SYNTHESES OF MIXED DONOR
HOMOGENEOUS AND IMMOBILIZED PALLADIUM(II) COMPLEXES
AS CATALYSTS FOR METHOXYCARBONYLATION AND HYDROGENATION
REACTIONS

By

Saphan Owino Akiri

A thesis submitted

In fulfilment of the academic requirements for the degree of

Doctor of Philosophy

in the College of Agriculture, Engineering and Science

School of Chemistry and Physics

University of KwaZulu-Natal

Pietermaritzburg, South Africa

Supervised by:

Professor Stephen Ojwach

August 2021

DECLARATION

I, **Saphan Akiri**, here in make a declaration that this thesis, entitled "syntheses of mixed donor homogeneous and immobilized palladium(II) complexes catalysts for methoxycarbonylation and hydrogenation reactions", entails my own and original research, accomplished at Inorganic laboratory, School of Chemistry and Physics, University of KwaZulu-Natal, Pietermaritzburg campus. Appropriate in-text citations and associated references have been included where others' work has been used. I also confirm that this thesis or part of it has never been submitted elsewhere for examination or award of a degree.
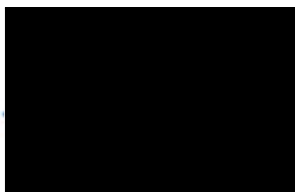
Signed: Date: 27/08/2021

Saphan Akiri

As the candidate's supervisor, I here approve that this PhD thesis be submitted for examination.

Signed: Date: 27/08/2021

Prof Stephen Ojwach

DEDICATION

I dedicate this work to my family members

ACKNOWLEDGEMENT

"No one who achieves success does so without acknowledging the help of others. The wise and confident acknowledge this help with gratitude". Alfred North Whitehead

I sincerely thank God for being the power in my life to guide me in making decisions and pursuing the right paths to culminate in achieving this feat. I also want to appreciate the immense work done and support offered by my supervisor, Professor Stephen Ojwach. The guidance, insights, positive criticisms, mentorship have been spot on during these years of intense research and write-ups. I am indebted to the DST-NRF Centre of Excellence in Catalysis for the incredible funding which supported my PhD project to completion.

My sincere gratitude to the University of KwaZulu-Natal technical staff for your unending support in characterizing every compound that I made, from NMR and GC spectroscopy, Mass spectrometry, X-ray crystallography to the Microscopy and Microanalysis Unit, thank so much. I also appreciate every assistance offered by the catalysis and organometallic research group Pietermaritzburg members; academic engagements during the group seminars were invaluable.

I express heartfelt appreciation to my marvellous family members. To my Wife Naomy, what a pillar you have been; your bravery and support were phenomenal. To my daughter Hilga Amani, your smiles and light mood was always a welcome distraction from the demanding lab work research; may you live long. I also appreciate my mum, Consolata Rose Akiri, who always prayed for the success of my PhD work. My siblings, Dan, Ruth, Ayub, Jemima and Susan, you are the best siblings one can ask for; your support and passion for education have encouraged me all the way.

PREFACE

This thesis is composed of seven chapters. **Chapter One** details a general introduction regarding recent advances in bridging the gap between heterogeneous and homogeneous catalyst systems. Various aspects have been covered, including techniques of immobilizing homogenous catalysts systems on solid supports and diverse techniques applied in biphasic catalysis. Furthermore, the chapter presents an insight into the methoxycarbonylation catalysis and industrial and domestic applications and the significance of methoxycarbonylation as an olefin value addition catalytic process. **Chapter two** is a comprehensive literature review of various catalytic systems that have been used as discrete catalysts in methoxycarbonylation reactions. In addition, this chapter also reviews supported catalysts used in the methoxycarbonylation catalysis.

Chapter three discusses the synthesis, characterization of N^N (pyridyl) benzamidine palladium complexes and their behaviour in methoxycarbonylation of a range of olefin substrates. The catalytic study focused on the role of ligand design in directing the product distribution of the produced esters. NMR kinetics study was applied in understanding the role played by phosphine and acid additives. The results obtained from this study has been published in Applied Organometallic Chemistry.

Chapter Four presents the synthesis and characterization of water-soluble and non-water soluble bischelated (phenoxyimine) palladium(II) complexes and their catalytic studies in methoxycarbonylation of 1-hexene. A detailed NMR study has also been done to understand the roles played by the addition of excess acid and phosphine promoters. Furthermore, the recyclability of the water-soluble complexes has been explored. The findings obtained from

this work have also been published in the Journal of Organometallic Chemistry (*Journal of Organometallic Chemistry 942 (2021): 121812*).

Chapter five entails the synthesis of homogeneous (amino)phenyl palladium(II) complexes and their respective silica and magnetic nanoparticle immobilized complexes. Various characterization techniques were also applied to fully characterize the new compounds formed. In addition, the catalytic behaviour of this set of complexes in methoxycarbonylation was evaluated, and the findings are reported in this chapter. The recyclability of the immobilized complexes was also examined in this chapter. **Chapter six** reports catalytic behaviour of homogeneous and silica-supported palladium(II) complexes bearing (phenoxy) imine ligands in the hydrogenation of styrene, alkenes, alkynes and functionalized benzenes. Further, this chapter reports recyclability studies of the supported complexes in this series in the hydrogenation of styrene and nitrobenzene. The results of this chapter have been published, *Catalysis Letters, 2020, 2850 - 2862*. The final chapter, **Chapter seven**, entails overall conclusions and future prospects for methoxycarbonylation catalysis systems.

RESEARCH OUTPUTS

Some parts of the research presented in this thesis have been published in peer-reviewed international journals, while the rest have been prepared as manuscripts and ready for submission as follows:

1. Akiri, Saphan O., Nondumiso L. Ngcobo, and Stephen O. Ojwach. "Comparative Study of Homogeneous and Silica Immobilized N^ N and N^ O Palladium (II) Complexes as Catalysts for Hydrogenation of Alkenes, Alkynes and Functionalized Benzenes." *Catalysis Letters* (2020): *2850 – 2862.* Doi: 10.1007/s10562-020-03192-1.

2. Akiri, Saphan O., and Stephen O. Ojwach. "Structural studies and applications of water-soluble (phenoxy) imine palladium (II) complexes as catalysts in biphasic methoxycarbonylation of 1-hexene." (*Journal of Organometallic Chemistry 942, 2021, 121812*). Doi: https://doi.org/10.1016/j.jorganchem.2021.121812.

3. Akiri, Saphan O., and Stephen O. Ojwach Sterically hindered (pyridyl) benzamidine palladium(II) complexes: Syntheses, structural studies and applications as catalysts in the methoxycarbonylation of olefins published by Applied Organometallic Chemistry. Doi:10.1002/aoc.6439.

4. Akiri, S. O., and Ojwach, S. O. A review of defined/ discrete palladium catalytic systems applied in the methoxycarbonylation/hydroesterification catalysis reactions (to be Submitted to Advanced Synthesis and Catalysis).

5. Akiri, Saphan O., and Stephen O. Ojwach. MCM-41 and SBA-15 supported (amino)phenyl palladium complexes as reusable catalysts in methoxycarbonylation of olefins: effects of support (manuscript to be submitted to Microporous and Mesoporous Materials).

6. Akiri, Saphan O., and Stephen O. Ojwach. Fe_3O_4 magnetic supported α, β diimine palladium(II) complexes as methoxycarbonylation of olefins recyclable catalysts (To be submitted to Applied Catalysis A: General)

CONFERENCE PRESENTATIONS

1. Saphan O. Akiri and Stephen O. Ojwach, DST-NRF Centre of Excellence in Catalysis: Centre for Catalysis Research Conference (November 2019), Krystal beach hotel, Cape Town. Oral presentation. Water-soluble monosodium sulfonato palladium II complexes: Structural studies and application in the methoxycarbonylation of olefins.

2. Saphan O. Akiri and Stephen O. Ojwach. Catalysis South Africa Conference (CATSA) (Virtual conference 2021). Structural studies and applications of water-soluble (phenoxy)imine palladium(II) complexes as catalysts in biphasic methoxycarbonylation of 1-hexene.

TABLE OF CONTENTS

ABSTRACT

Reactions of ligands (E)-N'-(2,6-diisopropylphenyl)-N-(4-methylpyridin-2-yl)benzimidamide (**L1),** (E)-N'-(2,6-diisopropylphenyl)-N-(6-methylpyridin-2-yl)benzimidamide (**L2**), (E)-N'-(2,6-dimethylphenyl)-N-(6-methylpyridin-2-yl)benzimidamide (**L3**), (E)-N'-(2,6-dimethylphenyl)-N-(4-methylpyridin-2-yl)benzimidamide (**L4**) and (E)-N-(6-methylpyridin-2-yl)-N'-phenylbenzimidamide (**L5**) with [Pd(NCMe)$_2$Cl$_2$] furnished the corresponding palladium(II) pre-catalysts (**Pd1-Pd5**), in good yields. Molecular structures of **Pd2** and **Pd3** revealed an N^N bidentate coordination mode to afford square planar compounds. Activation of the palladium(II) complexes with para tolyl sulfonic acid (PTSA) afforded active catalysts in the alkenes methoxycarbonylation. The resultant catalytic activities were controlled by both the complex structure and alkene substrate. While aliphatic substrates favoured the formation of linear esters (>70%), styrene substrate resulted in predominantly branched esters of up to 91%.

The water-soluble ligands; sodium 4-hydroxy-3-((phenylimino)methyl)benzenesulfonate (**L6**), sodium 3-(((2,6-dimethylphenyl)imino)methyl)-4-hydroxybenzenesulfonate (**L7**) and sodium 3-(2,6-diisopropylphenyl)imino)methyl)-4-hydroxybenzenesulfonate (**L8**) reacted with with Pd(OAc)$_2$ afford their respective palladium(II) complexes [Pd(**6**)$_2$] (**Pd6**), [Pd(**L7**)$_2$] (**Pd7**) and [Pd(**L8**)$_2$] (**PdL8**). In addition, treatment of the non-water-soluble ligands 2-((phenylimino)methyl)phenol (**L9**), 2-(((2,6-dimethylphenyl)imino)methyl)phenol (**L10**) and 2-((2,6-diisopropylphenyl)imino)methyl)phenol (**L11**) with Pd(OAc)$_2$ yielded complexes [Pd(**L9**)$_2$] (**Pd9**), [Pd(**10**)$_2$] (**Pd10)** and [Pd(**L11**)$_2$] (**Pd11),** respectively in good yields. Solid-state structures of compounds **Pd6** and **Pd9** revealed bis(chelated) square planar neutral compounds. All the complexes formed active catalysts in the methoxycarbonylation of 1-

hexene, affording yields of up to 92% within 20 h and regioselectivity of 73% in favour of linear esters. The activities and selectivities of the compounds depended on the steric encumbrance around the coordination centre. The water-soluble complexes displayed comparable catalytic behaviour to the non-water-soluble systems. The complexes could be recycled five times with minimal changes in both the catalytic activities and regio-selectivity.

Reactions of (amino)phenyl ligands, (E)-N-((Z)-4-(phenylamino)pent-3-en-2-ylidene)aniline (**L12**) and N,N'E,N,N'E)-N,N'-(3-(3-(triethoxysilyl)propyl)pentane-2,4-diylidene)dianiline (**L13**) with [Pd(NCMe)$_2$Cl$_2$] led to the formation of homogeneous complexes **Pd13** and **Pd14.** Besides, supporting of complex **Pd14** with either MCM-41, SBA-15, or Fe$_3$O$_4$ magnetic nanoparticles gave immobilized complexes **P15**-**Pd17,** respectively. Using varying metal loading in the MCM-41 immobilization of complex **Pd14** produced complexes **Pd18** and **Pd 19**. In addition, calcination of complex **Pd16** at 150ºC and 200ºC led to the formation of complexes **Pd20** and **Pd21,** respectively. All the complexes were received in good yields. The catalytic activities and selectivities of the homogeneous complexes were influenced by the coordination sphere, with the complexes predominantly forming linear esters. On the other hand, the catalytic behaviours of the immobilized catalysts depended on the nature of support and calcination temperatures. In addition, the catalytic activities were observed to depend on the reaction temperature, catalyst loading, amounts of PPh$_3$ and acid promoters. The immobilized complexes **Pd15**, **Pd16** and **Pd17,** were recycled up to five times.

The homogeneous and silica immobilized palladium(II) complexes of ligands (2-phenyl-2-((3(triethoxysilyl)propyl)imino)ethanol) (**L14),** (4-methyl-2-((3(triethoxysilyl)propyl)imino)methyl)phenol) (**L15**), [**L14**-MCM-41 (**L16),** and [**L15**-

MCM-41 (**L17**)]. The homogeneous complexes [Pd(**L14**)$_2$] (**Pd22**), [Pd(**L14**)$_2$] (**Pd23**), [Pd(**L14**)(Cl$_2$)] (**Pd24**), [Pd(**L15**)(Cl$_2$)] (**Pd25**) were obtained from homogenous ligands L14, **L15**, **L16** and **L17** respectively. In addition, the silica immobilized compounds [Pd(**L14**)$_2$]-MCM-41] (**Pd26**) and [Pd(**L15**)$_2$)-MCM-4] (**Pd27**) were obtained through convergence immobilization of complexes **Pd22** and **Pd23,** respectively. Comparatively, immobilized complexes [Pd (**L14**)(Cl$_2$)-MCM-41] (**Pd28**) and [Pd(**L15**)(Cl$_2$)]-MCM-41] (**Pd29**) were obtained from the complexation of immobilized ligands **L16** and **L17**. Both sets of complexes gave active catalysts in molecular hydrogenation of alkenes, alkynes and functionalized benzenes. The catalytic activities and product distribution in these reactions were largely dictated by the nature of the substrate. The kinetic studies revealed reaction orders dependence on styrene for both the homogeneous and supported catalysts. Significantly, the selectivity of both sets of catalysts was comparable in the hydrogenation of alkynes and multi-functionalized benzenes. The supported catalysts could be recycled up to four times with minimum reduction in catalytic activities and showed the absence of any leaching from hot filtration experiments. Kinetics and poisoning studies established the presence of active homogeneous species for complexes **Pd22**-**Pd5** and Pd(0) nanoparticles for the immobilized complexes **Pd26**-**Pd29,** respectively.

LIST OF FIGURES

LIST OF TABLES

LIST OF SCHEMES

ABBREVIATIONS and SYMBOLS

APTES	(Amino propyl)triethoxysilane
CTPES	Chloropropyl triethoxy silane.
DCM	Dichloromethane
EDX	Energy-dispersive X-ray spectroscopy
ESI	Electron spray ionization
FT-IR	Fourier transform Infrared spectroscopy
GC	Gas chromatography
GC-MS	Gas chromatography-mass spectrometry
mL	Millilitres
MS	Mass spectrometry
NMR	Nuclear Magnetic Resonance
ppm	Parts per million
PTSA	Para-toluene sulfonic Acid
SEM	Scanning electron microscopy
TEM	Transmission electron microscopy
TOF	Turn over frequency
TON	Turn over number
d	Doublet

J	Coupling constant
m	Multiplet
s	Singlet
t	Triplet
δ	Chemical shift

Chapter 1

Introduction and an overview of methoxycarbonylation reactions as catalysed by transition metal complexes through homogenous, heterogeneous, immobilised and biphasic systems.

1.1 Introductory remarks

The increasing demand for industrial products and by-products and their use as domestic wants and other industrial processes' feeder lines have led to an ever-increasing establishment of various industries to support the demand. One of such industrial processes which has presented with much growth is olefin value addition. The interplay between the commercial and financial considerations has commanded the use of improved catalytic systems, which have, over the years, developed and evolved to increase industrial output at a relatively lower cost. However, such an increased output has gone unfelt negatively in other areas as it has come with enhanced environment pollution and degradation, and thus, calling for a shift to green chemistry, which targets chemical processes and products that are reducing, if not eliminating the use and/or generation of hazardous chemicals. In response, the field of chemistry has seen a rise in the development of chemical and catalytic processes that minimise dangerous chemical emissions and waste production — for instance, the exploration of ease of recovery and reusability of catalysts in reducing the negative environmental impacts [1].

Metal complex catalysts have been the backbone of the manufacture of vast industrial products for decades. Examples of the olefin value addition which have attracted some attention are methoxycarbonylation and hydrogenation catalytic transformation reactions. While the former is versatile in the production of a range of useful commodities such as food flavours, solvents,

cosmetics, detergents, surfactants and pharmaceuticals [2, 3], the latter is vital in fine chemicals, petrochemical and pharmaceutical syntheses [4]. In efforts to maximise the profits using the catalyst systems while at the same time conserving the environment, numerous steps have been made to modify catalysts through catalyst design and modification of the reaction condition environments to find the most suitable catalytic conditions. One of the focuses of such modifications has been to tap the advantages of both homogenous and heterogeneous catalytic systems and create 'superior' catalytic systems which are both selective and recyclable. This chapter thus seeks to provide general principles of catalyst recycling and reuse with a major focus on methoxycarbonylation and hydrogen catalytic reactions as olefin value addition routes.

1.2 Bridging the gap between homogeneous and heterogeneous catalysis

Homogeneous catalysis has been for a long time applied in industrial production due to various advantages it has over heterogeneous catalysis. Notably, homogeneous catalysts are widely applied in various transformation reactions and syntheses since they can allow a multipronged control of selectivity; regioselectivity, chemoselectivity and stereoselectivity [5]. In addition, the mechanisms involved in homogeneous catalysis is easily understood [6], hence handing chemists a powerful tool of carefully controlling both activities and selectivities to get the targeted molecule or product. However, it is also known that homogeneous catalysts have poor separation of the precatalysts from the resulting catalysis mixture, thus, difficulty in recovering and reusing them. The use of organic solvents has therefore been employed in the past in efforts to separate the catalysts, a practice that leads to the creation of more chemical waste, violating the first and fifth green chemistry principles, which stress on lowering auxiliary substances and waste [7]. Besides, the separation of catalysts in the use of a homogeneous catalyst system may

require a high energy distillation process, which in turn impact negatively on the environment and at times damage the catalyst [8].

Heterogeneous catalysis comparatively has found its usefulness in industries since they can easily be separated and reused, even though they have limitations such as poor selectivity relative to the homogeneous catalysts [9]. In the last decades, various researchers have made deliberate efforts towards integrating the pros of heterogeneous and homogeneous catalytic systems to create a 'super' system that exhibits the desirable properties of both catalytic systems. In such catalytic designs, the goal is to have the system retain the recovery and reuse properties of heterogeneous systems and the superior selective property of the homogeneous systems. Various terms such as heterogenization, immobilisation and anchoring, among others, have been used to describe such a process. Two major synthetic protocols have been used in the immobilization of homogeneous catalysts; convergent and sequential protocols or synthetic routes [10]. Some of the methods that have been applied in heterogenizing homogeneous catalysts include the use of insoluble solid supports [11] and the use of biphasic catalytic systems [12].

1.3 Insoluble solid supports as agents of heterogenization.

Various solid supports have been used in creating a hybrid of homogenous and heterogeneous catalyst systems. While several of such materials exist in the literature, they can be broadly categorised into three classes; using magnetic supports, the application of inorganic supports like clay, silica, and alumina, [13] and the use of rigid-organic backbones [14], polymers [15] and dendrimers [16]. By using various synthetic routes, homogeneous catalysts can effectively be supported on these solid supports, which then render the whole catalyst system insoluble in

the reaction media, hence easy separation and reuse. While the catalysts supported on the inorganic solid supports are easily recycled through simple filtration, decantation or through centrifugation, a strong enough magnet is a requirement when separating the homogeneous catalysts supported on magnetic nanoparticles.

1.3.1 Magnetic nanoparticles

The use of iron magnetic nanoparticles as insoluble catalyst support has been on the rise due to various strengths such as thermal stability, relatively lower costs, high surface area, low toxicity, and chemical inertness [17]. In addition, iron magnetic particle versatility has also been shown in the application in a wide spectrum of fields such as electronic communication [18], magnetic fluids [19], environmental remediation [20], and biomedical [21], alongside catalysis (Figure 1.1). Iron magnetic nanoparticle immobilized catalysts are easily separated from a reaction mixture using an external magnet.
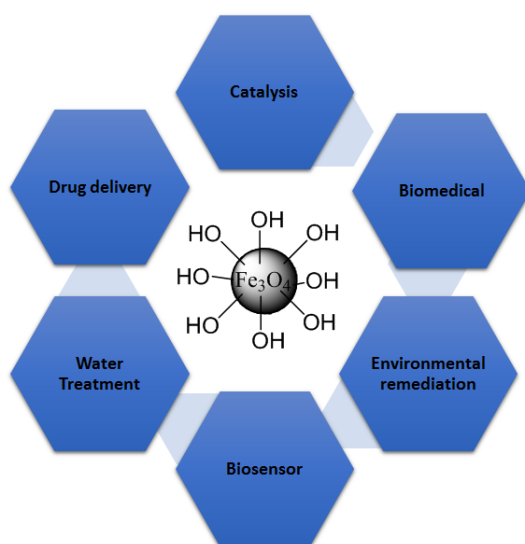
Figure 1.1: Uses of magnetic iron nanoparticles in immobilization of homogeneous catalysts

1.3.2 The use of silica as catalyst support

Silica is another class of insoluble inorganic supports that have been widely applied in the heterogenization of homogeneous catalysts for various catalytic transformations. Their wide application emanates from the fact that they are readily available as part of earth material, chemically inert, environment friendly, and they also have incredible thermal stability [22]. Most silica used as immobilization agents has large pore volumes, high surface area and mesoporous varying pore sizes as low as 2 nm up to 50 nm. However, microporous silica with sizes below 2 nm and macroporous with sizes above 50 nm have also been used [22]. Widely applied as supports, the mesoporous group of the silica materials exist in various forms possessing different orientations. For instance, while MCM-50 and MCM-48 have lamellar and cubic orientations, respectively, SBA-15 and MCM-41 (Figure 1.2) exist in hexagonal orientations [23].
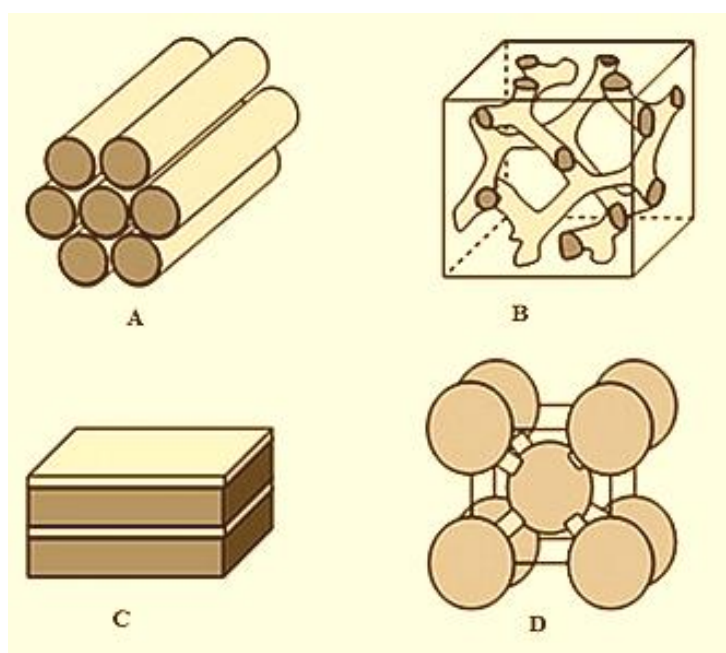
Figure 1.2: A diagram showing orientations of various silica support, MCM-41, SBA-15 (A), MCM-48 (B), MCM-50 (C) and SBA-16 (D).

1.4 Biphasic catalysts and recycling

Biphasic systems are generally liquid-liquid systems that contain the catalyst and the substrate in dissolved form. The two liquids used should have limited mutual solubility [24]. Even though the most widely used combination entails an organic-aqueous biphasic system, other combinations include organic-organic biphasic systems. More recently, the fluorous biphasic system, which contains immiscible normal organic solvent paired with a highly fluorinated organic solvent, and the use of ionic liquids have been applied [24]. In addition to biphasic catalysis having a potential of easier catalyst separation, recycling and reuse, water as a solvent is attractive since it is non-toxic, readily available, relatively cheap as well as its propensity of forming biphasic systems with numerous organic solvents and materials [24]. In most cases, the precatalysts dissolve in the more polar liquid, whereas the products and the substrate are in the organic phase. In a typical biphasic catalytic reaction, even though the two liquid phases are immiscible, the reaction normally takes place in the two phases due to enhanced stirring speeds, which in turn creates enough contact between the catalyst and the substrate (Figure 1.3). Various types of biphasic systems exist, including; ionic liquids [25-30], aqueous biphasic systems [8, 31], thermomorphic systems [32-34], supercritical fluid systems [35, 36] and fluorous systems [12].
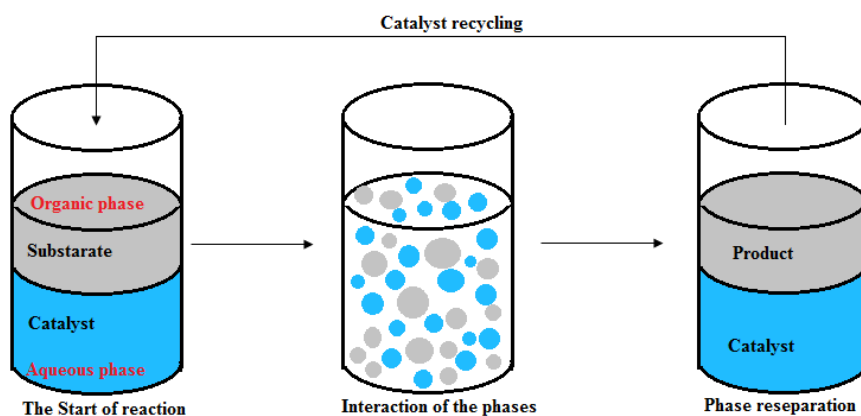
Figure 1.3: Depiction of biphasic catalysis, phase separation and recycling

Table 1.1: Industrial applications of biphasic catalysis

Industrial process	Industry name	Solvent/solvent system	Metal catalyst
Ethylene oligomerization	Universal Oil Products	Sulfolane	Nickel
Propylene dimerization	Institut Francais Du Pétrole	Ionic liquids	Nickel
Butadiene telomerization	Kuraray	Sulfolane/water	Palladium
Unsaturated aldehydes hydrogenation	Rhône-Poluenc	Water	Ruthenium
Butylene/Propylene hydroformylation	RuhrChemie/Rhone-Poluenc	Water	Rhodium
Ethylene oligomerization (SHOP)	Shell	Butane-1,4-diol	Nickel

1.5 Carbonylation: a synthetic route to olefin value addition

Introduced by Walter Reppe in the mid-20th century while at BASF, the word carbonylation refers to various reactions where the carbonyl moiety (C=O) is solely or together with other

substituents are inserted into nitro groups, alcohols, and amines, among other groups to obtain a target molecule or compound [37, 38]. The (C=O) can be obtained directly from carbon monoxide or from CO surrogates. Carbonylation catalytic reaction favourably proceeds upon the addition of transition metal catalysts like palladium, iridium, rhodium, cobalt, nickel and ruthenium [38]. Some of the most common carbonylation reactions include hydroformylation which mainly involves the formation of aldehydes [39], hydrocarboxylation, which is the synthesis of carboxylic acids [40] and alkoxycarbonylation [41], also referred to as hydroesterification, which involves the production of esters. Figure 1.4 gives a summary of common carbonylation reactions
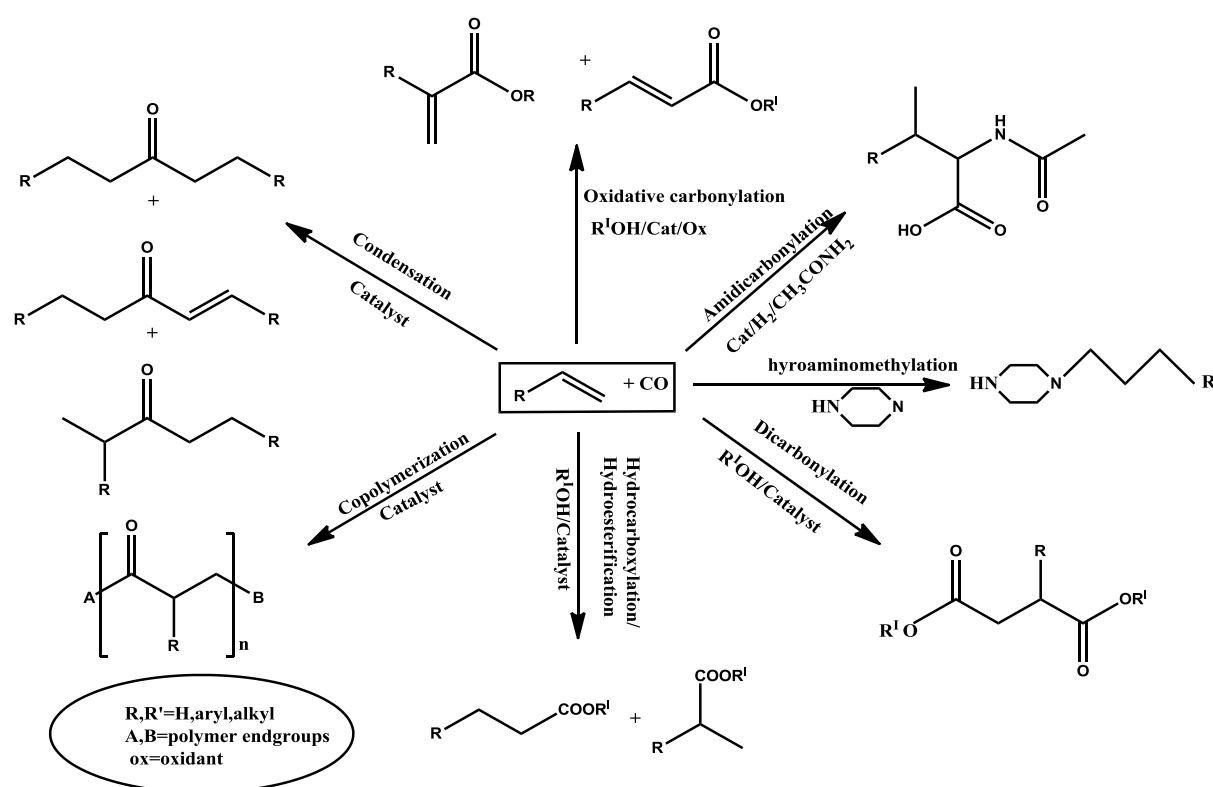
Figure 1.4: A diagram showing examples of carbonylation types

1.6 Carbonyl sources for carbonylation reactions

Carbon monoxide is one of the most vital reactants in carbonylation as its insertion in the cycle result in important transition metal intermediates, hence the carbonylation products. Traditionally, carbon monoxide has been used as the carbonyl source in carbonylation reactions in general. However, there is a range of problems surrounding CO use as the source of carbonyl, some of which include its transport and storage, combined with the fact that it is toxic [42]. As such, deliberate intentions to bypass the use of carbon monoxide and explore other carbonyl sources which can effectively drive carbonylation reactions such as methoxycarbonylation is a priority. Some of the advances which have been made in this regard include the use of formic acid [43] and its derivatives such as formates [44], formamides [45], use of aldehydes [46], and the use of metal carbonyls [47]. More recently, the use of more abundant carbon dioxide as a carbonyl source has been explored despite the difficulties faced in its activation [48, 49].

1.7 Methoxycarbonylation: An insight into the process

A type of carbonylation reaction, methoxycarbonylation, refers to the functionalisation of olefins and other groups in the presence of methanol, carbon monoxide, acid promoter and a phosphine stabiliser. The carbon monoxide is introduced into π- unsaturated compounds through oxidative addition, with the resulting ester formed *via* a reductive elimination in a methanolysis process [50]. Two ester products are possible- a branched ester, linear ester, or both, with the possibility of the selected ester product depending majorly on factors such as reaction conditions and nature of complex [51]. Even though a range of metal complexes such as ruthenium, platinum, cobalt, iridium, rhodium and nickel have been applied in the methoxycarbonylation reactions, palladium complexes have been the most preferred since they can be used in milder conditions and can catalyse a broad scope of substrates to respective

products. Methoxycarbonylation reaction can be done using two methods, one of them being oxidative methoxycarbonylation. In the oxidative methoxycarbonylation, stoichiometric amounts of methanol and a metal salt, in most cases palladium(II) chloride are used in the transformation of a suitable substrate into an ester product (Scheme 1.1) [52]. By using an appropriate oxidant such as benzoquinone, the reaction proceeds through a catalytic path where the production of diesters are possible through a further CO insertion [53].
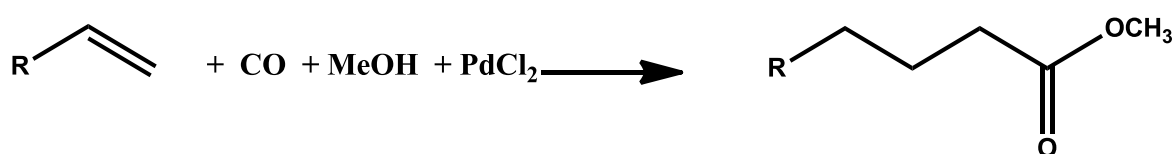
Scheme 1.1: Stoichiometric oxidative methoxycarbonylation.

The second type of methoxycarbonylation using palladium catalysts require a stabiliser as they have been shown in the absence of stabiliser to form inactive or less active moiety or palladium(0) which then precipitates off the catalytic reaction mixture leading to inactivity [54]. Ligands coordinated to the palladium centre together with the stabiliser additive and co-catalyst (Scheme 1.2), therefore play a major role in the catalyst stabilisation during a methoxycarbonylation reaction.
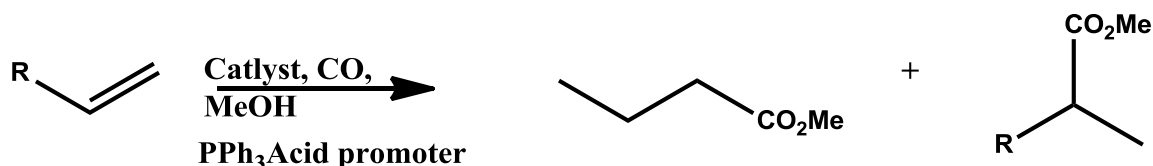
Scheme 1.2: A typical catalytic methoxycarbonylation reaction showing the conditions

1.7.1 Methoxycarbonylation mechanism

Several studies have been done in the past to unearth the possible mechanism of palladium(II) catalysed methoxycarbonylation reactions. Two of the most widely agreed mechanistic routes are carbomethoxy and the hydride routes [55]. While the carbomethoxy route entails inserting the olefin into the Pd-carbomethoxy bond, the olefin is inserted into the Pd-hydride bond when it comes to the hydride mechanism (Figure 1.5). The Pd-hydride moiety results from the combination of the precatalysts and hydrogen from a hydrogen source, mostly an acid promoter. On the other hand, the Pd-carbomethoxy group forms from a reaction between the precatalysts and methanol [56, 57]. The carbomethoxy route commences by acid promoter facilitated the formation of the Pd-Methoxy bond. The carbon monoxide then inserts into the formed bond, followed by the olefin coordination and insertion. The final ester product(s) is then produced through a methanolysis process [58, 59]. On the contrary, the hydride mechanism is triggered through the formation of a Pd-H followed by the olefin coordination to the created bond. This process then leads to coordination and migratory insertion of carbon monoxide to give a Pd-acyl intermediate. Attachment of methanol to the intermediate eventually yields the ester products [59]. Various factors have been implicated to have an influence on the mechanistic route, followed by a methoxycarbonylation under consideration. However, the majority of the studies indicate that the hydride mechanism is favoured [60-64].
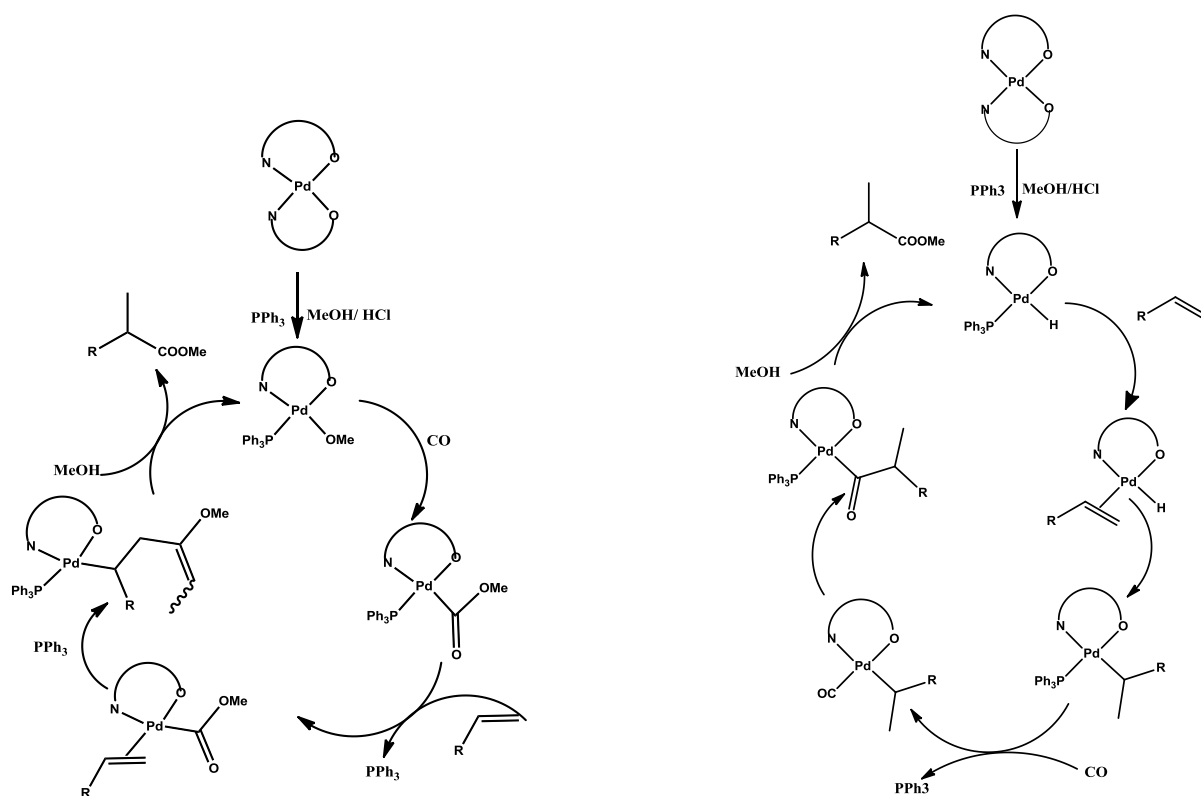
Figure 1.5: A representation of carbomethoxy and hydride methoxycarbonylation mechanisms.

1.8 Significance of methoxycarbonylation

Methoxycarbonylation is among the most industrially significant chemical reactions. One of the known wide-scale applications is the methoxycarbonylation of ethylene to produce methyl propanoate [65], a precursor in the manufacture of methacrylate. The polymer (polymethyl methacrylate) formed from methacrylate has numerous industrial uses like applications in touch screens and liquid-crystal display screen electronics [66]. Most recently, it has been applied in lightweight and transparent shielding equipment [67]. Another known application of methoxycarbonylation is in pharmaceuticals where, through the process, some of the most important classes of drugs- the non-steroidal anti-inflammatory drugs (NSAIDs) can be synthesised. Examples of such drugs include Naproxen, Ibuprofen, Fenoprofen and Ketoprofen

[68-72]. Some of the most widely applied methoxycarbonylation products are summarised in Table 1.2.

Table 1.2: Selected ester products and their domestic and industrial application

Methoxycarbonylation ester product	Major uses
Ethyl benzoate	-Preservative and fragrance ingredient [73], applied as a perfume scent [74], food flavouring agent [75].
Methyl propanoate/ Methyl propionate	Manufacture of (polymethyl methacrylate) [67], manufacture of varnishes and paints and resins[76].
Isobutyl acetate	Used as a solvent [77] flavouring agent and fuel supplement [78].
Methyl acetate	A solvent for ink resins and oils [79].
Isopropyl myristate	Applied in cosmetics and manufacture of topical medicine [80].

1.9 References

[1] P.J. Dunn, The importance of green chemistry in process research and development, Chem. Soc. Rev., 41 (2012) 1452-1461.

[2] B. Liu, F. Hu, B.-F. Shi, Recent advances on ester synthesis via transition-metal catalyzed C–H functionalization, ACS Catalysis, 5 (2015) 1863-1881.

[3] K. Kosswig, W. Schaefer, Hydrocarboxymethylation-an Attractive Route from Olefins to Fatty Acid Esters?, Ind. Eng. Chem., 19 (1980) 330-334.

[4] R. Abu-Reziq, D. Wang, M. Post, H. Alper, Platinum nanoparticles supported on ionic liquid-modified magnetic nanoparticles: Selective hydrogenation catalysts, Adv. Synth. Catal., 349 (2007) 2145-2150.

[5] A. Marr, P. Marr, Entrapping homogeneous catalysts by sol–gel methods: the bottom-up synthesis of catalysts that recycle and cascade, Dalton Trans., 40 (2011) 20-26.

[6] D.J. Cole-Hamilton, Homogeneous catalysis--new approaches to catalyst separation, recovery, and recycling, Science, 299 (2003) 1702-1706.

[7] P. Anastas, N. Eghbali, Green chemistry: principles and practice, Chem. Soc. Rev., 39 (2010) 301-312.

[8] E. Karakhanov, A. Maksimov, Biphasic catalysis in petrochemical processes, Russ. J. Gen. Chem., 79 (2009) 1370-1383.

[9] H.H. Brintzinger, D. Fischer, R. Mülhaupt, B. Rieger, R.M. Waymouth, Stereospecific olefin polymerization with chiral metallocene catalysts, Angew. Chem. Int. Ed., 34 (1995) 1143-1170.

[10] P. McMorn, G.J. Hutchings, Heterogeneous enantioselective catalysts: strategies for the immobilisation of homogeneous catalysts, Chem. Soc. Rev., 33 (2004) 108-122.

[11] A.E. Collis, I.T. Horvath, Heterogenization of homogeneous catalytic systems, Catal. Sci. Technol, 1 (2011) 912-919.

[12] I.T. Horváth, J. Rábai, Facile catalyst separation without water: fluorous biphase hydroformylation of olefins, Science, 266 (1994) 72-75.

[13] J.J. de Pater, B.J. Deelman, C.J. Elsevier, G. van Koten, Multiphase systems for the recycling of alkoxycarbonylation catalysts, Adv. Synth. Catal., 348 (2006) 1447-1458.

[14] H.P. Dijkstra, M.D. Meijer, J. Patel, R. Kreiter, G.P. van Klink, M. Lutz, A.L. Spek, A.J. Canty, G. van Koten, Design and performance of rigid nanosize multimetallic cartwheel pincer compounds as lewis-acid catalysts, Organometallics, 20 (2001) 3159-3168.

[15] D.E. Bergbreiter, B.L. Case, Y.-S. Liu, J.W. Caraway, Poly (N-isopropylacrylamide) soluble polymer supports in catalysis and synthesis, Macromolecules, 31 (1998) 6053-6062.

[16] J.W. Knapen, A.W. van der Made, J.C. de Wilde, P.W. van Leeuwen, P. Wijkens, D.M. Grove, G. van Koten, Homogeneous catalysts based on silane dendrimers functionalized with arylnickel (II) complexes, Nature, 372 (1994) 659.

[17] J. Govan, Y.K. Gun'ko, Recent advances in the application of magnetic nanoparticles as a support for homogeneous catalysts, Nanomaterials, 4 (2014) 222-241.

[18] X.-B. Li, Y.-J. Gao, Y. Wang, F. Zhan, X.-Y. Zhang, Q.-Y. Kong, N.-J. Zhao, Q. Guo, H.-L. Wu, Z.-J. Li, Self-assembled framework enhances electronic communication of ultrasmall-sized nanoparticles for exceptional solar hydrogen evolution, J. Am. Chem. Soc., 139 (2017) 4789-4796.

[19] S. Laurent, S. Dutz, U.O. Häfeli, M. Mahmoudi, Magnetic fluid hyperthermia: focus on superparamagnetic iron oxide nanoparticles, Adv. Colloid Interface Sci., 166 (2011) 8-23.

[20] S.C. Tang, I.M. Lo, Magnetic nanoparticles: essential factors for sustainable environmental applications, Water Res., 47 (2013) 2613-2632.

[21] L.H. Reddy, J.L. Arias, J. Nicolas, P. Couvreur, Magnetic nanoparticles: design and characterization, toxicity and biocompatibility, pharmaceutical and biomedical applications, Chem. Rev., 112 (2012) 5818-5878.

[22] Z.-A. Qiao, Q.-S. Huo, Synthetic Chemistry of the Inorganic Ordered Porous Materials, Modern Inorganic Synthetic Chemistry, Elsevier2017, pp. 389-428.

[23] B. Szczęśniak, J. Choma, M. Jaroniec, Major advances in the development of ordered mesoporous materials, Chem. Commun., 56 (2020) 7836-7848.

[24] F. Joo, Biphasic Catalysis-Homogeneous. Encyclopedia of Catalysis, John Wiley & Sons, Inc, 2012.

[25] T. Welton, Ionic liquids: a brief history, Biophys. rev., 10 (2018) 691-706.

[26] M. Haumann, A. Riisager, Hydroformylation in room temperature ionic liquids (RTILs): catalyst and process developments, Chem. Rev., 108 (2008) 1474-1497.

[27] V.I. Pârvulescu, C. Hardacre, Catalysis in ionic liquids, Chem. Rev., 107 (2007) 2615-2665.

[28] Y. Qiao, A.D. Headley, Ionic liquid immobilized organocatalysts for asymmetric reactions in aqueous media, Catalysts, 3 (2013) 709-725.

[29] S.G. Khokarale, E.J. Garcia-Suarez, R. Fehrmann, A. Riisager, Highly selective continuous gas-phase methoxycarbonylation of ethylene with supported ionic liquid phase (SILP) catalysts, ChemCatChem, 9 (2017) 1824-1829.

[30] E.J. García-Suárez, S.G. Khokarale, O.N. van Buu, R. Fehrmann, A. Riisager, Pd-catalyzed ethylene methoxycarbonylation with Brønsted acid ionic liquids as promoter and phase-separable reaction media, Green Chem., 16 (2014) 161-166.

[31] J. Herwig, R. Fischer in Rhodium Catalyzed Hydroformylation, Kluwer Academic, Dordrecht, 2000.

[32] T. Gaide, J.M. Dreimann, A. Behr, A.J. Vorholt, Overcoming Phase-Transfer Limitations in the Conversion of Lipophilic Oleo Compounds in Aqueous Media—A Thermomorphic Approach, Angew. Chem. Int. Ed., 55 (2016) 2924-2928.

[33] A. Behr, L. Johnen, A.J. Vorholt, Telomerization of myrcene and catalyst separation by thermomorphic solvent systems, ChemCatChem, 2 (2010) 1271-1277.

[34] Y. Brunsch, A. Behr, Temperature-controlled catalyst recycling in homogeneous transition-metal catalysis: minimization of catalyst leaching, Angew. Chem. Int. Ed., 52 (2013) 1586-1589.

[35] P.G. Jessop, T. Ikariya, R. Noyori, Homogeneous catalysis in supercritical fluids, Chem. Rev., 99 (1999) 475-494.

[36] J. Fang, H. Jin, T. Ruddy, K. Pennybaker, D. Fahey, B. Subramaniam, Economic and environmental impact analyses of catalytic olefin hydroformylation in CO2-expanded liquid (CXL) media, Ind. Eng. Chem. Res, 46 (2007) 8687-8692.

[37] G. Liu, Z. Li, H. Geng, X. Zhang, Rhodium-catalyzed regioselective hydroaminomethylation of terminal olefins with pyrrole-based tetraphosphorus ligands, Catal. Sci. Technol,, 4 (2014) 917-921.

[38] H. Colquhoun, D. Thompson, M.V. Twigg, Carbonylation, Springer Science & Business Media1991.

[39] D.M. Hood, R.A. Johnson, A.E. Carpenter, J.M. Younker, D.J. Vinyard, G.G. Stanley, Highly active cationic cobalt (II) hydroformylation catalysts, Science, 367 (2020) 542-548.

[40] A. Alkayal, V. Tabas, S. Montanaro, I.A. Wright, A.V. Malkov, B.R. Buckley, Harnessing applied potential: selective β-hydrocarboxylation of substituted olefins, J. Am. Chem. Soc., 142 (2020) 1780-1785.

[41] J. Yang, J. Liu, Y. Ge, W. Huang, C. Schneider, R. Dühren, R. Franke, H. Neumann, R. Jackstell, M. Beller, A general platinum-catalyzed alkoxycarbonylation of olefins, Chem. Commun., 56 (2020) 5235-5238.

[42] T. Morimoto, K. Kakiuchi, Evolution of carbonylation catalysis: no need for carbon monoxide, Angew. Chem. Int. Ed., 43 (2004) 5580-5588.

[43] J.-P. Simonato, T. Walter, P. Métivier, Iridium–formic acid based system for hydroxycarbonylation without CO gas, J. Mol. Catal. A: Chem., 171 (2001) 91-94.

[44] P. Isnard, B. Denise, R. Sneeden, J. Cognion, P. Durual, Transition metal catalysed interaction of ethylene and alkyl formates, J. Organomet. Chem., 256 (1983) 135-139.

[45] S. Ko, H. Han, S. Chang, Ru-catalyzed hydroamidation of alkenes and cooperative aminocarboxylation procedure with chelating formamide, Org. Lett., 5 (2003) 2687-2690.

[46] T. Shibata, N. Toshida, K. Takagi, Rhodium Complex-Catalyzed Pauson− Khand-Type Reaction with Aldehydes as a CO Source, J. Org. Chem, 67 (2002) 7446-7450.

[47] N.-F.K. Kaiser, A. Hallberg, M. Larhed, In situ generation of carbon monoxide from solid molybdenum hexacarbonyl. A convenient and fast route to palladium-catalyzed carbonylation reactions, J. Comb. Chem., 4 (2002) 109-111.

[48] Q. Liu, L. Wu, R. Jackstell, M. Beller, Using carbon dioxide as a building block in organic synthesis, Nat. Commun., 6 (2015) 5933.

[49] L. Wu, Q. Liu, I. Fleischer, R. Jackstell, M. Beller, Ruthenium-catalysed alkoxycarbonylation of alkenes with carbon dioxide, Nat. Commun., 5 (2014) 1-6.

[50] X.-F. Wu, X. Fang, L. Wu, R. Jackstell, H. Neumann, M. Beller, Transition-metal-catalyzed carbonylation reactions of olefins and alkynes: a personal account, Acc. Chem. Res., 47 (2014) 1041-1053.

[51] S. Zolezzi, S.A. Moya, G. Valdebenito, G. Abarca, J. Parada, P. Aguirre, Methoxycarbonylation of olefins catalyzed by palladium (II) complexes containing naphthyl (diphenyl) phosphine ligands, Appl. Organomet. Chem., 28 (2014) 364-371.

[52] A. Brennführer, H. Neumann, M. Beller, Palladium-catalyzed carbonylation reactions of alkenes and alkynes, ChemCatChem, 1 (2009) 28-41.

[53] C. Bianchini, A. Meli, W. Oberhauser, P.W. van Leeuwen, M.A. Zuideveld, Z. Freixa, P.C. Kamer, A.L. Spek, O.V. Gusev, A.M. Kal'sin, Methoxycarbonylation of Ethene by Palladium (II) Complexes with 1, 1 '-Bis (diphenylphosphino) ferrocene (dppf) and 1, 1 '-Bis (diphenylphosphino) octamethylferrocene (dppomf), Organometallics, 22 (2003) 2409-2421.

[54] G. Kiss, Palladium-catalyzed Reppe carbonylation, Chem. Rev., 101 (2001) 3435-3456.

[55] G. Cavinato, L. Toniolo, A. Vavasori, Characterization and catalytic activity of trans-[Pd (COCH$_2$CH$_3$)(TsO)(PPh$_3$)$_2$], isolated from the hydro-methoxycarbonylation of ethene catalyzed by [Pd (TsO)$_2$ (PPh$_3$)$_2$], J. Mol. Catal. A: Chem., 219 (2004) 233-240.

[56] E.J.G. Suárez, Palladium complexes containing diphosphine and sulfonated phosphine ligands for cc bond forming reactions. catalytic and mechanistic studies, Universitat Rovira i Virgili2008.

[57] I. del Río, C. Claver, P.W. van Leeuwen, On the mechanism of the hydroxycarbonylation of styrene with palladium systems, Eur. J. Inorg. Chem., 2001 (2001) 2719-2738.

[58] L. Crawford, D.J. Cole-Hamilton, M. Bühl, Uncovering the mechanism of homogeneous methyl methacrylate formation with p, n chelating ligands and palladium: favored reaction channels and selectivities, Organometallics, 34 (2015) 438-449.

[59] R. Heck, Dicarboalkoxylation of olefins and acetylenes, J. Am. Chem. Soc., 94 (1972) 2712-2716.

[60] P. Roesle, L. Caporaso, M. Schnitte, V. Goldbach, L. Cavallo, S. Mecking, A comprehensive mechanistic picture of the isomerizing alkoxycarbonylation of plant oils, J. Am. Chem. Soc., 136 (2014) 16871-16881.

[61] R.P. Tooze, K. Whiston, A.P. Malyan, M.J. Taylor, N.W. Wilson, Evidence for the hydride mechanism in the methoxycarbonylation of ethene catalysed by palladium–triphenylphosphine complexes, J. Chem. Soc., Dalton Trans., (2000) 3441-3444.

[62] G.R. Eastham, R.P. Tooze, M. Kilner, D.F. Foster, D.J. Cole-Hamilton, Deuterium labelling evidence for a hydride mechanism in the formation of methyl propanoate from carbon monoxide, ethene and methanol catalysed by a palladium complex, J. Chem. Soc., Dalton Trans., (2002) 1613-1617.

[63] G. Cavinato, A. Vavasori, L. Toniolo, F. Benetollo, Synthesis, characterization and X-ray structure of trans-[Pd (COOCH$_3$)(H$_2$O)(PPh$_3$)$_2$](TsO), a possible intermediate in the catalytic hydroesterification of olefins (TsO= p-toluenesulfonate), Inorg. Chim. Acta, 343 (2003) 183-188.

[64] V. de la Fuente, M. Waugh, G.R. Eastham, J.A. Iggo, S. Castillón, C. Claver, Phosphine Ligands in the Palladium-Catalysed Methoxycarbonylation of Ethene: Insights into the Catalytic Cycle through an HP NMR Spectroscopic Study, Chem. Eur. J., 16 (2010) 6919-6932.

[65] W. Clegg, M.R. Elsegood, G.R. Eastham, R.P. Tooze, X.L. Wang, K. Whiston, Highly active and selective catalysts for the production of methyl propanoate via the methoxycarbonylation of ethene, Chem. Commun., (1999) 1877-1878.

[66] B. Harris, Acrylics for the Future, Ingenia, 45 (2010) 18-23.

[67] S. Ahmad, L.E. Crawford, M. Bühl, Palladium-catalysed methoxycarbonylation of ethene with bidentate diphosphine ligands: a density functional theory study, PCCP, 22 (2020) 24330-24336.

[68] J. Li, W. Chang, W. Ren, J. Dai, Y. Shi, Palladium-catalyzed highly regio-and enantioselective hydroesterification of aryl olefins with phenyl formate, Org. Lett., 18 (2016) 5456-5459.

[69] F.D. Hart, The new antirheumatic drugs, Drugs, 9 (1975) 321-325.

[70] T.G. Kantor, Ketoprofen: a review of its pharmacologic and clinical properties, Pharmacoltherapy, 6 (1986) 93-102.

[71] P. Harrington, E. Lodewijk, Large-scale synthetic process for (S)-naproxen by Syntex, Org. Process Res. Dev, 1 (1997) 72-76.

[72] J.M. Lehmann, J.M. Lenhard, B.B. Oliver, G.M. Ringold, S.A. Kliewer, Peroxisome proliferator-activated receptors α and γ are activated by indomethacin and other non-steroidal anti-inflammatory drugs, J. Biol. Chem., 272 (1997) 3406-3410.

[73] J. Panten, E. Oelkers, J. Correll, P. Kurzenne, Use of carboxylic acid esters as a fragrance substance, Google Patents, 2013.

[74] L.C. 'Becker, W.F. Bergfeld, D.V. Belsito, R.A. Hill, C.D. Klaassen, D. Liebler, J.G. Marks Jr, R.C. Shank, T.J. Slaga, P.W. Snyder, Safety assessment of alkyl benzoates as used in cosmetics, Int. J. Toxicol.,, 31 (2012) 342S-372S.

[75] D. Sen, Esters, terpenes and flavours: Make the mood cheers by three musketeers, World J. Pharm. Res.,, 4 (2015) 01-40.

[76] S.G. Khokarale, J.-P. Mikkola, Efficient and catalyst free synthesis of acrylic plastic precursors: methyl propionate and methyl methacrylate synthesis through reversible CO_2 capture, Green Chem., 21 (2019) 2138-2147.

[77] S. Diab, D.I. Gerogiorgis, Process modelling, simulation and technoeconomic optimisation for continuous pharmaceutical manufacturing of (S)-warfarin, Comput. Aided Chem. Eng., Elsevier2018, pp. 1643-1648.

[78] Y. Tashiro, S.H. Desai, S. Atsumi, Two-dimensional isobutyl acetate production pathways to improve carbon yield, Nat. Commun., 6 (2015) 1-9.

[79] G. Krishna, T.H. Min, G. Rangaiah, Modeling and analysis of novel reactive HiGee distillation, Comput. Aided Chem. Eng., Elsevier2012, pp. 1201-1205.

[80] I. Brinkmann, C. Müller-Goymann, Role of isopropyl myristate, isopropyl alcohol and a combination of both in hydrocortisone permeation across the human stratum corneum, Skin Pharmacol Physiol, 16 (2003) 393-404.

Chapter 2

Literature review of defined/ discrete palladium catalytic systems applied in the methoxycarbonylation/hydroesterification catalysis reactions.

2.1 Introduction

Methoxycarbonylation forms part of the most important industrial catalytic processes. Therefore, methoxycarbonylation has been given much attention in the past decades [1, 2]. Indeed, apart from hydroformylation and other related olefin functionalization reactions [3-5], alkoxycarbonylation catalysis forms the next biggest industrial process when it comes to homogeneous catalysis [6]. Even though other metals like ruthenium have been used in methoxycarbonylation reactions, palladium has so far been preferred since it has high stability, catalytic activity and mild reaction conditions tolerance [7, 8]. However, most of the methoxycarbonylation reports presented over the years utilize the *in situ* generated catalysts [9-30].

Different classes of ligands have been applied in the presence of various palladium precursors to generate active catalysts in the methoxycarbonylation reactions. In the *in situ* generated catalyst systems, an acid promoter, either Lewis or Brønsted acid, a ligand and palladium salts such as $Pd(dba)_2$, $Pd(OAc)_2$, and $PdCl_2$ are used to transform a substrate into the desired ester product. One drawback of the *insitu* generated catalysts is that it is difficult to understand the coordination environment of the catalyst and, by extension, the true nature of the active species. It has been well documented that by carefully designing the ligand networks, a chemist possesses a powerful tool in controlling activities and selectivities [24, 31, 32], two of the most

important value addition aspects in catalysis. Such control can better be achieved through the synthesis of the complex or '*ex-situ*'. Besides, it has also been reported that a presynthesized catalyst can display superior catalytic activity to the corresponding *insitu* generated catalyst in the methoxycarbonylation reactions [33].

As a common practice, palladium catalysts derived from phosphorus have been the mainstay in the methoxycarbonylation reactions. However, in the search for more stable and impurity tolerance, other systems like nitrogen-phosphine, nitrogen-nitrogen and other mixed donor systems have been explored. This chapter, therefore, explores palladium metal complexes applied over the years in the methoxycarbonylation catalytic reactions. While various palladium donor atom systems are explored, attention has been paid to the exhibited catalytic activities and regiocontrol. Various catalyst designs such as P^P donor, P^N donor, P^O donor, N^N donor, tridentate mixed donor systems, and immobilized systems have all been explored in this chapter. In addition to reviewing active homogeneous and heterogeneous systems, this chapter also entails the products of effort to go greener in the industrial processes by reviewing systems that allow for recycling and reuse of catalysts.

2.2 Homogeneous palladium(II) systems applied in methoxycarbonylation catalysis reactions

2.2.1 P^P donor-based palladium(II) catalysts

Traditionally, methoxycarbonylation reactions have been done using P^P donor complexes. In one of such reports, Zolezzi *et al.* gave an account of methoxycarbonylation as catalysed by P^P palladium(II) complexes bearing naphthyl(diphenyl)phosphine derived ligands [34]. The activity of these complexes was found to slightly depend on their structure (Figure 2.1). For

instance, while complex **1** gives a conversion of 97% of styrene to ester products, complex **2** displays a slightly lower conversion of 93%. However, such a change in design does not present with alterations in the product distribution as both catalysts selectively give branched ester products of 93% and 92%, respectively. The catalysts show varied activities towards different substrates. For instance, while the use of complex **2** results in conversions of 93% of styrene to the ester products, the same catalysts only gives moderate catalytic activities of 40% to 61% using cyclohexene, α-methylstyrene and n-hexene substrates.
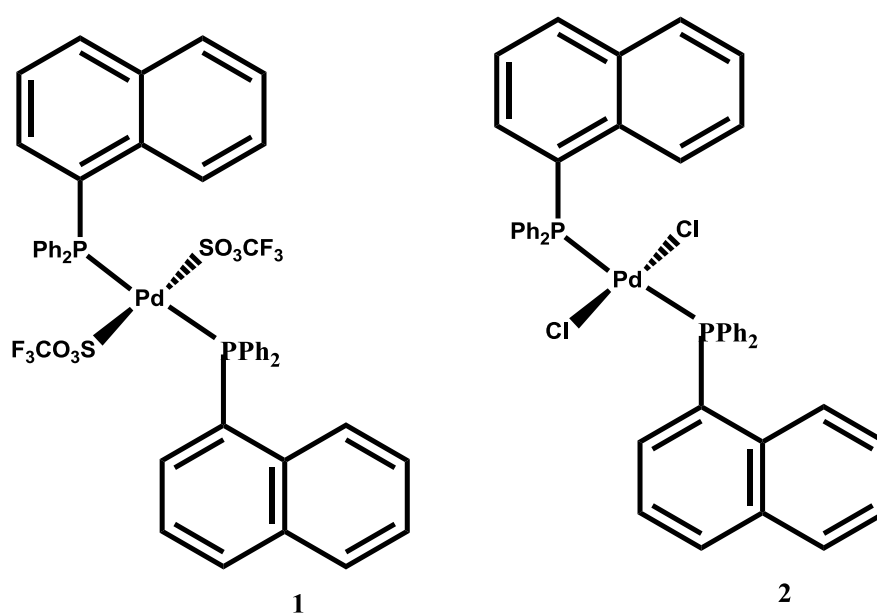
Figure 2.1: The P^P donor palladium(II) systems reported by Zolezzi *et al*. in the methoxycarbonylation of olefins [34].

De la Fuente *et al*. reported in their work the methoxycarbonylation of ethene using phosphine donor carbocyclic ligands of *cis*-1, 2- bis (di-tertbutyl-phosphinomethyl) [35]. The catalytic behaviour depends on the length of the carbocyclic backbone. For instance, the three, four and six-membered ring palladium(II) complexes **4**, **5** and **6** (Figure 2.2) respectively display a superior catalytic activity to the palladium catalyst derived from **3**, a ligand containing a six-

membered ring, with only the double bonds making it be different from **6**. The three complexes similarly exhibit higher catalytic activities superior to complex derived from **7** [35].
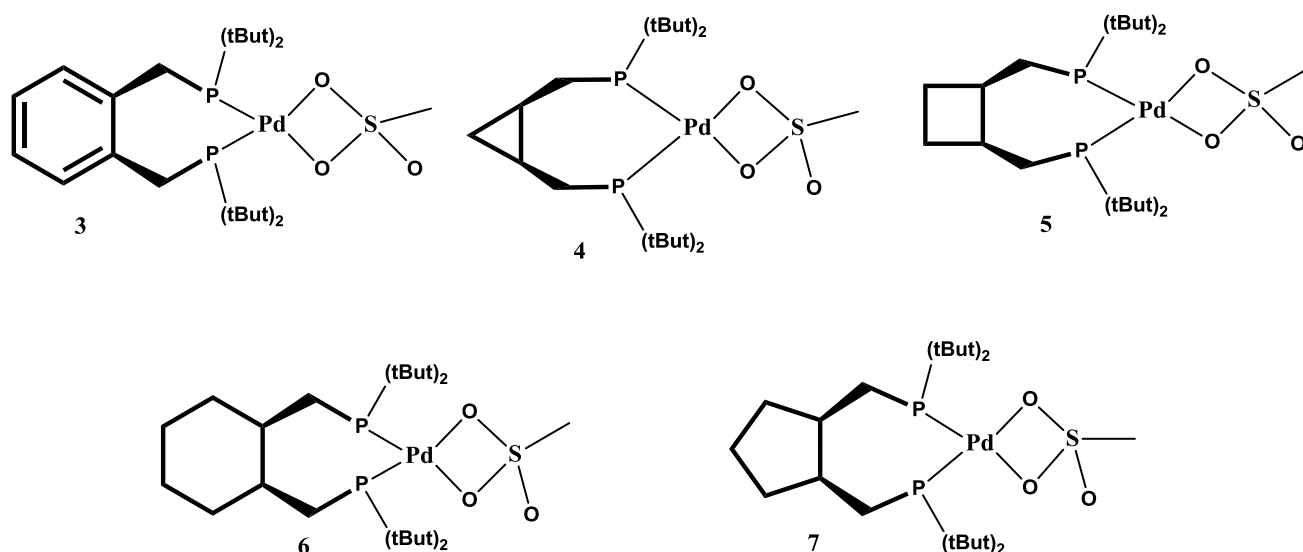
Figure 2.2: P^P- donor systems applied by de la Fuente *et al*. in the methoxycarbonylation of ethane [35].

Another system was reported by Bianchini *et al.* [36, 37]. The phosphine donor palladium(II) complexes were anchored on 1, 1-bis (diphenylphosphino) ruthenocene (dppr), 1, 1-bis (diphenylphosphino)osmocene (dppo), 1, 1-bis (diphenylphosphino) ferrocene (dppf), and 1, 1-bis(diphenylphosphino) octamethylferrocene (dppomf) ligands (Figure 2. 3). Using TsOH as the acid promoter, the 1, 1-bis (diphenylphosphino) metallocene palladium (II) complexes form active catalysts in the methoxycarbonylation of styrene. The catalytic activities were found to be influenced by the complex coordination nature; to demonstrate this, complex **11** exhibits the highest TOF of 334. Another factor that influences the catalytic activities of these systems is temperature variations. The catalysts are also predominantly selective towards methyl 3-phenylpropionate, the linear ester isomer with 77% to 84% observed. Variations made to the

metallocene metal Os, Fe, and Ru and replacing the cyclopentadienyl ligands with methyl cyclopentadienyl ligands do not have a substantial effect on regioselectivity or chemoselectivity.
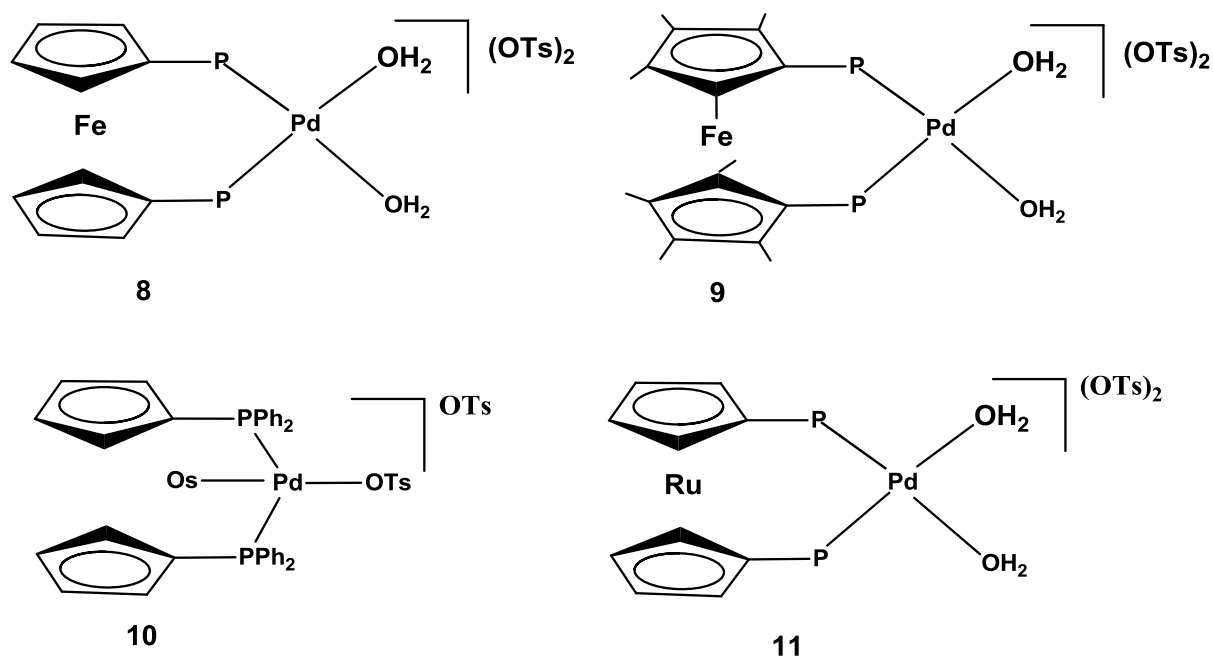
Figure 2.3: The P^P donor palladium systems applied by Bianchini *et al.* in the methoxycarbonylation of styrene [36-37].

The next P^P donor mononuclear palladium and dinuclear palladium system were investigated by Konrad *et al.* [38] in styrene methoxycarbonylation (Figure 2.4). These systems show a range of catalytic activities, with a low yield of 3% observed in the catalysis using complex **12** after 3 hours. Higher reaction times were necessary for the improvement of activities as the same catalyst gives 95% of the ester products after a 42 hrs reaction. The coordination chemistry of this set of complexes seems to control the activities as dinuclear catalysts display

superior yields. For instance, while complex **12** gives a yield of 95%, the dinuclear complex **14** bearing the same ligand network affords >99% within 42 hrs [38], showing the superiority of a double metal centre. One of the best regioselectivities achieved by this system is 90% in favour of the linear products, with complexes having greater steric hindrance around the metal centre favouring more of the linear products [39]. Modification of complex **15** by changing the PAr$_2$ group from 3,5-(Me$_2$C$_6$H$_3$) to 3,5-(CF$_3$)$_2$C$_6$H$_3$ triggers a dramatic change of regioselectivity from 36% to the formation branched ester product as the sole product [39].

Ar = Ph, 12
Ar= 3,5-(Me$_2$C$_6$H$_3$), 13

Ar= Ph, 14
Ar= 3,5-(Me$_2$C$_6$H$_3$), 15
Ar= 3,5-(CF$_3$)$_2$C$_6$H$_3$), 16
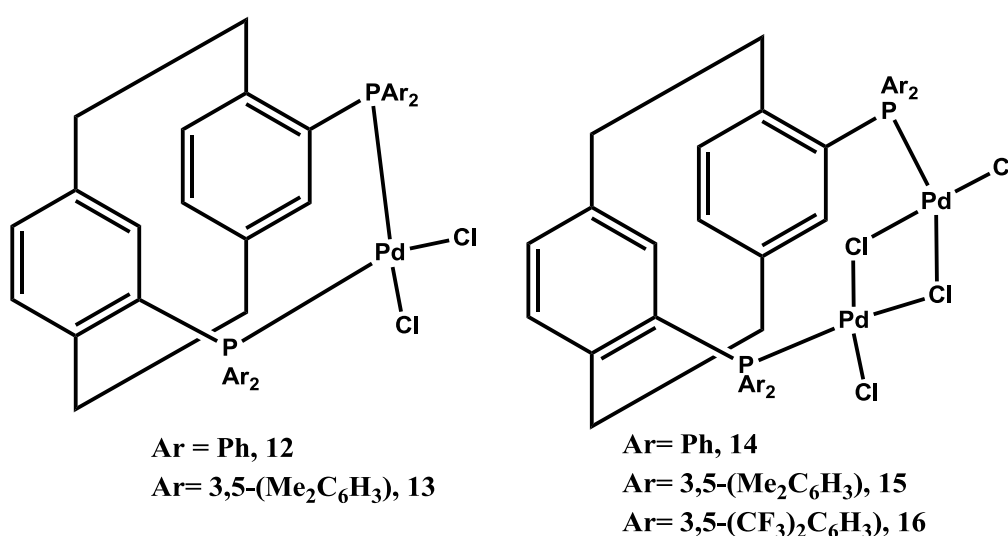
Figure 2.4: P^P donor mononuclear palladium and dinuclear palladium system reported by Konrad *et al* [38-39].

In yet another report, the use of palladium(II) system anchored on anthracene moiety show efficacy in catalysing the methoxycarbonylation of several aryl bromides and aryl iodides (Figure 2.5). The activity exhibited largely depend on the group connected to the substrate's aryl ring. For instance, the electron-rich methoxy and methyl-substituted iodides and bromides give corresponding esters (yields of 85-98%) in superior quantity to the electron-poor substrates bearing groups such as nitro, cyano, keto (yield of 72-86%) [33]. Such an

observation can be attributed to better coordination of the electron-rich substrates to the catalyst centre. However, the electronic nature of the substrates has no bearing on the selectivity [33].

R^1= R^2= Bu^t, X= H, **19**
R^1= R^2= Bu^t, X= NO$_2$, **20**
R^1= R^2= Bu^t, X= OMe, **21**
R^1= R^2= Pr^i, X= H, **22**
R^1= R^2= Cy, X= H, **23**
R^1= R^2= Ph, X= H, **24**
R^1= Bu^t, R^2= Cy, X= H, **25**
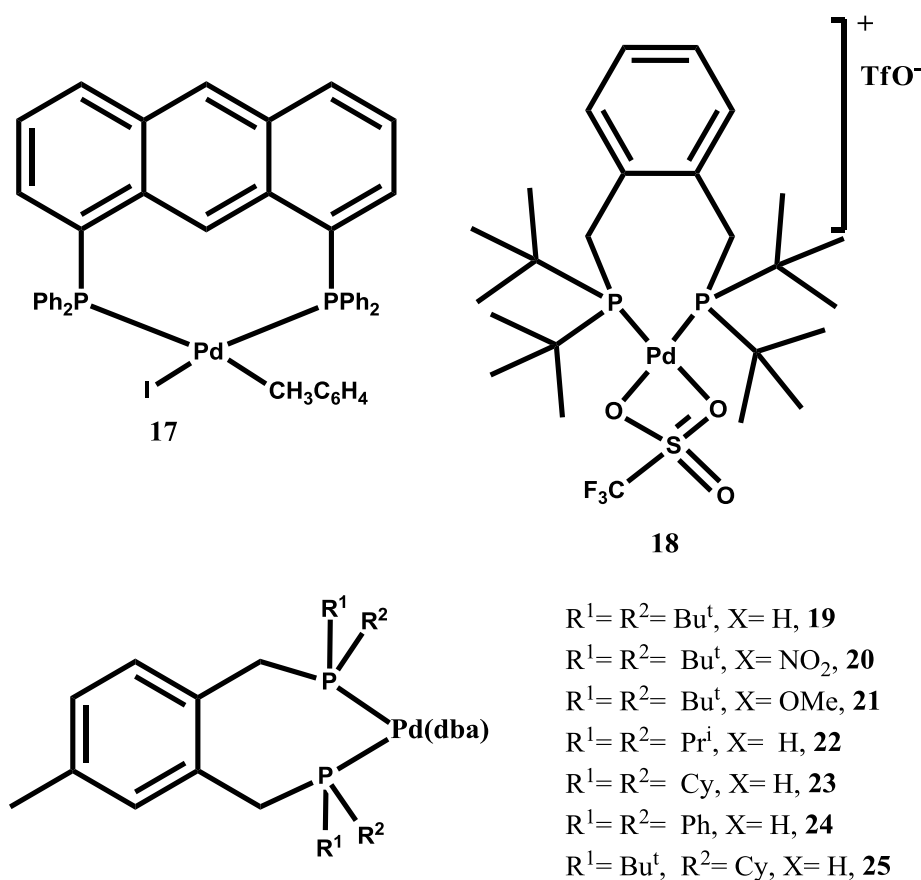
Figure 2.5: P^P donor palladium systems used by various researchers in methoxycarbonylation [40].

One of the rare reports to have discussed the *in-situ* versus *ex-situ* issue is work done by Mecking and co-workers. They applied both *insitu* generated and *ex-situ* synthesized forms of palladium complex **18** (Figure 2.5) in the isomerized methoxycarbonylation of methyl oleate to α,ω-diester [40]. While the defined *ex-situ* generated complex affords a conversion of 80%, the *in-situ* generated counterpart gives a mere 50%. An observation that the researchers do not explain.

Dibenzylideneacetone based palladium P^P donor systems have also been applied in the methoxycarbonylation of ethene (Figure 2.5). These complexes show exceptional catalytic activities. Complexes **19** leads to the conversion of up to 12000 moles of ethene per hour to the ester product. The ligand structure controls both activity and chemoselectivity. For instance, changing the R groups from tert butyl to the isopropyl significantly leads to a drop in the amount of converted ethene, 12000 moles and 200 moles, respectively. While complexes **19**-**21** give >99% chemoselectivity, complexes **22**-**25** exhibit a significant drop to 20-30% with other products such as polymers and polyketone oligomers observed, pointing to the delicate act of simultaneous control of both catalytic activity, chemoselectivity and regioselectivity.

Doherty *et al.* used a palladium system based on the ethano-anthracene ligand in the methoxycarbonylation of ethylene. Using complex **26** (Figure 2.6) in the methoxycarbonylation of ethylene produces 7300 moles of methyl propanoate within an hour of reaction with the production polyketones and polymers also observed [41].
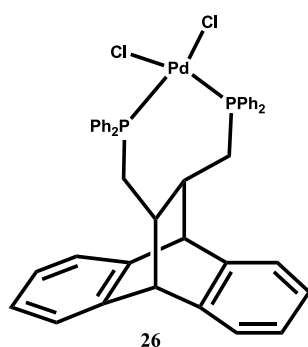
Figure 2.6: Tetramethylphospholylmethyl)-9,10-dihydro-9,10-ethanoanthracene}PdCl2] used by Doherty *et al.* in the methoxycarbonylation of ethylene [41].

In one of the few reports on palladium systems possessing osmocene ligands, Gusev *et al.* demonstrated that the [Pd(OTs)(dppo)]- OTs complex **27** (Figure 2.7) catalyses the methoxycarbonylation of both styrene and ethylene. The complex shows TOFs of 402 and 44 in the formation of methyl propanoate and methyl-3-phenylpropanoate, respectively [42].

27
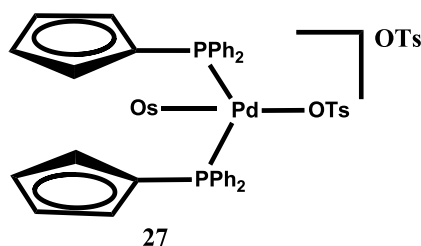
Figure 2.7: Palladium system of the nature [Pd(OTs)(dppo)]- OTs used by Gusev *et al.* in the methoxycarbonylation of styrene and ethylene [42].

Another palladium(II) system bearing diphenylphosphinecyrhetrene ligand system was also applied in the methoxycarbonylation of styrene (Figure 2.8). Complex **28** exhibits low to high catalytic activities depending on the reaction conditions (14-100%), with excellent chemoselectivities. The best conversion (100%) is obtained by using tenfold HCl with respect to the complex, a gas pressure of 50 bar, and at 75 °C [43]. By adjusting the reaction conditions, the complex is capable of 98% regioselectivity in favour of the branched ester product.

28
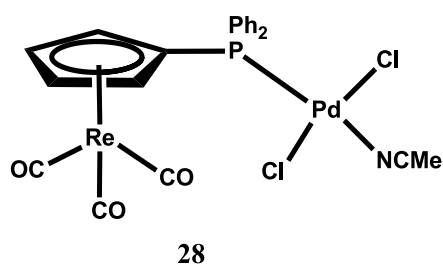
Figure 2.8: Dephenylphosphinecyrhetrene palladium system used by Zuniga *et al* [43].

A possible effect of diphosphines on the regioselectivity in methoxycarbonylation of styrene prompted Guiu *et al.* to apply a range of diphosphine palladium systems (Figure 2.9) in the methoxycarbonylation of styrene. Complex **30** show a good catalytic activity, giving a TOF of 834 h^{-1}. Similarly, the same catalyst shows enhanced regioselectivity, favouring the formation of 74% branched ester product [44]. The regiocontrol of this set of precatalysts is also impacted by the ligands electronic nature. For instance, while complexes **29** and **30** have near similar steric properties, they afford 23 and 74% of the branched ester product, respectively, pointing to regioselectivity not only depending on the obvious steric properties but also electronic properties. A plausible explanation for the phenomenon is that since complex **29** is electron poorer, it may form palladium alkoxy carbonyl moiety, which has been shown to direct olefins substrate insertion to the branched ester compounds.
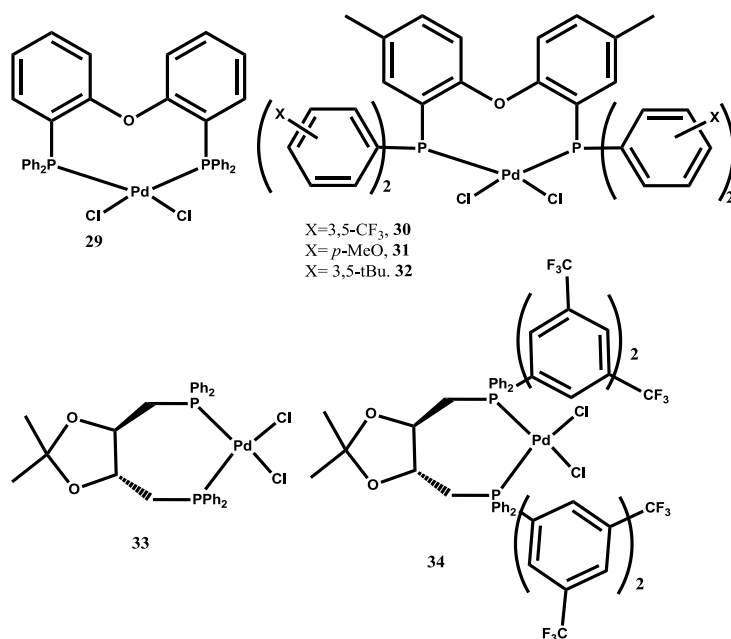
Figure 2.9: Palladium systems based on DPEphos ligands family applied in the methoxycarbonylation of styrene by Guiu *et al* [44].

The palladium phosphine donor systems in Figure 2.10 convert styrene to the ester products with appreciable activity. While **35** gives a yield of 88%, **36** performs slightly better, giving a yield of 98% under the same reaction conditions [45]—the complexes favour over 99% formation of the branched ester products. Complex **36** also shows appreciable catalytic activities in the conversion of styrene to respective ester products using i-PrOH alcohol and tert-butyl alcohol, giving yields of 96 and 48%, respectively.

35 **36**
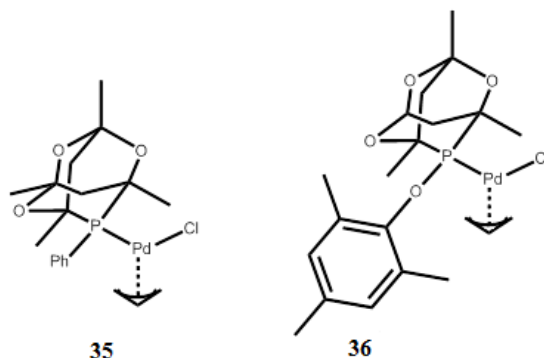
Figure 2.10: Palladium (trioxo-adamantyl cage phosphine) chloride complexes used in alkoxycarbonylation of styrene by Fuentes *et al* [45].

Modified P^P donor mononuclear palladium and dinuclear palladium system [38, 39] forms Flurbiprofen methyl ester through a methoxycarbonylation process (Figure 2.11). While all the complexes show activities towards the ester product formation, complex **37** shows the highest catalytic activity, forming >99 % ester product within 17 hours [46]. The complexes all show a range of regioselectivities, with complexes **38** and **41** giving up to over 99% of the branched products

Ar = 3,5- (xylyl), **37**
Ar= 3,5-(CF$_3$)$_2$C$_6$H$_3$, **38**
Ar= 3,5-Cl$_2$C$_6$H$_3$, **39**

Ar = 3,5- (xylyl), **40**
Ar= 3,5-(CF$_3$)$_2$C$_6$H$_3$, **41**
Ar= 3,5-Cl$_2$C$_6$H$_3$, **42**
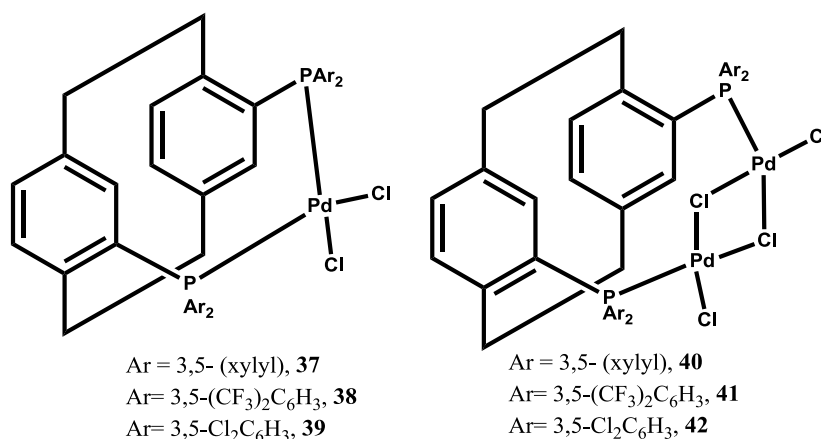
Figure 2.11: Palladium Phanephos systems applied in the methoxycarbonylation of vinyl arenes [46]

TROPP ligand based palladium(II) complexes display low to high catalytic activities in the methoxycarbonylation of various alkyne substrates (Figure 2.12). Complex **45** show the best catalytic activity (TOF of 960 h^{-1}) among these group of palladium complexes in the methoxycarbonylation of 4-tolylacetylene. Besides, the same complex exclusively gives the branched ester product. Complex **46** shows a slightly diminished activity (TOF 920 h^{-1}) [47], likely due to steric factors. However, this contribution does not report the results for the other four complexes, which could have been interesting, especially with the rest of the complexes coming in with completely different electronic properties.

R=Ph, **43**
R= 2-MeOPh, **44**

R= Ph, **45**
R= 2-MeOPh, **46**

R= Ph, **47**
R= 2-MeOPh, **48**
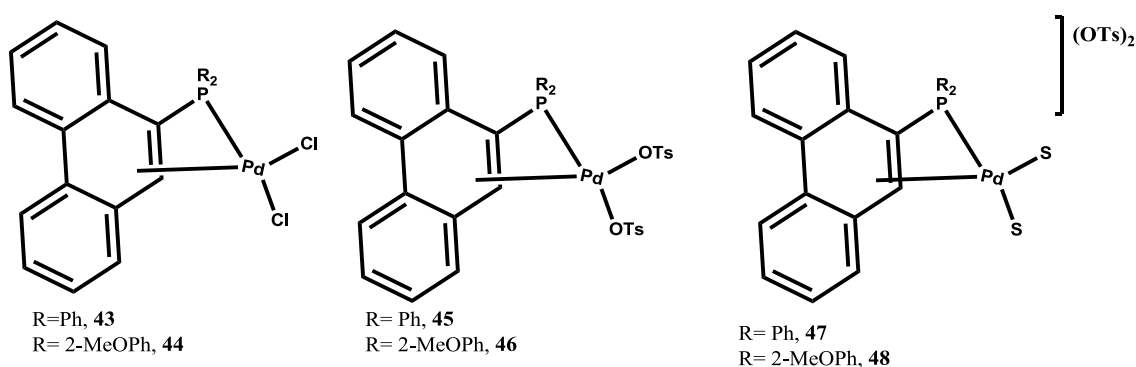
Figure 2.12: TROPP ligand based palladium complexes used in the methoxycarbonylation of terminal alkynes [47]

Palladium(II) complexes containing 1,1′-Bis(diphenylphosphino)ferrocenes ligands converts ethene to methyl propanoate as the major product in a methoxycarbonylation reaction. Under the same reaction conditions, complex **51** (Figure 2.13) gives the best yield of methyl propanoate (a TON of 1618) [48]. A similar complex **49**, except for the coordination environment, gives a slightly lower activity (a TON of 1378), showing the notable effects of the substituents on the ferrocene ring.
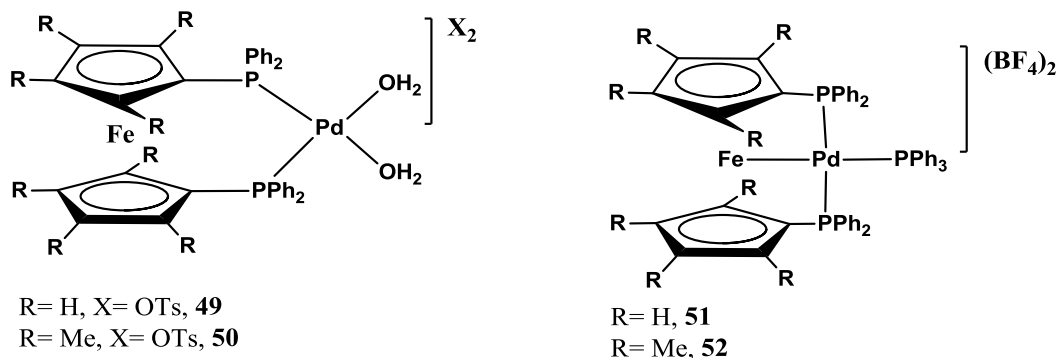
Figure 2.13: Palladium(II) Complexes bearing 1,1'-Bis(diphenylphosphino)ferrocenes ligands applied in methoxycarbonylation of ethane [48]

Palladium complexes bearing diphosphine ligands (Figure 2.14) convert methyl oleate to diesters with yields ranging from low to high (18-98%). The observed catalytic activities are largely controlled by the steric encumbrance of the ligand moieties attached to the phosphorus atoms. The researchers made a rather unusual observation of more sterically hindered complexes giving better activities, a reverse of observations elsewhere [49], pointing to the activity being influenced by other factors such as the electronic nature of the ligands groups attached to the donor atom. Regioselectivity is also controlled by steric hindrance, with more sterically hindered complexes yielding more of the branched ester products [48]. For instance, the most sterically hindered complex **53** gives the highest quantity of the branched ester products (30%).
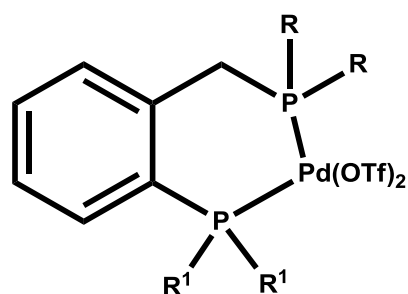
R= tBu, R¹= tBu, **53**   R= Ad, R¹= Cy, **57**
R= tBu, R¹= Cy, **54**   R= Cy, R¹= Cy, **58**
R= tBu, R¹= iPr, **55**   R= Ad, R¹= Ad, **59**
R= Ad, R¹= tBu, **56**

Figure 2.14: Palladium(II) complexes bearing diphosphine ligands used in the methoxycarbonylation of methyl oleate [49]

2.2.2 N^P donor palladium(II) catalysts

Apart from the P^P donor systems, the bidentate heteroatomic P^N donor systems are another group having great potential and use in a range of catalytic transformations, methoxycarbonylation included. One of such systems has been applied in the methoxycarbonylation of styrene by Abarca *et al.* [50]. The palladium(II) complexes with ligand frameworks of 2-diphenylphosphinoaniline (Ph$_2$Pan) and (2-diphenylphosphino) pyrimidine (Ph$_2$PNHpym), and N,2-bis(diphenylphosphino)benzeneamine (Ph$_2$PNHC$_6$H$_4$PPh$_2$) show a range of catalytic behaviour that is largely influenced by their structures (Figure 2.15).
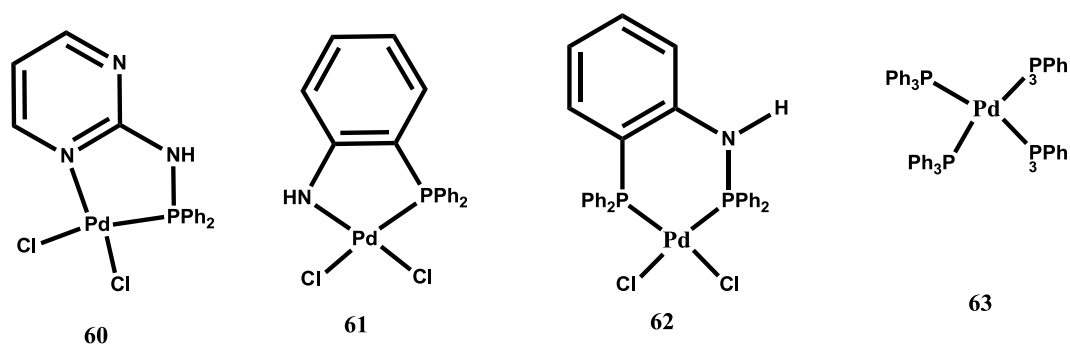
Figure 2.15: P^N donor palladium (II) systems applied by Abarca *et al.* in the methoxycarbonylation of styrene [50]

Using similar reaction conditions, complexes **60** and **61** afford moderate conversions of 48 and 46%, respectively, in the methoxycarbonylation of styrene in the absence of a phosphine stabilizer. Comparatively, adding equimolar quantities of ligand or PPh_3 leads to improved conversions. While the addition of $Ph_2PNHpym$ ligand to complex **60** affords an improved conversion of 78%, the addition of one equivalent of PPh_3 results in even a far much better conversion of 99% within 6 h, underpinning the need for phosphine stabilizer in the methoxycarbonylation reactions. The selectivities of the complexes similarly hinge on the identity of the complexes' structures and the reaction conditions. For instance, while complexes **60** and **61** respectively give chemoselectivities of 71 and 75% and regioselectivities of 75 and 82% towards the branched ester product without PPh_3, adding PPh_3 remarkably improve both chemoselectivity and regioselectivity to 99 and 92% and 92 and 96%, respectively. Even though the four complexes show remarkable selectivities in the methoxycarbonylation of styrene, complex **60** posts better results than the other complexes; such an observation has been implicated on complexes **60,** having the pyridine group [50].

Another mixed P, N donor palladium(II) complexes have been applied by Aguirre *et al*. in the methoxycarbonylation of various olefins [51]. Similar to the observation of Abarca and the group, the catalytic behaviour of these set of complexes are heavily influenced by the complex structure. While the use of complex **64** (Figure 2.18) without the addition of triphenylphosphine ligand yields a meagre conversion of 14%, the addition of one and two equivalents of triphenylphosphine relative to the palladium catalyst dramatically increase the conversions to 99 and 97%, respectively. The addition of the one and two equivalents of phosphine promoter also varies the selectivity from 75% to 92 and 89% of the branched product, respectively. Under similar conditions, complexes **66** and **67** (Figure 2.16) show far much inferior activities of 28 and 9%. Attempts to replace the 2-(diphenylphosphino)quinoline (Ph$_2$Pqn) in complex **67** with either 2-(diphenylphosphinoaminomethyl) pyridine (Ph$_2$PNMepy) or (diphenylphosphino), phenylamine (Ph$_2$PNHPh) further lowers the catalytic activities of the catalysts, highlighting that both the NH and the pyridine groups are important if higher catalytic activities are to be obtained in these set of complex design [51]. The complexes also give different activities in the methoxycarbonylation of various substrates. For example, while complex **64** affords 99% conversion of styrene to the ester products, it converts only 43 and 19% of 1-hexene and cyclohexene, respectively, to the expected ester products in 24 h [51].
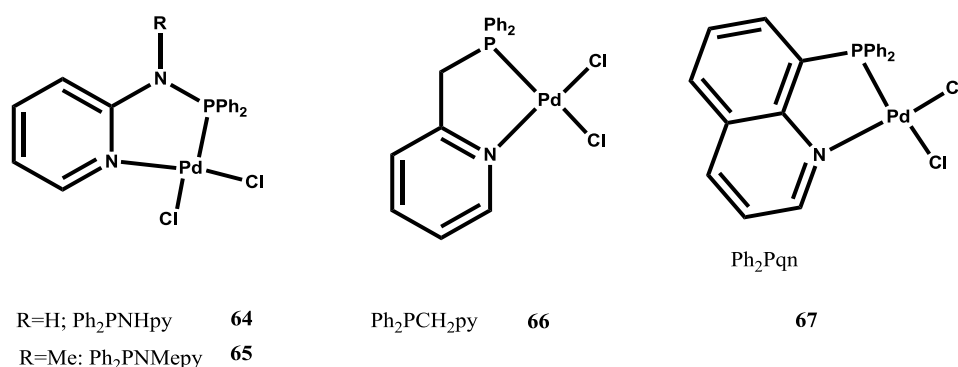
Figure 2.16: P^N donor palladium (II) systems used by Aguirre *et al*. in the methoxycarbonylation of olefins [51].

2.2.3 N^N donor palladium(II) catalysts

Recently, Zulu *et al.* reported N^N donor palladium(II) complexes bearing pyridyl imine ligands with pendant arms in the methoxycarbonylation of 1-hexene (Figure 2.17). The nature of the precatalysts largely impacts the catalytic behaviour of the complexes. For example, changing the nature of complex **68** by replacing a chloride ligand with methyl to form **69** only leads to a dip in conversion from 91 to 62%, an observation connected to the electron-donating behaviour of the CH_3 moiety. The pendant donor groups also controlled the observed activities, for instance, complex **70**, having an OH group as the pendant donor displays an inferior conversion of 58% as compared to complex **68** (91%), having a methoxy group at the same position [52]. The hemilabile nature of the methoxy group allows for easier substrate coordination as well as stabilization of the active intermediate, hence a superior activity. The structure of the complexes, however, do not have a notable effect on the regioselectivity as the steric encumbrance around the metal centres is the same due to the remote location of the pendant donor atoms.

37
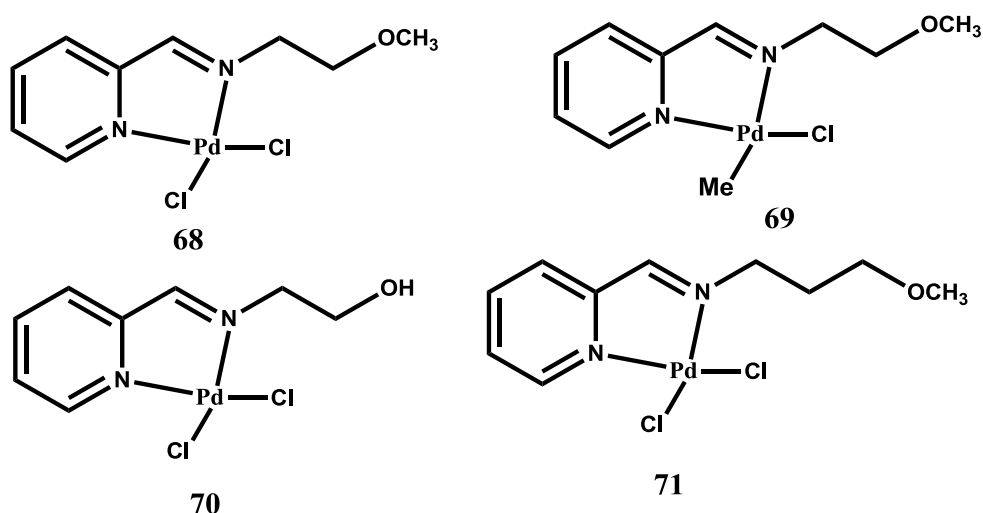
Figure 2.17: N^N donor palladium (II) systems used by Zulu *et al*. in the methoxycarbonylation of olefins [52].

Another N^N donor palladium(II) system has been reported by Alam *et al.* [53]. Bearing (pyrazolylmethyl) pyridine ligands, the coordination atmosphere of these palladium(II) complexes is the main factor behind observed varied catalytic behaviours. For example, the substituents of the pyrazolyl ring dictate the catalytic activity observed. Replacing the CH_3 substituent with a phenyl improves the activity from the conversion of 63 to 77% (Figure 2.18) posted by complex **73** in the methoxycarbonylation of 1-octene to the corresponding ester products. The cationic analogue, complex **74**, gives the least conversion of 47% under the same reaction conditions, an observation attributed to its relative instability [53]. Even though the varying complex design does not have a profound effect on the product distribution, phosphine additive appeared to vastly control the regioselectivity. For example, while complex **72** affords 41% of the branched products in the presence of triphenylphosphine, the branched selectivity increases up to 60% without the phosphine. The increased branched isomer selectivity without the use of PPh_3 is attributed to the lower steric encumbrance around the coordination sphere, thereby enhancing chain migration or isomerization [53].
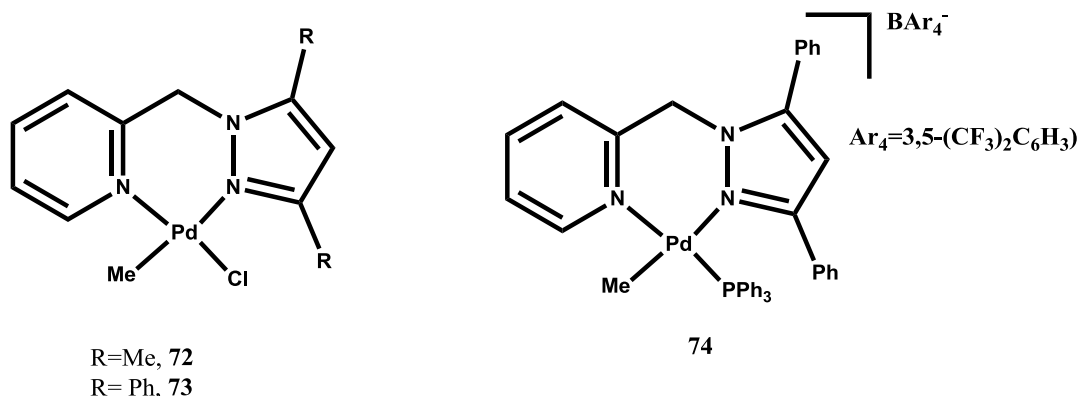
Figure 2.18: (Pyrazolylmethyl) pyridine palladium(II) complexes used by Alam *et al.* in the methoxycarbonylation of different olefins [53].

Tshabalala and Ojwach reported an N^N donor palladium(II) system bearing (benzimidazolylmethyl)amine ligands. By using a range of various internal olefin substrates and phosphine derivatives, these palladium(II) complexes show a range of catalytic activities and selectivities [54]. The compounds' catalytic behaviour was found to heavily hinge on the coordination environment of the metal centre. For instance, modification of complex **76** by replacing the chloro and methyl group with triphenyl phosphine and tosylate ligands to form complex **78** (Figure 2.19) leads to improved catalytic activity. While complex **76** gives a conversion of 39%, complex **78** displays 84% under the same reaction conditions, an observation attributed to the stability of complex **76,** which result from the stabilizing nature of the tolyl and PPh$_3$ groups. The shift in catalyst design from **76** to **78** similarly has a strong influence on regioselectivity. Whereas precatalysts **76** display 60% of the branched products, **78** gives 74% of the branched ester products, a phenomenon attributed to the bulkier OTs and PPh$_3$ ligand hindering the isomerization of the coordinated substrate.
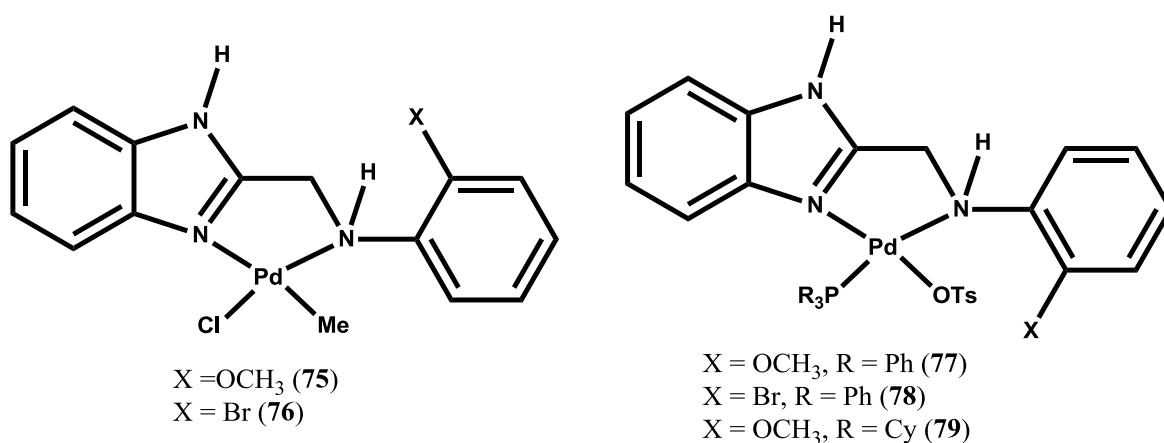
Figure 2.19: (Benzimidazolylemethyl)amine palladium(II) complexes used by Tshabalala and Ojwach in the methoxycarbonylation of the terminal and internal olefins [54].

In the absence of a phosphine stabilizer, palladium(II) bearing *bis*(oxazoline)-phosphine ligands only gives traces of products in the methoxycarbonylation of phenylacetylene. However, the addition of PPh$_3$ dramatically improves the catalytic activities. For instance, complex **80** (Figure 2.20) gives a high activity of 90% in the presence of 2 fold equivalent of PPh$_3$. Under similar reaction conditions, complexes **81** and **82** both give conversions of 99% within 1 hr. Complex **81** further shows moderate activity in conversion of various alkynes to respective ester products; for instance, the complex showed a conversion of 79 and 76% of 4-ethynylbenzaldehyde and 1-decyne, respectively to various ester products [55]. Under the same reaction conditions, both complexes **81** and **82** afford near-complete regioselectivity of 97 and 98% respectively of branched products in the methoxycarbonylation of phenylacetylene.
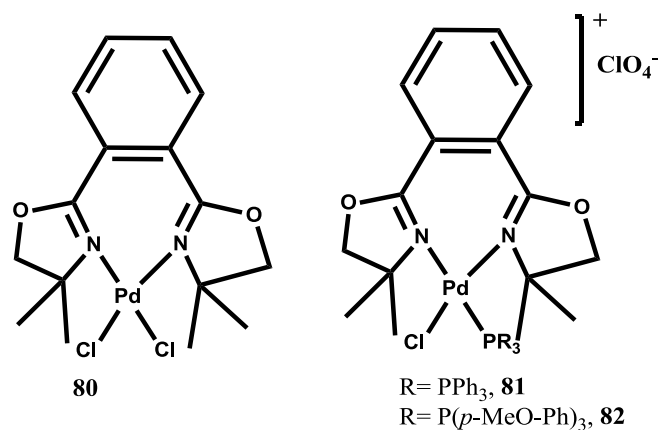
Figure 2.20: Bis(oxazoline)-phosphine palladium system used in the methoxycarbonylation of alkynes Ibrahim *et al* [55].

N^N donor palladium(II) complexes of (pyrazolyl-ethyl)pyridine ligands show a range of catalytic activities in the methoxycarbonylation of higher olefins giving TOFs of 3.9 to 7.6 h^{-1}, under various reaction conditions. The catalytic activities observed are controlled by the nature of the complexes as more sterically hindered complexes gave fewer % conversions [56]. For instance, complex **83** bearing methyl groups gives a conversion of 91% in the methoxycarbonylation of 1-octene, compared to complex **86** bearing Ph groups which give a lower conversion of 84%.

R= Me, X= Cl, **83**
R= Me, X= Me, **84**
R= Ph, X= Me, **85**
R= Ph, X= Cl, **86**
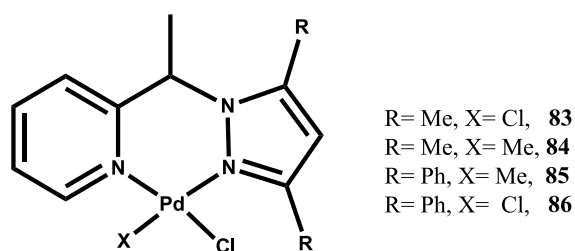
Figure 2.21: (Pyrazolyl-ethyl)pyridine palladium(II) complexes reported by Zulu *et al*. in the methoxycarbonylation of higher olefins [56]

N^N donor pyridinimine palladium catalysts show varied catalytic behaviour in the methoxycarbonylation of styrene to the ester products. The activities shown by this set of complexes are greatly influenced by the steric nature of the alkyl substituent attached to the imine aryl moiety (Figure 2.22). For example, complexes **87** and **88** having CH$_3$ moiety as R$_3$ groups exhibit better yield of 57 and 53% respectively in comparison to similar complexes **89** and **90** bearing isopropyl groups at the same positions (39 and 36%) respectively [57]. Such a behaviour can be due to the possibility of isopropyl groups stabilizing reaction intermediates hence shielding the palladium centre from the substrate, CO and methanol, leading to limited access [58]. Product distribution is influenced by the nature of the group on the imine carbon. For instance, even though all the complexes (except for complex **91,** which is inactive) gave a mixture of products, dimethyl-2,5-diphenyl-4-oxoheptanedioate, methyl-3,6-diphenyl-4-oxohex-5-enoate, methyl-2,6-diphenyl-4-oxohexanoate, dimethyl phenylsuccinate and methyl cinnamate, the complexes bearing H on the imine carbon are more selective towards dimethyl phenylsuccinate, product **E** [57].
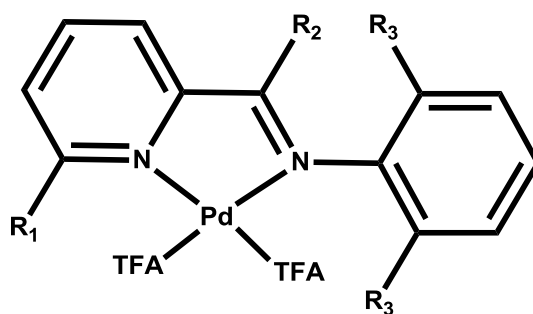
R$_1$= H, R$_2$= H, R$_3$= Me, **87**   R$_1$= H, R$_2$= Me, R$_3$= i-Pr, **90**

R$_1$= H, R$_2$= Me, R$_3$= Me, **88**   R$_1$= Me, R$_2$= H, R$_3$= i-Pr, **91**

R$_1$= H, R$_2$= H, R$_3$= i-Pr, **89**   R$_1$= H, R$_2$= H, R$_3$= H, **92**

Figure 2.22: Pyridinimine palladium(II) catalysts applied in the methoxycarbonylation of styrene [57].

Palladium(II) complexes bearing (benzoimidazol-2-ylmethyl)amine ligands promote methoxycarbonylation of olefins in moderate to high conversions within 24 h. The catalytic activities displayed by the complexes (Figure 2.23) are mainly dependent on their structures. The electronic nature of the R groups influences the conversions observed. For instance, the cationic complex **95** bearing the methoxy group on the ring displays the highest conversion of 86% [59]. By contrast, a similar complex **96** having an electron-withdrawing Br group gives only a conversion of 29%. Such an observation is due to the difference in the stability of the resulting complexes. The electron-withdrawing nature of Br tends to form less stable complexes which have a higher probability of decomposition, thus lower catalytic activity.

R = OCH₃, X = Me , **93**
R = Br, X = Me,   **94**

R = OCH₃, X= Me, **95**
R = Br, X= Me,   **96**
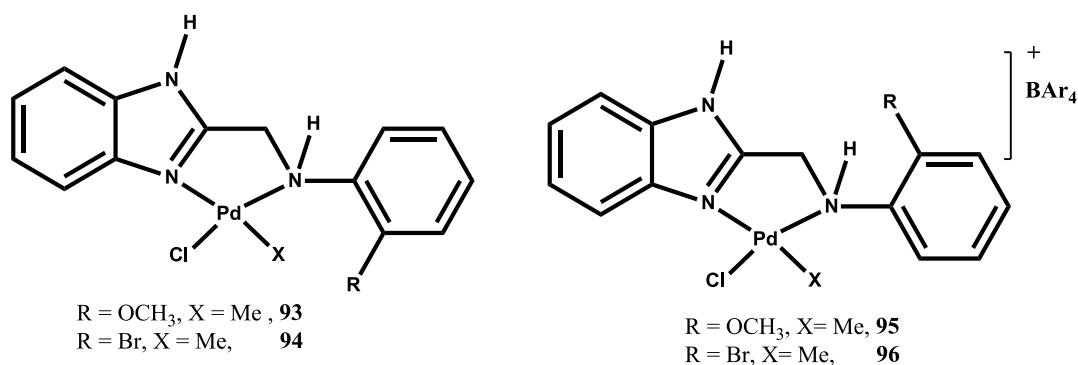
Figure 2.23:(Benzoimidazol-2-ylmethyl)amine palladium(II) complexes used in the methoxycarbonylation of olefins [59]

2.2.4 Other mixed donor systems

While most palladium(II) systems reported in the methoxycarbonylation catalysis are bidentate ligand coordinated systems, there are reports of tridentate systems. Not long ago, Kumar and Darkwa reported palladium complexes bearing mixed N^N^O and N^N^S donor ligands in the methoxycarbonylation of olefins [60]. The catalytic behaviour of this set of complexes is influenced by their structural nature. One of the interesting observations made from this research is that while all the neutral complexes do not give any activity in the absence of phosphine promoter, the cationic complexes display some notable activities. However, it is not surprising since the cationic complexes bear a coordinated phosphine, able to stabilize the active species. Even though there is no clear difference between the catalytic activities of the cationic and neutral complexes, all the catalysts display conversions of 66-96% in the methoxycarbonylation of 1-hexene into the ester products (Figure 2.24). One of the reasons for the wide range of activities observed could be variations of donor atoms, as N^S donors generally display lower activity than the N^N donors. For instance, while complex **98** shows conversion of 95%, complex **102** displays a conversion of 66%.
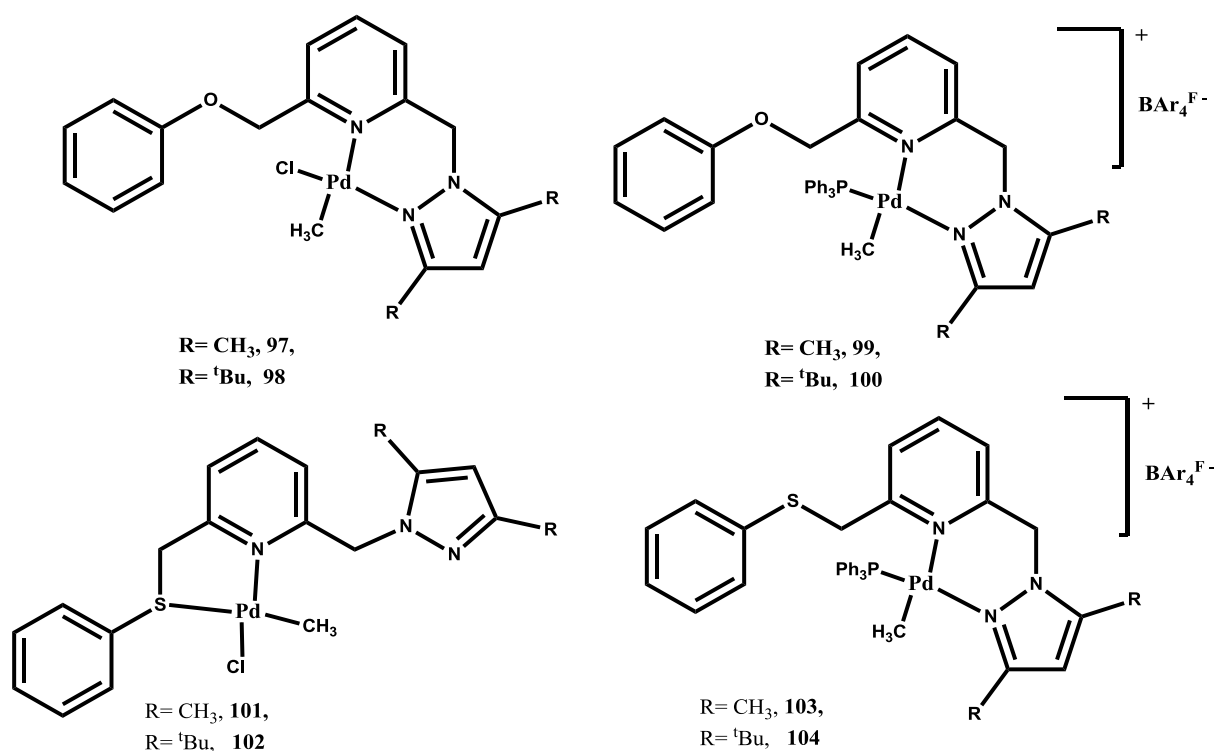
Figure 2.24: Palladium (II) complexes used by Kumar and Darkwa in the methoxycarbonylation of selected 1-alkenes [60].

Recently, we applied mixed N^N and N^O palladium(II) complexes bearing phenoxyimine alkoxysilane ligands in the methoxycarbonylation of a range of olefin substrates. The bischelated complexes **105** and **106** exhibit superior catalytic activities to the monochelated complexes **107** and **108** (Figure 2.25). The observation is largely attributed to better stability of the bischelated complexes hence resisting catalyst decomposition at the reaction temperature. Complexes **105**-**108** yield predominantly linear esters in the methoxycarbonylation of 1-hexene, with 58-67% of linear esters yields observed [61]. The complexes convert alkenes such as 1-heptene, 1-octene, 1-nonene and 1-decene to their respective ester products, with the observed % conversions decreasing with increasing carbon chain length.

R= CH$_3$, X= H, **105**
R= H, X= CH$_3$, **106**

R= CH$_3$, X= H, **107**
R= H, X= CH$_3$, **108**
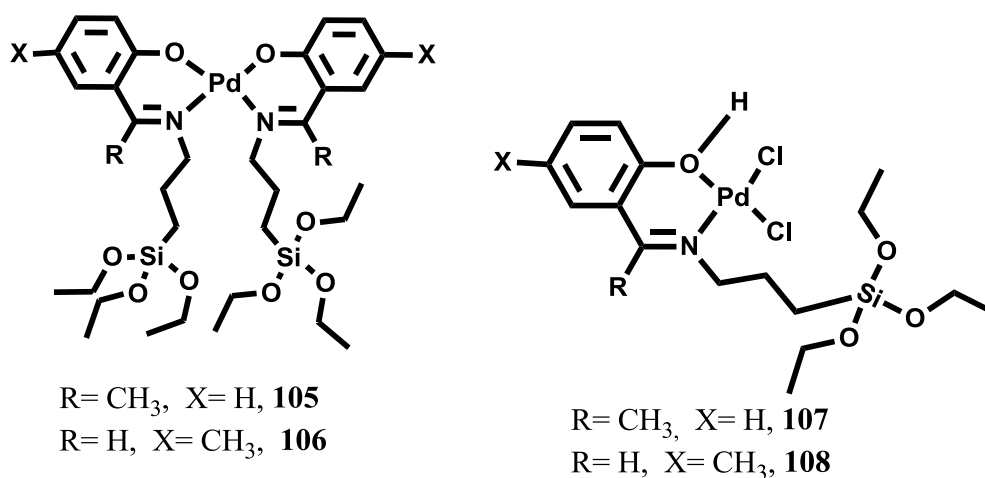
Figure 2.25: Palladium(II) complexes bearing phenoxyimine alkoxysilane ligands used in the methoxycarbonylation of a range of olefin substrates [61].

2.2.5 Immobilized palladium catalysts in the methoxycarbonylation reactions

In present times and past decades, attempts have been made to capitalize on the strengths of both homogeneous catalysts and heterogeneous catalysts to design catalysts that are active, selective and recyclable through the heterogenization process. Even though heterogenized systems have been widely applied in other catalytic transformation reactions, it is glaringly evident that alkoxycarbonylation has just but a handful of reports. It is, therefore, an area that has a tapping potential through the use of biphasic catalysis, using insoluble inorganic supports like silica, magnetic supports and polymer supports. The activities and selectivities on such heterogenized systems can effectively be controlled and improved if the clear and correct structures and coordination chemistry of their homogeneous counterparts are understood through synthesis and characterization before using them for catalysis.

2.2.5.1 Silica supported palladium(II) catalysts

In one of the rare efforts to make homogeneous catalysts recyclable, we have recently reported methoxycarbonylation using palladium(II) complexes bearing phenoxyimine alkoxysilane ligands immobilized on silica (Figure 2.26). Using PTSA as an acid promoter, this set of immobilized complexes display moderate to high catalytic conversions in the methoxycarbonylation of 1-hexene. For instance, under the same reaction conditions, complex **110** displays the highest conversion of 78%, while complex **111** gives the least (59 %). These complexes are recyclable up to four times with little loss in catalytic activities [62].

R= CH$_3$; X= H, **109**
R= H; X= CH$_3$, **110**

R= CH$_3$; X= H, **111**
R= H; X= CH$_3$, **112**
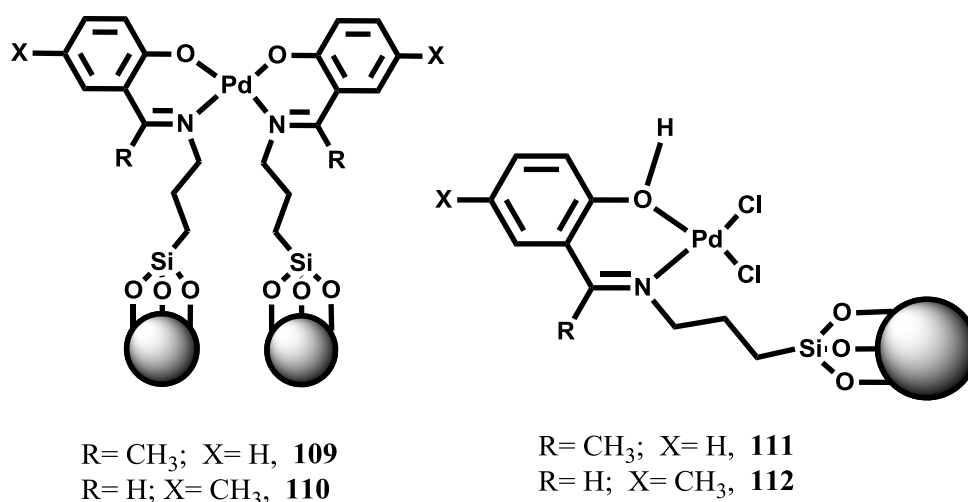
Figure 2.26: Palladium(II) complexes bearing phenoxyimine alkoxysilane ligands immobilized on silica [62].

Another silica-supported palladium catalyst shows catalyst activities in the methoxycarbonylation of various substrates. While all the immobilized complexes show activities in the methoxycarbonylation of 1-decene, complex **114** shows the highest conversion of 82% of 1-decene to the ester products, with optimized quantities of PPh$_3$ and acid promoters of 25 and 35, respectively, relative to the metal content loading. Complexes **113**-**116** (Figure 2.27) also yield predominantly linear esters in the methoxycarbonylation of all screened

substrates such as styrene, *o*-methylstyrene, *p*-chlorostyrene, 1-decene, 1-octene, and 1-hexene, with the steric factors the major determinant [63]. For example, complex **114** affords 78 and 69% of linear ester products in the methoxycarbonylation of 1-decene and styrene, respectively. Complex **114** is also recyclable and has been reused up to five times in the methoxycarbonylation of 1-decene.
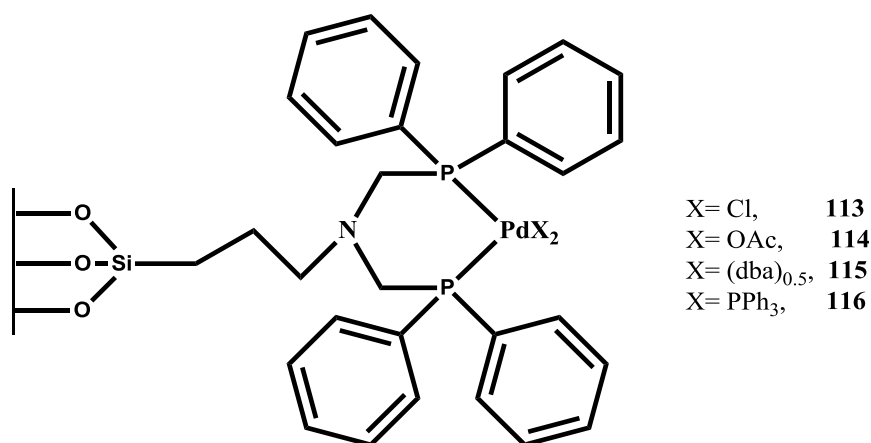
Figure 2.27: Palladium-Complexed PAMAM Dendrimers Immobilized on Silica used in the methoxycarbonylation of 1-decene [63].

Silica supported palladium catalysts of (2-diphenylphosphinoethyl functionalized silica) of the nature $PdCl_2\_PPh_2Et@SiO_2$ (**117**) and Pd $(OAc)_2\_PPh_2Et@SiO_2$ (**118**) transform a range of aryl iodides to ester products [64]. Complexes **117** and **118** show a range of catalytic activities under various reaction conditions. Complex **117** and **118** give a yield of 99 and 92% respectively in the methoxycarbonylation of iodobenzene to the ester products. Reaction aspects like solvent, temperature, gas pressure and catalyst loading all influence the catalytic behaviour displayed by the supported complexes. While a methanol and trimethylamine system gives the best yield of 99%, the optimum CO pressure is 0.5 MPa. Besides, the optimum catalyst loading is 0.6 mol% [64].

2.2.5.2 Polymer supported palladium(II) catalysts

Apart from silica-supported catalysts, polymer-supported palladium catalysts have also been used in methoxycarbonylation. Homogeneous catalysts heterogenized on polymer support from active catalysts in the methoxycarbonylation of acetylene (Figure 2.28). Interestingly, the catalysts supported on porous 2-vinyl-functional diphenyl-2 pyridylphosphine (2V-P, N) polymer (POL-2V-P, N) exhibit superior catalytic activity (TOF of 2983.3 h^{-1}) in comparison to the homogeneous derivative (TOF of 1238.8 h^{-1}) [65]. Complex **119** show a range of catalytic activities under varied catalytic reaction parameters. An interesting result obtained from this research is that the polymer-supported complex **119** shows superior catalytic activity as compared to its non-supported counterpart. Complex **119** is reused up to three cycles.

119
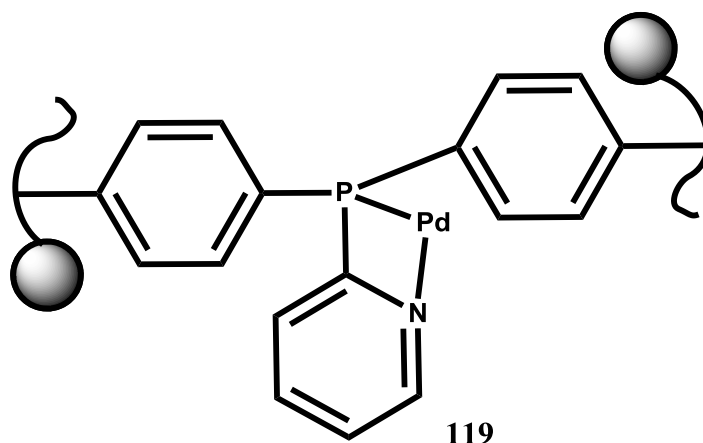
Figure 2.28: Palladium catalysts supported on porous 2-vinyl-functional diphenyl-2 pyridylphosphine (2V-P, N) polymer (POL-2V-P, N) used in the methoxycarbonylation of acetylene [65].

Another polymer-supported palladium catalyst of the nature, Pd/PPh$_3$@POP, catalyses methoxycarbonylation of a range of olefin substrates to yield respective ester products [66]. Using various forms of the catalyst Pd/PPh$_3$@POP possessing different loadings of palladium, a range of catalytic activities is observed. For instance, 0.2Pd/PPh$_3$@POP, 0.5 Pd/PPh$_3$@POP, and 0.7 Pd/PPh$_3$@POP give TOFs of 16, 31 and 36 h^{-1} respectively. Upon optimization of the reaction conditions, 0.7 Pd/PPh$_3$@POP affords an improved catalytic activity of TOF of 70 h^{-1} in the methoxycarbonylation of styrene. The heterogenized catalyst also shows appreciable activities in the methoxycarbonylation of other substrates such as 1-octene, 1-hexene, 4-tertbutylstyrene, 4-methoxystyrene, 4-bromostyrene, 4-chlorostyrene and 4-fluorostyrene [66]. The complex 0.7 Pd/PPh$_3$@POP was recycled through a simple centrifugation process and reused up to four times [66].

2.2.6 Biphasic methoxycarbonylation catalysis

Over the years, the call for green chemistry has led to the development of various catalytic systems which minimize waste, reduce solvent use, and discard the use of harmful chemicals. One of such efforts has been the use of biphasic catalysis. Having been applied successfully on a large scale in the Ruhrchemie/Rhône-Poulenc process in forming butanal from propene [67], biphasic catalysis has since been applied in other important value addition catalytic processes. Even though biphasic catalysis has featured in many of the carbonylation catalytic reactions, methoxycarbonylation has just a handful of reports where one of the phase liquids is water, probably due to the possibility of such reaction going the route of the undesired hydroxycarbonylation. It is also surprising that no reports of "clearly defined catalyst" or the *ex-situ* generated biphasic catalysts have been applied in methoxycarbonylation. This section, therefore, reviews the *insitu* generated catalysts applied in the biphasic methoxycarbonylation reactions

Using an *in situ* generated water-soluble complexes bearing SulfoXantPhos ligands (Figure 2.29), Schmidt *et al.* achieved methoxycarbonylation of 1-dodecene to its ester products in biphasic environments [68]. With water and methanol making the polar phase and the substrate making the non-polar phase, the activities obtained were found to be dependent on the composition of the polar phase. While a reaction containing 5% water gives a conversion of 95% within 20 h, increasing the polarity by adding more water gradually reduces the activity until a complete inhibition at 50% water, a trend resulting from the reduced substrate and CO solubility in the polar phase. By increasing the amount of water, the regioselectivity of the products formed is also significantly affected as more linear products are obtained. For instance, while 68% of the linear ester is exhibited at 5% water, this value increases to 72% with 20% of water in the polar phase [68]. This system is recyclable up to four times. Interestingly the quantity of the produced ester increases with the number of runs; for example, while the first run affords a conversion of 32%, the second run gives 55%, and the fourth run, 70%. The researchers attributed such an observation to the presence of induction period in the first run and lack of the same in subsequent runs. In addition, possible remains of the ester products in the catalyst phase after every run enhance substrate solubility in the phase, thus higher yields in subsequent runs [68].
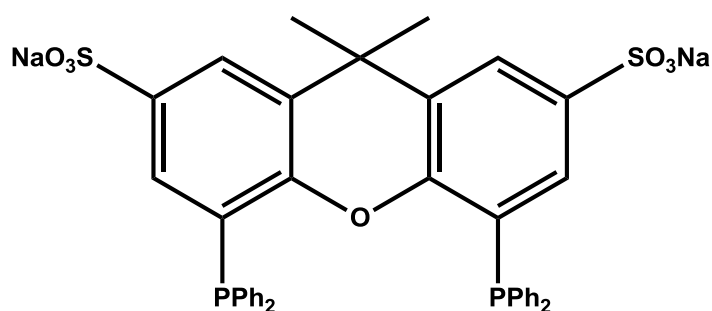
Figure 2.29: SulfoXantPhos ligand used by Schmidt *et al.* in biphasic methoxycarbonylation of 1-dodecene [68].

2.3 Comparisons of *in situ* and discrete catalysts

As previously mentioned, methoxycarbonylation catalysis has traditionally been done using *in situ* generated catalyst systems. Such systems have shown a range of catalytic activities, selectivities. Some of the best systems include 3 bis-(di-tert-butylphosphinomethyl)benzene (DTBPMB) ligand with tris(dibenzylideneacetone)dipalladium precursor used in the methoxycarbonylation of various substrates [69] . In the presence of methane sulfonic acid as an acid promoter and CO pressure of 30 bar and 80 °C, this system converts to completion, 3-methyl-1-pentene, 4-methyl-1-pentene and 4-methyl-2-pentene with 3 hrs of reaction. In addition, the system selectively forms respective linear products with over 99% selectivity observed [69]. The DTBPMB ligand-based palladium systems have shown efficacy in catalysing a range of substrates to desired ester products.

In another report, the system completely converts vinyl acetate to respective ester products with chemoselectivity of 100% within a reaction time of 3 hrs [70]. Another ligand system that has shown good results in the methoxycarbonylation is 2,2'-bis(diphenylphosphino)-1,10 -

binaphthyl (BINAP). In one of the reports, a system-generated using Pd(OAc)$_2$ and BINAP under optimized reaction conditions convert phenylacetylene to the ester products, with a TOF of up to 1600 h^{-1} observed [28]. In the same work, a palladium system based on SiXantphos ligand achieves complete conversion of phenyl acetylene, giving 65% of branched ester products [28]. *In-situ* formed palladium catalysts formed from Pd(OAc)$_2$ and 2-pyridyldiphenylphosphine show a TON of up to 40000 h^{-1} in the methoxycarbonylation of propyne. This system is also able to selectively form the expected ester product with up to selectivity of 99% observed [71].

Even though a range of *in situ* generated systems has been successfully applied in methoxycarbonylation, incredibly effective discrete palladium systems have also been used. An example is the palladium system bearing trans, trans-dibenzylideneacetone ligand and coordinated to 1,2-bis(di-tert-butylphosphinomethyl)benzene. This system gives an extremely high TOF of 12000 h^{-1} in the methoxycarbonylation of ethene [72]. This catalyst also shows selectivity of over 99% towards the desired methyl propanoate. Due to the excellent catalysts behaviour, this system has been commercialized in the Lucite Alpha process, where 370 000 tons of methyl methacrylate is produced per year [73]. With the ever-growing concerns of industrial waste as well as environmental pollution, industrial processes geared towards greener approaches, minimization of industrial waste and elimination of toxic solvents are ever welcome. There is an evident potential of discrete or isolated catalyst systems resulting in a better atom economy which can effectively push industries towards achieving a better balance of the ever tricky balancing act between profit generation and environmental conservation. Coupled with heterogenization of the homogeneous systems using various methods, the discrete systems upon heterogenization can give a further advantage of recycling and reusing the catalyst. Heterogenized systems are conspicuously few in the field of

methoxycarbonylation, as pointed earlier and therefore presents another area that requires further study.

Table 2.1: A comparison between some of the best-selected *insitu* and discrete catalysts in the methoxycarbonylation reactions.

Entry	Catalyst type	Substrate	Conversion/Activity	Regioselectivity/chemoselectivity
1	*Insitu*	Propyne	50000 mol (mol Pd)$^{-1}$ h^{-1})	>99 of methyl crotonate the linear product [71]
2	*Insitu*	1-Octene	100% within 3 hrs	99% of the linear ester product [69]
3	*Insitu*	Ethene	25000 mol (mol Pd)$^{-1}$ h^{-1})	97% of methyl propionate [74]
4	*Insitu*	Ethene	10000 mol (mol Pd)$^{-1}$ h^{-1})	>99% of methyl propanoate [75]
5	*Insitu*	cyclohexene	TOF of 150 h^{-1}	Complete selectivity towards methyl cyclohexanecarboxylate [76].
6	Discrete	Ethene	50000 mol of product per mol of Pd h-1	>99 methyl propanoate [72]
7	Discrete	Ethene	$62\ 270$ g methyl propanoate (mol cat)-1 h-1	93% of methyl propanoate [77]

2.4.1 Problem statement

While both heterogeneous and homogeneous catalysts have been widely utilized in numerous catalytic transformations, it has been shown that both catalytic systems have setbacks. For instance, even though homogeneous catalysts are excellent in terms of selectivity, they have a major drawback of difficulty in catalyst recycling. Comparatively, heterogeneous catalysts are easily separable and recoverable for use in subsequent reactions. However, the heterogeneous catalysts suffer from poor selectivity. As such, it is imperative to design catalyst systems that integrate the strengths of the heterogeneous and homogeneous catalysts of recyclability and selectivity, respectively.

2.4.2 Justification of the research

Transition metal catalysts have formed the backbone of various catalytic transformations in the pharmaceutical, chemical and petrochemical industries. With the continued demand for better efficiency and environmental protection strategies from industrial waste, it is important to design better catalysts that can catalyse various reactions such as methoxycarbonylation. From the literature review, it is evident that most literature methoxycarbonylation catalysts are generated *in situ.* While some of these systems have shown excellent catalytic activities, understanding the nature of active species is a challenge. For these reasons, it is vital to design homogenous discrete systems. Besides, it is imperative to design active, selective, stable, and recyclable catalysts.

2.4.3 Aim of the project

The aim of this research is to synthesize efficient homogeneous and immobilized palladium(II) complexes as methoxycarbonylation and hydrogenation catalysts.

2.4.4 Specific objectives

With the use of the mentioned aim as the guiding light, the following specific objectives were arrived at:

1. To synthesize, structurally characterize and study sterically hindered (pyridyl)benzamidine palladium(II) complexes as catalysts in the methoxycarbonylation of olefins.

2. To synthesize and characterize water-soluble (phenoxy)imine palladium(II) complexes and study their behaviour in the methoxycarbonylation of olefins under biphasic conditions.

3. To synthesize and characterize MCM-41, SBA-15 and Fe_3O_4 immobilized (amino)phenyl palladium(II) complexes and investigate the influence of the identity of the support in the methoxycarbonylation of olefins.

4. To investigate the comparative behaviour of homogeneous and silica immobilized N^N and N^O palladium(II) complexes as catalysts in the hydrogenation of alkenes, alkynes and functionalized benzenes.

Chapters 3-6 give an account of the work done to achieve every specific objective. Finally, Chapter 7 gives the overall conclusions, summary and future recommendations based on the findings in Chapters 3-6.

2.5 References

[1] G. Kiss, Palladium-catalyzed Reppe carbonylation, Chem. Rev., 101 (2001) 3435-3456.
[2] J.D. Nobbs, C.H. Low, L.P. Stubbs, C. Wang, E. Drent, M. van Meurs, Isomerizing methoxycarbonylation of alkenes to esters using a bis (phosphorinone) xylene palladium catalyst, Organometallics, 36 (2017) 391-398.

[3] R. Franke, D. Selent, A. Börner, Applied hydroformylation, Chem. Rev., 112 (2012) 5675-5732.

[4] J.R. Zbieg, E. Yamaguchi, E.L. McInturff, M.J. Krische, Enantioselective CH crotylation of primary alcohols via hydrohydroxyalkylation of butadiene, Science, 336 (2012) 324-327.

[5] P.W. Van Leeuwen, C. Claver, Rhodium catalyzed hydroformylation, Springer Science & Business Media2002.

[6] J. Liu, Z. Wei, H. Jiao, R. Jackstell, M. Beller, Toward Green Acylation of (Hetero) arenes: Palladium-Catalyzed Carbonylation of Olefins to Ketones, ACS central science, 4 (2018) 30-38.

[7] L. Wu, X. Fang, Q. Liu, R. Jackstell, M. Beller, X. Wu, A. Catal, 4, 2977–2989; d) X, F. Wu, X. Fang, L. Wu, R. Jackstell, H. Neumann, M. Beller, Acc. Chem. Res, 47 (2014) 1041-1053.

[8] A. Brennführer, H. Neumann, M. Beller, Palladium-catalyzed carbonylation reactions of alkenes and alkynes, ChemCatChem, 1 (2009) 28-41.

[9] P. Kalck, M. Urrutigoity, Recent improvements in the alkoxycarbonylation reaction catalyzed by transition metal complexes, Inorg. Chim. Acta, 431 (2015) 110-121.

[10] J. Liu, K. Dong, R. Franke, H. Neumann, R. Jackstell, M. Beller, Selective Palladium-Catalyzed Carbonylation of Alkynes: An Atom-Economic Synthesis of 1, 4-Dicarboxylic Acid Diesters, J. Am. Chem. Soc., 140 (2018) 10282-10288.

[11] J. Liu, J. Yang, F. Ferretti, R. Jackstell, M. Beller, Pd-Catalyzed Selective Carbonylation of gem-Difluoroalkenes: A Practical Synthesis of Difluoromethylated Esters, Angew. Chem., 131 (2019) 4738-4742.

[12] I.E. Nifant'ev, N.T. Sevostyanova, S.A. Batashev, A.A. Vinogradov, A.A. Vinogradov, A.V. Churakov, P.V. Ivchenko, Synthesis of methyl β-alkylcarboxylates by Pd/diphosphine-catalyzed methoxycarbonylation of methylenealkanes RCH_2CH_2C (R)= CH_2, Appl Catal A-gen, 581 (2019) 123-132.

[13] J. Liu, K. Dong, R. Franke, H. Neumann, R. Jackstell, M. Beller, Development of efficient palladium catalysts for alkoxycarbonylation of alkenes, Chem. Commun., 54 (2018) 12238-12241.

[14] M. Amézquita-Valencia, G. Achonduh, H. Alper, Pd-Catalyzed Regioselective Alkoxycarbonylation of 1-Alkenes Using a Lewis Acid [$SnCl_2$orTi (OiPr)4] and a Phosphine, J. Org. Chem, 80 (2015) 6419-6424.

[15] J. Li, W. Chang, W. Ren, J. Dai, Y. Shi, Palladium-catalyzed highly regio-and enantioselective hydroesterification of aryl olefins with phenyl formate, Org. Lett., 18 (2016) 5456-5459.

[16] C. Arderne, l.A. Guzei, C.W. Holzapfel, T. Bredenkamp, Branched Selectivity in the Pd-Catalysed Methoxycarbonylation of 1-Alkenes, ChemCatChem, 8 (2016) 1084-1093.

[17] K. Dong, R. Sang, X. Fang, R. Franke, A. Spannenberg, H. Neumann, R. Jackstell, M. Beller, Efficient Palladium-Catalyzed Alkoxycarbonylation of Bulk Industrial Olefins Using Ferrocenyl Phosphine Ligands, Angew. Chem., 129 (2017) 5351-5355.

[18] H. Qi, Z. Huang, M. Wang, P. Yang, C.-X. Du, S.-W. Chen, Y. Li, Bifunctional ligands for Pd-catalyzed selective alkoxycarbonylation of alkynes, J. Catal., 363 (2018) 63-68.

[19] R. Sang, C. Schneider, R. Razzaq, H. Neumann, R. Jackstell, M. Beller, Palladium-catalyzed carbonylations of highly substituted olefins using CO-surrogates,
Org. Chem. Front. , 7 (2020) 3681-3685.

[20] I. Fleischer, R. Jennerjahn, D. Cozzula, R. Jackstell, R. Franke, M. Beller, A unique palladium catalyst for efficient and selective alkoxycarbonylation of olefins with formates, ChemSusChem, 6 (2013) 417-420.

[21] A. Pews-Davtyan, X. Fang, R. Jackstell, A. Spannenberg, W. Baumann, R. Franke, M. Beller, Synthesis of New Diphosphine Ligands and their Application in Pd-Catalyzed Alkoxycarbonylation Reactions, Chem. Asian J., 9 (2014) 1168-1174.

[22] T. Bredenkamp, C. Holzapfel, Toward the development of efficient and stable Pd-catalysts for the methoxycarbonylation of medium chain alkenes, J. Iran. Chem. Soc. , 13 (2016) 421-427.

[23] Q. Liu, K. Yuan, P.B. Arockiam, R. Franke, H. Doucet, R. Jackstell, M. Beller, Regioselective Pd-catalyzed methoxycarbonylation of alkenes using both paraformaldehyde and methanol as CO surrogates, Angew. Chem. Int. Ed., 54 (2015) 4493-4497.

[24] K. Dong, R. Sang, Z. Wei, J. Liu, R. Dühren, A. Spannenberg, H. Jiao, H. Neumann, R. Jackstell, R. Franke, Cooperative catalytic methoxycarbonylation of alkenes: uncovering the role of palladium complexes with hemilabile ligands, Chemical science, 9 (2018) 2510-2516.

[25] A.J. Rucklidge, G.E. Morris, A.M. Slawin, D.J. Cole-Hamilton, The Methoxycarbonylation of Vinyl Acetate Catalyzed by Palladium Complexes of [1, 2-Phenylenebis (methylene)] bis [di (tert-butyl) phosphine], Helv. Chim. Acta, 89 (2006) 1783-1800.

[26] L. Diab, M. Gougou, E. Manoury, P. Kalck, M. Urrutigoïty, Highly regioselective palladium-catalyzed methoxycarbonylation of styrene using chiral ferrocene-and biphosphole-based ligands, Tetrahedron Lett., 49 (2008) 5186-5189.

[27] C. Holzapfel, T. Bredenkamp, An Empirical Study of Phosphine Ligands for the Methoxycarbonylation of Medium-Chain Alkenes, ChemCatChem, 7 (2015) 2598-2606.

[28] D.B.G. Williams, M.L. Shaw, T. Hughes, Recyclable Pd (OAc) 2/Ligand/Al (OTf) 3 Catalyst for the Homogeneous Methoxycarbonylation and Hydrocarboxylation Reactions of Phenylacetylene, Organometallics, 30 (2011) 4968-4973.

[29] D. Olivieri, F. Fini, R. Mazzoni, S. Zacchini, N. Della Ca', G. Spadoni, B. Gabriele, R. Mancuso, V. Zanotti, C. Carfagna, Diastereospecific Bis-alkoxycarbonylation of 1, 2-Disubstituted Olefins Catalyzed by Aryl α-Diimine Palladium (II) Catalysts, Adv. Synth. Catal., 360 (2018) 3507-3517.

[30] J. Tijani, R. Suleiman, B. El Ali, Palladium–dppb–borate-catalyzed regioselective synthesis of cinnamate esters by alkoxycarbonylation of phenylacetylene, Appl. Organomet. Chem., 22 (2008) 553-559.

[31] G.S. Nyamato, S.O. Ojwach, M.P. Akerman, Ethylene oligomerization studies by nickel (II) complexes chelated by (amino) pyridine ligands: Experimental and density functional theory studies, Dalton Trans., 45 (2016) 3407-3416.

[32] C. Bianchini, A. Meli, Alternating copolymerization of carbon monoxide and olefins by single-site metal catalysis, Coord. Chem. Rev., 225 (2002) 35-66.

[33] L. Kaganovsky, D. Gelman, K. Rueck-Braun, Trans-chelating ligands in palladium-catalyzed carbonylative coupling and methoxycarbonylation of aryl halides, J. Organomet. Chem., 695 (2010) 260-266.

[34] S. Zolezzi, S.A. Moya, G. Valdebenito, G. Abarca, J. Parada, P. Aguirre, Methoxycarbonylation of olefins catalyzed by palladium (II) complexes containing naphthyl (diphenyl) phosphine ligands, Appl. Organomet. Chem., 28 (2014) 364-371.

[35] V. de la Fuente, M. Waugh, G.R. Eastham, J.A. Iggo, S. Castillón, C. Claver, Phosphine Ligands in the Palladium-Catalysed Methoxycarbonylation of Ethene: Insights into the Catalytic Cycle through an HP NMR Spectroscopic Study, Chem. Eur. J., 16 (2010) 6919-6932.

[36] C. Bianchini, A. Meli, W. Oberhauser, S. Parisel, O.V. Gusev, A.M. Kal'sin, N.V. Vologdin, F.M. Dolgushin, Methoxycarbonylation of styrene to methyl arylpropanoates

catalyzed by palladium (II) precursors with 1, 1′-bis (diphenylphosphino) metallocenes, J. Mol. Catal. A: Chem., 224 (2004) 35-49.

[37] C. Bianchini, A. Meli, W. Oberhauser, P.W. van Leeuwen, M.A. Zuideveld, Z. Freixa, P.C. Kamer, A.L. Spek, O.V. Gusev, A.M. Kal'sin, Methoxycarbonylation of Ethene by Palladium (II) Complexes with 1, 1 '-Bis (diphenylphosphino) ferrocene (dppf) and 1, 1 '-Bis (diphenylphosphino) octamethylferrocene (dppomf), Organometallics, 22 (2003) 2409-2421.

[38] T.M. Konrad, J.A. Fuentes, A.M. Slawin, M.L. Clarke, Highly enantioselective hydroxycarbonylation and alkoxycarbonylation of alkenes using dipalladium complexes as precatalysts, Angew. Chem., 122 (2010) 9383-9386.

[39] T.M. Konrad, J.T. Durrani, C.J. Cobley, M.L. Clarke, Simultaneous control of regioselectivity and enantioselectivity in the hydroxycarbonylation and methoxycarbonylation of vinyl arenes, Chem. Commun., 49 (2013) 3306-3308.

[40] F. Stempfle, D. Quinzler, I. Heckler, S. Mecking, Long-chain linear C19 and C23 monomers and polycondensates from unsaturated fatty acid esters, Macromolecules, 44 (2011) 4159-4166.

[41] S. Doherty, E.G. Robins, J.G. Knight, C.R. Newman, B. Rhodes, P.A. Champkin, W. Clegg, Selectivity for the methoxycarbonylation of ethylene versus CO・ethylene copolymerization with catalysts based on C4-bridged bidentate phosphines and phospholes, J. Organomet. Chem., 640 (2001) 182-196.

[42] O.V. Gusev, A.M. Kalsin, P.V. Petrovskii, K.A. Lyssenko, Y.F. Oprunenko, C. Bianchini, A. Meli, W. Oberhauser, Synthesis, Characterization, and Reactivity of 1, 1 '-Bis (diphenylphosphino) osmocene: Palladium (II) Complexes and Their Use as Catalysts in the Methoxycarbonylation of Olefins, Organometallics, 22 (2003) 913-915.

[43] C. Zuniga, D. Sierra, J. Oyarzo, A. Klahn, Methoxycarbonylation of styrene by palladium (II) complex containing the diphenylphosphinocyrhetrene ligand, J. Chil. Chem. Soc., 57 (2012) 1101-1103.

[44] E. Guiu, M. Caporali, B. Munoz, C. Müller, M. Lutz, A.L. Spek, C. Claver, P.W. van Leeuwen, Electronic effect of diphosphines on the regioselectivity of the palladium-catalyzed hydroesterification of styrene, Organometallics, 25 (2006) 3102-3104.

[45] J.A. Fuentes, A.M. Slawin, M.L. Clarke, Application of palladium (trioxo-adamantyl cage phosphine) chloride complexes as catalysts for the alkoxycarbonylation of styrene; Pd catalysed tert-butoxycarbonylation of styrene, Catal. Sci. Technol., 2 (2012) 715-718.

[46] G.J. Harkness, M.L. Clarke, A highly enantioselective alkene methoxycarbonylation enables a concise synthesis of (S)-flurbiprofen, Eur. J. Org. Chem., (2017).

[47] L. Bettucci, C. Bianchini, W. Oberhauser, M. Vogt, H. Grützmacher, Chemoselective methoxycarbonylation of terminal alkynes catalyzed by Pd (II)-TROPP complexes, Dalton Trans., 39 (2010) 6509-6517.

[48] O.V. Gusev, A.M. Kalsin, M.G. Peterleitner, P.V. Petrovskii, K.A. Lyssenko, N.G. Akhmedov, C. Bianchini, A. Meli, W. Oberhauser, Palladium (II) Complexes with 1, 1 '− Bis (diphenylphosphino) ferrocenes [Fe (η5-C5R4PPh2) 2] n+(dppf, R= H, n= 0; dppomf, R= Me, n= 0; dppomf+, R= Me, n= 1). Synthesis, Characterization, and Catalytic Activity in Ethene Methoxycarbonylation, Organometallics, 21 (2002) 3637-3649.

[49] I. Pryjomska, H. Bartosz-Bechowski, Z. Ciunik, A.M. Trzeciak, J.J. Ziółkowski, Chemistry of palladium phosphinite (PPh$_2$(OR)) and phosphonite (P(OPh)$_2$(OH)) complexes: catalytic activity in methoxycarbonylation and Heck coupling reactions, Dalton Trans., (2006) 213-220.

[50] G. Abarca, K. Brown, S.A. Moya, J.C. Bayón, P.A. Aguirre, Methoxycarbonylation of Styrene Using a New Type of Palladium Complexes Bearing P, N-donor Ligands as Catalysts, Catal. Lett., 145 (2015) 1396-1402.

[51] P.A. Aguirre, C.A. Lagos, S.A. Moya, C. Zúñiga, C. Vera-Oyarce, E. Sola, G. Peris, J.C. Bayón, Methoxycarbonylation of olefins catalyzed by palladium complexes bearing P, N-donor ligands, Dalton Trans., (2007) 5419-5426.

[52] Z. Zulu, G.S. Nyamato, T.A. Tshabalala, S.O. Ojwach, Palladium (II) complexes of (pyridyl) imine ligands as catalysts for the methoxycarbonylation of olefins, Inorg. Chim. Acta, 501 (2020) 119270.

[53] M.G. Alam, T.A. Tshabalala, S.O. Ojwach, Metal-Catalyzed Alkene Functionalization Reactions Towards Production of Detergent and Surfactant Feedstocks, J Surfactants Deterg, 20 (2017) 75-81.

[54] T.A. Tshabalala, S.O. Ojwach, Tuning the regioselectivity of (benzimidazolylmethyl) amine palladium (II) complexes in the methoxycarbonylation of hexenes and octenes, Transition Met. Chem., 43 (2018) 339-346.

[55] M.B. Ibrahim, R. Suleiman, B. El Ali, New palladium-bis (oxazoline)-phosphine complexes: synthesis, characterization and catalytic application in alkoxycarbonylation of alkynes, J. Coord. Chem., 69 (2016) 1346-1357.

[56] S. Zulu, M.G. Alam, S.O. Ojwach, M.P. Akerman, Structural and theoretical studies of the methoxycarbonylation of higher olefins catalysed by (Pyrazolyl-ethyl) pyridine palladium (II) complexes, Appl. Organomet. Chem., 33 (2019) e5175.

[57] C. Bianchini, H.M. Lee, G. Mantovani, A. Meli, W. Oberhauser, Bis-alkoxycarbonylation of styrene by pyridinimine palladium catalysts, New J. Chem., 26 (2002) 387-397.

[58] W.P. Mul, H. Oosterbeek, G.A. Beitel, G.J. Kramer, E. Drent, In Situ Monitoring of a Heterogeneous Palladium-Based Polyketone Catalyst, Angew. Chem. Int. Ed., 39 (2000) 1848-1851.

[59] T.A. Tshabalala, S.O. Ojwach, M.A. Akerman, Palladium complexes of (benzoimidazol-2-ylmethyl) amine ligands as catalysts for methoxycarbonylation of olefins, J. Mol. Catal. A: Chem., 406 (2015) 178-184.

[60] K. Kumar, J. Darkwa, Palladium (II) complexes bearing mixed N^ N^ X (X= O and S) tridentate ligands as pre-catalysts for the methoxycarbonylation of selected 1-alkenes, Polyhedron, 138 (2017) 249-257.

[61] S.O. Akiri, S.O. Ojwach, Methoxycarbonylation of olefins catalysed by homogeneous palladium (II) complexes of (phenoxy) imine ligands bearing alkoxy silane groups, Inorg. Chim. Acta, 489 (2019) 236-243.

[62] S.O. Akiri, S.O. Ojwach, Synthesis of MCM-41 Immobilized (Phenoxy) Imine Palladium (II) Complexes as Recyclable Catalysts in the Methoxycarbonylation of 1-Hexene, Catalysts, 9 (2019) 143.

[63] J.P. Reynhardt, H. Alper, Hydroesterification reactions with palladium-complexed PAMAM dendrimers immobilized on silica J. Org. Chem., 68 (2003) 8353-8360.

[64] R.S. Mane, T. Sasaki, B.M. Bhanage, Silica supported palladium-phosphine as a reusable catalyst for alkoxycarbonylation and aminocarbonylation of aryl and heteroaryl iodides, RSC Adv., 5 (2015) 94776-94785.

[65] X. Chen, H. Zhu, T. Wang, C. Li, L. Yan, M. Jiang, J. Liu, X. Sun, Z. Jiang, Y. Ding, The 2V-P, N polymer supported palladium catalyst for methoxycarbonylation of acetylene, J. Mol. Catal. A: Chem., 414 (2016) 37-46.

[66] M. Chen, X. Mou, S. Wang, X. Chen, Y. Tan, M. Chen, Z. Zhao, C. Huang, W. Yang, R. Lin, Porous organic polymer-supported palladium catalyst for hydroesterification of olefins, Molecular Catalysis, 498 (2020) 111239.

[67] C.W. Kohlpaintner, R.W. Fischer, B. Cornils, Aqueous biphasic catalysis: Ruhrchemie/Rhône-Poulenc oxo process, Appl Catal A- Gen, 221 (2001) 219-225.

[68] M. Schmidt, T. Pogrzeba, L. Hohl, A. Weber, A. Kielholz, M. Kraume, R. Schomäcker, Palladium catalyzed methoxycarbonylation of 1-dodecene in biphasic systems–optimization of catalyst recycling, Molecular Catalysis, 439 (2017) 1-8.

[69] C.J. Rodriguez, D.F. Foster, G.R. Eastham, D.J. Cole-Hamilton, Highly selective formation of linear esters from terminal and internal alkenes catalysed by palladium complexes of bis-(di-tert-butylphosphinomethyl) benzene, Chem. Commun., (2004) 1720-1721.

[70] A.J. Rucklidge, G.E. Morris, D.J. Cole-Hamilton, Methoxycarbonylation of vinyl acetate catalysed by palladium complexes of bis (ditertiarybutylphosphinomethyl) benzene and related ligands, Chem. Commun., (2005) 1176-1178.

[71] E. Drent, P. Arnoldy, P. Budzelaar, Efficient palladium catalysts for the carbonylation of alkynes, J. Organomet. Chem., 455 (1993) 247-253.

[72] W. Clegg, M.R. Elsegood, G.R. Eastham, R.P. Tooze, X.L. Wang, K. Whiston, Highly active and selective catalysts for the production of methyl propanoate via the methoxycarbonylation of ethene, Chem. Commun., (1999) 1877-1878.

[73] R. Sang, Y. Hu, R. Razzaq, R. Jackstell, R. Franke, M. Beller, State-of-the-art palladium-catalyzed alkoxycarbonylations, Organic Chemistry Frontiers, (2020).

[74] R.I. Pugh, E. Drent, Methoxycarbonylation versus hydroacylation of ethene; dramatic influence of the ligand in cationic palladium catalysis, Adv. Synth. Catal., 344 (2002) 837-840.

[75] R.I. Pugh, E. Drent, P.G. Pringle, Tandem isomerisation–carbonylation catalysis: highly active palladium (II) catalysts for the selective methoxycarbonylation of internal alkenes to linear esters, Chem. Commun., (2001) 1476-1477.

[76] I. Nifant'ev, S. Batashev, S. Toloraya, A. Tavtorkin, N. Sevostyanova, A. Vorobiev, V. Bagrov, V. Averyanov, Effect of the structure and concentration of diphosphine ligands on the rate of hydrocarbomethoxylation of cyclohexene catalyzed by palladium acetate/diphosphine/TsOH system, J. Mol. Catal. A: Chem., 350 (2011) 64-68.

[77] J.G. Knight, S. Doherty, A. Harriman, E.G. Robins, M. Betham, G.R. Eastham, R.P. Tooze, M.R. Elsegood, P. Champkin, W. Clegg, Remarkable Differences in Catalyst Activity and Selectivity for the Production of Methyl Propanoate versus CO− Ethylene Copolymer by a Series of Palladium Complexes of Related C4-Bridged Diphosphines, Organometallics, 19 (2000) 4957-4967.

Chapter 3

Sterically hindered (pyridyl)benzamidine palladium(II) complexes: Syntheses, structural studies and applications as catalysts in the methoxycarbonylation of olefins

This chapter is adapted from the paper published in Applied Organometallic Chemistry. Doi:10.1002/aoc.6439, and is wholly based on the work of the first author, Saphan Akiri. The contribution of the first author, Saphan Akiri, include ligand and complex synthesis and characterization, methoxycarbonylation catalysis as well as drafting the manuscript.

3.1 Introduction

Value addition of olefins *via* transition metal catalysts constitute some of the most versatile and industrially relevant processes [1-3]. Some of these reactions include but are not limited to carbonylation [4], polymerization [5-7], oxidation [8], Suzuki cross-coupling reactions [9], hydrogenation [10, 11] and metathesis [12]. Among the carbonylation reactions, methoxycarbonylation of olefins has continued to gain much traction as various industrial and domestic products such as food additives, pesticides, fragrances and solvents can be accessed through this protocol [13, 14].

Traditionally, metal catalysed methoxycarbonylation reactions have been driven by phosphine-based palladium(II) based catalysts, as they exhibit superior catalytic activity as well as selectivity [13, 15]. Similarly, the catalytic process has employed mostly *in situ* generated active catalysts from the reactions of various palladium(II) metal salts and phosphine based ligands [16-20]. However, despite the success of these phosphine-based palladium(II) catalysts, they are not without any blemish. Key among the limitations is the relatively high

costs of their establishment, in addition to their isolation and handling. Besides, insufficient knowledge on the true nature of the active species and mechanistic insights of the *in situ* catalysts limits rationale catalyst design and development.

Pursuant to these limitations, significant efforts are being channelled towards the invention of alternative donor-ligands, which are cheaper and amenable to synthetic manipulations such as N^N [21-27], N^P [28, 29], N^O [30, 31], among others [32]. In addition, the design, isolation, and structural characterization of discrete palladium(II) catalysts are attractive as it allows for a better understanding of the catalytic process in terms of kinetics, mechanistic and deactivation profiles. All these have the benefit of the discovery of improved catalysts that can effectively be used in methoxycarbonylation catalysis. In this Chapter, we delineate the synthesis and structural characterization of palladium(II) complexes anchored on structurally rigid (pyridyl)benzamidine ligand networks. Moreover, methoxycarbonylation of various alkenes using this set of complexes are expounded. Detailed understanding of the contribution of the phosphine additives and acid promoters in active species generation and the influence of the various alkene substrates have been undertaken and are presented herein.

3.2 Experimental section

3.2.1 General materials and Instrumentation

The chemicals benzoyl chloride (97%), triethylamine (99%), thionyl chloride (95%), 2-amino-4-methyl pyridine, 2-amino-6-methyl pyridine, 2, 6- diisopropylaniline (90%), 2,6-dimethyl aniline (99%), aniline (>99.5%), and $PdCl_2$ were procured from Sigma-Aldrich and used in synthesis with no additional purification. The solvents acquired from Merck were of analytical grade, and various procedures were followed to dry them prior to use. Whereas

dichloromethane was dried by distilling over P_2O_5 and subsequently storing in molecular sieves, drying of methanol was done by heating over iodine-activated magnesium metal. In addition, drying of toluene was done over sodium wire and benzophenone. A Bruker Ultrashield 400 (^{1}H NMR 400 MHz, ^{13}C NMR 100 MHz) spectrometer was used in recording ^{1}H NMR and ^{13}C NMR spectra in deuterated chloroform at ambient temperature. The residual carbon and proton peaks at 77.0 ppm and 7.24 ppm, respectively, were used in referencing the chemical shift values (δ). In addition, the recording of the IR spectra was done on a Perkin-Elmer Spectrum 100 in the 600–4000 cm^{-1} range. While a Thermal Scientific Flash 2000 was used for elemental analyses, LC premier micromass was applied in carrying out the analysis of mass spectra. Moreover, Varian QP2010 and CP-3800 were used in GC–MS and GC analyses, respectively.

3.2.2 Synthesis and characterization of (pyridyl)benzamidine ligands the respective palladium(II) complexes

*3.2.2.1 (E)-N'-(2,6-diisopropylphenyl)-N-(4-methylpyridin-2-yl)benzimidamide (**L1**).*

To a stirred solution of 2, 6-diisopropylaniline (0.95 mL, 5.00 mmol) in dichloromethane (30 mL), was added benzoyl chloride (0.55 mL, 5.00 mmol) and triethylamine (0.80 mL. 5.50 mmol). After 3 h, the solvent was reduced under vacuum after filtration to obtain a brown oil. An excess of thionyl chloride (1.00 mL, 14.00 mmol) was then introduced and the reaction left to proceed for a further 2 h at 80 ºC. The unreacted thionyl chloride was then eliminated under a reduced pressure to afford imidoyl chloride as a yellow oil. Immediately, toluene (30.00 mL), trimethylamine (0.80 mL, 5.50 mmol) and 2-amino-4-methyl pyridine (0.54 g, 5.00 mmol) were introduced and the resultant mixture heated under reflux for 24 h under nitrogen atmosphere. The obtained crude substance was then filtered and the solvent removed under vacuum to obtain a dark brown oil, followed by recrystallization in methanol to afford white

66

crystalline compound **L1**. Yield = 1.28 g (69%.) ^{1}H NMR (400 MHz, CDCl$_3$): δ$_H$ (ppm) (Isomer (*E-anti* and *E-syn*) ratio 1: 5), major isomer, 1.17 (d, 12H, ^{3}J$_{HH}$ = 6.80 Hz, CH(C*H*$_3$)$_2$, 2.43 (s, 3H, CH$_3$), 3.18 (m, 2H, C*H*(CH$_3$)$_2$), 7.02–7.44 (m, 11H, pyridyl and phenyl protons). Minor isomer: 0.96 (d, 12H, ^{3}J$_{HH}$ = 6.80 Hz CH(C*H*$_3$)$_2$, 2.43(s, 3H, CH$_3$), 3.08 (m, 2H, C*H*(CH$_3$)$_2$), 7.02–7.44 (m, 11H, pyridyl and phenyl protons). ^{13}C NMR (100 MHz, CDCl3, δ ppm); major isomer: 162.5 (N=C), 147.4 (2pyC), 144.3 (6PyC), 132.6 (4PyC), 132.2 (*iPr*C), 129.8 (2,6 *iPr*C), 128.8 (1ArC), 128.3(4ArC) 127.1 (5PyC), 126.1 (3,5 ArC), 123.4 (3,5 ArC) 121.1 (3,5 *iPr*C), 119.6 (4 *iPr*C), 114.6 (3PyC), 29.8 (*C*H(CH$_3$)$_2$), 22.8 (PyCH$_3$), 21.6 (CH(*C*H$_3$)$_2$). Minor isomer: 162.5 (N=C), 147.4 (2pyC), 144.3 (6PyC), 132.6 (4PyC), 132.2 (1iPrC), 129.8 (2,6 *iPr*C), 128.8 (1ArC), 128.3(4ArC) 127.1 (5PyC), 126.1 (3,5 ArC), 123.4 (3,5 ArC) 121.1 (3,5 *iPr*C), 119.6 (4 *iPr*C), 114.6 (3PyC), 25.1 (*C*H(CH$_3$)$_2$), 22.8 (PyCH$_3$), 21.4 (CH(*C*H$_3$)$_2$). ESI-MS: *m*/*z* (%) 372 [(M$^+$+ H,100%)]F. IR ν_{max}/ cm^{-1}: $\nu_{(C=N)}$ = 1637.

*3.2.2.2 (E)-N'-(2,6-diisopropylphenyl)-N-(6-methylpyridin-2-yl)benzimidamide (**L2**)*

L2 was synthesised following the procedure for **L1** using 2, 6-diisopropylaniline (0.95 mL, 5.00 mmol), benzoyl chloride (0.55 mL, 5.00 mmol), triethylamine (0.80 mL. 5.50 mmol), thionyl chloride (1.00 mL, 14.00 mmol) and 2-amino-6-methyl pyridine (0.54 g, 5.00 mmol). The resulting yellow product was recrystallized from ethanol to give light yellow crystals. Yield =1.36 g (73%). ^{1}H NMR (400 MHz, CDCl$_3$): δ$_H$ (ppm) [Isomer (*E-anti* and *E-syn*) ratio 1: 1. 6], major isomer, 1.19 (d, 12H, CH(C*H*$_3$)$_2$, 2.50 (s, 3H, CH$_3$), 3.24 (m, 2H, C*H*(CH$_3$)$_2$), 6.96–7.71 (m, 11H, pyridyl and phenyl protons). Minor isomer: 1.00 (d, 12H, CH(C*H*$_3$)$_2$, 2.50 (s, 3H, CH$_3$), 3.06 (m, 2H, C*H*(CH$_3$)$_2$), 7.02–7.44 (m, 11H, pyridyl and phenyl protons). ^{13}C NMR (100 MHz, CDCl3, δ ppm); major isomer: 154.2 (N=C), 144.6 (2pyC), 139.3 (6PyC), 138.7 (4PyC), 132.2 (*iPr*C), 129.6 (2,6 iPrC), 128.8 (1ArC), 128.1(4ArC) 127.1 (5PyC), 126.1 (3,5 ArC), 123.9 (3,5 ArC) 123.4(3,5 *iPr*C), 119.4 (4 *iPr*C), 110.9 (3PyC), 28.8 (*C*H(CH$_3$)$_2$), 24.0 (PyCH$_3$), 22.8 (CH(*C*H$_3$)$_2$). Minor isomer: 154.2 (N=C), 144.6 (2pyC), 139.3 (6PyC),

138.7 (4PyC), 132.2 (*iPr*C), 129.6 (2,6 iPrC), 128.8 (1ArC), 128.1(4ArC) 127.1 (5PyC), 126.1 (3,5 ArC), 123.9 (3,5 ArC) 123.4(3,5 iPrC), 119.4 (4 iPrC), 110.9 (3PyC), 25.4 (*C*H(CH$_3$)$_2$), 24.0 (PyCH$_3$), 21.6.8 (CH(*C*H$_3$)$_2$). ESI-MS: *m/z* (%) 372 [(M$^+$,100%)]. IR ν_{max}/ cm^{-1}: $\nu_{(C=N)}$ = 1637.

3.2.2.3 (E)-N'-(2,6-dimethylphenyl)-N-(6-methylpyridin-2-yl)benzimidamide (*L3*)

Ligand **L3** was synthesised by applying the same protocol for **L1** using 2, 6-dimethylaniline (1.23 mL, 10.00 mmol), benzoyl chloride (1.10 mL, 10.00 mmol), triethylamine (1.60 mL. 11.00 mmol), thionyl chloride (2.00 mL, 28.00 mmol) and 2-amino-6-methyl pyridine (1.08 g, 10.00 mmol). The solvent was eliminated under reduced pressure to afford **L3** as a brown solid . Yield =2.72 g (73%). ^{1}H NMR (400 MHz, CDCl$_3$): δ_H (ppm): 2.21 (s, 6H, CH$_3$-Ar), 2.58 (s, 3H, CH$_3$-Py), 7.18 (m, 3H, H-Py), 7.38 (m, 3H, H-ArPy), 7.54 (t, 1H, ^{3}J$_{HH}$ = 7.6 Hz, H-Ar), 7.61 (d, 2H, ^{3}J$_{HH}$ = 7.6 Hz, H-Ar), 7.85 (t, 1H, ^{3}J$_{HH}$ = 7.8 Hz, H-Ar), 8.63 (d, 1H, ^{3}J$_{HH}$ = 8.2 Hz, H-Ar). ^{13}C NMR (100 MHz, CDCl3, δ ppm); 160.7 (N=C), 158.4 (2pyC), 152.9 (6PyC), 145.5 (ArC), 137.1 (4PyC), 136.8 ArC), 130.2 (ArC), 129.9(4ArC), 128.8 (ArC), 128.7 (ArC), 128.6 (5PyC) 128.5 (ArC), 127.9 (ArC), 125.4 (3PyC), 24.5 (PyCH$_3$), 18.8 (ArCH$_3$). ESI-MS: *m/z* (%) 316 [(M+ H, 100%)]. IR ν_{max}/ cm^{-1}: $\nu_{(C=N)}$ = 1642.

3.2.2.4 (E)-N'-(2,6-dimethylphenyl)-N-(4-methylpyridin-2-yl)benzimidamide (*L4*)

Ligand **L4** was synthesized following the synthetic route for **L1** using 2, 6-dimethylaniline (1.23 mL, 10.00 mmol), benzoyl chloride (1.10 mL, 10.00 mmol), triethylamine (1.60 mL. 11.00 mmol), thionyl chloride (2.00 mL, 28.00 mmol) and 2-amino-4-methyl pyridine (1.08 g, 10.00 mmol). **L4** was then revealed as a dark brown oil upon solvent removal under reduced pressure. Yield =2.76 g (74%). ^{1}H NMR (400 MHz, CDCl$_3$): δ_H (ppm): 2.21 (s, 6H, CH$_3$-Ar), 2.58 (s, 3H, CH$_3$-Py), 7.18 (m, 3H, H-Py), 7.38 (m, 3H, H-ArPy), 7.54 (t, 1H, ^{3}J$_{HH}$ = 7.6 Hz,

H-Ar), 7.61 (d, 2H, $^3J_{HH}$ = 7.6 Hz, H-Ar), 7.85 (t, 1H, $^3J_{HH}$ = 7.8 Hz, H-Ar), 8.63 (d, 1H, $^3J_{HH}$ = 8.2 Hz, H-Ar). ^{13}C NMR (100 MHz, CDCl3, δ ppm); 160.5 (N=C), 158.8 (2pyC), 153.9 (4PyC), 148.5 (ArC), 137.8 (6PyC), 136.1 ArC), 130.5 (ArC), 129.3(4ArC), 128.9 (ArC), 128.7 (ArC), 128.5 (5PyC) 128.2 (ArC), 127.9 (ArC), 125.8 (3PyC), 21.4 (PyCH₃), 18.8 (ArCH₃), ESI-MS: m/z (%) 316 [(M+ H, 100%)]. IR ν_{max}/ cm^{-1}: $\nu_{(C=N)}$ = 1647.

3.2.2.5 (E)-N-(6-methylpyridin-2-yl)-N'-phenylbenzimidamide (L5)

L5 was synthesised following the procedure for L1 using aniline (0.45 mL, 5.00 mmol), benzoyl chloride (0.55 mL, 5.00 mmol), triethylamine (0.80 mL. 5.50 mmol), thionyl chloride (1.0 mL, 14.00 mmol) and 2-amino-6-methyl pyridine (0.54 g, 5.00 mmol). Upon evaporating the solvent, ligand L5 was obtained as brown oil. Yield =0.91 g (80%). ^{1}H NMR (400 MHz, CDCl₃): δ_H (ppm) 2.38 (s, 3H, CH₃), 7.18-7.91 (m, 13H, H, pyridyl and phenyl protons). ^{13}C NMR (100 MHz, CDCl3, δ ppm);166.3 (N=C), 151.3 (pyC), 146.1 (PyC), 137.9 (4PyC), 131.8 (ArC), 129.1 (ArC), 129.0 (ArC), 128.8(ArC) 128.2 (PyC), 127.0 (ArC), 125.3 (ArC) 124.6(ArC), 121.4 (ArC), 120.2 (PyC), 21.4 (PyCH₃). ESI-MS: m/z (%) 288 [(M$^+$ + H, 100%)]. IR ν_{max}/ cm^{-1}: $\nu_{(C=N)}$ = 1658.

3.2.2.6 (E)-N'-(2,6-diisopropylphenyl)-N-(4-methylpyridin-2-yl)benzimidamide palladium(II) (Pd1)

A solution of [Pd(NCMe)₂Cl₂] (0.05 g, 0.19 mmol) in DCM (10 mL) was mixed with a solution L1 (0.07 g, 0.19 mmol) in DCM (5 mL), affording a yellow solution. Under stirring, the set up was let to run for 24 h at ambient temperature. Upon the reduction of the solvent under reduced pressure, and a recrystallization using hexane (5 mL) complex Pd1 was afforded as a pure bright yellow solid. Yield = 0.08 g (76%). ^{1}H NMR (400 MHz, CDCl₃): δ_H (ppm) 0.01 (d, 3H, $^3J_{HH}$ = 6.60 Hz, CH(CH₃)₂), 1.24 (d, 3H, $^3J_{HH}$ = 6.88 Hz CH(CH₃)₂), 1.51 (d, 3H,

$^3J_{HH} = 6.88$ Hz CH(CH_3)$_2$) , 2.07 (d, 3H, $^3J_{HH} = 6.88$ Hz CH(CH_3)$_2$), 2.70 (s, 3H, CH$_3$), 4.12 (m, 2H, CH(CH$_3$)$_2$), 6.76 (m, 1H, H-Py), 6.91 (m, 2H, H-Py), 7.04 (m, 6H, H-Ar,Py), 7.22 (t, 1H, $^3J_{HH} = 7.68$ Hz, H-Ar), 7.24 (m, 1H, H-py). ^{13}C NMR (100 MHz, CDCl3, δ ppm) 147.1 (N=C), 146.1 (2pyC), 144.4 (6PyC), 140.7 (4PyC), 139.1 (1iPrC), 131.0 (2,6 iPrC), 130.7 (1ArC), 129.6 (4ArC) 129.4 (5PyC), 129.1 (3,5 ArC), 128.4 (3,5 ArC) 127.0(3,5 iPrC), 123.4 (4 iPrC), 129.0 (3PyC), 29.1(CH(CH$_3$)$_2$) 28.1 (PyCH$_3$), 25.8 (CH(CH_3)$_2$), 22.4(CH(CH_3)$_2$), 22.3(CH(CH_3)$_2$), 21.5 (CH(CH_3)$_2$),. ESI-MS: m/z (%) 548 [(M$^+$ + H, 100%)]. IR ν_{max}/ cm^{-1}: $\nu_{(C=N)}$ = 1602. CHN. Anal. Calc. for C$_{25}$H$_{29}$Cl$_2$N$_3$Pd: C, 54.71; H, 5.33; N, 7.66. Found: C, 54.60; H, 5.51; N, 7.51.

3.2.2.7 (E)-N'-(2,6-diisopropylphenyl)-N-(6-methylpyridin-2-yl)benzimidamide palladium(II) (Pd2)

Complex **Pd2** was made by applying the synthetic protocol for complex **Pd1** using ligand **L5** (0.07 g, 0.19 mmol) and [Pd(NCMe)$_2$Cl$_2$] (0.05 g, 0.19 mmol). Bright yellow solid. Yield = 0.09 g (85%). 0.02 (d, 3H, $^3J_{HH} = 6.60$ Hz, CH(CH_3)$_2$), 1.23 (d, 3H, $^3J_{HH} = 6.88$ Hz CH(CH_3)$_2$), 1.47 (d, 3H, $^3J_{HH} = 6.88$ Hz CH(CH_3)$_2$) , 2.06 (d, 3H, $^3J_{HH} = 6.88$ Hz CH(CH_3)$_2$), 3.51 (s, 3H, CH$_3$), 4.10 (m, 2H, CH(CH$_3$)$_2$), 6.94 (m, 1H, H-Py), 7.08 (m, 2H, H-Py), 7.27 (m, 6H, H-Ar,Py), 7.85 (t, 1H, $^3J_{HH} = 7.68$ Hz, H-Ar), 8.39 (m, 1H, H-py). ^{13}C NMR (100 MHz, CDCl3, δ ppm) 147.1 (N=C), 146.1 (2-pyC), 145.5 (6-PyC), 144.3 (4-PyC), 140.7 (1iPrC), 139.1 (2,6 *iPr*C), 132.0 (1ArC), 130.9(4-ArC) 129.6 (5-PyC), 129.4 (3,5-ArC), 126.9 (3,5-ArC) 124.3(3,5 *iPr*C), 123.4 (4 *iPr*C), 119.9 (3PyC), 29.1(CH(CH$_3$)$_2$) 28.1 (PyCH$_3$), 25.8 (CH(CH_3)$_2$), 22.4 (CH(CH_3)$_2$), 22.3 (CH(CH_3)$_2$), 21.5 (CH(CH_3)$_2$). ESI-MS: m/z (%) 548 [(M$^+$ + H, 100%)]. IR ν_{max}/ cm^{-1}: $\nu_{(C=N)}$ = 1604. CHN. Anal. Calc. for C$_{25}$H$_{29}$Cl$_2$N$_3$Pd: C, 54.71; H, 5.33; N, 7.66. Found: C, 54.83; H, 5.35; N, 7.47.

3.2.2.8 (E)-N'-(2,6-dimethylphenyl)-N-(6-methylpyridin-2-yl)benzimidamide palladium(II)

(Pd3)

Complex **Pd3** was made by applying the synthetic protocol for **Pd1** using [Pd(NCMe)$_2$Cl$_2$] (0.05 g, 0.19 mmol) and **L3** (0.06 g, 0.19 mmol). Brown solid. Yield = 0.083 g (87 %). ^{1}H NMR (400 MHz, CDCl$_3$): δ_H (ppm): 2.24 (s, 6H, CH$_3$-Ar), 2.60 (s, 3H, CH$_3$-Py), 7.10 (d, 3H, $^3J_{HH}$ = 7.6 Hz, H-Ar ,H-Py), 7.21 (t, 2H, $^3J_{HH}$ = 7.68 Hz, H-ArPy), 7.54 (m, 2H, H-Ar), 7.62 (m, 1H, H-Ar), 7.76 (m, 2H, H-Ar), 7.95 (m, 1H, H-Ar). ^{13}C NMR (100 MHz, CDCl3, δ ppm); 158.8 (2pyC), 157.8 (6PyC), 155.5 (N=C), 147.5 (ArC), 137.1 (4PyC), 136.4(ArC), 130.2 (ArC), 129.9(4ArC), 128.8 (ArC), 128.7 (ArC), 128.6 (5PyC) 128.5 (ArC), 127.9 (ArC), 125.3 (3PyC), 21.8 (PyCH$_3$), 18.9 (ArCH$_3$). IR ν_{max}/ cm^{-1}: $\nu_{(C=N)}$ = 1607. CHN. Anal. Calc. for C$_{21}$H$_{21}$Cl$_2$N$_3$Pd: C, 51.19; H, 4.30; N, 8.53. Found: C, 51.35; H, 4.11; N, 8.51.

3.2.2.9 (E)-N'-(2,6-dimethylphenyl)-N-(4-methylpyridin-2-yl)benzimidamide palladium(II)

(Pd4)

Complex **Pd4** was made by applying the synthetic protocol for **Pd1** using [Pd(NCMe)$_2$Cl$_2$] (0.05 g, 0.19 mmol) and **L4** (0.06 g, 0.19 mmol). Brown solid. Yield = 0.08 g (84 %). ^{1}H NMR (400 MHz, CDCl$_3$): δ_H (ppm): 2.22 (s, 6H, CH$_3$-Ar), 2.36 (s, 3H, CH$_3$-Py), 6.78 (d, 2H, $^3J_{HH}$ = 7.6 Hz, H-Ar ,H-Py), 7.14 (t, 4H, $^3J_{HH}$ = 7.68 Hz, H-Ar), 7.25 (m, 3H, H-Ar), 7.32 (m, 2H, H-Ar). ^{13}C NMR (100 MHz, CDCl3, δ ppm); 158.1 (2-pyC), 157.1 (N=C), 153.1 (4PyC), 146.1 (ArC), 144.3 (6-PyC), 140.7 ArC), 130.9 (ArC), 130.7(4-ArC), 129.6 (ArC), 129.4 (ArC), 129.1(5-PyC) 128.4 (ArC), 126.9 (ArC), 123.4 (3-PyC), 21.8 (PyCH$_3$), 18.9 (ArCH$_3$) IR ν_{max}/ cm^{-1}: $\nu_{(C=N)}$ = 1610. CHN. Anal. Calc. for C$_{21}$H$_{21}$Cl$_2$N$_3$Pd: C, 51.19; H, 4.30; N, 8.53. Found: C, 51.20; H, 4.52; N, 8.64.

3.2.2.10 (E)-N-(6-methylpyridin-2-yl)-N'-phenylbenzimidamide palladium(II) (Pd5)

Complex **Pd5** was made by applying the synthetic protocol for complex **Pd1** using ligand **L5** (0.05 g, 0.19 mmol) and [Pd(NCMe)$_2$Cl$_2$] (0.05g, 0.19 mmol). Brown solid. Yield = 0.07 g

(78%). ^{1}H NMR (400 MHz, CDCl$_3$): δ_H (ppm) 2.47 (s, 3H, CH$_3$), 7.50-8.04 (m, 13H, H, pyridyl and phenyl protons). ^{13}C NMR (100 MHz, CDCl$_3$, δ ppm);166.3 (N=C), 147.2 (pyC), 143.4 (PyC), 137.9 (4-PyC), 130.8 (ArC), 128.4 (ArC), 128.2 (ArC), 127.3(ArC) 126.9 (PyC), 126.0 (ArC), 125.4 (ArC) 123.8(ArC), 121.1 (ArC), 119.2 (PyC), 20.8 (PyCH$_3$). ESI-MS: m/z (%) 417 [(M$^+$ -CH$_3$-Cl), 100%)]. IR ν_{max}/ cm^{-1}: $\nu_{(C=N)}$ = 1619. CHN. Anal. Calc. for C$_{19}$H$_{17}$Cl$_2$N$_3$Pd: C, 49.11; H, 3.69; N, 9.04. Found: C, 49.33; H, 3.67; N, 8.92.

3.2.3 Typical experimental protocol for methoxycarbonylation catalysis

All the methoxycarbonylation catalytic reactions were carried out in a stainless steel autoclave Parr reactor furnished with a sampling valve, an in-built cooling system and a unit for controlling temperature. As an example of the catalytic experiment, **Pd1** (0.03 g, 0.05 mmol), PTSA (0.09 g), 1-hexene (1.3 mL, 10.00 mmol) and PPh$_3$ (0.03 g, 0.1 mmol) which translates to 0.5 mol % were mixed in a Schlenk tube. A methanol and toluene mixture (each 20 mL) was then introduced. The resulting solution was emptied into the reactor and purged with the carbon monoxide gas three times, and the unit adjusted to the desired pressure, temperature and stirring speed. Upon the reaction's completion, the unit's temperature was left to adjust to ambient temperature, and the surplus CO was taken off through an outlet. For analysis, some amounts of the product were obtained, and a micro-filter was used to filter the sample prior to a GC analysis with ethylbenzene as the internal standard to obtain percentage yields. GC–MS was employed in identifying the catalysis products, whereas the commercial methyl heptanoate ester was used in assigning the linear and the branched yield. The GC analyses were carried out following our previously published method [33].

3.3 Results and discussion

3.3.1 Synthesis of (pyridyl)benzamidine ligands and their palladium(II)complexes

The (pyridyl)benzamidine ligands (**L1** - **L5**) were prepared according to modified literature protocols [34, 35] in moderate yields (69%-73%) (Scheme 3.1). Reactions of (pyridyl)benzamidine synthons with [Pd(NCMe)$_2$Cl$_2$] precursor afforded the corresponding palladium(II) complexes (**Pd1**- **Pd5**) in high yields of 76%-87% (Scheme 3.1).

R$_1$= ipr, R$_2$= CH$_3$, R$_3$= H,   L1, Pd1
R$_1$= ipr, R$_2$= H, R$_3$= CH$_3$,   L2, Pd2
R$_1$= CH$_3$, R$_2$= H, R$_3$= CH$_3$,   L3, Pd3
R$_1$= CH$_3$, R$_2$= CH$_3$, R$_3$= H, L4, Pd4
R1= H, R2= H, R3= CH3,   L5, Pd5
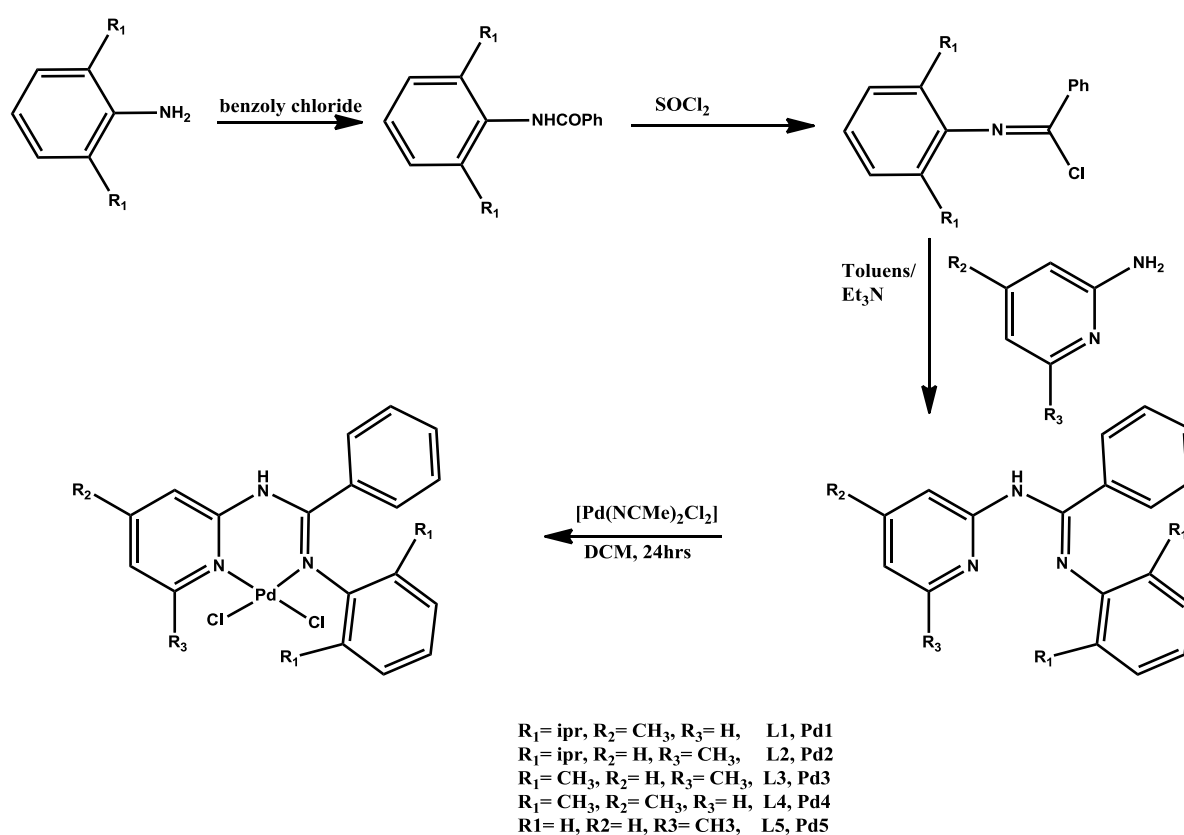
Scheme 3.1: Synthesis of (pyridyl) benzamidine ligands and their palladium(II) complexes

The ^{1}H NMR, ^{13}C NMR, FT-IR spectroscopies, elemental analyses, mass spectrometry were employed in characterizing the synthesized compounds and single-crystal analyses for compounds **Pd2** and **Pd3**. ^{1}H NMR characterization tool was instrumental in inferring the

successful synthesis of both the ligands and their respective palladium coordination compounds. For instance, the methyl-pyridyl protons in ligand **L2** and **Pd2** were recorded at 2.50 ppm to 3.51 ppm, respectively (Figure 3.1). A more outstanding feature was observed in the isopropyl proton signals in ligands **L1** and **L2**. Whereas two sets of signals of the C*H* protons were observed in ligands **L1** and **L2**, only one set of signals were recorded in their respective palladium(II) complexes, **Pd1** and **Pd2**. The two sets of signals in ligands **L1** and **L2** are accredited to the existence of isomeric *E* anti and *E* syn mixtures due to the unhindered rotation in the ligands. Upon complexation, this rotation is hindered due to the rigidity imposed by the chelating effect of the ligand in the complex coordination sphere [36-38].
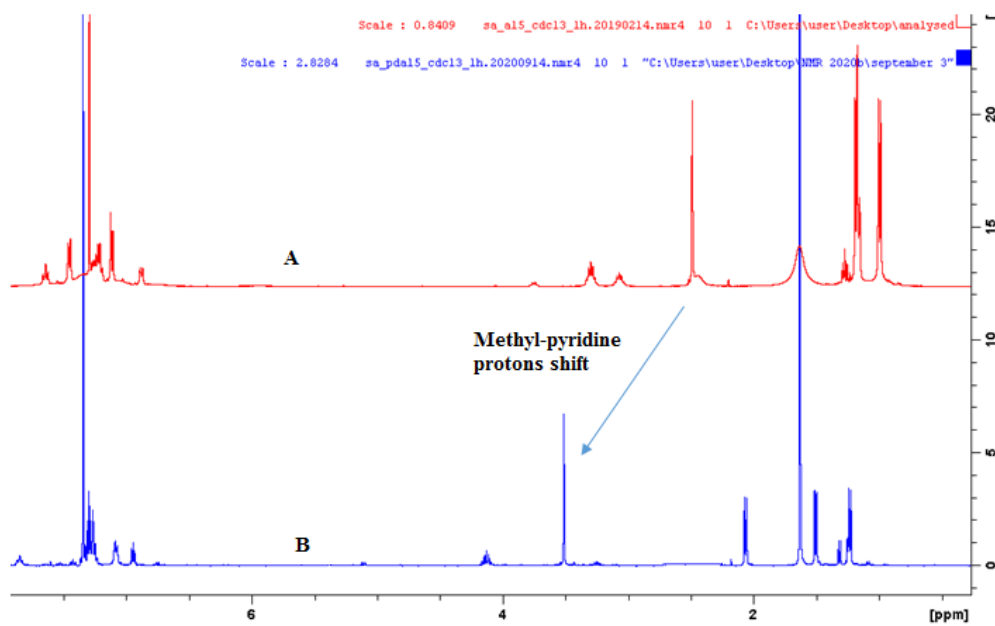
Figure 3.1: An overlaid ^{1}H NMR spectra of ligand **L2** (A) and corresponding complex **Pd2** (B) showing the downfield shift of methyl-pyridine protons

^{13}C NMR spectra were also beneficial in the structural elucidation of the formed ligands and complexes. The methyl-pyridine carbons in ligand **L2** and its complex corresponding **Pd2**

were displayed at 24.0 and 28.1 ppm, respectively (Figure 3.2. This signalled a change in the chemical environment upon complexation, hence further supporting a successful formation of the complex.
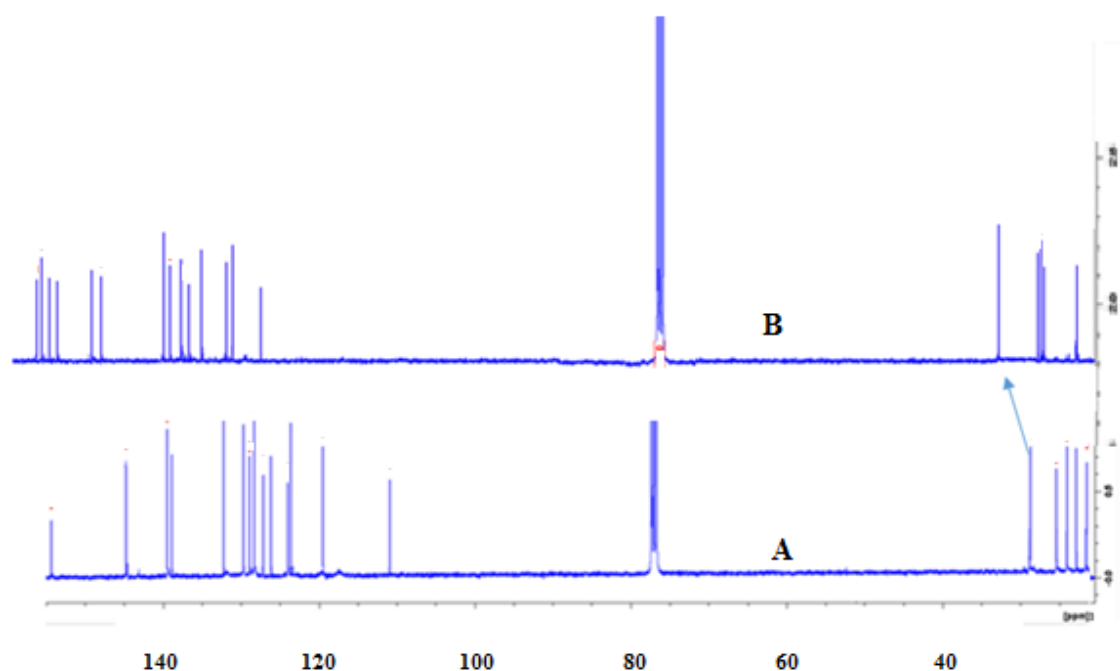
Figure 3.2: An overlaid ^{13}H NMR spectra of ligand **L2** (A) and corresponding complex **Pd2** (B) showing the downfield shift of methyl-pyridine carbons

In the IR spectral data, the ν*(C=N)* imine bond was employed to confer both the formation and successful coordination of the ligands to form the complexes. As a demonstration, the ν*(C=N)* signals for **L1** and the corresponding complex **Pd1** were was displayed at 1618 and 1602 cm$^-$^{1}, respectively (Figure 3.3). Besides, the ν*(N-H)* stretching was observed in every ligand and palladium(II) complex, indicating the absence of deprotonation (Table 3.1).
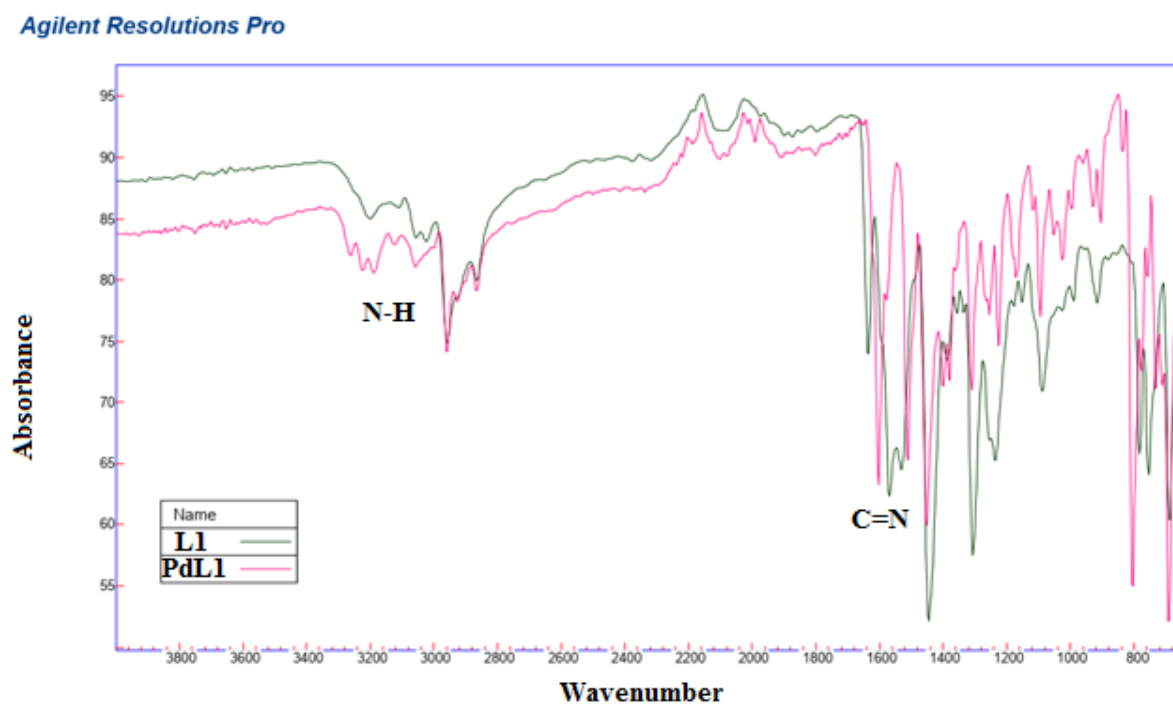
Figure 3.3: An overlaid IR spectrum of ligand **L1** and complex **PdL1** showing the expected

peaks

Table 3.1: FTIR spectroscopy and mass spectral data for ligands and complexes

Compounds	$\nu_{(C=N)}$ frequency (cm^{-1})	$\nu_{(N-H)}$ frequency (cm^{-1})	Molar mass $(gmol^{-1})$	m/z (amu)
L1	1618	3320	371.24	372 $(M^+ + H)$
Pd1	1602	3317	547.08	548 $(M^+ + H)$
L2	1637	3201	371.24	372 $(M^+ + H)$
Pd2	1604	3224	547.08	548 $(M^+ + H)$
L3	1642	3184	315.17	316 $(M^+ + H)$
Pd3	1607	3186	491.01	492 $(M^+ + H)$
L4	1647	3265	315.17	316 $(M^+ + H)$
Pd4	1610	3236	491.01	492 $(M^+ + H)$
L5	1658	3335	287.14	288 $(M^+ + H)$
Pd5	1619	3315	462.98	448 $(M^+ - CH_3)$

Mass spectrometry was applied in substantiating the molecular masses of all the synthesized compounds (Table 3.1). In general, all the compounds showed m/z signals that relate to their individual molecular ions. For instance, in the mass spectra of ligand **L3** and complex **Pd3,** m/z peaks at 316.21 amu and 492.11 amu were recorded, corresponding to their molar masses of 315.17 $gmol^{-1}$ and 491.01 $gmol^{-1,}$ respectively (Figure 3.4).
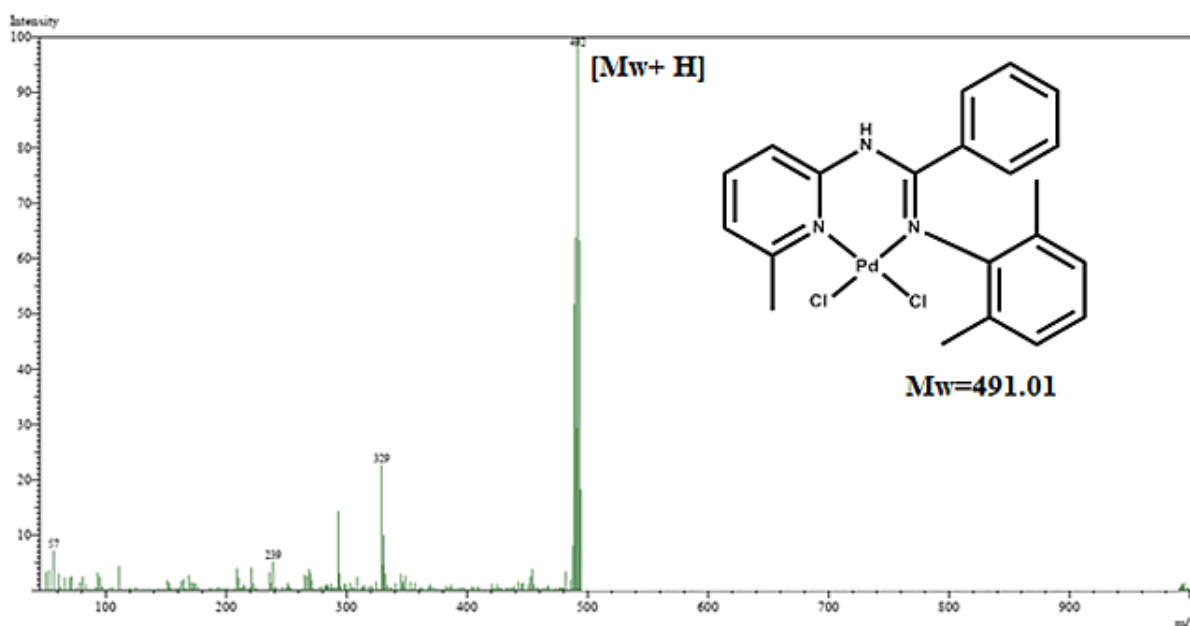
Figure 3.4: Mass spectrum of complex **Pd3** showing the molecular peak at 492 amu

3.3.2 Molecular structures of palladium(II) complexes Pd2 and Pd3

Single crystals of compounds **Pd2** and **Pd3** appropriate for X-ray screening were grown through slow diffusion of hexane solvent into corresponding concentrated acetonitrile solutions at ambient temperature. Table 3.2 represents the crystallographic data and structural refinement parameters, whereas the **Pd2** and **Pd3** molecular structures are given in Figures 3.5 and 3.6, respectively. Complex **Pd3** crystallized with one acetonitrile solvent molecule in its lattice. Both complexes **Pd2** and **Pd3** exhibited six-membered chelate rings, containing one N^N bidentate ligand and two chloride ligands to complete a four coordination environment (Figures 3.5 and 3.6).
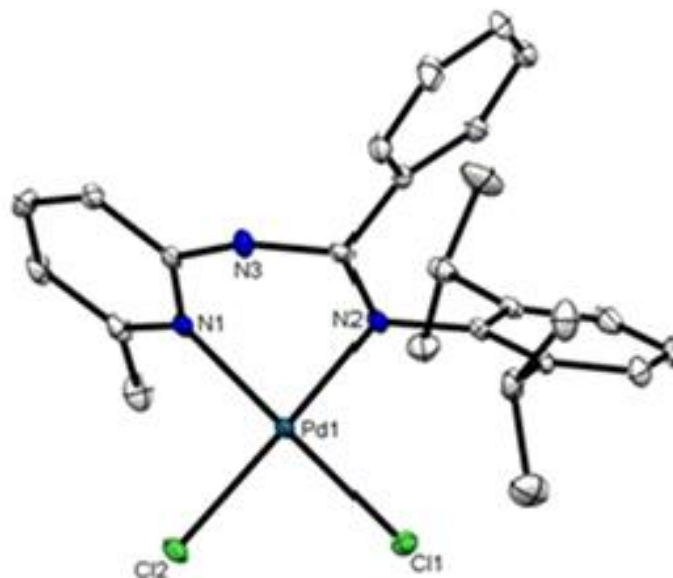
Figure 3.5: Molecular structure of **Pd2** drawn at 50% probability ellipsoids
Selected bond lengths [Å]: Pd(1)-N(1), 2.0383 (16); Pd(1)-N(2), 2.0426(16) ; Pd(1)-Cl(2), 2.2945(5); Pd(1)-Cl(1), 2.2996(5); N(2)-C(5), 1.399(2); N(2)-C(6), 1.372(2). Selected bond angles [°]: N(1)-Pd(1)-N(3), 87.74(6); N(1)-Pd(1)-Cl(2), 176.1 0(5); N(3)-Pd(1)-Cl(2), 92.81(5); N(1)-Pd(1)-Cl(1), 92.37(5); N(3)-Pd(1)-Cl(1), 169.59(5); Cl(2)-Pd(1)-Cl(1), 87.781(18).

Table 3.2: Structure refinement and crystallographic data summary for complexes **Pd2** and

Pd3

Parameter	Pd2	Pd3
Empirical formula	$C_{25} H_{29} Cl_2 N_3 Pd$	$C_{23} H_{24} Cl_2 N_4 Pd$
Formula weight	548.81	533.76
Temperature	100.02 K	100(2) K
Wavelength	0.71073Å	0.71073 Å
Crystal system	Monoclinic	Monoclinic
Space group	P 21/n	C 2/c
Unit cell dimensions		
a (Å)	11.9925(6)	21.0638(14) Å
b (Å)	13.1943(6)	16.2935(10) Å
c (Å)	16.0911(8)	13.3045(9) Å
α (°)	90°	90°
β (°)	107.868(3)°	105.638(3)°.
γ (°)	90º	90°
Volume	2423.3(2) $Å^3$	4397.1(5) $Å^3$
Z	4	8
Density (calculated)	1.504 Mg/m^3	1.613 Mg/m^3
Absorption coefficient	1.004 mm^{-1}	1.105 mm^{-1}
F(000)	1120	2160
Crystal size	0.240 x 0.140 x 0.120 mm^3	0.232 x 0.178 x 0.173 mm^3
Theta range for data collection	1.870 to 26.725°	1.603 to 26.779°
R	0.02	0.02

The average Pd-Cl bond lengths for complexes **Pd2** and **Pd3** of 2.29705± 0.0025 Å and

2.30765± 0.020 Å respectively are comparable. The Pd-N_{imine} and Pd-N_{py} bond lengths are

2.0426 and 2.0383 Å respectively for complex **Pd2**; values comparable to 2.0200 and 2.0353

Å observed for complex **Pd3**, pointing to similar electronic properties of the complexes. The

average Pd-Cl, Pd-N_{imine} and Pd-N_{py} of 2.30232± 0.015 Å 2.0313 ± 0.012 and 2.0368 ± 0.009

Å for complexes **Pd2** and **Pd3** are statistically similar to the average lengths of 2.2993± 0.012

Å and 2.021± 0.018 Å reported for related palladium complexes [37-39]. Complex **Pd3**

exhibits bite angles for N(1)-Pd(1)-N(3) of 86.32(6) and N(3)-Pd(1)-Cl(2) of 93.01(4), while

complex **Pd2** has bite angles for N(1)-Pd(1)-N(3) of   87.74(6) and Cl(2)-Pd(1)-Cl(1) of

92.81(5), confirming slightly distorted square planar geometries in both compounds. A closer

examination of the bite angles reveals that complex **Pd2** experiences slightly more distortion

as compared to complex **Pd3**, as the average deviation of the bite angles from the typical 90°

is 2.5 and 2.3, respectively. The calculated Tau parameters (τ) for complexes **Pd2** and **Pd3** of

0.14 and 0.08, respectively, further supported this trend.
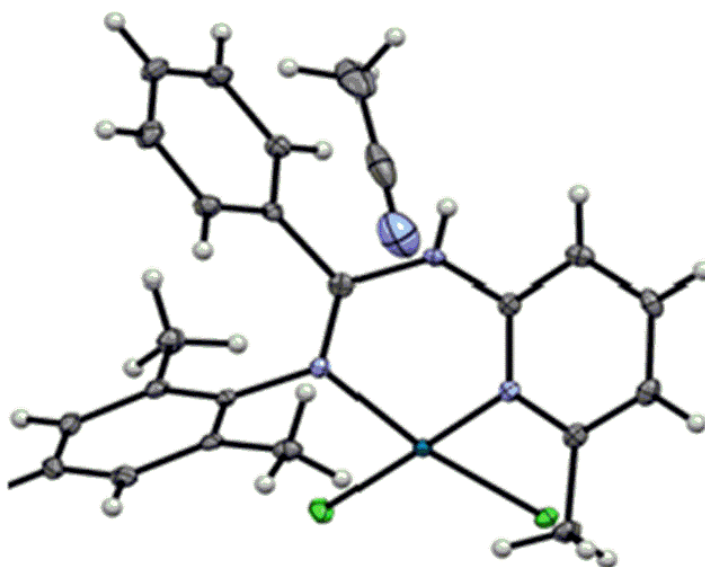
Figure 3.6: Molecular structure of **Pd3** with atom numbering Scheme. The displacement

ellipsoids of atoms are shown at the 50% probability level**:** Selected bond lengths [Å] Pd(1)-

N(1), 2.0200(14); Pd(1)-N(3), 2.0353(14); Pd(1)-Cl(2), 2.2878(5); Pd(1)-Cl(1), 2.3275(4);

N(2)-C(7), 1.375(2); N(2)-C(6), 1.401(2). Selected bond angles [°]: N(1)-Pd(1)-N(3), 86.32(6);

N(1)-Pd(1)-Cl(2), 179.24(4); N(3)-Pd(1)-Cl(2),   93.01(4); N(1)-Pd(1)-Cl(1), 91.72(4); N(3)-

Pd(1)-Cl(1), 169.36(4); Cl(2)-Pd(1)-Cl(1), 88.878(16).

3.4 Methoxycarbonylation catalysed by (pyridyl)benzamidine palladium(II) complexes Pd1-Pd5.

3.4.1 Preliminary investigations of complexes Pd1-Pd5 behaviour in methoxycarbonylation of 1-hexene

Preliminary investigation of the propensity of complexes **Pd1**- **Pd5** to catalyse the methoxycarbonylation 1-hexene was studied using ratios of 1:2:10:200 (the Pd:PPh$_3$:PTSA: hexene). The initial reaction temperature and CO of 90 °C and 60 bar were employed, respectively (Table 3.3). The identification and quantification of the catalysis products were accomplished using GC and GC-MS techniques, as indicated in Figure 3.7. Under these reaction conditions, complex **Pd5** was found to be the most active with affording percentage yields of 68% (Table 3.3, entry 5). Thus complex **Pd5** was used for further optimization reactions and investigations.
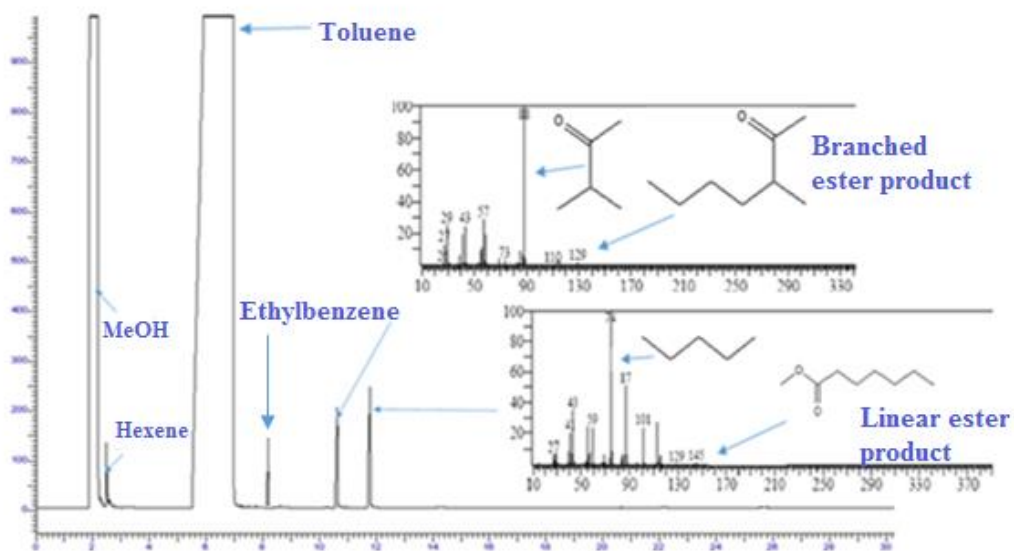
Figure 3.7: GC and GC-Ms spectra of products identified as branched (methyl 2-methylhexanoate) and linear (methyl heptanoate) esters using ethyl benzene as internal standard in the methoxycarbonylation of 1-hexene.

Table 3.3: Initial screening of the behaviour of pyridyl benzamidine palladium(II) complexes in methoxycarbonylation of 1-hexene[a]

Entry	Complex	Yield (%)[b]	B/L(%)[c]	TON[d]
1	**Pd1**	58	29/71	116
2	**Pd2**	53	30/70	102
3	**Pd3**	61	35/65	122
4	**Pd4**	66	34/66	132
5	**Pd5**	68	37/63	136
6[e]	**Pd5**	trace	-	-

[a] Reaction conditions: Methanol and toluene(both 20 mL) as solvent system;

[Pd]:[PPh$_3$][PTSA]:[hexene] ratio; 1:2:10:200; time, 24 h. %yield determined from GC using ethylbenzene as an internal standard and linear methyl heptanoate commercial sample. [c] Molar ratio between branched and linear products. [d] TON = (mol.prod/mol. Pd). [e]Reaction without PPh$_3$

We first probed the effect of the Pd: PPh$_3$ ratio of 1:1, 1:2 and 1:3 (Table 3.4, entries 1-4). Expectedly, only traces of products were observed in the absence of PPh$_3$, underpinning the importance of the PPh$_3$ to stabilize the generated active species [40, 41]. This is also augmented by the decomposition of the catalyst, and the formation of Pd(0) observed in the reaction chamber. Increasing the amount of the PPh$_3$ from one fold to two folds was marked with improved yields from 52% to 68% (Table 3.4, entries 2 and 3). Notably, increasing the PPh$_3$ quantity to (Pd: PPh$_3$ of 1:3) led to a slight drop in percentage yields 62%. The diminished catalytic performance at enhanced amounts of PPh$_3$ could be connected to the competition between PPh$_3$ and 1-hexene to coordinate to the palladium active site [42, 43]. Comparatively, no observable shift in regioselectivity was noted with a change in Pd: PPh$_3$ ratios, linear esters of 63%-66% were obtained in all the reactions (Table 3.4, entries 2-4).

Table 3.4: Optimization of the Pd:PPh3 and Pd:PTSA ratios using complex **Pd5**[a]

Entry	Pd:PPh$_3$	Pd: PTSA	Yield (%)[b]	B/L(%)[c]	TON[d]
1[b]	0	1:10	trace	-	-
2	1:1	1:10	52	38/62	104
3	1:2	1:10	68	37/63	136
4	1:3	1:10	62	34/66	124
5	1:2	1:20	79	40/60	158
6	1:2	1:30	88	37/63	176
7	1:2	1:40	73	40/60	146

[a]Reaction conditions: Solvent: methanol/toluene (40 mL); Pd: hexene ratio, 1:200; time, 24 h; temp: 90 °C; Pressure: 60 bar ; [b]% yields and conversions obtained using an internal standard (ethylbenzene) from GC. [c]Molar ratio between branched and linear esters computed using commercial sample (linear methyl heptanoate). [d]TON = (mol. prod/mol. Pd). [b] reaction carried out with no PPh$_3$

Considering the observed significant influence of PPh$_3$ and its inherence concentration in controlling the catalytic activities in the methoxycarbonylation reactions, we sought to gain more insights on its role on the possible active species formation using *in situ* NMR spectroscopy. Thus, **Pd5**:PPh$_3$ ratios of 1:1 and 1:2 were used to monitor the changes in the ^{31}P NMR spectral data over a period of 6 h (Figure 3.8). The spectra data obtained at **Pd5**:PPh$_3$ ratio of 1:1 displayed two peaks at around 23 ppm and 32 ppm, indicating possible ([Pd(PPh$_3$)Cl(**L5**)]$^+$ intermediate formation as shown in Eq. 1. The two peaks in the ^{31}P NMR spectral data could be assigned to PPh$_3$ ligands in the [Pd(PPh$_3$)Cl(**L5**)],$^+$ *cis* and *trans* to the pyridyl and imine nitrogen atoms. The active catalyst ([Pd(PPh$_3$)Cl(L5)]$^+$ is formed in both

cases when Pd:PPh₃ ratios are 1:1 and 1:2. However, excess PPh₃ is necessary to shift the reactions towards the active species ([Pd(PPh₃)Cl(L5]⁺ as opposed to the inactive [Pd(L5)Cl₂)] complex. The use of the **Pd5**:PPh₃ ratio of 1:2 resulted in an additional peak at -5 ppm, assigned to the free PPh₃ group. The higher catalytic activities observed at a higher Pd: PPh₃ ratio of 2, compared to the ratio of 1:1, therefore avers that excess amounts of PPh₃ are necessary to stabilize the active species.
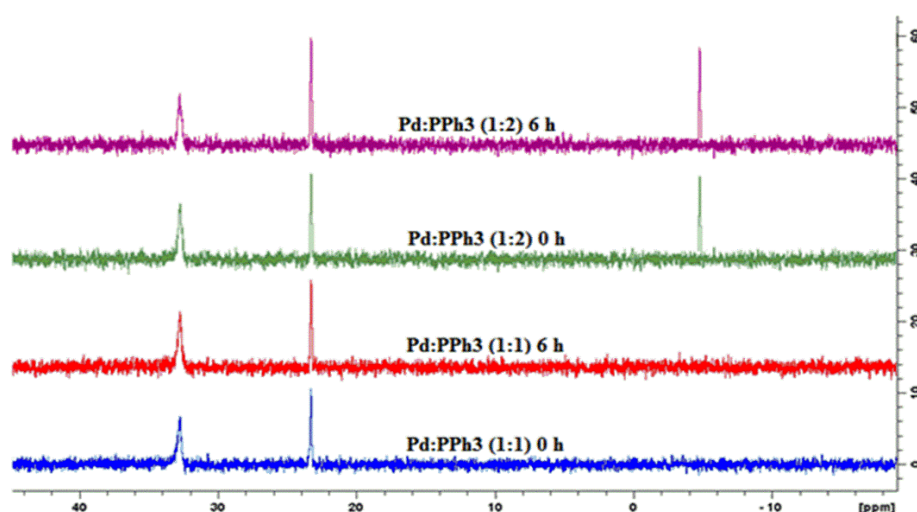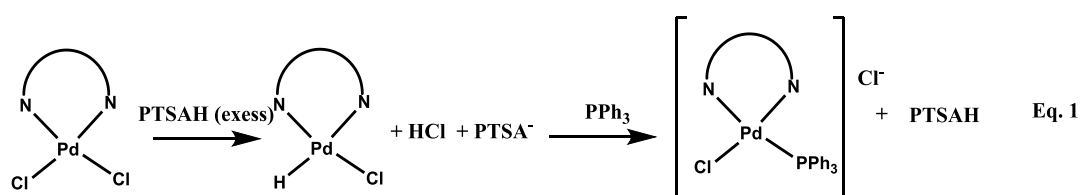
Figure 3.8: In situ ³¹P NMR spectral variation over time at different Pd:PPh₃ ratios using complex **Pd5**.

In attempts to further understand the role played by the PTSA acid, we varied the **Pd5**:PTSA ratio from 1:10 to 1:40 (Table 3.4, entries 3-7). It was evident that the amount of the acid promoter had a profound influence on the catalytic activity of complex **Pd5**. For example, percentage yields of 68% and 88% were recorded at **Pd5**:PTSA ratios of 1:10 and 1:30,

respectively (Table 3.4, entries 5-7). However, a further increase of the **Pd5**:PTSA ratio to 1:40 saw a drop in percentage yields to 73%. Lower catalytic activities at higher PTSA concentrations could be attributed to ligand hydrolysis [44], leading to catalyst decomposition. To confirm this hydrolysis, ^{1}H NMR spectral data of the mixtures (**Pd5**:PTSA ratios of 1:30 and 1:40) were monitored over a 6 h using period (Figure 3.9). While the spectrum acquired at the **Pd5**:PTSA ratio of 1:30 did not exhibit any observable changes, the spectral data for the **Pd5**:PTSA ratio of 1:40 exhibited new signals corresponding to the free ligands. This therefore established catalyst decomposition via ligand dissociation at higher PTSA concentrations, consistent with the low catalytic activities observed.
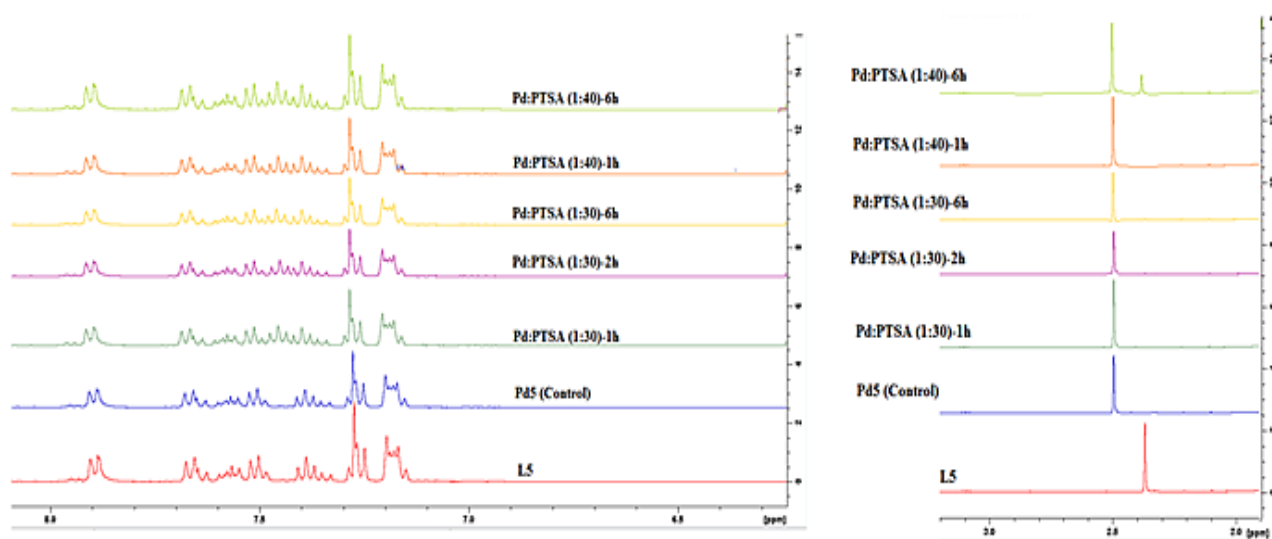
Figure 3.9: ^{1}H NMR of complex **Pd5** in the presence of PTSA and PPh$_3$ (Pd:PTSA ratios of 1:30 and 1:40) showing the stability of the complex **Pd5** at low acid concentration (Pd:PTSA ratio of 1:30) and possible ligand dissociation at high acid concentrations.

3.4.2 Investigation of the impacts of reaction conditions.

To qualitatively determine the optimum catalyst concentration in the methoxycarbonylation reaction, we determined the TON values at Pd loadings of 0.25 mol% (1:400) to 1 mol%

(1:100) using complex **Pd5** (Table 3.5, entries 1-4). While an increase in percentage yields was observed at higher Pd loadings, there was a general decline in the TON (Figure 3.6). For example, at 0.25 mol% (1:400) and 1 mol% (1:100), percentage yields of 60% and 95% were reported, while TONs of 252 and 95 were obtained, respectively (Table 3.5, entries 1 *vs* 4). Lower TONs at higher catalyst loading may result from catalyst aggregation [45, 46]. An optimum catalyst loading of 1:300 (0.33%) corresponding to a TON of 252 was thus established (Table 3.5, entry 3).

Next, we turned our attention to establishing the optimum reaction pressure and temperature. We noted that raising the catalyst systems' temperature from 90 ^{o}C to 100 ^{o}C was marked by a notable increase in yields from 84% to 94%, respectively. However, a higher temperature of 105 ^{o}C was met with a sharp decline in the percentage yields to 71% (Table 3.5, entries 3–5). Poor catalytic activities at elevated temperatures are correlated with the thermal decomposition of the catalyst, as deduced from the presence of palladium(0), observed in the catalyst reaction chamber at 100 ^{o}C [47]. It is worth mentioning the increased amounts of branched esters at elevated temperatures. For instance, 34% and 43% of the branched esters were produced at 90 ^{o}C and 110 ^{o}C, respectively (Table 3.5, entries 3 vs 6). Such an observation has been made before and associated is with enhanced isomerization reactions at higher temperatures [48].

Table 3.5: Optimization of reaction conditions in 1-hexene methoxycarbonylation using complex **Pd5**[a]

Entry	Pd:1-hexene	Temperature	Pressure	Yield (%)[b]	B/L(%)[c]	TON[d]
1	1:100	90	60	95	35/65	95
2	1:200	90	60	92	34/66	184
3	1:300	90	60	84	34/66	252
4	1:400	90	60	60	35/65	240
5	1:300	100	60	94	39/61	282
6	1:300	110	60	71	43/57	213
7	1:300	100	50	66	38/62	198
8	1:300	100	70	77	37/63	231
9	1:300	70	60	68	39/61	204
10[e]	1:300	100	60	8	43/57	24
11[f]	1:300	100	60	35	41/59	105
12[g]	1:300	100	60	59	40/60	186
13[h]	1:300	100	60	78	40/60	234

[a]Reaction conditions: Solvent, methanol/toluene (40 mL); Pd:PPh$_3$:PTSA:hexene ratio; 1: 2: 30; time, 24 h. [b]% yields and conversions obtained using an internal standard (ethylbenzene) from GC. [c]Molar ratio between branched and linear esters computed using commercial sample (linear methyl heptanoate). [d] TON = (mol.prod/mol. Pd).[efgh] Reactions done for 2, 6, 12 and 18 hrs respectively.

The dependence of the catalytic performance of complex **Pd5** on CO pressure was scrutinized by varying it from 50 bar to 70 bar (Table 3.5, entries 5, 7and 8). Expectedly, the higher pressure of 60 bar concomitantly led to enhanced yields of 94%, in comparison to percentage yields of 66%, observed at 50 bar. This is consistent with rapid CO insertion at higher pressures

and is well supported by previous literature reports [49]. Contrary to the catalytic activity trends reported, no notable effects of CO pressure on product regio-selectivity was evident. Lastly, the stability profile of complex **Pd5** was ventilated by comparisons of TOFs at reaction times from 2 h to 24 h (Figure 3.10). From Figure 3.6, lower yields were observed at fewer hours of reaction time. For instance, while percentage yields of 8% and 35% were observed after 2 h and 6 h respectively, increases to 59% and 78% at 12 h and 18 h were reported respectively. Quantitatively, 24 h reaction time could be regarded as the optimum reaction time as maximum percentage yields of 94% was realized. However, qualitatively, shorter reaction times gave better results. For instance, while a yield of only 35% was observed at 6 h reaction, it coincided with the highest turnover frequency of 17.5 h^{-1}, versus 11.9 h^{-1} observed at 24 h. This shows that while the catalytic activity of complex **Pd5** is appreciably retained over time, there is some catalyst deactivation occurring with longer reaction times.
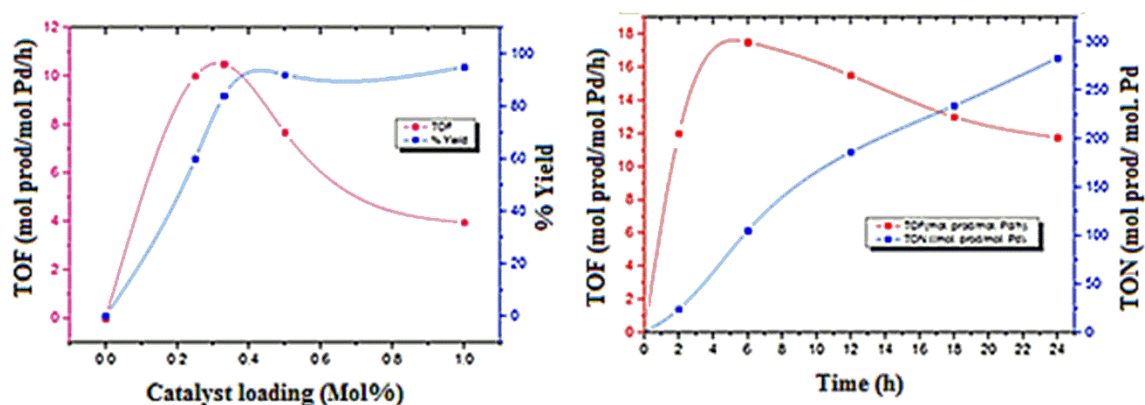
Figure 3.10: Graphical plots showing TON and TOF at different reaction times and catalyst loadings using complex **Pd5**. Reaction conditions: Solvent system, methanol/toluene (40 mL); [Pd]:[PPh$_3$][PTSA]:[hexene] ratio; 1:2:30:300; time,24 h, Temp, 100 $^{\circ}$C.

3.4.3 The influence of complex structure

Having established the best reaction conditions using complex **Pd5**, the complex/ligand structure influence was then studied by testing the other complexes **Pd1**-**Pd4** in 1-hexene methoxycarbonylation (Table 3.6, entries 1-5). From the data, it was apparent that the ligand structure controlled the behaviour of the pre-catalyst in terms of catalytic performance. For instance, complexes **Pd5** and **Pd2,** with unsubstituted and *isopropyl* substituted aryls close to their coordination sphere, afforded percentage yields of 94% and 73%, respectively (Table 3.6, entries 2 vs 5). The lower catalytic activities reported for, the more sterically hindered complex **Pd2** is anticipated and is linked to the limited access of the alkene substrate to the active metal site [50]. In terms of selectivity, the more sterically hindered complex **Pd2** expectedly afforded more of the sterically less demanding linear esters (75%) in comparison to 65% reported for the less bulky complex **Pd5** [51]. Similar observations were made for the remaining complexes. The catalytic performance observed for complexes **Pd1**-**Pd5** compares well with similar palladium complexes reported in the literature. In terms of catalytic activity, while some systems have reported slightly higher catalytic activities, for instance, palladium(II) system anchored on the 2-(diphenylphosphinoamino) pyridine ligands (a TON of 340), others have reported similar catalytic activities. For example, palladium(II) catalysts based on mixed N^N^O(S) (a TON of 264) in the methoxycarbonylation reaction [29, 32]. While there is no significant improvement in terms of catalytic activities in comparison to our previous outputs in this area [21, 25, 30, 52], this latest contribution brings the insight of controlling the regioselectivity by varying the steric encumbrance around the metal coordination sphere. For instance, while most of our previous reports gave linear and branched products in almost equal quantities, this new contribution has one of the catalysts giving up to 75% of the linear product in the methoxycarbonylation of 1-hexene.

Table 3.6: Influence of complex structure in 1-hexene methoxycarbonylation[a].

Entry	Complex	Yield (%)[b]	B/L(%)[c]	TON[d]
1	**Pd1**	80	28/72	240
2	**Pd2**	74	25/75	222
3	**Pd3**	83	31/69	249
4	**Pd4**	88	32/68	264
5	**Pd5**	94	35/65	282
6[e]	-	48	33/67	144
7[f]	-	72	47/53	216
8[g]	**Pd5**	89	37/63	264

[a]Reaction conditions: Solvent, methanol/toluene (both 20 mL); Pd:PPh$_3$:PTSA:hexene ratio; 1:2:30:300; time,24 h, Temp, 100 °C. [b]% yields and conversions obtained using an internal standard (ethylbenzene) from GC. [c]Molar ratio between branched and linear esters computed using commercial sample (linear methyl heptanoate). [d]TON = (mol.prod/mol. Pd). [e][Pd(NCMe)$_2$Cl$_2$]/**L5** system, [f]PdCl$_2$(PPh$_3$)$_2$] as a catalyst, [g]Hg poisoning investigation.

Two sets of control experiments were undertaken in an effort to establish the isolated palladium(II) complexes and ligands roles (Table 3.6, entries 6 and 7). First, we compared the behaviour of complex **Pd5** with an *in situ* generated palladium catalyst using [Pd(NCMe)$_2$Cl$_2$]/**L5** system. A notable reduction in catalytic activity (48%) was observed in the catalytic set-up with the *in situ* generated catalyst compared to 94% attained by complex **Pd5** (Table 3.6, entries 5 vs 7). This affirms the crucial role played by discrete catalysts, consistent with previous findings [33, 53]. The use of [PdCl$_2$(PPh$_3$)$_2$] salt in the methoxycarbonylation reactions have also been reported [54]. We thus compared its catalytic performance with our complexes under similar conditions. Even the catalytic activity displayed by [PdCl$_2$(PPh$_3$)$_2$] of 72% was lower than 94% for complex **Pd5;** it was comparable

to complexes **Pd1** and **Pd2.** With respect to regio-selectivity, expectedly **[PdCl$_2$(PPh$_3$)$_2$]** produced 53% of the linear products, compared to compositions of 65%-75% reported for the more sterically hindered complexes **Pd1-Pd5** (Table 3.6, entries 1-5). These differences in catalytic behaviour thus confirm that the active species in complexes. **Pd1**-**Pd5** contain a coordinated ligand and differ from **[PdCl$_2$(PPh$_3$)$_2$].** Finally, we used Hg(0) drop test to elucidate whether the active species is purely homogeneous or contain some active Pd(0) nanoparticles using complex **Pd5**. The addition of five drops of Hg(0) marginally reduced the percentage yields from 94% to 89% (Table 3.6, entries 5 vs 8). This points to the largely homogeneous nature of the active species using complex **Pd5** [55].

3.4.4 Investigation of the substrate scope using complex Pd5

The alkene substrate was studied using terminal alkenes of varying chain lengths, internal alkenes and styrene at optimized reaction conditions of Pd:PPh$_3$:substrate: PTSA (1:2:300:30), at 100 ºC and CO pressure of 60 bar (Table 3.7). From the data, it was evident the olefin substrate's identity affected the regio-selectivity and catalytic activity of complex **Pd5**. In general, terminal alkenes afforded higher percentage yields than the internal analogues, while styrene recorded the highest catalytic activity. For instance, styrene, 1-hexene, and 1-tetradecene alkenes gave percentage yields of 99%, 94% and 32%, respectively. Similarly, percentage yields of 68% and 51% were observed for 1-octene and *trans*-4-octene, respectively (Table 3.7). These results are in good agreement with previous reports and have been associated with steric and electronic contributions from various alkenes [22, 25, 30, 52]. The superior percentage yields recorded for styrene (>99%) is normal and is attributed to the resultant benzylic palladium(II) intermediate, which is more active as compared to alkyl palladium(II) species in aliphatic alkenes [56]. The identity of the olefin substrate also controlled the type of ester products yielded. As expected, percentage compositions of the

92

branched esters of 39% and 81% for 1-hexene and 2-hexene substrates, respectively. Similarly, 1-hexene and 1-tetradecene gave branched esters of 39% and 67%, respectively (Table 3.7, entries 1 vs 9). Preference to branched ester products with increased carbon chain length can be explained by the higher number of possible isomers [57, 58]. The small quantities of the linear esters observed in methoxycarbonylation of internal olefins are associated with isomerization. For instance, 14% of the linear ester product formed in the methoxycarbonylation *trans*-4-octene is due to its isomerization to form 1-octene

Table 3.7: Effects of substrate identity on methoxycarbonylation using complex **Pd5**[a]

Entry	Substrate	Yield (%)[b]	B/L(%)[c]	TON[d]
1	1-hexene	94	31/69	282
2	*Trans*-2-hexene	71	81/19	213
3	Styrene	99	91/09	297
4	1-heptene	83	43/57	249
5	1-octene	68	48/52	204
6	1-decene	54	54/46	162
7	*Trans*-4-octene	51	86/14	153
8	1-dodecene	42	60/40	126
9	Tetradecene	32	67/33	96

[a]Reaction conditions: Solvent, methanol/toluene (both 20 mL); Pd:PPh$_3$:PTSA: substrate ratio; 1:2:30:300; time,24 h, Temp, 100 °C. [b]% yields and conversions obtained using an internal standard (ethylbenzene) from GC. [c]Molar ratio between branched and linear esters computed using commercial sample. [d]TON = (mol.prod/mol. Pd).

The higher catalytic activities and regio-selectivity observed for complex **Pd5** in the methoxycarbonylation of styrene led us to explore the other complexes **Pd1**-**Pd4** in the styrene

reaction (Table 3.8). Similar to the trends observed in the reactions involving 1-hexene, with complex **Pd5** being the most active (99%), while complex **Pd2** was the least active (81%). More significantly, while linear esters were predominantly obtained in the methoxycarbonylation of 1-hexene (65%-75%), styrene substrate gave predominantly branched esters within the range of 79% - 91% (Table 3.6 *vs* Table 3.8). This points to the possible role of electronic and steric contributions in controlling the product distributions [59].

Table 3.8: Methoxycarbonylation of styrene using palladium complexes **Pd1**-**Pd5**[a]

Entry	Complex	Yield (%)[b]	B/L(%)[c]	TON[d]
1	**Pd1**	85	82/18	255
2	**Pd2**	81	79/21	243
3	**Pd3**	88	88/12	264
4	**Pd4**	94	86/14	282
5	**Pd5**	99	91/09	297

[a]Reaction conditions: Solvent system, methanol/toluene (40 mL); [Pd]:[PPh$_3$][PTSA]:[hexene] ratio; 1: 2: 30:300; time,24 h, Temp, 100 $^{\circ}$C. [b]% yields and conversions obtained using an internal standard (ethylbenzene) from GC. [c]Molar ratio between branched and linear esters computed using commercial sample (linear methyl heptanoate). [d] TON = (mol.prod/mol. Pd).

3.5 Conclusions

This chapter established the coordination behaviour of five palladium(II) complexes (**Pd1**-**Pd5**) anchored on rigid (pyridyl)benzamidine ligands with different steric requirements. The molecular structures of the palladium compounds revealed distorted square planer geometries containing a single bidentate neutral ligand and two chloride ligands. All the complexes formed active species in the methoxycarbonylation of various alkene substrates. Both the catalytic activities and regioselectivities were impacted by the steric and electronic dispositions

of the palladium(II) complexes and the identity of the alkene substrate. Sterically hindered complexes favoured the formation of linear esters. Terminal olefins produced mostly linear esters, while internal alkenes and styrene formed predominantly branched esters. NMR kinetics established the stabilization role of PPh$_3$ and catalyst deactivation through ligand hydrolysis at high acid concentrations.

The next chapter entails the synthesis of both non-water soluble and water-soluble bischelated palladium(II) complexes bearing (phenoxy)imine ligands. Both the comparative study of the sets of complexes and recyclability studies in the methoxycarbonylation has been done.

3.6 References

[1] T.P. Vispute, H. Zhang, A. Sanna, R. Xiao, G.W. Huber, Renewable chemical commodity feedstocks from integrated catalytic processing of pyrolysis oils, Science, 330 (2010) 1222-1227.

[2] F. Chen, T. Wang, N. Jiao, Recent advances in transition-metal-catalyzed functionalization of unstrained carbon–carbon bonds, Chem. Rev., 114 (2014) 8613-8661.

[3] C. Bolm, M. Beller, Transition metals for organic synthesis, Wiley-VCH: Weinheim2004.

[4] M. Sperrle, G. Consiglio, Olefin Carbonylation Catalysis with Cationic Palladium Complexes: Selectivity and Possible Intermediates, Chem. Ber., 130 (1997) 1557-1565.

[5] A.F. Mason, G.W. Coates, New phenoxyketimine titanium complexes: Combining isotacticity and living behavior in propylene polymerization, J. Am. Chem. Soc., 126 (2004) 16326-16327.

[6] F. Marchetti, G. Pampaloni, Y. Patil, A.M.R. Galletti, F. Renili, S. Zacchini, Ethylene Polymerization by Niobium (V) N, N-Dialkylcarbamates Activated with Aluminum Co-catalysts, Organometallics, 30 (2011) 1682-1688.

[7] T.R. Younkin, E.F. Connor, J.I. Henderson, S.K. Friedrich, R.H. Grubbs, D.A. Bansleben, Neutral, single-component nickel (II) polyolefin catalysts that tolerate heteroatoms, Science, 287 (2000) 460-462.

[8] A.A. Khandar, K. Nejati, Z. Rezvani, Syntheses, Characterization and Study of the Use of Cobalt (II) Schiff–Base Complexes as Catalysts for the Oxidation of Styrene by Molecular Oxygen, Molecules, 10 (2005) 302-311.

[9] N. Miyaura, A. Suzuki, Palladium-catalyzed cross-coupling reactions of organoboron compounds, Chem. Rev., 95 (1995) 2457-2483.

[10] R. Waymouth, P. Pino, Enantioselective hydrogenation of olefins with homogeneous Ziegler-Natta catalysts, J. Am. Chem. Soc., 112 (1990) 4911-4914.

[11] S.O. Akiri, N.L. Ngcobo, S.O. Ojwach, Comparative Study of Homogeneous and Silica Immobilized N^ N and N^ O Palladium (II) Complexes as Catalysts for Hydrogenation of Alkenes, Alkynes and Functionalized Benzenes, Catal. Lett., (2020) 1-13.

[12] R.H. Grubbs, S. Chang, Recent advances in olefin metathesis and its application in organic synthesis, Tetrahedron, 54 (1998) 4413-4450.

[13] P. Kalck, M. Urrutigoity, Recent improvements in the alkoxycarbonylation reaction catalyzed by transition metal complexes, Inorg. Chim. Acta, 431 (2015) 110-121.

[14] B. Liu, F. Hu, B.-F. Shi, Recent advances on ester synthesis via transition-metal catalyzed C–H functionalization, ACS Catal., 5 (2015) 1863-1881.

[15] A. Brennführer, H. Neumann, M. Beller, Palladium-catalyzed carbonylation reactions of alkenes and alkynes, ChemCatChem, 1 (2009) 28-41.

[16] J. Liu, K. Dong, R. Franke, H. Neumann, R. Jackstell, M. Beller, Development of efficient palladium catalysts for alkoxycarbonylation of alkenes, Chem. Commun., 54 (2018) 12238-12241.

[17] I.E. Nifant'ev, N.T. Sevostyanova, S.A. Batashev, A.A. Vinogradov, A.A. Vinogradov, A.V. Churakov, P.V. Ivchenko, Synthesis of methyl β-alkylcarboxylates by Pd/diphosphine-catalyzed methoxycarbonylation of methylenealkanes RCH_2CH_2C (R)= CH_2, Appl Catal A-gen, 581 (2019) 123-132.

[18] C. Arderne, C.W. Holzapfel, T. Bredenkamp, Branched Selectivity in the Pd-Catalysed Methoxycarbonylation of 1-Alkenes, ChemCatChem, 8 (2016) 1084-1093.

[19] K. Dong, R. Sang, X. Fang, R. Franke, A. Spannenberg, H. Neumann, R. Jackstell, M. Beller, Efficient Palladium-Catalyzed Alkoxycarbonylation of Bulk Industrial Olefins Using Ferrocenyl Phosphine Ligands, Angew. Chem., 129 (2017) 5351-5355.

[20] A.J. Rucklidge, G.E. Morris, A.M. Slawin, D.J. Cole-Hamilton, The Methoxycarbonylation of Vinyl Acetate Catalyzed by Palladium Complexes of [1, 2-

Phenylenebis (methylene)] bis [di (tert-butyl) phosphine], Helv. Chim. Acta, 89 (2006) 1783-1800.

[21] Z. Zulu, G.S. Nyamato, T.A. Tshabalala, S.O. Ojwach, Palladium (II) complexes of (pyridyl) imine ligands as catalysts for the methoxycarbonylation of olefins, Inorganica Chimica Acta, 501 (2020) 119270.

[22] M.G. Alam, T.A. Tshabalala, S.O. Ojwach, Metal-Catalyzed Alkene Functionalization Reactions Towards Production of Detergent and Surfactant Feedstocks, J Surfactants Deterg, 20 (2017) 75-81.

[23] T.A. Tshabalala, S.O. Ojwach, Tuning the regioselectivity of (benzimidazolylmethyl) amine palladium (II) complexes in the methoxycarbonylation of hexenes and octenes, Transition Met. Chem., 43 (2018) 339-346.

[24] M.B. Ibrahim, R. Suleiman, B. El Ali, New palladium-bis (oxazoline)-phosphine complexes: synthesis, characterization and catalytic application in alkoxycarbonylation of alkynes, J. Coord. Chem., 69 (2016) 1346-1357.

[25] S. Zulu, M.G. Alam, S.O. Ojwach, M.P. Akerman, Structural and theoretical studies of the methoxycarbonylation of higher olefins catalysed by (Pyrazolyl-ethyl) pyridine palladium (II) complexes, Appl. Organomet. Chem., 33 (2019) e5175.

[26] C. Bianchini, H.M. Lee, G. Mantovani, A. Meli, W. Oberhauser, Bis-alkoxycarbonylation of styrene by pyridinimine palladium catalysts, New J. Chem., 26 (2002) 387-397.

[27] N.L. Ngcobo, S.O. Akiri, A.O. Ogweno, S.O. Ojwach, Structural elucidation of chiral (imino) pyridine/phosphine palladium (II) complexes and their applications as catalysts in methoxycarbonylation of styrene, Polyhedron, (2021) 115243.

[28] G. Abarca, K. Brown, S.A. Moya, J.C. Bayón, P.A. Aguirre, Methoxycarbonylation of Styrene Using a New Type of Palladium Complexes Bearing P, N-donor Ligands as Catalysts, Catal. Lett., 145 (2015) 1396-1402.

[29] P.A. Aguirre, C.A. Lagos, S.A. Moya, C. Zúñiga, C. Vera-Oyarce, E. Sola, G. Peris, J.C. Bayón, Methoxycarbonylation of olefins catalyzed by palladium complexes bearing P, N-donor ligands, Dalton Trans., (2007) 5419-5426.

[30] S.O. Akiri, S.O. Ojwach, Methoxycarbonylation of olefins catalysed by homogeneous palladium (II) complexes of (phenoxy) imine ligands bearing alkoxy silane groups, Inorg. Chim. Acta, 489 (2019) 236-243.

[31] S.O. Akiri, S.O. Ojwach, Synthesis of MCM-41 Immobilized (Phenoxy) Imine Palladium (II) Complexes as Recyclable Catalysts in the Methoxycarbonylation of 1-Hexene, Catalysts, 9 (2019) 143.

[32] K. Kumar, J. Darkwa, Palladium (II) complexes bearing mixed N^ N^ X (X= O and S) tridentate ligands as pre-catalysts for the methoxycarbonylation of selected 1-alkenes, Polyhedron, 138 (2017) 249-257.

[33] S.O. Akiri, S.O. Ojwach, Structural studies and applications of water soluble (phenoxy) imine palladium (II) complexes as catalysts in biphasic methoxycarbonylation of 1-hexene, J. Organomet. Chem., 942 (2021) 121812.

[34] R.T. Boeré, V. Klassen, G. Wolmershäuser, Synthesis of some very bulky N, N′-disubstituted amidines and initial studies of their coordination chemistry, J. Chem. Soc., Dalton Trans., (1998) 4147-4154.

[35] A.M. Winter, K. Eichele, H.-G. Mack, S. Potuznik, H.A. Mayer, W.C. Kaska, Rhodium pincer complexes of 2, 2′-bis (diphenylphosphino) diphenylamine, J. Organomet. Chem., 682 (2003) 149-154.

[36] F.-S. Liu, H.-Y. Gao, K.-M. Song, L. Zhang, F.-M. Zhu, Q. Wu, Nickel complexes bearing [N, N] 2-pyridylbenzamidine ligands: Syntheses, characterizations, and catalytic properties for ethylene oligomerization, Polyhedron, 28 (2009) 1386-1392.

[37] Y.T. Huang, X. Tang, Y. Yang, D.S. Shen, C. Tan, F.S. Liu, Efficient pyridylbenzamidine ligands for palladium-catalyzed Suzuki–Miyaura reaction, Appl. Organomet. Chem., 26 (2012) 701-706.

[38] A. Tognon, V. Rosar, N. Demitri, T. Montini, F. Felluga, B. Milani, Coordination chemistry to palladium (II) of pyridylbenzamidine ligands and the related reactivity with ethylene, Inorg. Chim. Acta, 431 (2015) 206-218.

[39] Y. Lai, Z. Zong, Y. Tang, W. Mo, N. Sun, B. Hu, Z. Shen, L. Jin, W.-h. Sun, X. Hu, Highly bulky and stable geometry-constrained iminopyridines: Synthesis, structure and application in Pd-catalyzed Suzuki coupling of aryl chlorides, Beilstein J. Org. Chem., 13 (2017) 213-221.

[40] I. del Río, C. Claver, P.W. van Leeuwen, On the mechanism of the hydroxycarbonylation of styrene with palladium systems, Eur. J. Inorg. Chem., 2001 (2001) 2719-2738.

[41] G. Cavinato, L. Toniolo, Carbonylation of ethene catalysed by Pd (II)-phosphine complexes, Molecules, 19 (2014) 15116-15161.

[42] G. Kiss, Palladium-catalyzed Reppe carbonylation, Chem. Rev., 101 (2001) 3435-3456.

[43] C.-M. Tang, X.-L. Li, G.-Y. Wang, A highly efficient catalyst for direct synthesis of methyl acrylate via methoxycarbonylation of acetylene, Korean J. Chem. Eng., 29 (2012) 1700-1707.

[44] K. Dong, R. Sang, Z. Wei, J. Liu, R. Dühren, A. Spannenberg, H. Jiao, H. Neumann, R. Jackstell, R. Franke, Cooperative catalytic methoxycarbonylation of alkenes: uncovering the role of palladium complexes with hemilabile ligands, Chemical science, 9 (2018) 2510-2516.

[45] A.F. Schmidt, A. Al-Halaiqa, V.V. Smirnov, Effect of macrokinetic factors on the ligand-free Heck reaction with non-activated bromoarenes, J. Mol. Catal. A: Chem., 250 (2006) 131-137.

[46] H.A. Ghaly, A.S. El-Kalliny, T.A. Gad-Allah, N.E.A. El-Sattar, E.R. Souaya, Stable plasmonic Ag/AgCl–polyaniline photoactive composite for degradation of organic contaminants under solar light, RSC adv., 7 (2017) 12726-12736.

[47] T. Iwasawa, M. Tokunaga, Y. Obora, Y. Tsuji, Homogeneous palladium catalyst suppressing Pd black formation in air oxidation of alcohols, J. Am. Chem. Soc., 126 (2004) 6554-6555.

[48] C. Arderne, l.A. Guzei, C.W. Holzapfel, T. Bredenkamp, Branched Selectivity in the Pd-Catalysed Methoxycarbonylation of 1-Alkenes, ChemCatChem, 8 (2016) 1084-1093.

[49] B. Hendriksen, J. Frenken, CO oxidation on Pt (110): scanning tunneling microscopy inside a high-pressure flow reactor, Phys. Rev. Lett., 89 (2002) 046101.

[50] R.E. Harmon, S. Gupta, D. Brown, Hydrogenation of organic compounds using homogeneous catalysts, Chem. Rev., 73 (1973) 21-52.

[51] H.S. Yun, K.H. Lee, J.S.J.J.o.M.C.A.C. Lee, The regioselective hydrocarboalkoxylation of 4-methylstyrene catalyzed by palladium complexes, 95 (1995) 11-17.

[52] T.A. Tshabalala, S.O. Ojwach, M.A. Akerman, Palladium complexes of (benzoimidazol-2-ylmethyl) amine ligands as catalysts for methoxycarbonylation of olefins, J. Mol. Catal. A: Chem., 406 (2015) 178-184.

[53] F. Stempfle, D. Quinzler, I. Heckler, S. Mecking, Long-chain linear C19 and C23 monomers and polycondensates from unsaturated fatty acid esters, Macromolecules, 44 (2011) 4159-4166.

[54] M. Rosales, I. Pacheco, J. Medina, J. Fernández, Á. González, R. Izquierdo, L.G. Melean, P.J. Baricelli, Kinetics and mechanisms of homogeneous catalytic reactions. Part 12. Hydroalcoxycarbonylation of 1-hexene using palladium/triphenylphosphine systems as catalyst precursors, Catal. Lett., 144 (2014) 1717-1727.

[55] J.A. Widegren, R.G. Finke, A review of the problem of distinguishing true homogeneous catalysis from soluble or other metal-particle heterogeneous catalysis under reducing conditions, J. Mol. Catal. A: Chem., 198 (2003) 317-341.

[56] P. Santra, P. Sagar, Dihydrogen reduction of nitroaromatics, alkenes, alkynes using Pd (II) complexes both in normal and high pressure conditions, J. Mol. Catal. A: Chem., 197 (2003) 37-50.

[57] R. Pruvost, J. Boulanger, B. Léger, A. Ponchel, E. Monflier, M. Ibert, A. Mortreux, T. Chenal, M. Sauthier, Synthesis of 1, 4: 3, 6-Dianhydrohexitols Diesters from the Palladium-Catalyzed Hydroesterification Reaction, ChemSusChem, 7 (2014) 3157-3163.

[58] H. Schulz, M. Claeys, Reactions of α-olefins of different chain length added during Fischer–Tropsch synthesis on a cobalt catalyst in a slurry reactor, Appl Catal A- Gen, 186 (1999) 71-90.

[59] E. Guiu, M. Caporali, B. Munoz, C. Müller, M. Lutz, A.L. Spek, C. Claver, P.W. van Leeuwen, Electronic effect of diphosphines on the regioselectivity of the palladium-catalyzed hydroesterification of styrene, Organometallics, 25 (2006) 3102-3104.

Chapter 4

Structural studies and applications of water-soluble (phenoxy)imine palladium(II) complexes as catalysts in biphasic methoxycarbonylation of 1-hexene

This chapter is adapted from the paper published in the Journal of Organometallic Chemistry 942, 2021, 121812 and is wholly based on the work of the first author, Saphan Akiri. The contribution of the first author, Saphan Akiri, include ligand and complex synthesis and characterization, methoxycarbonylation catalysis as well as drafting the manuscript.

4.1 Introduction

The use of catalysts in industrial processes has triggered a significant increase in the production of various domestic and industrial products [1]. This mass production has, on the other hand, led to environmental concerns, which in turn has triggered the search and development of greener catalytic processes [2, 3]. While the principles of green chemistry call for catalysts that can be recycled and reused to minimize waste, the use of homogeneous catalysts in various industrial processes is still unavoidable [4]. This is mainly due to the selective nature of the homogeneous catalyst systems [5, 6]. As such, various methods have been developed to make the homogeneous catalysts recyclable while maintaining their selectivity. Some approaches that are currently being adopted include the use of inorganic supports such as silica [7], magnetic supports [8], and polymer supports [9] and, more recently, the use of supported ionic liquid phases [10].

Another technology that has also not been left behind in this venture is the use of biphasic homogeneous catalyst systems [11]. Even though the most widely used combination of liquids

in biphasic catalysis entails an organic-aqueous biphasic system, other combinations include organic-organic biphasic, and of more recent, fluorinated solvents, and ionic liquids [12]. In addition to the ease of separation and recycling of biphasic systems, utilizing water is attractive due to its lower cost and non-toxicity [13, 14]. While biphasic catalysts have been widely applied in hydroformylation reactions [15-17], Heck-coupling [18, 19], Suzuki-Miyaura coupling [20, 21], olefin oligomerization [22, 23] and hydrogenation reactions [24-26], among others, there are limited reports of the same in the methoxycarbonylation reactions [27, 28].

Methoxycarbonylation of olefins has gained interest due to the production of valuable ester products. Despite the fact that biphasic catalysis provides a suitable route for catalyst recycling and reuse, far much fewer reports on the use of water-soluble catalysts in methoxycarbonylation. This chapter reports the design of water-soluble palladium(II) complexes and their applications as biphasic catalysts in the methoxycarbonylation of 1-hexene. The non-water-soluble palladium(II) analogues have also been studied for comparison purposes. Detailed structural studies of the palladium(II) complexes, the influence of catalyst structure on catalytic behaviour and catalyst recycling have been investigated and are herein discussed.

4.2 Experimental section

4.2.1 Instrumentation and general materials

The reagents aniline (>99.5%), 2,6- dimethyl aniline (99%), 2, 6- diisopropylaniline (90%), salicylaldehyde (98%), sodium carbonate, glacial acetic acid (>98%), palladium acetate (98%), sulphuric acid, 2-methoxyethylamine (98%) were purchased from Sigma-Aldrich and were used as received without further purification. Sodium 3-formyl-4-

hydroxybenzenesulfonate was synthesised following a modified route of a previously reported procedure. Ligands **L9** and **L10** and their respective complexes **Pd9** and **Pd10**, having been reported before [29], were synthesised and used for comparison purposes with their water-soluble analogues. NMR, IR, elemental analyses and single-crystal X-ray crystallography was done as indicated in Chapter 3

4.2.2 Synthesis of water-soluble (phenoxy)imine ligands and palladium(II) complexes

*4.2.2.1 Sodium (E)-4-hydroxy-3-((phenylimino)methyl)benzenesulfonate (**L6**)*

To a solution of sodium 3-formyl-4-hydroxybenzenesulfonate (0.30 g, 1.34 mmol) in toluene 15 (ml) was added aniline (0.18 ml, 2.00 mmol). The mixture was then heated under reflux for 72 h using a Dean-Stark apparatus to give a yellow solution. The solvent was eliminated under reduced pressure to afford a yellow solid. The crude product was subsequently washed with 2 ml each of chloroform, dichloromethane and diethyl ether to give **L6** as bright yellow solid. Yield = 0.26 g (84 %). ^{1}H NMR (400 MHz, DMSO): δ_H (ppm); 6.91 (d, 1H, $^3J_{HH}$ = 8.40 Hz, 6-PhOH), 7.33 (t, 1H, $^3J_{HH}$ = 6.80 Hz, 4-Ph), 7.46 (m, 4H, 2,3,5 6-Ph), 7.63 (dd, 1H, $^3J_{HH}$ = 6.40 Hz, 5-PhOH, $^4J_{HH}$ = 2.20 Hz, 5-PhOH), 7.95(d, 1H, $^4J_{HH}$ = 2.20 Hz, 3-PhOH), 9.02 (s, 1H, H$_{imine}$), 13.28 (s, OH, 1H). ^{13}C NMR (100 MHz, DMSO, δ ppm): 163.7 (C-OH), 160.8 (CH-N), 148.4 (Ar-C), 140.4 (C-SO$_3$), 131.3 (Ar-C), 129.9 (Ar-C), 127.4 (Ar-C), 121.9 (Ar-C), 118.4 (Ar-C), 116.2 (Ar-C), 114.3 (Ar-C). IR ν_{max}/ cm^{-1}: $\nu_{(C=N)}$ = 1615, $\nu_{(O-H)}$ = 3428. HRMS-ESI; Calc: 299.0228; Found: 299.0221.

*4.2.2.2 Sodium (E)-3-(((2,6-dimethylphenyl)imino)methyl)-4-hydroxybenzenesulfonate (**L7**)*

To a solution of 3-formyl-4-hydroxybenzenesulfonate (0.20 g, 0.89 mmol) in toluene (15 ml), was added 2, 6 dimethyl aniline (0.12 ml, 1.34 mmol) and a 0.5 mol% of *para*-tolyl sulfonic acid. The mixture was then refluxed using a Dean-Stark apparatus for 48 h to afford a yellow solution. The solvent was then removed under reduced pressure to give ligand **L7** as a yellow

solid. Yield = 0.25 g (86 %). ^{1}H NMR (400 MHz, DMSO): δ_H (ppm); 2.14 (s, 6H, Ph-CH$_3$), 6.61 (d, 2H, $^3J_{HH}$ = 7.40 Hz, 3,5-Ph), 6.94 (d, 1H, $^3J_{HH}$ = 8.40 Hz, 6-PhOH), 7.05 (t, 1H, $^3J_{HH}$ = 7.20 Hz, 4-Ph) 7.68 (dd, 1H, $^3J_{HH}$ = 8.00 Hz, $^4J_{HH}$ = 2.36 Hz, 5-PhOH), 7.93(d, 1H, $^4J_{HH}$ = 2.12 Hz, 3-PhOH), 8.66 (s, 1H, H$_{imine}$). ^{13}C NMR (100 MHz, DMSO, δ ppm): 164.6 (C-OH), 161.9 (CH-N), 157.7 (Ar-C), 149.9 (C-SO$_3$), 148.6 (Ar-C), 133.7 (Ar-C), 133.4 (Ar-C), 123.6 (Ar-C), 121.1 (Ar-C), 119.1 (Ar-C), 117.2 (Ar-C) , 20.9 (C-H$_3$): IR ν_{max}/ cm^{-1}: $\nu_{(C=N)}$ =1617, $\nu_{(O-H)}$ =3401. HRMS-ESI; Calc: 327.0541; Found: 327.0502.

*4.2.2.3 Sodium(E)-3-(((2,6-diisopropylphenyl)imino)methyl)-4-hydroxybenzenesulfonate (**L8**)*

L8 was synthesized following the procedure described for ligand **L7** using 3-formyl-4-hydroxybenzenesulfonate (0.20 g, 0.89 mmol) and 2, 6 diisopropylaniline (0.23 ml, 1.34 mmol). Yield = 0.30 (88 %). ^{1}H NMR (400 MHz, DMSO): δ_H (ppm); 1.16 (d, 12H, $^3J_{HH}$ = 5.50 Hz ipr), 3.05 (m, 2H, CH$_3$CH$_3$C$\underline{H}$), 6.96 (d, 2H, $^3J_{HH}$ = 6.80 Hz, 3,5-Ph), 7.20 (t, 1H, $^3J_{HH}$ = 10.40 Hz, 4-Ph) 7.68 (dd, 1H, $^3J_{HH}$ = 8.00 Hz, $^4J_{HH}$ = 1.76 Hz, 5-Ph-OH), 7.96 (d, 1H, $^4J_{HH}$ = 1.72 Hz, 3-PhOH), 8.63 (s, 1H, H$_{imine}$). ^{13}C NMR (100 MHz, DMSO, δ ppm): 167.4 (C-OH), 160.7 (CH-N), 140.4 (Ar-C), 138.4 (C-SO$_3$), 131.4 (Ar-C), 129.8 (Ar-C), 128.5 (Ar-C), 126.0 (Ar-C), 123.6 (Ar-C), 118.1 (Ar-C), 116.3 (Ar-C), 31.1 (C-CH$_3$), 28.2 (C-H$_3$): IR ν_{max}/ cm^{-1}: $\nu_{(C=N)}$ = 1619, $\nu_{(O-H)}$ = 3464. HRMS-ESI; Calc: 383.1167; Found: 383.1103.

*4.2.2.4 (E)-2-((phenylimino)methyl)phenol (**L9**)*

To a solution of salicylaldehyde (0.85 ml, 8.00 mmol) in methanol (15 ml) was added aniline (0.73 ml, 8.00 mmol) with stirring. The reaction was the stirred for a further 24 h under room temperature. The solvent was then removed under reduced pressure to afford **L9** as bright yellow solid. Yield =1.48 g (94%). ^{1}H NMR (400 MHz, CDCl3): δ_H (ppm); 6.97 (m, 1H, 6PhOH), 7.07 (d, 1H, $^3J_{HH}$ = 6.60 Hz, 4Ph), 7.30 (m, 3H, Ar), 7.43 (m 4H, Ar), 8.65 (s, 1H, H$_{imine}$). 13.28 (s, OH, 1H). ^{13}C NMR (100 MHz, DMSO, δ ppm): 162.7 (C-OH), 161.2 (CH-N), 148.5 (Ar-C), 133.1 (Ar-C), 132.2 (Ar-C), 129.4 (Ar-C), 126.9 (Ar-C), 121.2 (Ar-C), 119.1

(Ar-C), 117.2 (Ar-C). IR $\nu_{max}/$ cm^{-1}: $\nu_{(C=N)} = 1612$, $\nu_{(O-H)} = 3054$. HRMS-ESI; Calc: 197.0841; Found: 197.0785.

*4.2.2.5 (E)-2-(((2,6-dimethylphenyl)imino)methyl)phenol (**L10**)*

To a solution of salicylaldehyde (0.85 ml, 8.00 mmol) in methanol (20 ml) was added 2,6 dimethyl aniline (0.99 ml, 8.00 mmol). The mixture was then refluxed for 24 hrs to give a yellow solution. The solvent was then removed under reduced pressure to reveal **L10** as a yellow oil. Yield = 1.6 g (89 %). ^{1}H NMR (400 MHz, CDCl$_3$): δ_H (ppm); 2.10 (s, 6H, Ar-CH$_3$), 6.99 (d, 2H, $^{3}J_{HH}$ = 7.80 Hz, 3,5Ph), 7.03 (d, 1H, $^{3}J_{HH}$= 6.84 6PhOH),7.10 (d, 2H, $^{3}J_{HH}$ = 7.60 Hz, 4Ph,4PhOH), 7.45 (t, 1H, $^{3}J_{HH}$ = 7.36 Hz, 5PhOH), 7.59 (d, 1H, $^{3}J_{HH}$ = 6.36, 3PhOH), 8.51 (s, 1H, H$_{imine}$). ^{13}C NMR (100 MHz, CDCl3, δ ppm): 166.8 (*C*-OH), 161.3 (*C*H=N), 148.2 (Ar-C), 133.2 (Ar-C), 134.2 (Ar-C), 128.4 (Ar-C), 128.3(Ar-C), 125.0 (Ar-C), 119.0 (Ar-C) ,118.8 (Ar-C), 117.3 (Ar-C), 18.5 (C-H$_3$): IR $\nu_{max}/$ cm^{-1}: $\nu_{(C=N)} = 1619$, $\nu_{(O-H)} = 3019$. HRMS-ESI; Calc: 225.1154; Found: 225.1002.

*4.2.2.6 (E)-2-(((2,6-diisopropylphenyl)imino)methyl)phenol (**L11**)*

To a solution of salicylaldehyde (0.85 ml, 8.00 mmol) in toluene (15 ml), was added 2, 6 diisopropylaniline (1.51 ml, 8.00 mmol) with stirring. The reaction was then refluxed using a Dean-Stark apparatus for 72 h to give a yellow solution. The solvent was then removed under reduced pressure to afford **L11** as a yellow oil yield. Yield = 2.08 g (92%). ^{1}H NMR (400 MHz, CDCl$_3$): δ_H (ppm); 1.26 (d, 24 H, $^{3}J_{HH}$ = 5.48 Hz, ipr), 3.10 (m, 4H, CH$_3$CH$_3$C$\underline{H}$) 7.04 (d, 2H, $^{3}J_{HH}$ = 6.00 Hz, 4-PhO), 7.14 (d, 2H, $^{3}J_{HH}$ = 6.60 Hz, 6-PhO),7.28 (m, 3H, 3,5-PhN, 5-PhOH), 7.42 (d, 1H, $^{3}J_{HH}$ = 6.20 Hz, 3-PhO), 7.49 (t, 1H, $^{3}J_{HH}$ = 7.00 Hz, 4-Ph), 8.38 (s, 1H, H$_{imine}$). ^{13}C NMR (100 MHz, CDCl$_3$, δ ppm):166.6 (CH-N), 161.2 (C-O), 146.1 (Ar-C), 138.8 (Ar-C), 134.9 (Ar-C), 133.3 (Ar-C), 132.3(Ar-C), 125.5 (Ar-C), 123.3 (Ar-C) ,119.1 (Ar-C),

117.4 (Ar-C), 28.1(C(CH$_3$)$_2$), 23.5(C-iPr): IR ν_{max}/ cm^{-1}: $\nu_{(C=N)}$ = 1617, $\nu_{(O-H)}$ = 3060. HRMS-ESI; Calc: 281.1779; Found: 281.1543.

*4.2.2.7 Sodium (E)-4-hydroxy-3-((phenylimino)methyl)benzenesulfonate palladium(II) (**Pd6**)*

To a solution of Pd(OAc)$_2$ (0.07 g, 0.31 mmol) in methanol (10 ml), was added a solution of **L6** (0.19 g, 0.62 mmol) in methanol (5 ml). The mixture was then stirred under nitrogen atmosphere for 24 h to give a yellow mixture which was filtered and recrystallized using small portions of hexane to afford a bright yellow solid. Yield = 0.17 g (78 %). ^{1}H NMR (400 MHz, DMSO): δ$_H$ (ppm); 5.85 (d, 2H, $^3J_{HH}$ = 8.80 Hz, 6PhO), 7.34-7.47 (m, 12H, Ar) 7.71 (d, 2H, $^4J_{HH}$ = 2.28 Hz, 3-PhO), 8.07 (s, 2H, H$_{imine}$). ^{13}C NMR (100 MHz, DMSO, δ ppm): 164.6 (CH-N), 164.2 (C-O), 149.2 (Ar-C), 136.2 (C-SO$_3$),133.4 (Ar-C), 132.7 (Ar-C), 128.4 (Ar-C), 126.8 (Ar-C), 125.1 (Ar-C), 119.2 (Ar-C), 119.1 (Ar-C).IR ν_{max}/ cm^{-1}: $\nu_{(C=N)}$ = 1605, ESI-MS (m/z) = 678([M-Na]$^+$,95%). CHN. Anal. Calc. for C$_{26}$H$_{18}$N$_2$Na$_2$O$_8$PdS$_2$: C, 44.42; H, 2.58; N, 3.99. Found: C, 44.59; H, 2.50; N, 4.03.

*4.2.2.8 Sodium (E)-3-(((2,6-dimethylphenyl)imino)methyl) benzenesulfonate palladium(II) (**Pd7**)*

Complex **Pd7** was synthesized using the method outlined for **Pd6** using Pd(OAc)$_2$ (0.05 g, 0.22 mmol) and **L7** (0.14 g, 0.44 mmol). Yield = 0.13 g (81%). ^{1}H NMR (400 MHz, DMSO): δ$_H$ (ppm); 2.14 (s, 12H, Ar-CH$_3$), δ$_H$ 5.78 (d, 2H, $^3J_{HH}$ = 8.8 Hz, Ar), 6.80 (d, 2H, $^3J_{HH}$ = 7.2 Hz, Ar), 7.34-7.47 (m, 6H, Ar) 7.65 (d, 2H, $^3J_{HH}$ = 2.0 Hz, Ar), 7.89 (s, 2H, H$_{imine}$). ^{13}C NMR (100 MHz, DMSO, δ ppm): 166.1 (CH-N), 162.9 (C-O), 149.1 (Ar-C), 146.1 (C-SO$_3$), 136.2 (Ar-C), 133.7(Ar-C), 128.1 (Ar-C), 124.6 (Ar-C), 121.1 (Ar-C), 119.1 (Ar-C) ,115.1 (Ar-C), 23.5 (C-H$_3$) IR ν_{max}/ cm^{-1}: $\nu_{(C=N)}$ = 1607, ESI-MS (m/z) = 780.99([M+Na]$^+$,25%). CHN. Anal. Calc. for C$_{30}$H$_{26}$N$_2$Na$_2$O$_8$PdS$_2$: C, 47.47; H, 3.45; N, 3.69. Found: C, 47.41; H, 3.50; N, 3.58.

*4.2.2.9 Sodium (E)-3-(((2,6-diisopropylphenyl)imino)methyl)benzenesulfonate (**Pd8**)*

Compound **Pd8** was synthesized using the method described for **Pd6** using Pd(OAc)$_2$ (0.05 g, 0.22 mmol) and **L8** (0.17 g, 0.44 mmol). Yield = 0.16 g (84%). ^{1}H NMR (400 MHz, DMSO): δ_H (ppm); 1.16 (d, 24H, $^3J_{HH}$ = 6.8 Hz ipr), 3.05 (m, 4H, CH$_3$CH$_3$C$\underline{H}$), δ_H 5.73 (d, 2H, $^3J_{HH}$ = 8.8Hz, Ar), 6.80 (d, 2H, $^3J_{HH}$ = 7.2 Hz, Ar), 7.34-7.47 (m, 6H, Ar) 7.65 (d, 2H, $^3J_{HH}$ = 2.0 Hz), 7.95 (s, 2H, H$_{imine}$). ^{13}C NMR (100 MHz, DMSO, δ ppm): 165.4 (CH-N), 162.7(C-O), 146.1 (Ar-C), 140.2 (C-SO$_3$), 134.4 (Ar-C), 133.7 (Ar-C), 128.1 (Ar-C), 124.6 (Ar-C), 123.5 (Ar-C), 120.7(Ar-C), 119.2 (Ar-C), 31.2 (C-CH$_3$), 28.1 (C-H$_3$). IR ν_{max}/ cm^{-1}: $\nu_{(C=N)}$ = 1604. ESI-MS (m/z) = 893.20([M+Na]$^+$,100%). CHN. Anal. Calc. for C$_{38}$H$_{42}$N$_2$Na$_2$O$_8$PdS$_2$: C, 52.38; H, 4.86; N, 3.22. Found: C, 52.29; H, 4.80; N, 3.33.

*4.2.2.10 (E)-2-((phenylimino)methyl)phenol palladium(II) (**Pd9**)*

To solution of **L9** (0.18 g, 0.88 mmol) in chloroform (10 ml) was added a solution of Pd(OAc)$_2$ (0.10 g, 0.44 mmol) in chloroform (5 ml). The mixture was then stirred for 24 h to give a yellow product which was then filtered and recrystallized using hexane to afford bright yellow crystals. Yield = 0.19 g (86%).^{1}H NMR (400 MHz, CDCl$_3$): δ_H (ppm); 6.14 (d, 2H, $^3J_{HH}$ = 8.4Hz, Ar), 6.52 (t, 2H, $^3J_{HH}$ = 7.8 Hz, Ar), 7.16 (m, 4H), 7.37 (m, 6H, Ar), 7.45 (m, 4H, Ar), 7.76 (s, 2H, H$_{imine}$). 13.28 (s, OH, 1H). ^{13}C NMR (100 MHz, CDCl3, δ ppm): 165.1 (CH-N), 162.8 (C-O), 149.5 (Ar-C), 135.2 (Ar-C), 134.4 (Ar-C), 128.1 (Ar-C), 126.4 (Ar-C), 124.6 (Ar-C), 120.7, (Ar-C), 120.1 (Ar-C), 115.1 (Ar-C).IR ν_{max}/ cm^{-1}: $\nu_{(C=N)}$ = 1588, ESI-MS (m/z) = 475.05([M+Na]$^+$, 90%).

*4.2.2.11(E)-2-(((2,6-dimethylphenyl)imino)methyl)phenol palladium (II)(**Pd10**)*

Pd10 was synthesized following the procedure used for **Pd9** using Pd(OAc)$_2$ (0.17 g, 0.78 mmol) and **L10** (0.34 g, 1.55 mmol). Yield = 0.38 g (88 %). ^{1}H NMR (400 MHz, CDCl$_3$): δ_H (ppm); 2.40 (s, 12 H, Ar-CH$_3$), 6.09 (d, 2H, $^3J_{HH}$ = 8.8 Hz, Ar), 6.49 (m, 2H, Ar),7.16 (m, 10H, Ar), 7.53 (s, 2H, H$_{imine}$). ^{13}C NMR (100 MHz, CDCl3, δ ppm):165.7 (CH-N), 163.0 (C-

O), 147.4 (Ar-C), 135.0 (Ar-C), 134.2 (Ar-C), 132.0 (Ar-C), 127.5(Ar-C), 126.0 (Ar-C), 120.6 (Ar-C) , 120.3 (Ar-C), 114.6 (Ar-C), 18.9(C-H$_3$): IR ν_{max}/ cm^{-1}: $\nu_{(C=N)}$ = 1605.

4.2.2.12 (E)-2-(((2,6-diisopropylphenyl)imino)methyl)phenol palladium(II) (Pd11)

Complex **Pd11** was synthesized following the procedure used for **Pd9** using Pd(OAc)$_2$ (0.17 g, 0.44 mmol) and **L11** (0.25 g, 0.88 mmol). Yield = 0.25 g (84 %). ^{1}H NMR (400 MHz, CDCl$_3$): δ_H (ppm); 1.20 (d, 24 H, $^3J_{HH}$ = 5.4 Hz, ipr), 3.54 (m, 4H, CH$_3$CH$_3$C$\underline{H}$) 6.01 (d, 2H, $^3J_{HH}$ = 6.72 Hz, 4-PhO), 6.46 (m, 2H, 4-PhO),7.10(m, 4H, 3,5-Ph), 7.21 (d, 4H, $^3J_{HH}$ = 6.2 Hz, 5-PhO, 4Ph), 7.35 (t, 2H, $^3J_{HH}$ = 6.12 Hz 3-PhO), (s, 2H, H$_{imine}$). ^{13}C NMR (100 MHz, CDCl3, δ ppm):165.5 (CH-N), 162.7 (C-O), 144.8 (Ar-C), 142.4 (Ar-C), 134.8 (Ar-C), 134.3 (Ar-C), 126.6(Ar-C), 122.8 (Ar-C)120.8 (Ar-C), 119.5 (Ar-C) ,114.2 (Ar-C), 28.8 (C(CH3)$_2$) 24.3 (C-iPr): IR ν_{max}/ cm^{-1}: $\nu_{(C=N)}$ = 1603. CHN. Anal. Calc. for C$_{38}$H$_{44}$N$_2$O$_2$Pd: C, 68.41; H, 6.65; N, 4.20. Found: C, 68.36; H, 6.70; N, 4.26.

4.2.2.13 Reactions of Pd9 with PPh$_3$ to form [Pd(PPh$_3$)$_2$(L9)]$^+$(Pd12)

To a solution of complex **Pd9** (0.10 g, 0.20 mmol) in chloroform (10.0 ml) was added NaBPh$_4$ (0.07 g, 0.20 mmol) and PPh$_3$ (0.11 g, 0.40 mmol) in chloroform (5.0 ml). The resulting yellow solution mixture was then stirred at room temperature for 24 h. The solution was the filtered, concentrated in *vacuo* and hexane (10 ml) used to precipitate compound [Pd(PPh$_3$)$_2$(**L9**)]$^+$ as a yellow solid. Yield = 0.12 g (80%). ^{1}H NMR (400 MHz, CDCl3): δ_H (ppm); 6.13 (d, 1H, $^3J_{HH}$ = 8.4 Hz, Ar), 6.54 (t, 1H, $^3J_{HH}$ = 7.8 Hz, Ar), 6.83 (m, 1H, Ar), 7.05 (m, 2H, Ar), 7.23 (m, 6H, Ar), 7.33-7.50 (m, 30H, Ar, BPh$_4$), 7.52-7.68 (m, 8H, Ar), 7.71-7.78 (m, 10H, Ar) 7.84 (s, 1H, H$_{imine}$). ^{31}P NMR (CDCl3): δ 23.24 (s, 1P, PPh$_3$), 29.30 (s, 1P, PPh$_3$).

4.2.3 Catalyst recycling experiments

The water-soluble complexes were recycled using a developed procedure. For instance, by the end of a reaction using complex **Pd6**, the reactor's temperature was let to adjust to the ambient temperature. The unused carbon monoxide was then eliminated by venting, and the reactor contents were placed into a measuring cylinder and given time to stand for phase separation. Using a decantation procedure, the organic phase was obtained and taken back to the reactor, followed by the addition of toluene, HCl, PPh$_3$ and substrate. The reaction was then commenced for the subsequent run.

4.3. Results and discussion

4.3.1 Synthesis of (phenoxy)imine ligands and their palladium(II) complexes

The sulfonated salicylaldehyde sodium 3-formyl-4-hydroxybenzenesulfonate synthon was synthesized according to a modified reported procedure [30, 31]. While the (phenoxy)imine sulfonate ligand **L6** was synthesised by refluxing using a Dean-Stark apparatus for 72 h, ligands **L7** and **L8** were synthesised under reflux using catalytic amounts of *para*-tolyl sulfonic acid for 48 h (Scheme 4.1). The non-water-soluble (phenoxy)imine analogue **L9** was synthesized by stirring at room temperature, while compounds **L10** and **L11** were synthesized by reflux in toluene. All the new ligands were obtained in high yields of 84-88%. Reactions of ligands **L6**-**L11** with Pd(OAc)$_2$ acetate at room temperature afforded the respective complexes **Pd6**-**Pd11** in moderate to good yields (Scheme 4.1).
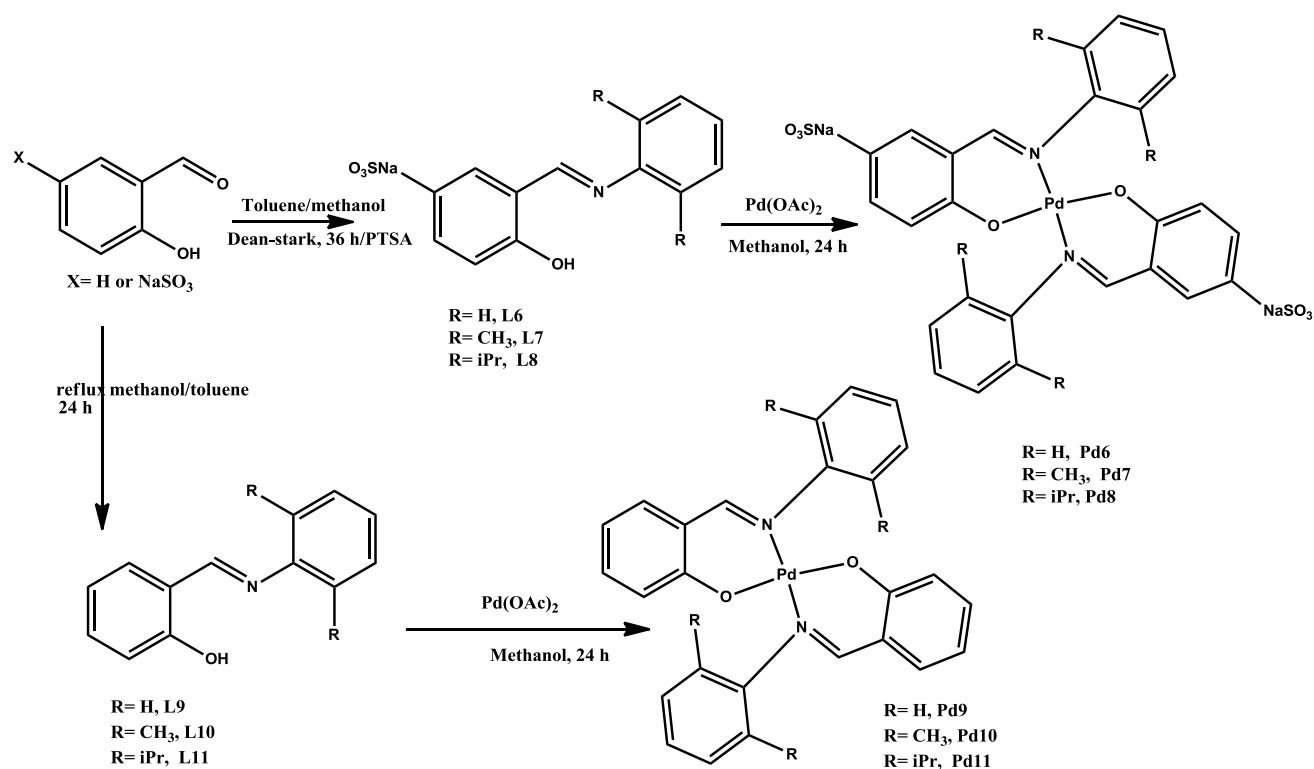
Scheme 4.1: Synthesis of water and non-water-soluble (phenoxy)imine ligands and their respective palladium(II) complexes

^{1}H NMR, ^{13}C NMR and IR spectroscopies, mass spectrometry and elemental analyses were employed to identify all the new compounds. In the ^{1}H NMR spectra, the aldimine protons were observed between 8.52 to 9.02 ppm for ligands **L6- L11,** consistent with previous reports [32, 33]. The same imine proton was traced and used to infer the formation of the respective palladium(II) complexes. For instance, whereas the imine proton was observed at 9.02 ppm in ligand **L6,** the same proton shifted up-field to 8.07 ppm in the respective complex **Pd6** (Figure 4.1).
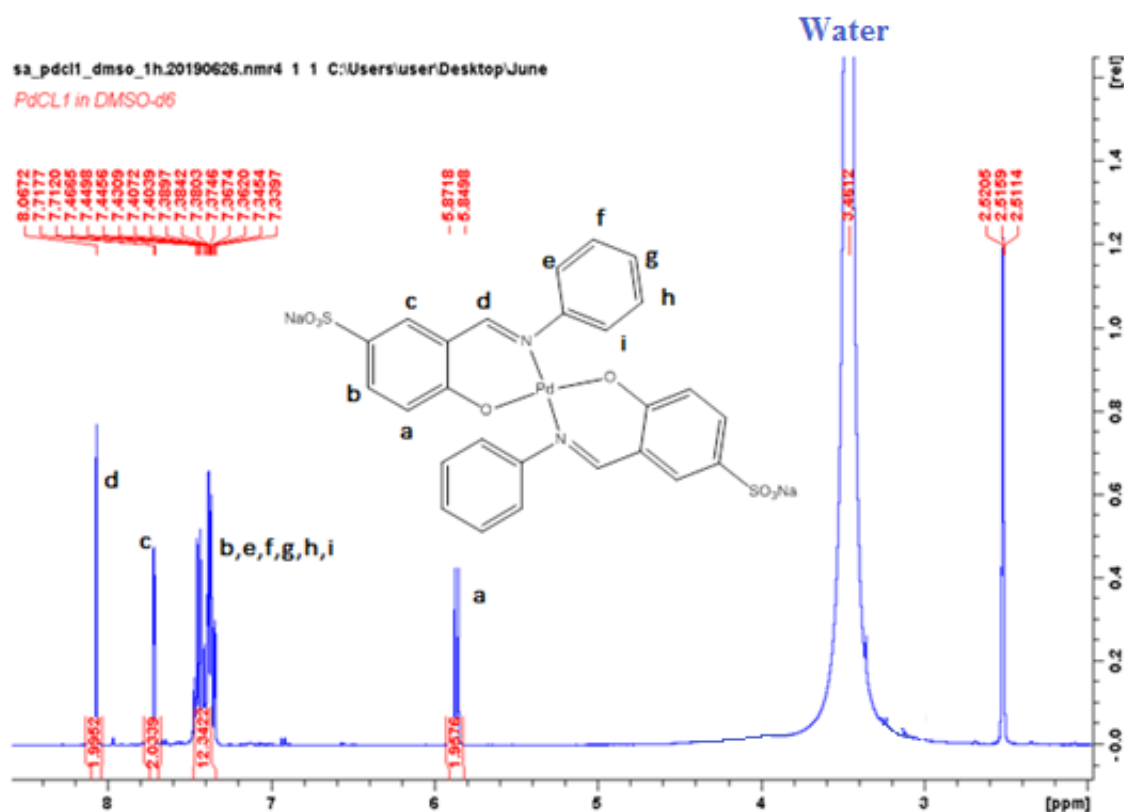
Figure 4.1: ¹HNMR of complex **Pd6** showing the shift in imine peak to 8.07 ppm from 9.02 ppm observed in the respective ligand **L6**.

¹³C NMR was also used as a characterization tool for the synthesized ligands and complexes. The expected carbon shifts were observed in all the complexes and ligands. For example, the shift of imine carbon shift was useful in inferring the successful formation of the expected compounds. While the imine carbon resonated at 160.8 ppm in ligand **L6,** the same carbon was observed to resonate at 164.1 ppm in complex **PdL6** (Figure 4.2), showing a change in the chemical environment upon the complex formation.
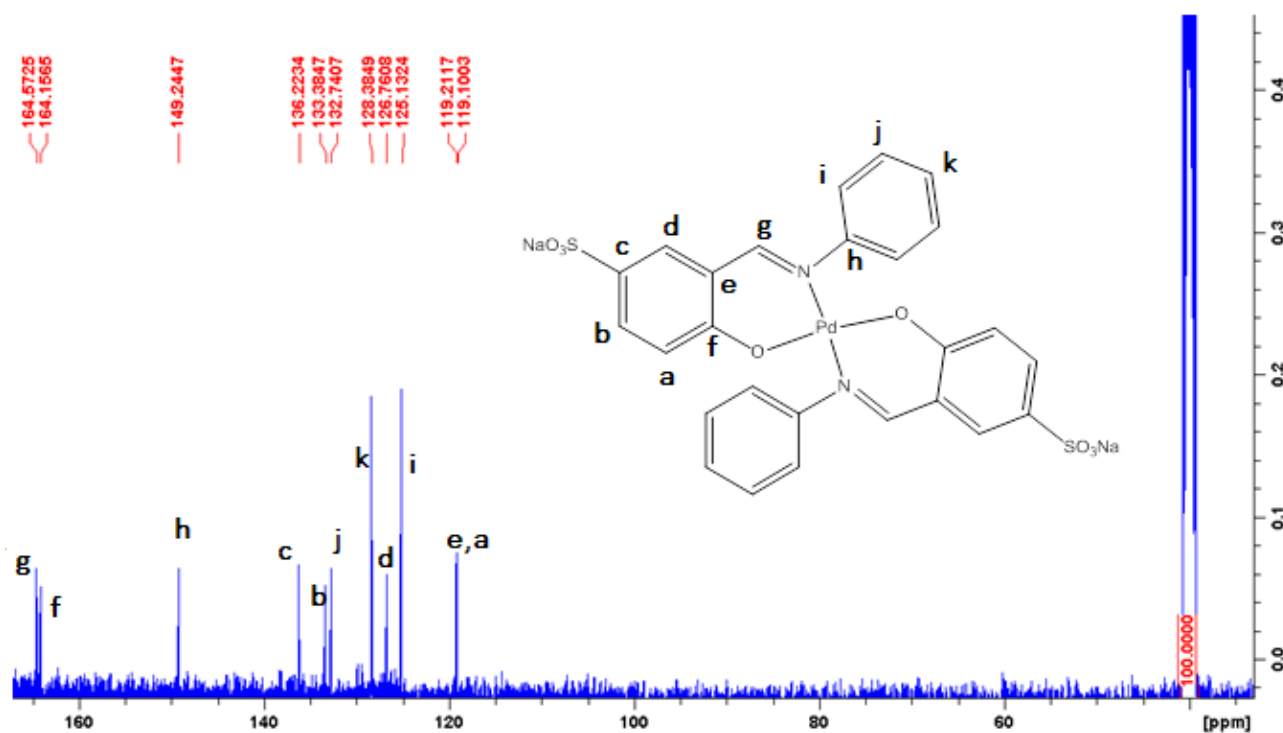
Figure 4.2: ^{13}C NMR of complex **Pd6** showing a downward shift of imine carbon to 164.1 ppm from 160.8 ppm observed in ligand **L6**

The FT-IR data of the ligands showed $v_{(C=N)}$ diagnostic peaks between 1605 and 1619 cm^{-1} [33]. Upon complexation, general shifts in the absorption ranges of the imine bond were recorded. To demonstrate this, while the $v_{(C=N)}$ for **L6** was recorded at 1605 cm^{-1}, complex **Pd6** showed the same signal at 1615 cm^{-1}. Another important feature of the IR spectra was the OH functionality. While the IR spectra of the ligands showed the $v_{(O-H)}$ signals between 3 060 cm^{-1} to 3 464 cm^{-1}, the respective complexes did not display this peak (Figure 4.3), confirming deprotonation of the phenolic proton upon coordination to give the anionic ligands [34].

Figure 4.3: IR spectrum of complex **Pd6** showing the disappearance of the OH peak and the shifting of imine peak to 1615 cm^{-1} from 1605 as observed in ligand **L6**.

Mass spectrometry was further used to confirm the molecular masses of both the ligands and the respective complexes by comparing the experimental and theoretical isotopic mass distribution patterns. For instance, complex **Pd6** (Mw = 701.93) showed a molecular ion peak at 678.93 ([M-Na]$^+$, consistent with the theoretical isotopic mass distribution (Figure 4.4). Similar observations were recorded for all the ligands and the respective palladium(II) complexes (Table 4.1). The elemental analyses data supported the presence of two ligand units per palladium(II) atom, thus confirming that the bulk material is pure.
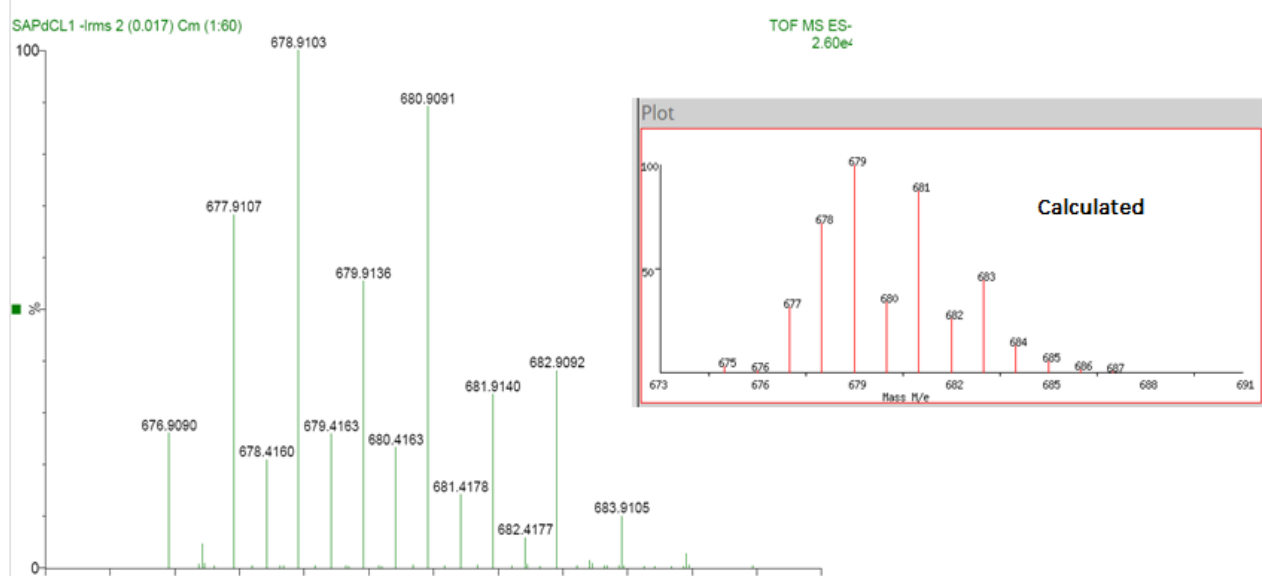
Figure 4.4: An overlaid mass spectra of ligand **Pd6** (ESI-MS (m/z) = 678([M-Na]+) showing the found and calculated peak patterns.

Table 4.1: A table showing mass spectra of the ligands and complexes

Compound	Molar mass (gmol^{-1})	m/z (amu)
L6	299.02	276.02 [M-Na]$^+$
L7	327.05	304.05 [M-Na]$^+$
L8	383.12	360.12 [M-Na]$^+$
Pd6	701.93	724.93([M+Na]$^+$
Pd7	757.99	780.99([M+Na]$^+$
Pd8	870.12	893.20([M+Na]$^+$

4.3.2. X-ray molecular structures of complexes Pd6 and Pd11

Single crystal suitable for X-ray analyses of complexes **Pd6** and **Pd11** were obtained by slow diffusion of hexane into their respective concentrated solutions in chloroform at room temperature. Table 4.2 shows the structural refinement parameters and crystallographic data, while Figures 4.4 and 4.5 represent the molecular structures, selected bond angles and bond lengths of complexes **Pd6** and **Pd11,** respectively. Complex **Pd6** consists of the Pd centre atom with two anionic bidentate ligand units to form a square planar coordination environment around the palladium(II) atom and the two O and two N donor atoms in a *trans*-configuration. The charge stabilization of the **Pd6** is accomplished by the cationic sodium-aqua complex. Only half of the anionic Pd complex, one hydrate molecule and a cationic sodium-aqua complex exist in the asymmetric unit (Figure 4.5 b). The Pd atom rests on an inversion centre; hence it has a site occupancy factor of 0.5. The oxidation state of Pd in the asymmetric unit, thus +1 whilst the ligand bears a -2 charge from the phenolate (-1) and sulfonate (-1) moieties. Thus, the Pd complex is anionic (-1 overall charge) and is balanced by the cationic sodium-aqua complex (+1 overall charge). The complete complex **Pd6**, therefore, forms a one dimensional, homometallic sodium-aqua coordination polymer upon the execution of the inversion symmetry operation. For every complete complex Pd(II), there are two Na-aqua complexes that form 1D coordination polymers via bridging aqua molecules. Complex **Pd11,** like **Pd6,** has a Pd atom centre with two anionic bidentate N^O-donor (phenoxy)imine ligand units, affording a distorted square planar coordination mode. The coordination chemistry of complexes **Pd6** and **Pd11** as established from the solid structures concur with the IR spectra (absence of O-H frequency).
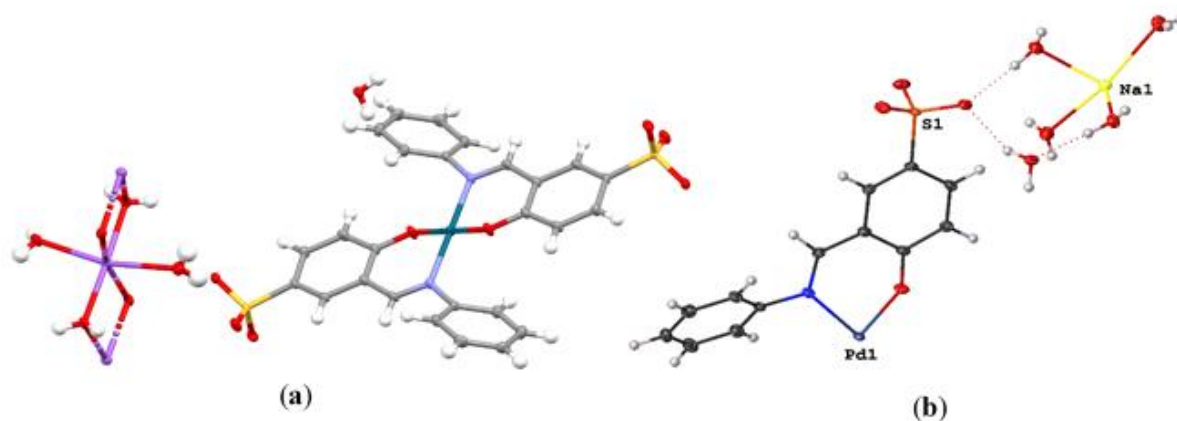
Figure 4.5: Molecular structure of **Pd6** with atom numbering Scheme

(**a**) Molecular structure of **Pd6** with atom numbering Scheme. The displacement ellipsoids of atoms are shown at the 50% probability level. Selected bond lengths [Å]: Pd(1)- O(1), 1.9764(15) ; Pd(1)-N(1), 2.0282(19); Selected bond angles (°): O(1)- Pd(1)- O(1), 180.00(10) ; N(1)-Pd(1)- N(1), 180.00(10); O(1)-Pd(1)-N(1), 88.80(7); O(1)-Pd(1)-N(1)#1, 91.20(7). (**b**) Asymmetrical view of the unit showing only half of the anionic Pd complex, one hydrate molecule and the cationic sodium-aqua complex.
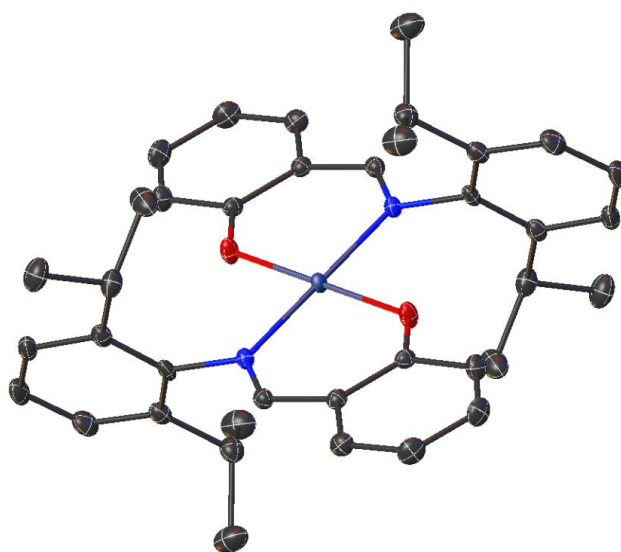
Figure 4.6: Molecular structure of **Pd11** with atom numbering Scheme

The displacement ellipsoids of atoms are shown at the 50% probability level. Selected bond lengths [Å]: Pd(1)- O(1), 1.976(12); Pd(1)- O(2), 1.972(12); Pd(1)-N(1), 2.013(15); Pd(1)-N(2), 2.013(15); O(1)-C(6), 1.301(2). Selected bond angles (°): O(1)- Pd(1)- O(2), 180.0; N(2)-Pd(1)- N(1), 180.0; O(1)-Pd(1)-N(2), 87.86(5); O(1)-Pd(1)-N(1), 92.14(6).

The average Pd(1)- O(1) bond distances of 1.9764 (15)Å and 1.9776(15) Å for complexes **Pd6** and **Pd11,** respectively, are comparable. On the other hand, the average Pd-N$_{imine}$ bond length for complex **Pd6** of 2.0282(19) Å is marginally longer as compared to the Pd-N$_{imine}$ bond distance of 2.013(15) Å for complex **Pd11** because of the inductive effects resulting from the iPr groups present in **Pd11** (Figure 4.6)**.** The bond lengths exhibited by complexes **Pd6** and **Pd11** are comparable to similar reported compounds, where bond lengths for Pd(1)- O and Pd(1)-N$_{imine}$ were recorded as 2.026 (16)Å and 2.067 (18)Å respectively [29]. Complex **Pd6** displays bite angles for O(1)-Pd(1)-N(1) and O(1)-Pd(1)-N(2) of 88.80(7)° and 91.20(7)° respectively, well within those recorded for complex **Pd11** of 92.14(6)°and 87.86(5)° respectively. This is consistent with minimal Pd centre sphere steric encumbrance in both **Pd6** and **Pd11** as the alkyl substituents are remotely located from the Pd centres. In general, complexes **Pd6** and **Pd11**, thus, have adopted distorted square planar coordination geometry, with the bite angles marginally deviating from typical square planar geometry of 90°.

Table 4.2: Summary of the crystallographic data and structure refinement for complexes

Parameter	Pd6	Pd11
Empirical formula	$C_{13} H_{19} N Na O_9 Pd_{0.50} S$	$C_{38}H_{44}N_2O_2Pd$
Formula weight	441.54	667.15
Temperature	100(2) K	100.02 K
Wavelength	0.71073 Å	0.71073Å
Crystal system	Monoclinic	triclinic
Space group	P 21/c	P-1
Unit cell dimensions		
a (Å)	19.9891(17) Å	7.9427(5)
b (Å)	6.8752(6) Å	10.1922(6) 11.1065(7)
c (Å)	13.5220(12) Å	91.295(2)
		11.1065(7)
α (°)	90°	113.803(3)
β (°)	103.238(2)°	96.819(3)
γ (°)	90°	97.945(3)
Volume	1808.9(3) Å^3	799.48(9)
Z	4	1
Density (calculated)	1.621 Mg/m^3	1.386 Mg/m^3
Absorption coefficient	0.730 mm^{-1}	0.616 mm^{-1}
F(000)	904.0	348.0
Crystal size	0.260 x 0.140 x 0.020 mm^3	$0.24 \times 0.19 \times 0.11$ mm^3
Theta range for data collection	1.046 to 26.609°	4.084 to 58.026°
R	0.03	0.03

4.4. Methoxycarbonylation reactions catalysed by complexes Pd6-Pd11.

4.4.1 Initial screening and optimization of the reaction conditions in the methoxycarbonylation of 1-hexene

The initial screening of the complexes in the methoxycarbonylation reactions of 1-hexene was done using the non-water-soluble complex **Pd9**. The ester products were identified and quantified using GC and GC-MS by employing a commercial methyl heptanoate (linear ester) sample and ethylbenzene as an internal standard (Figure 4.7). These allowed us to determine both the percentage conversions and yields. The TONs were calculated based on percentage yields. The comparable values in percentage yields and conversions suggest selectivity towards the ester products, as depicted in Scheme 4.2.
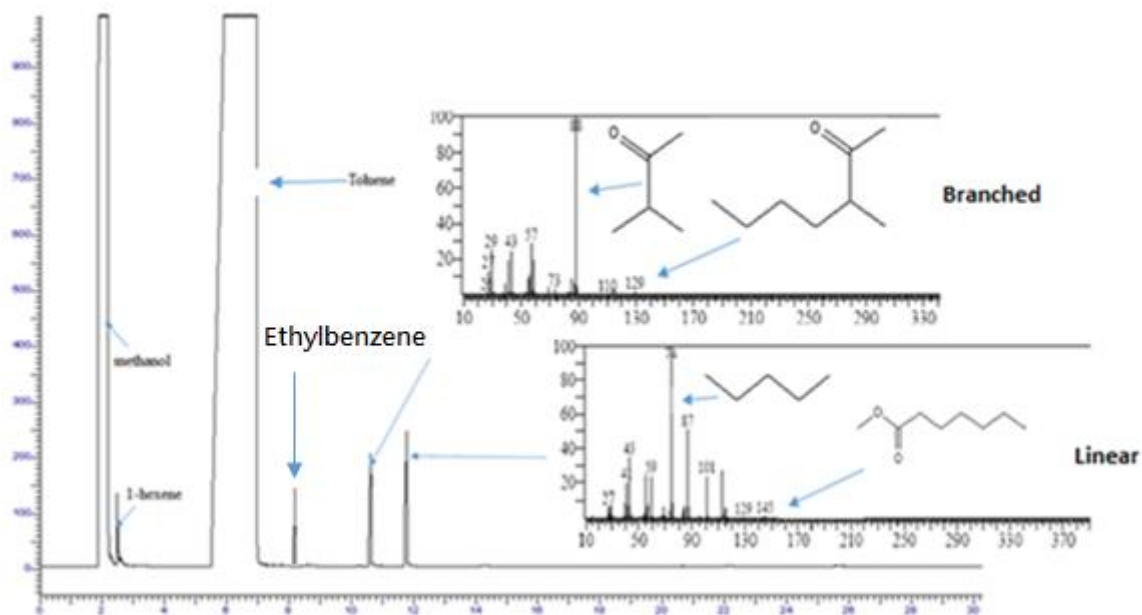
Figure 4.7: GC and GC-Ms spectra of methoxycarbonylation products identified as branched (methyl 2-methylhexanoate) and linear (methyl heptanoate) esters using ethyl benzene as internal standard

The typical reactions conditions of 1-hexene:HCl: PPh$_3$:Pd molar ratios of 200:10:2:1 were employed (Scheme 4.2 and Table 4.3). Under these conditions, complex **Pd9** afforded yields of 52% within 20 h and 64 % of the linear ester (Table 4.3, entry 2). The importance of the triphenyl phosphine additive in stabilizing the active species [35] was displayed from the catalytic inactivity when a reaction was done without the additive (Table 4.3, entry 1).
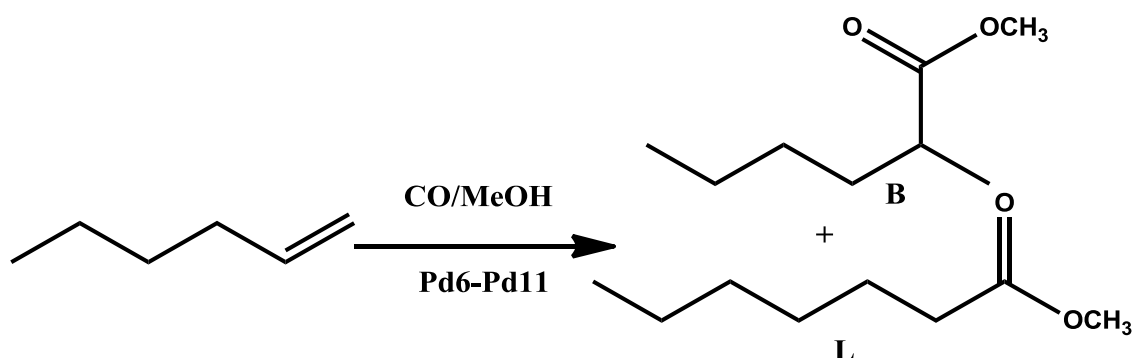
Scheme 4.2: Methoxycarbonylation of 1-hexene using complexes **Pd6**-**Pd11** as catalysts to give branched (A) and linear (B) esters.

4.4.1.1: Variations of Pd/PPh$_3$ ratios

Informed by the bis(chelated) coordination chemistry of the complexes (Figures 4.4 and 4.5), we envisioned that varying the amount of PPh$_3$ would have a major influence on the resultant catalytic activities of the complexes [36]. The use of phosphine additives and acid promoters in the methoxycarbonylation reactions is believed to generate and stabilize the active species, respectively [36-38]. Thus, we varied the PPh$_3$/**Pd9** ratio from 2 to 8 (Table 4.3, entries 2 -5). We observed an increase in catalytic activity with an increase in the amount of PPh$_3$, giving an optimum yield of 83% at a PPh$_3$/**Pd9** ratio of 6 (Table 4.3, entry 4). Interestingly, a further increase of PPh$_3$/**Pd9** ratio to 8 was marked by a decline in percentage yield to 78% (Table 4.3, entry 5). Lower catalytic activities reported at higher PPh$_3$/**Pd9** implies a possible competition

between the PPh_3 and the substrate for the coordination centre [39]. Similar results were reported in the methoxycarbonylation of acetylene [40].

Separately, the lower catalytic activities observed at lower PPh_3/Pd ratios of 2 and 4 could be attributed to the bis(chelated) nature of the complexes, hence higher amounts of PPh_3 is required to displace the coordinated ligand units. Interestingly, the PPh_3/Pd ratio also influenced the regio-selectivity of the ester products. For example, PPh_3/ **Pd9** ratios of 2 and 8 afforded 64% and 73% of the linear esters, respectively (Table 4.3, entries 2 *vs* 5). The higher linear ester products produced at higher PPh_3/**Pd9** ratios may be assigned to increased steric bulk due to PPh_3 groups around the metal centre, thus favouring the less sterically demanding linear products [41].

Table 4.3: Initial screening and optimization of phosphine and acid promoter ratios in the methoxycarbonylation of 1-hexene using complex **Pd9**[a]

Entry	Pd: Acid	Pd:PPh$_3$	Conv(%)[b]	Yield (%)[b]	B/L(%)[c]	TON[d]
1[e]	1:10	0	0	0	-	-
2	1:10	1:2	55	52	36/64	104
3	1:10	1:4	69	68	31/69	136
4	1:10	1:6	85	83	30/70	166
5	1:10	1:8	80	78	27/73	156
6	1:20	1:6	92	92	30/70	184
7	1:5	1:6	46	43	30/70	86
8	1:30	1:6	71	68	31/69	136
9	1:40	1:6	44	43	29/71	86
10[f]	1:20	1:6	44	41	29/71	82
11[g]	1:20	1:6	70	67	30/70	134
12[h]	1:20	-	-	-	-	-
13[i]	1:20	1:6	9	7	30/70	20
14[j]	1:20	1:6	23	20	32/68	80
15[k]	1:20	1:6	84	82	34/66	164
16[l]	1:20	1:6	72	71	30/70	142

[a]Reaction conditions: Pressure: 60 bar, temp: 90 °C, Solvent: methanol 20 mL and toluene 20 mL; [Pd]:[hexene] ratio; 1:200; time, 20 h; [b]% Conversions and yields determined from GC using ethylbenzene as internal standard. [c]Molar ratio between branched and linear esters calculated using linear methyl heptanoate commercial sample. [d]TON = (mol. prod/mol. Pd). [e] reaction done in the absence of PPh$_3$ [f]40 bar; [g]70 bar. [h]Pd(OAc)$_2$/**L9**, [i]Pd(OAc)$_2$/**L9**/PPh$_3$; [j]Pd(OAc)$_2$/PPh$_3$. [k]para tolyl sulfonic acid (PTSA; [l]methane sulfonic acid (MSA).

4.4.1.2: Variation of Pd: Acid ratios

Using the optimized PPh_3/**Pd9** ratio of 6, we then varied the ratio of HCl/**Pd9** between 5 and 40 (Table 4.3, entries 4 and 6 - 9). From Table 4.3, an optimum HCl/**Pd9** ratio of 20 (92% yield) was realized. Increasing the amount of acid promoter is known to initiate efficient reactivation of palladium(0) formed under the reducing conditions [42]. Similarly, lower concentrations of the acid promoter have been shown to favour the formation of the less active palladium carbomethoxy intermediate [43]. In addition, excess acid is needed to achieve catalyst stability since the acid promoter is consumed during the catalytic cycle. Apart from the acid promoter playing a role in active species formation, it is also required to shift the equilibrium from the inactive Pd(0) species to the active intermediate species. However, further increase of the HCl concentration (HCl/Pd > 20) coincided with a decrease in catalytic activities (Table 4.3, entries 8 and 9). We also probed the behaviour of para-tolyl sulfonic acid (PTSA) and methanesulfonic acid (MSA) due to their mild natures as opposed to HCl in the methoxycarbonylation of olefins [40]. However, both PTSA and MSA displayed diminished catalytic activities in comparison with HCl. As a demonstration, using complex **Pd9**, conversions of 92%, 84% and 72% were realized for HCl, PTSA and MSA, respectively (Table 4.3, entries, 6, 15 and 16). The observation is in sync with the dependence of catalytic activities on acid strengths, as previously reported by Zúñiga *et al.* [44].

To fully grasp the coordinated ligands and isolated complexes' role in the generation of the active catalysts, we performed control experiments using $Pd(OAc)_2$/**L9** and $Pd(OAc)_2$/**L9**/ PPh_3 systems (Table 4.3, entries 12-14). The $Pd(OAc)_2$/**L9** and $Pd(OAc)_2$/**L9**/ PPh_3 combinations yielded much lower percentages of 7% and 20% when compared to percentage yields of 92% displayed by complex **Pd9/**PPh_3 catalyst system, respectively (Table 4.3, entries

12-14 and 6). From this data, it is conceivable that the coordinated ligands and the discrete metal complexes play a significant role in the formation of the active species.

4.4.1.3: Variations of catalyst loading

Having established the optimum amounts of PPh_3 and HCl, we turned out attention to the catalyst concentration impact by using the 1-hexene/**Pd9** ratio from 1000 (0.1 mol %) to 100 (1 mol %) as shown in Figure 4.8. The percentage yields were observed to increase with an increase in catalyst loading. For example, at 1-hexene/**Pd9** ratio 500 (0.2 mol %) and 200 (0.5 mol %), percentage yields of 56%, and 92% were obtained respectively. However, a further increase of catalyst loading to 1.0 mol% resulted in a slight drop in percentage yield to 85% (Figure 4.8). The decrease in catalyst activities at higher catalyst loading is not new and has been associated with catalyst aggregation [45, 46]. Even though higher catalyst loadings led to higher percentage yields, it is important to note that these were accompanied by lower TON values (Figure 4.8). For instance, loadings of 0.2 mol% and 1.0 mol% recorded TON values of 280 (56%) and 80 (87%) respectively.   The highest TON value of 292 (95%) was recorded at a lower catalyst loading of 0.25% (substrate/Pd = 400). Thus, from this data, it is evident that higher catalyst loadings are not beneficial to the system. In terms of selectivity, the change in catalyst loading did not cause any substantial changes in the regio-selectivity of the esters. For instance, catalyst loadings of 0.2 mol% and 0.5 mol% gave 71% and 70% of the linear esters, respectively.
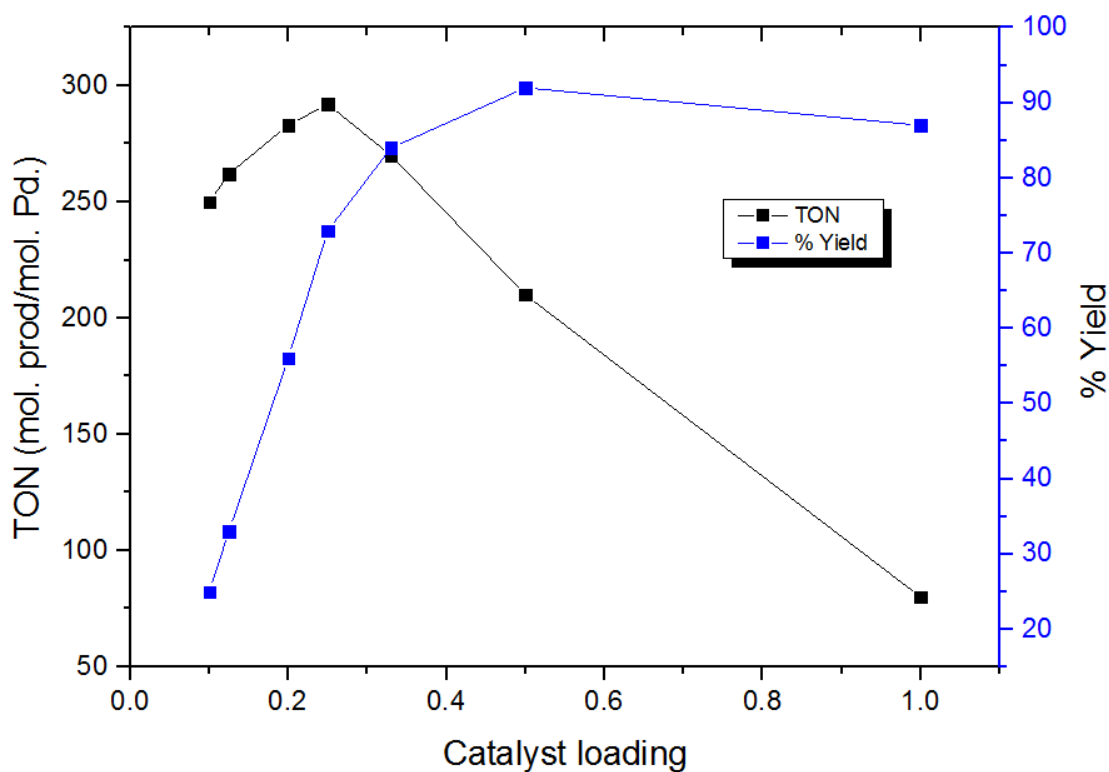
Figure 4.8: A graphical plot showing the variations of TON and % yields with catalyst loading for complex **Pd9**. Catalyst loading varied from 0.1% (1:1000) to 1% (1:100).

4.4.1.4: Effects of temperature variation

The influence of temperature was studied by changing the reaction temperatures from 50 °C to 90 °C (Figure 4.9). Expectedly reaction temperatures of 90 °C gave yields of 72%, while lower temperatures of 70 and 50 °C witnessed diminished yields of 59 % and 40%, respectively [47]. On the other hand, elevated temperatures of 100 °C resulted in lower yields of 65%, a trend that can be connected to partial catalyst decomposition to form palladium black [48] as observed from the reactor. On the other hand, temperature variations did not affect the regio-selectivity as values 68% to 71% of the linear products were obtained across all the temperature variations.
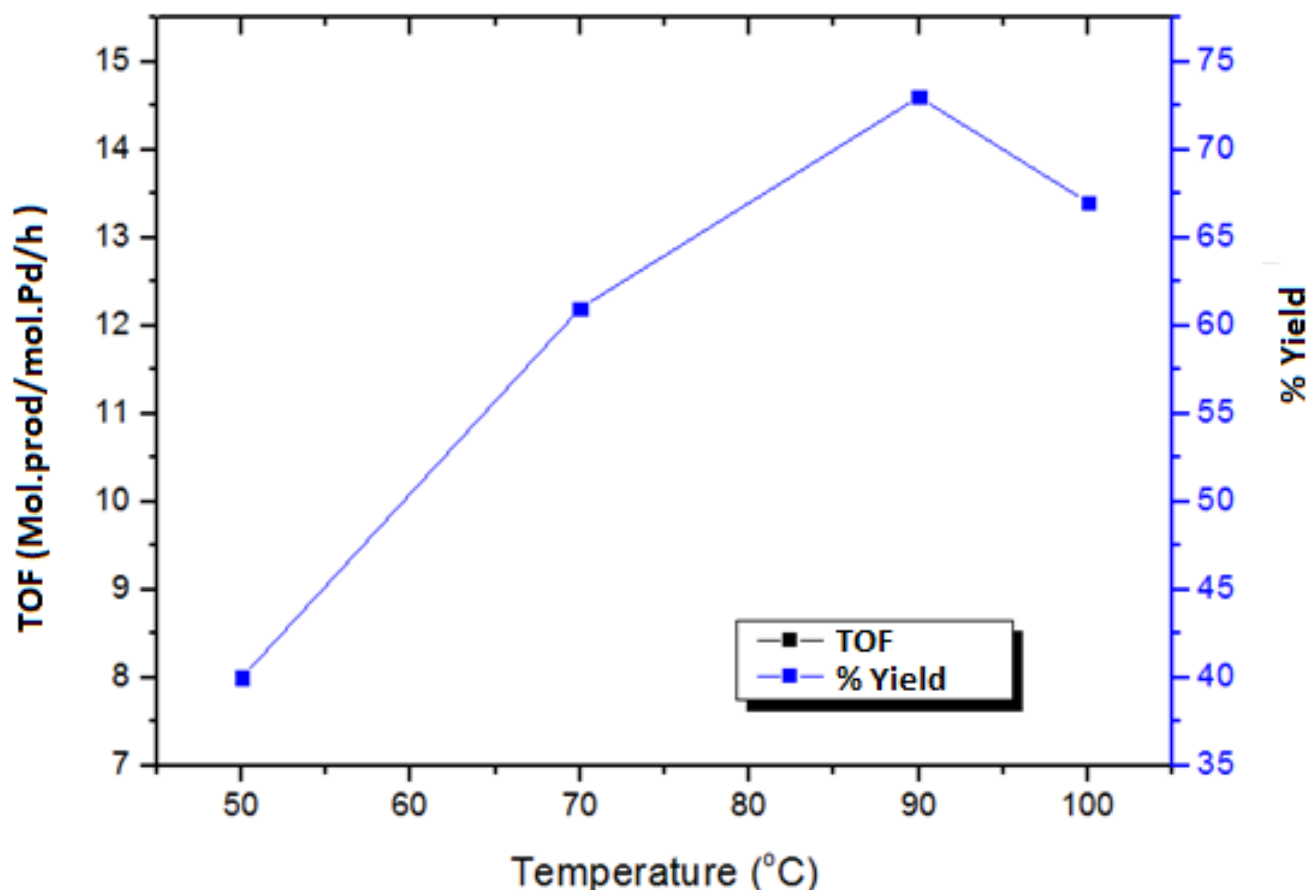
Figure 4.9: A graphical plot showing the variations of TOF and % yield with temperature for **Pd6** in the methoxycarbonylation of 1-hexene

4.4.2 Investigation of the role of PPh$_3$ and HCl in the methoxycarbonylation reactions via in situ NMR techniques

Having observed the significant dependence of catalytic activities of complex **Pd9** on the amounts of PPh$_3$ and HCl, our curiosity led us to try and understand the exact role these two play in regulating the catalytic activity. Thus *in situ* ^{1}H and ^{31}P NMR studies were employed to monitor the kinetics of formation and relative stabilities of possible active intermediates. The ^{31}P NMR experiment was performed using **Pd9**:PPh$_3$ ratios of 1:1, 1:2, 1:6 and 1:8 (Figure 4.10). The ^{31}P NMR spectra showed multiple peaks within the region of 22 ppm to 33 pm,

indicating the formation of a number of Pd-PPh$_3$ adducts/intermediates [48-50]. Expectedly, the use of excess PPh$_3$ (PPh$_3$/Pd ratios of 6 and 8) gave signals at -5 ppm, pointing to the presence of an uncoordinated PPh$_3$ group. More significantly, the absence of the free PPh$_3$ signal at PPh$_3$/Pd ratio of 2 points to the coordination of two PPh$_3$ units to Pd to give [Pd(PPh$_3$)$_2$(**L9**)]$^+$ adduct, as a possible active species. Indeed, the lower yields reported at this PPh$_3$/Pd ratio of 2, point to insufficient stabilization of the active species.
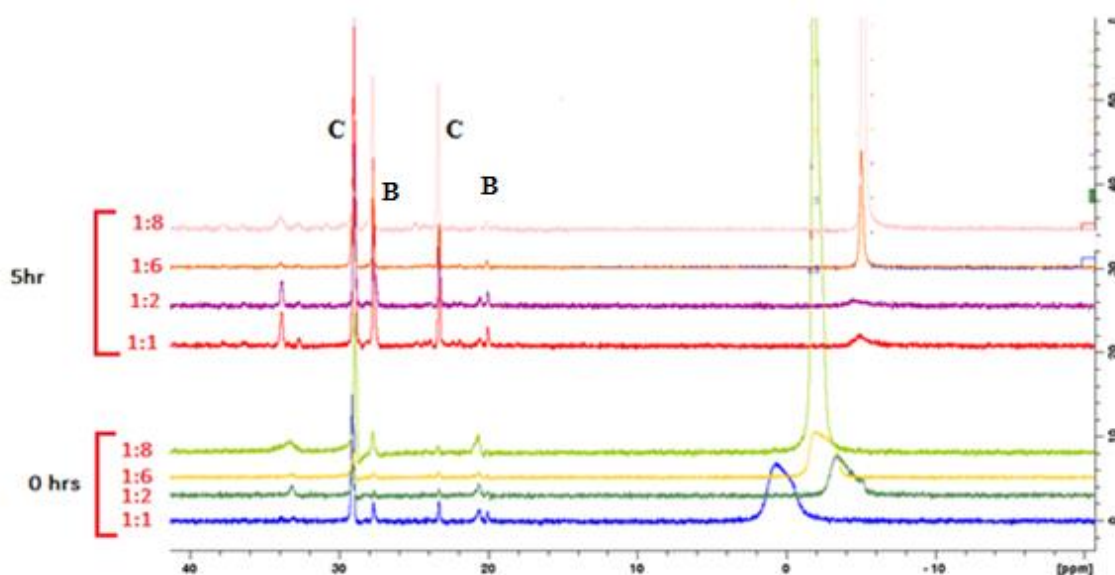
Figure 4.10: ^{31}P NMR spectra showing various peaks for different concentrations of PPh$_3$ as a stabilizing agent using complex **Pd9**.

We also performed *in situ* ^{1}H NMR spectroscopy using a **Pd9**/ PPh$_3$/HCl ratio of 1:8:20 by monitoring the changes in the ligand proton signals over a period of 9 h (Figure 4.11). The main objective here was to establish if there is any hydrolysis of the imine group upon the addition of HCl. Interestingly, no observable change to the imine signal at around 8.07 ppm was recorded over the 9 h period (Figure 4.10). This was evident from the absence of the ligand

L6 (8.37 ppm) or aldehyde (9.80 ppm) signals. The invariable spectra over the 9 h period thus pointed to the stability of complex **Pd9** under the experimental acidic conditions. The formation of the Pd-H group was expected, but unfortunately, no such signal at around 0 to -13 ppm was observed [51, 52]. Instead, a signal at around 0.10 ppm was recorded, which at this stage, we are unable to unambiguously assign to the Pd-H species.
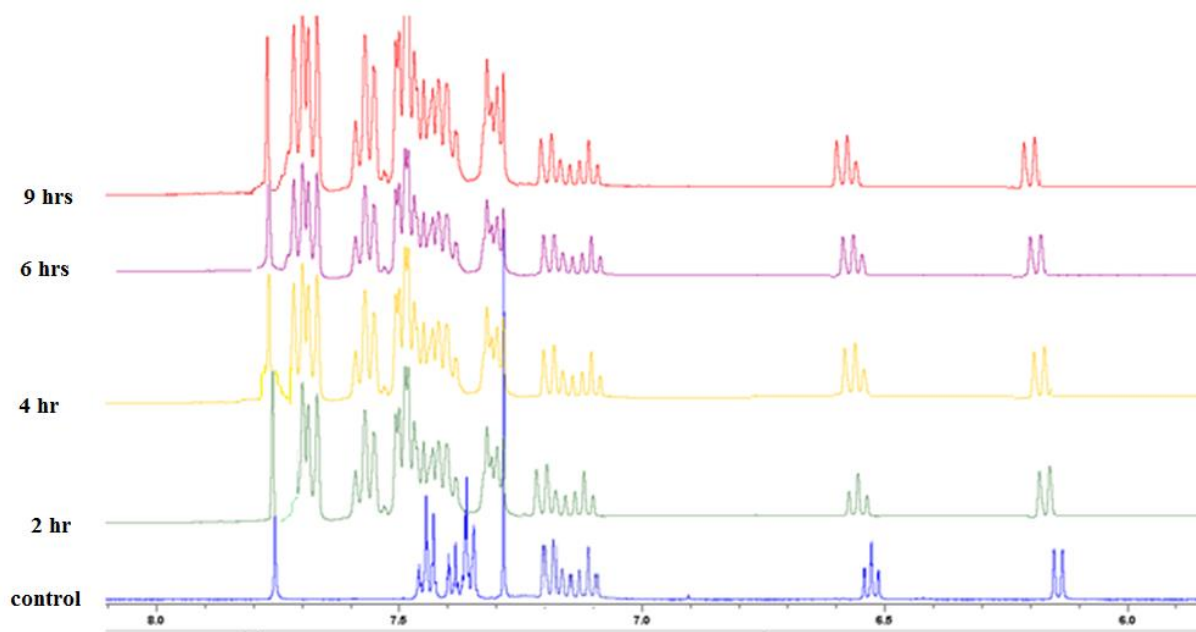
Figure 4.11: ^{1}H NMR of complex **Pd9** in the presence of HCl and PPh$_3$ showing the stability of the complex in acid media over a 9 period.

From the ^{1}H and ^{31}P NMR spectral studies, possible stabilization and mechanistic routes in the active species formulation for the methoxycarbonylation reaction using complex **Pd9** as depicted in Scheme 4.3 can be proposed. From Scheme 4.3, it is evident that the addition of HCl/PPh$_3$ mixture leads to complete dissociation of one ligand **L9** group to give the PPh$_3$ intermediate [PdCl(**L9**)PPh$_3$] (**B**). This is derived from the signals shown in the ^{31}P NMR data at 21 ppm and 28 ppm, corresponding to the mono-coordinated PPh$_3$ units either *trans* to the

N- or O-donor atoms in **L9**. Similar palladium(II) complexes, bearing monodentate coordinated PPh$_3$ ligands, show the PPh$_3$ peaks at 32.49 and 23.28 respectively in their ^{31}P NMR spectra [50]. The formation of the bis-coordinated PPh$_3$ intermediate [Pd(**L9**)(PPh$_3$)$_2$]$^+$ (**C**) was evident from the observation of two signals at 23.8 ppm and 29.3 ppm (Figure 4.14).
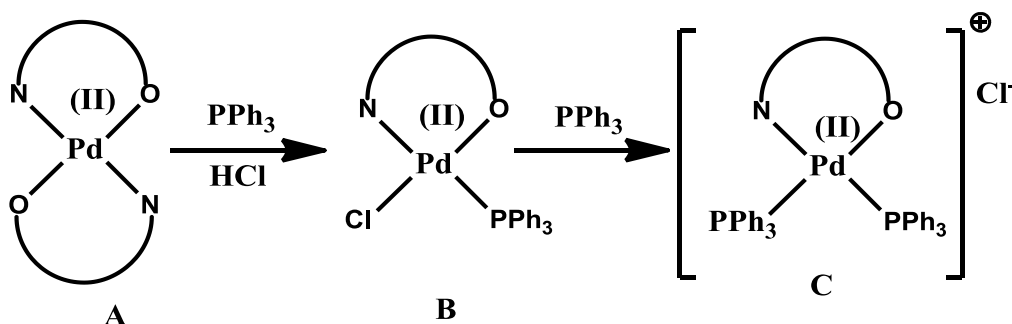
Scheme 4.3: Proposed activation and stabilization pathways of **Pd9** in the presence of PPh$_3$ and HCl.

We also obtained the ^{1}H, and ^{31}P NMR data of the catalyst residue from the **Pd9**/PPh$_3$/HCl (1:8:20) system ran under the catalytic conditions of 60 bar of CO and 90 °C to investigate how stable the compounds are when subjected to the catalytic conditions. This was done by isolation of the spent catalyst after 20 h of reaction time. The used catalyst spectrum was comparable to that of the original complex **Pd9,** with the imine proton being intact (Figure 4.12). Indeed, the ^{31}P NMR spectra of the spent catalyst were comparable to the spectra obtained at room temperature as well as that of the original complex. Moreover, the two signals recorded at around 23 ppm and 30 ppm do not compare to the one signal at around 24 ppm expected for the [Pd(PPh$_3$)$_2$Cl$_2$] species [53]. This also points to the coordination of ligand **L9** to the metal atom to possibly give compound [Pd(PPh$_3$)$_2$(**L9**)]$,^+$ consistent with the proposed as shown in

Scheme 4.3. This data, therefore, unequivocally unveiled that the active species are stable and that the complex coordination environment is retained under the conditions.
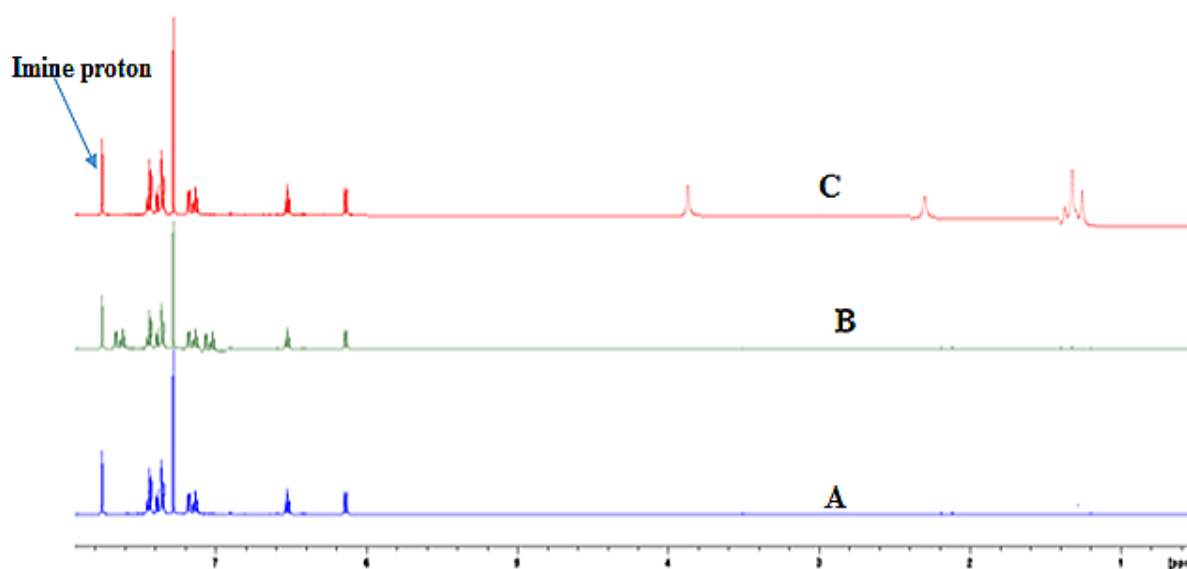
Figure 4.12: (A) ^{1}H NMR spectrum of complex **Pd9**, (B) ^{1}H NMR spectrum obtained from the reactions of **Pd9** with PPh$_3$ under CO (60 bar) in the presence of HCl at 90 ºC (catalytic conditions), (C) ^{1}H NMR spectrum of the catalytic reaction mixture.

We further attempted to confirm the presence of [Pd(PPh$_3$)$_2$(**L9**)]$^+$ intermediate (Scheme 4.3) and if it can indeed catalyse the methoxycarbonylation reaction of styrene. This was done by isolation of the product of the reactions of two equivalent of PPh$_3$ with **Pd9.** Both the ^{1}H NMR and ^{31}P NMR spectra (Figures 4.13 and 4.14) of the isolated residue pointed to the formation of [Pd(PPh$_3$)$_2$(**L9**)]$^+$ compound. For example, all the aromatic protons (60) were accountable for in the ^{1}H NMR spectrum (Figure 4.13), confirming the presence of one ligand **L9** unit and two coordinated PPh$_3$ ligands in the Pd coordination sphere. This was augmented by the signals at 23.2 ppm and 29.3 ppm in the ^{31}P NMR spectrum (Figure 4.14). Even though a $^2J_{(P-P)}$

coupling was expected, ^{31}P NMR spectrum of [Pd(PPh₃)₂(**L9**)]⁺ did not exhibit such coupling/splitting as the two PPh₃ groups appeared as singlets. The observation could be attributed to a rapid ligand exchange resulting in exchange-averaged resonances [54].

Figure 4.13: ^{1}H NMR spectrum of complex **Pd12** showing all the expected peaks and the incorporation of PPh₃ ligand protons. Inset is the ^{1}H NMR spectrum of the original complex **Pd9**.

Complex **Pd12** was then used as a catalyst in the presence and absence of PPh₃ additive (Table 4.4, entries 8-10). Interestingly, the catalyst [Pd(PPh₃)₂(**L9**)]⁺ showed comparable catalytic activities to complex **Pd9.** For instance, percentage yields of 72% and 74% were recorded for complexes **Pd9** and [Pd(PPh₃)₂(**L9**)]⁺, respectively (Table 4.4, entries 4 vs 8). Most significantly, complex [Pd(PPh₃)₂(**L9**)]⁺ did not require the addition of PPh₃, as appreciable yields of 70% were recorded in the absence of PPh₃ (Table 4.4, entry 10). These observations,

therefore, implicated $[Pd(PPh_3)_2(\textbf{L9})]^+$ intermediate as the possible active species in these reactions.
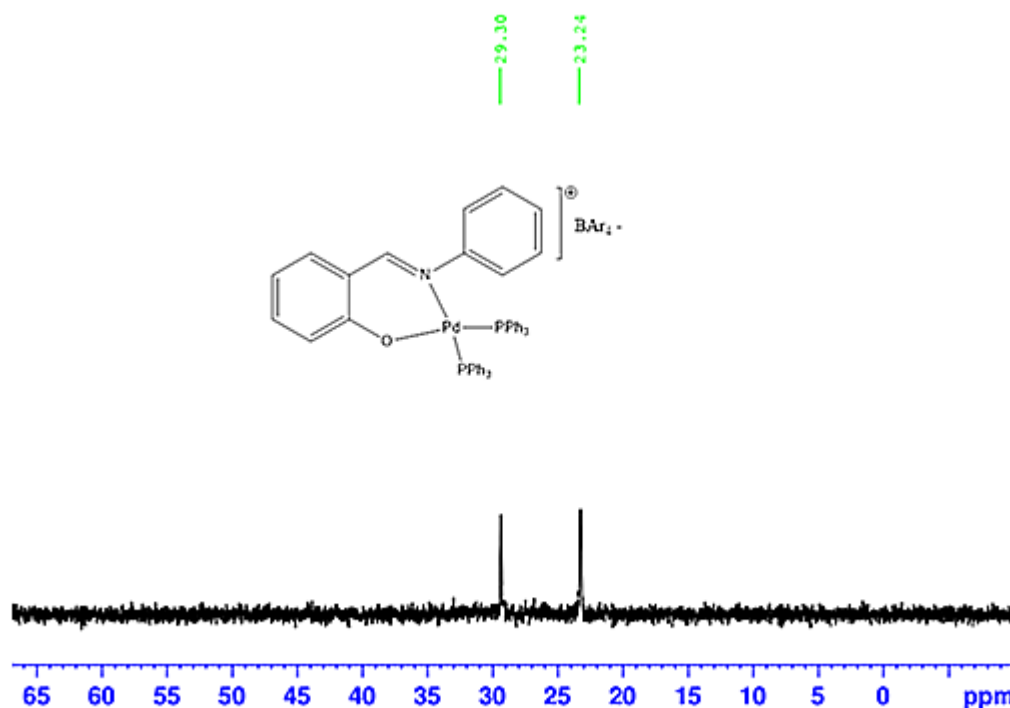
Figure 4.14: ^{31}P NMR spectrum of complex **Pd12.** The peak two signals (23 ppm and 31 ppm) represent the two PPh$_3$ groups showing coordination of PPh$_3$ to form complex **Pd12**

4.4.3 Effect of complex structure on methoxycarbonylation reactions

Upon establishing the optimum conditions of temperature, catalyst loading, acid and phosphine additives for the methoxycarbonylation reactions using complex **Pd9**, we then investigated the comparative catalytic performance of the six complexes as shown in Table 4.4. From the data in Table 4.4, we observed some dependence of catalytic activities on the steric parameters of the complexes. For example, the unsubstituted complex **Pd6** recorded yields of 69%, while the isopropyl substituted complex **Pd8** afforded yields of 56% (Table 4.4, entries 1 vs 3). This trend can be assigned to the increased steric encumbrance around the metal atom, thus

hindering substrate coordination. This observation mirrors those of Harmon *et al.*, where sterically hindered ruthenium(III) complex showed reduced catalytic activities [55].

Interestingly, the water-soluble complexes **Pd6**-**Pd8** showed comparable catalytic activities to their respective non-water-soluble counterparts **Pd9**-**Pd11** (Table 4.4). For instance, while the water-soluble **Pd6** displayed yields 69%, the corresponding complex **Pd9** exhibited yields of 72% (Table 4.4, entries 1 vs 4). This showed that incorporation of the water-soluble motif did not compromise the catalytic activities of the complexes, hence a major achievement in the design of separable catalyst systems. The activities observed for the non-water-soluble complexes compare well with similar systems reported in the literature. While some systems performed better in methoxycarbonylation [35], others reported lower activities. For instance, 2-(diphenylphosphinoamino)pyridine palladium complexes by Aguirre *et al.* reported showed TONs of 340, compared to our TONs of 276 in the methoxycarbonylation of 1-hexene. On the other hand, palladium complexes of naphthyl(diphenyl)phosphines, benzimidazolylemethyl)amine palladium complexes and mixed N^N^X (X = O and S) ligands reported lower TONs of 190 in the methoxycarbonylation of 1-hexene.

Table 4.4: Effects of complex structure on catalytic activity and regio-selectivity[a]

Entry	Catalyst	Conv(%)[b]	Yield (%)[b]	B/L(%)[c]	TON[d]
1	Pd6	71	69	31/69	276
2	Pd7	66	64	29/71	256
3	Pd8	59	56	23/77	184
4	Pd9	73	72	30/70	288
5	Pd10	68	66	27/73	264
6	Pd11	60	59	23/77	236
7[e]	Pd9	70	68	31/69	272
8[f]	$[Pd(PPh_3)_2(L9)]^+$	76	74	31/69	296
9[g]	$[Pd(PPh_3)_2(L9)]^+$	74	73	30/70	292
10[h]	$[Pd(PPh_3)_2(L9)]^+$	71	70	32/68	280

[a]Reaction conditions: Solvent: methanol 20 mL and toluene 20 mL; [Pd]:[PPh$_3$][acid]:[hexene] ratio; 1:6:20:400; time, 20 h. [b]%Conversion and %yield determined from GC using ethylbenzene as an internal standard and linear methyl heptanoate commericial sample. [c]Molar ratio between branched and linear ester. [d]TON = (mol. prod/mol. Pd). [e]Hg drop experiment. [f, g, h] Pd:PPh$_3$ ratios of 1:6, 1:1, 1:0 respectively.

In terms of regio-selectivity, the formation of either the linear or branched ester products were also affected by the steric crowding around the complexes. For instance, while the unsubstituted catalyst **Pd6** gave 69% of the linear isomer, the more sterically demanding isopropyl complex **Pd8** produced 77% of the linear ester. Increased steric bulk around the coordination centre is known to favour 1,2 olefin insertion, hence preference to the less bulky linear products [41]. The increase in linear products with steric crowding of the catalyst supports the operation of a hydride mechanism [41, 42]. More importantly, the regio-

selectivity of the water-soluble complexes were similar to those of the non-water analogues. For example, complexes **Pd6** and **Pd9** gave 69% and 70% of the linear esters, respectively (Table 4.4, entries 1 vs 4). This clearly shows that incorporation of the water-soluble motif on the ligand backbone did not alter the selectivity of the resultant catalysts.

4.4.4 Biphasic methoxycarbonylation reactions using water-soluble complexes Pd6 – Pd8

Even though the use of water-soluble complexes in methoxycarbonylation of olefins is considered environmentally benign, to date, there are few reports on such catalysts [56-58]. Herein, we have carried out the methoxycarbonylation of 1-hexene under biphasic conditions (water/toluene/methanol system) using the water-soluble complexes **Pd6 – Pd8**. First, we established the best solvent ratio by changing the water quantities using complex **Pd6** (Table 4.5). While keeping the volume of the organic phase (toluene) constant at 20 mL, we varied the amounts of water (0-40%) and methanol to give a total volume of 20 mL of the aqueous phase at any given time. It was noted that the introduction of 1 mL of water (5% of the aqueous phase) to the toluene/methanol system gave yields of 67%, in comparison to 70% recorded in the pure toluene/methanol solvent (Table 4.5, entries 1 vs 2). However, under these conditions, phase separation required up to 10 h (Figure 4.15).
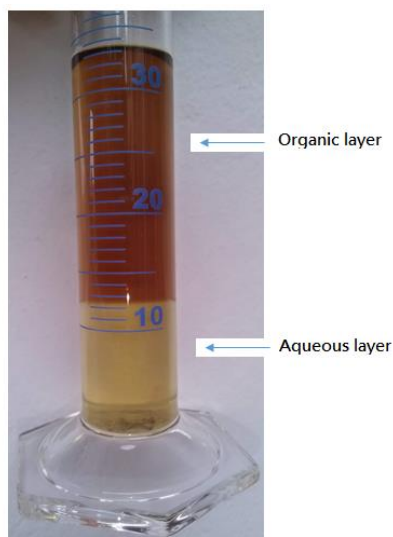
Figure 4.15: An image of the catalysis phase separation within 10 h (with 5% water)

Increasing the water content to 2 mL (10%) resulted in a slight decrease in percentage yield to 63%, but significantly, phase separation occurred within 2 h. A further increase in the water contents had detrimental effects, giving only 22% percentage yields at 6 mL (30%) of water content, while no activity was observed upon addition of 8 mL (40%) of water (Table 4.5, entries 4-7). This phenomenon has been observed by Schmidt *et al.*, where the use of 50% of water in the aqueous phase led to a complete loss of catalytic activity [27]. The lower yields observed with increased water has been attributed to reduced solubilities of 1-hexene and CO in the aqueous phase [27], since CO has a low solubility value of 0.03 mol/L in pure water, compared to solubility of 0.28 mol/L in pure methanol [59]. As expected, complete decomposition of the catalyst was observed at 40% water, as deduced from the extensive formation of Pd(0) black in this experiment.

Table 4.5: Biphasic catalysis and aqueous phase modification [a]

Entry	Complex	Volume of Water (mL)	Conv(%)[b]	Yield %)[b]	B/L(%)[c]	TON[d]
1	**Pd6**	0	71	70	31/69	280
2	**Pd6**	1(5%)	68	67	30/70	268
3	**Pd6**	2 (10%)	65	63	32/68	252
4	**Pd6**	3(15%)	60	58	30/70	232
5	**Pd6**	4(20%)	51	50	31/69	200
6	**Pd6**	6(30%)	25	22	29/71	88
7	**Pd6**	8(40%)	Trace	-	-	-
8	**Pd7**	1(5%)	64	62	26/74	248
9	**Pd8**	1(5%)	55	52	22/78	208
10[e]	**Pd6**	1(5%)	66	64	31/69	256

[a]Reaction conditions: Pressure: 60 bar, temp: 90 °C, Solvent: methanol (varying volumes) and toluene 20 mL; %water in the aqueous phase. [Pd]:[PPh$_3$][acid]:[hexene] ratio; 1:6:20:400; time, 20 h; [b]%Conversions and yields determined from GC using ethylbenzene as internal standard and linear methyl heptanoate commercial sample. [d]Molar ratio between branched and linear ester. [d]TON = (mol. prod/mol. Pd h^{-1}). [e]Hg drop experiment

The product distribution, however, remained unaltered as 68% -71% of the linear esters was observed. Surprisingly, no carboxylic acidic products were observed even with increased water content through hydroxycarbonylation, as has been observed in other related contributions [60]. We thus applied the conditions which led to higher catalytic activities to the water-soluble complexes **Pd7** and **Pd8** in the methoxycarbonylation of 1-hexene (Table 4.4, entries 8 and 9). Consistent with the homogeneous trends, the catalytic activities of the complexes followed the order of **Pd6> Pd8> Pd9**. It is important to note that the catalytic activities recorded in both the homogeneous and biphasic media were comparable. For example, complex **Pd6** gave a

yield of 70% and 67% under homogeneous and biphasic conditions, respectively (Tables 4.4 and 4.5).

4. 4. 5 Catalyst recycling studies

The promising performance of the water-soluble complexes **Pd6** – **Pd8** under biphasic conditions prompted us to investigate their potential to be recycled in the methoxycarbonylation of 1-hexene. This was achieved by carrying out the reactions for 24 h, followed by the organic phase from aqueous layer separation and reusing the aqueous phase (Figure 4.16). From Figure 4.16, the complexes significantly retained their yields in the five cycles investigated, recording drops of between 11% -15%. For example, catalyst **Pd6** recorded yields of 93% and 79% in the first and fifth runs, respectively. It is worth noting that the selectivity of the complexes was not affected in the recycling experiments. For instance, complex **Pd6** afforded regio-selectivities towards the linear esters of 70% and 71% in the first and fifth cycles.
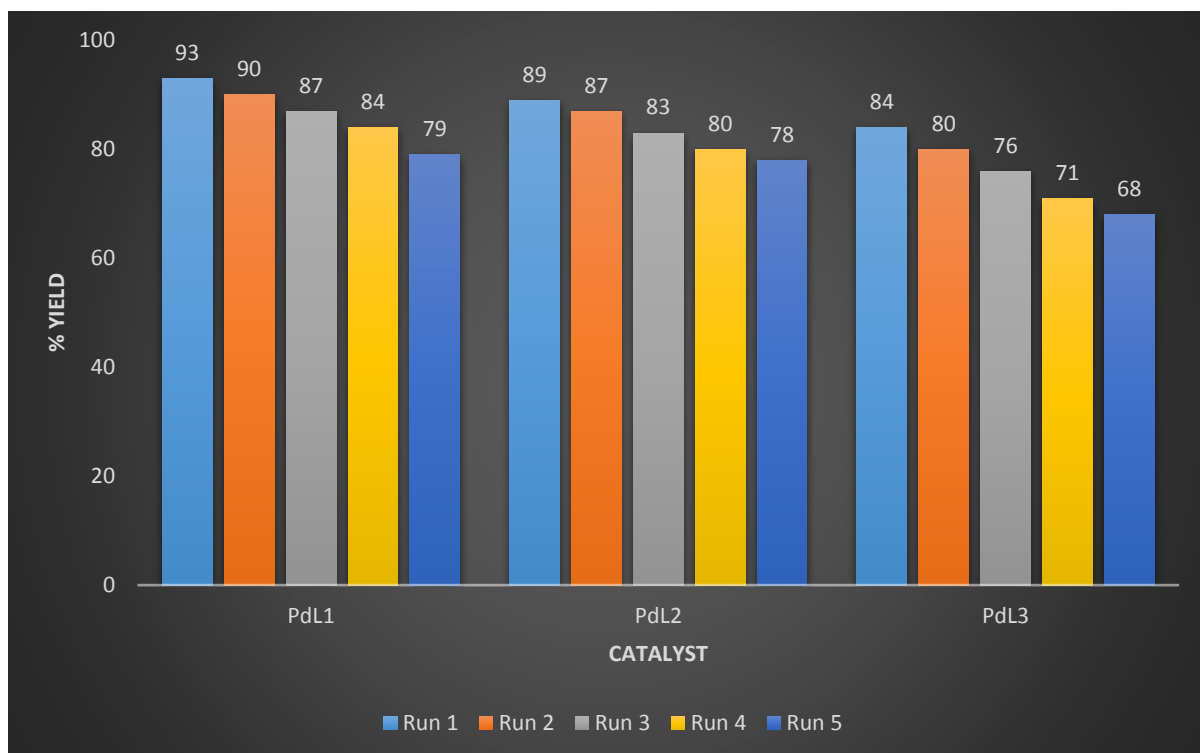
Figure 4.16: A graph showing catalytic activities of complexes **Pd6**- **Pd8** with % yields of subsequent cycles in the methoxycarbonylation of 1-hexene. Reaction conditions: time, 24 h; CO: 60 bar; temp, 90 oC; solvent, toluene (20 mL), methanol (18 ml), water (2 ml).

The observed decline in catalytic activities may be associated with leached catalysts into the organic layer and or catalytic degradation in subsequent cycles [61, 62]. In order to ventilate if leaching may be the reason for the decline in catalytic activities, we performed hot filtration tests using complex **Pd6**. This was accomplished by running the reaction for 12 h, followed by separation of the aqueous layer. The organic phase was then reintroduced into the reactor with fresh methanol, and the reaction allowed to run for a further 24 h to mimic the recycling experiments. While in the first 12 h, percentage yields of 36% were reported, the next 12 h (24 h total time) only realized percentage yields of 39%. This translates to an increase of 3% in the next 12 h, suggesting the presence of some traces of the active species in the organic phase. In addition, this 3% increase is comparable to a drop in catalytic activity from 95% to 90% in the

first and second cycles. Thus, the loss of the catalytic activities in the recycling experiments could be due to leached catalyst.

To determine the true nature of the active species (possible formation of any Pd(0) active nanoparticles), centrifugation of the **Pd6** catalyst was carried out after 10 h of reaction time. The supernatant liquid was then decanted off and reintroduced into the reactor, and the reaction ran for a further 10 h. An increase in percentage yield from 27% within the first 10 h to 66% (original yield was 67%, Table 4.5, entry 1) in the next 10 h, points to a purely homogeneous system without the formation of any active Pd(0) nanoparticles. We also carried out Hg(0) experiments to further establish the homogeneity of the active species using the water-soluble and non-water soluble catalysts (**Pd6** and **Pd9**). While the control reactions gave percentage yields of 68% and 72%, the experiments carried out using 5 drops of Hg(0) recorded percentage yields of 64% and 70% for complexes **Pd6** and **Pd9** respectively (Table 4.4, entry 7 and Table 4.5, entry 10). These comparable catalytic activities support the absence of any active Pd(0) nanoparticles and thus the homogeneity of the active species, consistent with the data obtained in the hot filtration and centrifugation experiments.

4.5 Conclusions

In summary, water-soluble and non-water-soluble palladium(II) complexes anchored on anionic N^O (phenoxy)imine ligands have been synthesized and structurally characterized. The solid structures of the complexes establish the existence of two anionic bidentate ligand units to form distorted square planar complexes. All the palladium(II) complexes transformed substrates into products in favour of the formation of linear esters. Both the catalytic activity and regioselectivity appeared to be controlled by steric encumbrance around the palladium(II)

atom. The water-soluble complexes exhibited comparable catalytic activities and regio-selectivities to their homogeneous systems. Under biphasic conditions, the complexes were reused five times with the minimum decline of catalytic activity but without any change in regio-selectivity. Hot filtration, centrifugation, and Hg(0) drop experiments signalled the homogeneity of the active species under biphasic conditions.

The next chapter covers the synthesis of homogeneous and immobilized palladium catalysts anchored on SBA-15, MCM-41 and magnetic Fe_3O_4 nanoparticles solid supports. The behaviours of these complexes in methoxycarbonylation reaction have been explored, with interest given to the effect of support and calcination temperatures.

4.6 References

[1] I. Delidovich, R. Palkovits, Catalytic versus stoichiometric reagents as a key concept for Green Chemistry, Green Chem., 18 (2016) 590-593.

[2] P. Anastas, N. Eghbali, Green chemistry: principles and practice, Chem. Soc. Rev., 39 (2010) 301-312.

[3] R.A. Sheldon, Fundamentals of green chemistry: efficiency in reaction design, Chem. Soc. Rev., 41 (2012) 1437-1451.

[4] J. Hagen, Industrial catalysis: a practical approach, John Wiley & Sons2015.

[5] C. Copéret, F. Allouche, K.W. Chan, M.P. Conley, M.F. Delley, A. Fedorov, I.B. Moroz, V. Mougel, M. Pucino, K. Searles, Bridging the Gap between Industrial and Well-Defined Supported Catalysts, Angew. Chem. Int. Ed., 57 (2018) 6398-6440.

[6] J. Pritchard, G.A. Filonenko, R. van Putten, E.J. Hensen, E.A. Pidko, Heterogeneous and homogeneous catalysis for the hydrogenation of carboxylic acid derivatives: history, advances and future directions, Chem. Soc. Rev., 44 (2015) 3808-3833.

[7] E.A. Karakanov, A.V. Zolotukhina, A.O. Ivanov, A.L. Maximov, Dendrimer-encapsulated Pd nanoparticles, immobilized in silica pores, as catalysts for selective hydrogenation of unsaturated compounds, ChemistryOpen, 8 (2019) 358.

[8] A. Vavasori, S. Bravo, F. Pasinato, N. Kudaibergenov, L. Pietrobon, L. Ronchin, Supported palladium metal as heterogeneous catalyst precursor for the methoxycarbonylation of cyclohexene, Mol catal, 484 (2020) 110742.

[9] Y. Wan, Z. Chen, D. Liu, Y. Lei, Palladium Nanoparticles Supported on Triphenylphosphine-Functionalized Porous Polymer as an Active and Recyclable Catalyst for the Carbonylation of Chloroacetates, Catalysts, 8 (2018) 586.

[10] S.G. Khokarale, E.J. Garcia-Suarez, R. Fehrmann, A. Riisager, Highly selective continuous gas-phase methoxycarbonylation of ethylene with supported ionic liquid phase (SILP) catalysts, ChemCatChem, 9 (2017) 1824-1829.

[11] M. Illner, M. Schmidt, T. Pogrzeba, C. Urban, E. Esche, R. Schomäcker, J.-U. Repke, Palladium-Catalyzed Methoxycarbonylation of 1-Dodecene in a Two-Phase System: The Path toward a Continuous Process, Ind. Eng. Chem. Res., 57 (2018) 8884-8894.

[12] F. Joo, Biphasic Catalysis-Homogeneous. Encyclopedia of Catalysis, John Wiley & Sons, Inc, 2012.

[13] T. Welton, Solvents and sustainable chemistry, Proc. R. Soc. Lond. Ser. A Math. Phys. Eng. Sci, 471 (2015) 20150502.

[14] K.H. Shaughnessy, Hydrophilic ligands and their application in aqueous-phase metal-catalyzed reactions, Chem. Rev., 109 (2009) 643-710.

[15] K. Künnemann, L. Schurm, D. Lange, T. Seidensticker, S. Tilloy, E. Monflier, D. Vogt, J. Dreimann, Continuous hydroformylation of 1-decene in an aqueous biphasic system enabled by methylated cyclodextrins, Green Chem., 22 (2020) 3809-3819.

[16] J. Bianga, N. Herrmann, L. Schurm, T. Gaide, J.M. Dreimann, D. Vogt, T. Seidensticker, Improvement of Productivity for Aqueous Biphasic Hydroformylation of Methyl 10-Undecenoate: A Detailed Phase Investigation, Eur. J. Lipid Sci. Technol., 122 (2020) 1900317.

[17] A. Cocq, H. Bricout, F. Djedaïni-Pilard, S. Tilloy, E. Monflier, Rhodium-Catalyzed Aqueous Biphasic Olefin Hydroformylation Promoted by Amphiphilic Cyclodextrins, Catalysts, 10 (2020) 56.

[18] S. Jagtap, R. Deshpande, True water soluble palladium-catalyzed Heck reactions in aqueous–organic biphasic media, Tetrahedron Lett., 54 (2013) 2733-2736.

[19] S.V. Jagtap, R.M. Deshpande, PdCl2 (bipy) complex—An efficient catalyst for Heck reaction in glycol–organic biphasic medium, Catal. Today, 131 (2008) 353-359.

[20] H.B. Wang, Y.-L. Hu, D.-J. Li, Facile and efficient Suzuki–Miyaura coupling reaction of aryl halides catalyzed by Pd2 (dba) 3 in ionic liquid/supercritical carbon dioxide biphasic system, J. Mol. Liq., 218 (2016) 429-433.

[21] A. Mahanta, M. Mondal, A.J. Thakur, U. Bora, An improved Suzuki–Miyaura cross-coupling reaction with the aid of in situ generated PdNPs: Evidence for enhancing effect with biphasic system, Tetrahedron Lett., 57 (2016) 3091-3095.

[22] K.M.N. Borba, M.O. de Souza, R.F. de Souza, K. Bernardo-Gusmão, β-Diimine nickel complexes in BMI· AlCl4 ionic liquid: a catalytic biphasic system for propylene oligomerization, Appl Catal A-gen, 538 (2017) 51-58.

[23] A. Behr, Z. Bayrak, G. Samli, D. Yildiz, V. Korkmaz, S. Peitz, G. Stochniol, Recycling and oligomerization Activity of Ni/Al catalyst in a biphasic system with ionic liquids, Chem Eng Technol, 40 (2017) 196-204.

[24] Z. Császár, J. Bakos, G. Farkas, Sulfonated Phosphine Ligands in the Ruthenium Catalyzed Biphasic Hydrogenation of Unsaturated Hydrocarbons, Catal. Lett., (2020) 1-8.

[25] A. Joumaa, S. Chen, S. Vincendeau, F. Gayet, R. Poli, E. Manoury, Rhodium-catalyzed aqueous biphasic hydrogenation of alkenes with amphiphilic phosphine-containing core-shell polymers, Mol catal, 438 (2017) 267-271.

[26] S. Weber, J. Brünig, V. Zeindlhofer, C. Schröder, B. Stöger, A. Limbeck, K. Kirchner, K. Bica, Selective Hydrogenation of Aldehydes Using a Well-Defined Fe (II) PNP Pincer Complex in Biphasic Medium, ChemCatChem, 10 (2018) 4386-4394.

[27] M. Schmidt, T. Pogrzeba, L. Hohl, A. Weber, A. Kielholz, M. Kraume, R. Schomäcker, Palladium catalyzed methoxycarbonylation of 1-dodecene in biphasic systems–optimization of catalyst recycling, Molecular Catalysis, 439 (2017) 1-8.

[28] F. Monteil, P. Kalck, Carbonylation of bromobenzene in a biphasic medium catalysed by water-soluble palladium complexes derived from tris (3-sulphophenyl) phosphine, J. Organomet. Chem., 482 (1994) 45-51.

[29] N. Kumari, V.K. Yadav, S. Záliš, L. Mishra, Pd (II) catalyzed transformation of Schiff bases in complexes of the type trans-[PdCl 2 (NH 2 Ar-X) 2](X= H, CH 3, Cl): Reactivity with aldehydes and Heck coupling reaction, Indian J. Chem., 51A (2012) 554-563.

[30] M. Botsivali, D.F. Evans, P.H. Missen, M.W. Upton, Studies on singlet oxygen in aqueous solution. Part 2. Water-soluble square-planar nickel complexes as quenchers, J. Chem. Soc., Dalton Trans., (1985) 1147-1149.

[31] B. Choudary, T. Ramani, H. Maheswaran, L. Prashant, K. Ranganath, K.V. Kumar, Catalytic Asymmetric Epoxidation of Unfunctionalised Olefins using Silica, LDH and Resin-Supported Sulfonato-Mn (salen) Complex, Adv. Synth. Catal., 348 (2006) 493-498.

[32] C. Fasina, Synthesis, electronic spectra and inhibitory study of some Salicylaldehyde Schiff bases of 2-aminopyridine, Afr. J. *Pure* Appl. *Chem*, 5 (2011) 13-18.

[33] T. Stringer, P. Chellan, B. Therrien, N. Shunmoogam-Gounden, D.T. Hendricks, G.S. Smith, Synthesis and structural characterization of binuclear palladium (II) complexes of salicylaldimine dithiosemicarbazones, Polyhedron, 28 (2009) 2839-2846.

[34] S.O. Akiri, S.O. Ojwach, Methoxycarbonylation of olefins catalysed by homogeneous palladium (II) complexes of (phenoxy) imine ligands bearing alkoxy silane groups, Inorg. Chim. Acta, 489 (2019) 236-243.

[35] P.A. Aguirre, C.A. Lagos, S.A. Moya, C. Zúñiga, C. Vera-Oyarce, E. Sola, G. Peris, J.C. Bayón, Methoxycarbonylation of olefins catalyzed by palladium complexes bearing P, N-donor ligands, Dalton Trans., (2007) 5419-5426.

[36] G. Cavinato, L. Toniolo, Carbonylation of ethene catalysed by Pd (II)-phosphine complexes, Molecules, 19 (2014) 15116-15161.

[37] I. del Río, C. Claver, P.W. van Leeuwen, On the mechanism of the hydroxycarbonylation of styrene with palladium systems, Eur. J. Inorg. Chem., 2001 (2001) 2719-2738.

[38] C. Bianchini, A. Meli, W. Oberhauser, P.W. van Leeuwen, M.A. Zuideveld, Z. Freixa, P.C. Kamer, A.L. Spek, O.V. Gusev, A.M. Kal'sin, Methoxycarbonylation of Ethene by Palladium (II) Complexes with 1, 1 '-Bis (diphenylphosphino) ferrocene (dppf) and 1, 1 '-Bis (diphenylphosphino) octamethylferrocene (dppomf), Organometallics, 22 (2003) 2409-2421.

[39] G. Kiss, Palladium-catalyzed Reppe carbonylation, Chem. Rev., 101 (2001) 3435-3456.

[40] C.-M. Tang, X.-L. Li, G.-Y. Wang, A highly efficient catalyst for direct synthesis of methyl acrylate via methoxycarbonylation of acetylene, Korean J. Chem. Eng., 29 (2012) 1700-1707.

[41] H.S. Yun, K.H. Lee, J.S. Lee, The regioselective hydrocarboalkoxylation of 4-methylstyrene catalyzed by palladium complexes, J. Mol. Catal. A: Chem., 95 (1995) 11-17.

[42] A. Seayad, A. Kelkar, L. Toniolo, R. Chaudhari, Hydroesterification of styrene using an in situ formed Pd (OTs) 2 (PPh3) 2 complex catalyst, J. Mol. Catal. A: Chem., 151 (2000) 47-59.

[43] R. Bertania, G. Cavinato, L. Toniolol, G. Vasapollo, New alkoxycarbonyl complexes of palladium (II) and their role in carbonylation reactions carried out in the presence of an alkanol, J. Mol. Catal., 84 (1993) 165-176.

[44] C. Zuniga, D. Sierra, J. Oyarzo, A. Klahn, Methoxycarbonylation of styrene by palladium (II) complex containing the diphenylphosphinocyrhetrene ligand, J. Chil. Chem. Soc., 57 (2012) 1101-1103.

[45] H.A. Ghaly, A.S. El-Kalliny, T.A. Gad-Allah, N.E.A. El-Sattar, E.R. Souaya, Stable plasmonic Ag/AgCl–polyaniline photoactive composite for degradation of organic contaminants under solar light, RSC adv., 7 (2017) 12726-12736.

[46] A.F. Schmidt, A. Al-Halaiqa, V.V. Smirnov, Effect of macrokinetic factors on the ligand-free Heck reaction with non-activated bromoarenes, J. Mol. Catal. A: Chem., 250 (2006) 131-137.

[47] R.B. Bernstein, Atom-molecule collision theory: a guide for the experimentalist, Springer Science & Business Media2013.

[48] J.J. de Pater, D. Tromp, D.M. Tooke, A.L. Spek, B.-J. Deelman, G. van Koten, C.J. Elsevier, Palladium (0)-Alkene Bis (triarylphosphine) complexes as catalyst precursors for the methoxycarbonylation of styrene, Organometallics, 24 (2005) 6411-6419.

[49] M.K. YILMAZ, S. İnce, Palladium (II) Complexes of Monodentate Phosphine Ligands and Their Application as Catalyst in Suzuki-Miyaura CC Coupling Reaction at Room Temperature, J. Turkish chem. soc., 5 (2018) 895-902.

[50] Z. Kokan, B. Perić, G. Kovačević, A. Brozovic, N. Metzler-Nolte, S.I. Kirin, cis-versus trans-Square-Planar Palladium (II) and Platinum (II) Complexes with Triphenylphosphine Amino Acid Bioconjugates, Eur. J. Inorg. Chem., 2017 (2017) 3928-3937.

[51] C. Blanco, C. Godard, E. Zangrando, A. Ruiz, C. Claver, Room temperature asymmetric Pd-catalyzed methoxycarbonylation of norbornene: highly selective catalysis and HP-NMR studies, Dalton Trans., 41 (2012) 6980-6991.

[52] J.S. Kim, A. Sen, I.A. Guzei, L.M. Liable-Sands, A.L. Rheingold, Synthesis and reactivity of bimetallic palladium (II) methyl complexes with new functional phosphine ligands, J. Chem. Soc., Dalton Trans., (2002) 4726-4731.

[53] Y. Cabon, I. Reboule, M. Lutz, R.J. Klein Gebbink, B.-J. Deelman, Oxidative Addition of Sn− C Bonds on Palladium (0): Identification of Palladium− Stannyl Species and a Facile Synthetic Route to Diphosphinostannylene− Palladium Complexes, Organometallics, 29 (2010) 5904-5911.

[54] J.H. Nelson, Aspects of equivalence as illustrated by phosphine complexes of transition metals, Concepts in Magnetic Resonance: An Educational Journal, 14 (2002) 19-78.

[55] R.E. Harmon, S. Gupta, D. Brown, Hydrogenation of organic compounds using homogeneous catalysts, Chem. Rev., 73 (1973) 21-52.

[56] R. Pruvost, J. Boulanger, B. Leger, A. Ponchel, E. Monflier, M. Ibert, A. Mortreux, M. Sauthier, Biphasic Palladium-Catalyzed Hydroesterification in a Polyol Phase: Selective Synthesis of Derived Monoesters, ChemSusChem, 8 (2015) 2133-2137.

[57] T. Gaide, A. Behr, M. Terhorst, A. Arns, F. Benski, A.J. Vorholt, Catalyst Comparison in the Hydroesterification of Methyl 10-Undecenoate in Thermomorphic Solvent Systems, Chem. Ing. Tech., 88 (2016) 158-167.

[58] A. Behr, A. Vorholt, N. Rentmeister, Recyclable homogeneous catalyst for the hydroesterification of methyl oleate in thermomorphic solvent systems, Chem. Eng. Sci., 99 (2013) 38-43.

[59] S.B. Dake, R.V. Chaudhari, Solubility of carbon monoxide in aqueous mixtures of methanol, acetic acid, ethanol and propionic acid, J. Chem. Eng. Data, 30 (1985) 400-403.

[60] R. Sang, P. Kucmierczyk, R. Dühren, R. Razzaq, K. Dong, J. Liu, R. Franke, R. Jackstell, M. Beller, Synthesis of Carboxylic Acids by Palladium-Catalyzed Hydroxycarbonylation, Angew. Chem. Int. Ed., 58 (2019) 14365-14373.

[61] B. Richter, A.L. Spek, G. van Koten, B.-J. Deelman, Fluorous versions of Wilkinson's catalyst. Activity in fluorous hydrogenation of 1-alkenes and recycling by fluorous biphasic separation, J. Am. Chem. Soc., 122 (2000) 3945-3951.

[62] J. Dupont, P.A. Suarez, A.P. Umpierre, R.F.d. Souza, Pd (II)-dissolved in ionic liquids: a recyclable catalytic system for the selective biphasic hydrogenation of dienes to monoenes, J. Braz. Chem. Soc., 11 (2000) 293-297.

Chapter 5

Effects of MCM-41, SBA-15 and Fe$_3$O$_4$ solid supports and calcination temperature on methoxycarbonylation of olefins

5.1 Introduction

Heterogeneous and homogeneous catalyst systems have played a vital role in increasing industrial outputs and greatly reducing the time required to manufacture various industrial products and feedstocks through various catalytic transformation reactions [1]. However, such an improvement has not come without challenges, some of which include environmental pollution, excess use of solvents, and the concern about the purity of the produced industrial products [2]. Accordingly, there have been efforts in recent times to shift to more robust, greener and more sustainable industrial strategies that can use feedstocks efficiently, do away with the application of hazardous and toxic compounds as well as eliminate waste [3]. Besides, both homogeneous catalysts and heterogeneous catalysts face various drawbacks. For instance, while homogeneous catalysts suffer from a lack of catalyst separation and recyclability, heterogeneous catalysts suffer from poor selectivity and complexity of the mechanistic paths involved. As such, efforts have been made in recent times to integrate the pros of heterogeneous and homogeneous catalysts to come up with a "hybrid" system that can be reused and also selective [4, 5].

To date, various methods have been applied in attempts to design catalysts combining the strength of both the homogeneous and the heterogeneous catalysts. Some of the strategies include immobilization on magnetic nanoparticles [6], polymer supports [7-9], silica supports [10, 11], metal-organic frameworks [12]. An important observation is that the use of silica

supports have been favoured and preferred as support to catalysts used in various catalytic transformations [13, 14]. Among the possible reasons for such a trend is that silica shows appreciable thermal and chemical stability hence can be used in a range of chemical environments such as high and low temperatures as well as high and low pressures [15]. Even though immobilization of catalysts on various supports has been extensively used in various catalytic reactions, methoxycarbonylation as one of the carbonylation reactions has just but a handful of reports, hence presenting an opportunity that chemists can exploit.

Industrially, the methoxycarbonylation ester products are applied in producing polymer-building blocks and detergents. It is, therefore, not surprising that a palladium-based catalyst system for methoxycarbonylation of ethylene is being used as the major process in the Lucite Alpha reaction in the manufacture of methyl methacrylate polymers [16]. In efforts to integrate homogeneous and heterogeneous catalysis, this chapter reports the synthesis and characterization of homogeneous palladium(II) complexes bearing diimine ligands. In addition, synthesis and characterization of the complexes immobilized on silica (MCM-41 and SBA-15) and magnetic nanoparticles are also reported. This chapter further reports a detailed comparative study between the homogeneous palladium(II) complexes and their immobilized counterparts in the methoxycarbonylation of olefins. The effects of support and calcination temperature on the behaviour of the immobilized catalysts have also been explored.

5.2 Experimental section

5. 2.1 Instrumentation and material

The reagents aniline, 2,6- dimethyl aniline, 2, 6- diisopropylaniline, sodium hydride, sodium carbonate, and palladium dichloride, 3-chloropropyl triethoxy silane, iron(III) chloride

hexahydrate ($FeCl_3 \cdot 6H_2O$) SBA 15 and MCM41 were purchased from Sigma-Aldrich and were used as received without further purification. In addition, the Fe_3O_4 magnetic support was synthesised following previously published literature [17]. A transmission electron microscope (JEOL JEM, 1400 model) operating at 200 kV accelerating voltage was used in acquiring the TEM images. The compounds were sonicated in ethanol before placing on carbon-coated copper grids. The morphology of the surfaces and particles sizes were studied using a scanning electron microscope of the ZEISS EVO LS15 model operating at an accelerating voltage of 20kV. Besides, the qualitative elemental contents of the supported palladium(II) complexes were acquired by using an Oxford make EDX detector. The X-ray diffraction spectra of the synthesized materials were analyzed using an XPERT-PRO XRD instrument with $CuK\alpha$ radiation with 4.01 to 89.9° used as the 2θ range

5.2.2 Synthesis and characterization of (amino)phenyl ligands and their homogeneous palladium(II) complexes

*5.2.2.1(E)-N-((Z)-4-(phenylamino)pent-3-en-2-ylidene)aniline (**L12**)*

To a mixture of rapidly stirred aniline (3.60 ml, 40.00 mmol) and acetylacetone (2.10 ml, 20.00 mmol) in a flask put in ice, concentrated hydrochloric acid (1.70 ml) was slowly added, forming a yellow mixture immediately. After stirring for 12 h, filtration was done, and the yellow precipitate was washed with hexane. The precipitate was then dissolved in 10.00 ml of water, 4.00 ml of triethylamine and 2.00 ml of dichloromethane. The aqueous phase was further extracted using diethyl ether and combined with the organic phase. The mixture was then dried over magnesium sulphate and the solvent evaporated under vacuum to result in **L12** as a yellow oil. Yield =2.13 g (43 %). ^1H NMR (400 MHz, $CDCl_3$): δ_H (ppm) 2.07 (s, 6H, CH_3), 4.92 (s, 2H, CH_2), 7.12 (d, 4H, $^3J_{HH}$ =8.0 Hz, *o*-ArH, 7.22 (t, 2H, $^3J_{HH}$ =8.0 Hz, *p*-ArH), 7.36(t, 4H, $^3J_{HH}$ =8.0, *m*-ArH), 12.52 (s, 1H NH). ^{13}C NMR (100 MHz, CDCl3, δ ppm); 196.2 (C=N), 191.2

(C-N), 160.26 (C-Ar), 138.8 (C-Ar), 129.1 (C-Ar), 125.6 (C-Ar), 124.8 (C-Ar), 97.7 (β-CH), 29.2 (α-CH3), 24.8 (α-CH3). IR ν_{max}/ cm^{-1}: $\nu_{(C=N)}$ = 1635. ESI-MS (m/z) = 251(M$^+$ + H)$^+$,100%)

*5.2.2.2 N,N'E,N,N'E)-N,N'-(3-(3-(triethoxysilyl)propyl)pentane-2,4-diylidene)dianiline (**L13**)*

To solution of ligand **L12** (1.5 g, 6.00 mmol) in dichloromethane (20 ml) was added NaH (0.21, 9.00 mmol) under nitrogen and stirred for 30 min at 35 °C. A solution of 3-chloropropyl triethoxy silane (CTPES) (1.44 ml, 6.00 mmol) in 5 ml of toluene was then added to the resulting mixture and refluxed for a further 3 h. The resulting product was then cooled and centrifuged for a duration of 20 min. The supernatant liquid was then taken and the solvent removed *in vacuo* to give **L13** as a dark yellow oil. Yield =2.37 g (87 %). ^{1}H NMR (400 MHz, CDCl$_3$): δ_H (ppm) 0.77 (t, 2H, $^3J_{HH}$ = 8.0 Hz, CH$_2$-Si), 1.25 (t, 9H, $^3J_{HH}$ = 7.0 Hz, SiOCH$_2$*CH$_3$*), 1.90 (m, 2H, Si-βCH$_2$), 2.05 (s, 3H, CH$_3$), 2.11 (s, 3H, CH$_3$), 3.54 (t, 2H, $^3J_{HH}$ = 6.8 Hz, Si-γCH$_2$) 3.84 (q, 6H, $^3J_{HH}$ = 7.0 Hz, SiO*CH$_2$*CH$_3$) 7.15 (d, 4H, $^3J_{HH}$ =8.0 Hz, *o*-ArH, 7.24 (t, 2H, $^3J_{HH}$ =8.0 Hz, *p*-ArH), 7.38 (t, 4H, $^3J_{HH}$ =8.0, *m*-ArH), 12.52 (s, 1H NH). ^{13}C NMR (100 MHz, CDCl3, δ ppm); 169.2 (C=N), 161.2 (C-N), 160.26 (C-Ar), 138.8 (C-Ar), 129.1 (C-Ar), 125.6 (C-Ar), 124.8 (C-Ar), 97.7 (β-CH), 59.5 (SiO*CH$_2$*CH$_3$), 29.2 (α-CH3), 26.2 (Si-γCH$_2$), 24.8 (α-CH3) ,20.3(SiOCH$_2$*CH$_3$*), 17.5 (Si-βCH$_2$), 14.4 (CH$_2$-Si). IR ν_{max}/ cm^{-1}: $\nu_{(C=N)}$ = 1642. ESI-MS (m/z) = 455 (M$^+$ + H)$^+$,100%).

*5.2.2.3 (E)-N-((Z)-4-(phenylamino)pent-3-en-2-ylidene)aniline (**Pd13**)*

To a solution of ligand **L12** (0.10 g, 0.40 mmol) in CH$_2$Cl$_2$ (5.00 ml) was added [Pd(NCMe)Cl$_2$] (0.10 g, 0.40 mmol) to give a brown mixture. The mixture was then stirred for 12 h, followed by solvent elimination *in vacuo* and the formed solid washed with hexane to give **Pd13** as bright yellow solid. Yield = 0.13 g (76%). ^{1}H NMR (400 MHz, CDCl$_3$): δ_H (ppm) 2.07 (s, 6H, CH$_3$), 4.83 (s, 2H, CH$_2$), 7.12 (d, 4H, $^3J_{HH}$ =8.0 Hz, *o*-ArH, 7.22 (t, 2H, $^3J_{HH}$ =8.0 Hz, *p*-ArH), 7.36(t, 4H, $^3J_{HH}$ =8.0, *m*-ArH), 12.52 (s, 1H NH). ^{13}C NMR (100 MHz, CDCl3, δ ppm); 196.2

(C=N), 191.2 (C-N), 160.26 (C-Ar), 138.8 (C-Ar), 129.1 (C-Ar), 125.6 (C-Ar), 124.8 (C-Ar), 97.7 (β-CH), 29.2 (α-CH3), 24.8 (α-CH3). IR ν_{max}/ cm^{-1}: $\nu_{(C=N)}$ = 1644. ESI-MS: m/z (%) 355 [(M$^+$ -2Cl), 100%)]. Anal. Calc. for $C_{17}H_{17}Cl_2N_2Pd$: C, 47.86 , H, 4.02, N, 6.57. Found: C, 47.77, H. 4.18, N, 6.50.

5.2.2.4 N,N'E,N,N'E)-N,N'-(3-(3-(triethoxysilyl)propyl)pentane-2,4-diylidene)dianiline

*palladium(II) (**Pd14**)*

To a solution of [PdCl$_2$(CH$_3$CN)$_2$] (0.15 g ,0.57 mmol) in dichlomethane (5 ml) was added a solution of **L13** (0.26 g, 0.57 mmol) in 5 ml of dichloromethane. The resulting mixture was then stirred under nitrogen at room temperature for 24 h to give a yellow solution. The solvent was then removed *in vacuo* to afford **Pd14** as bright yellow solid. Yield = 0.31 g (86%). ^{1}H NMR (400 MHz, CDCl$_3$): δ$_H$ (ppm) 0.79 (t, 2H, $^3J_{HH}$ = 8.0 Hz, CH$_2$-Si), 1.22 (t, 9H, $^3J_{HH}$ = 7.0 Hz, SiOCH$_2$*CH$_3$*), 1.95 (m, 2H, Si-βCH$_2$), 2.11 (s, 3H, CH$_3$), 2.32 (s, 3H, CH$_3$), 3.64 (t, 2H, $^3J_{HH}$ = 6.8 Hz, Si-γCH$_2$) 3.88 (q, 6H, $^3J_{HH}$ = 7.0 Hz, SiO*CH$_2$*CH$_3$) 7.11 (d, 4H, $^3J_{HH}$ =8.0 Hz, *o*-ArH, 7.20 (t, 2H, $^3J_{HH}$ =8.0 Hz, *p*-ArH), 7.40 (t, 4H, $^3J_{HH}$ =8.0, *m*-ArH), 12.52 (s, 1H NH). ^{13}C NMR (100 MHz, CDCl3, δ ppm); 167.5 (C=N), 161.8 (C-N), 160.55 (C-Ar), 137.8 (C-Ar), 130.5 (C-Ar), 124.8 (C-Ar), 123.6 (C-Ar), 96.8 (β-CH), 58.3 (SiO*CH$_2$*CH$_3$), 30.1 (α-CH3), 27.0 (Si-γCH$_2$), 24.4 (α-CH3), 20.8(SiOCH$_2$*CH$_3$),   17.2 (Si-βCH$_2$), 14.7 (CH$_2$-Si). IR ν_{max}/ cm^{-1}: $\nu_{(C=N)}$ = 1642. ESI-MS (m/z) = 631.09 (M$^+$ + H)$^+$,100%).

5.2.3. Synthesis of diimine palladium(II) complexes immobilized on silica and Fe$_3$O$_4$ magnetic nanoparticles.

*5.2.3.1 Synthesis of (**Pd14-MCM41**) (**Pd15**).*

To a solution of **Pd14** (0.1 g, 0.16 mmol) in toluene (15 ml) was added MCM-41 (1.0 g), and the mixture was sonicated for 20 min. The mixture was then refluxed for 24 h, cooled and

filtered. The residue was then washed with ethanol (2x3 ml) and dried in the oven for 24 h to give **Pd15** as a yellow powder. Yield, 0.95 g. IR vmax/ cm^{-1}: ν *(C=N)* = 1641,ν *(Si-O-Si)* = 1056

*5. 2.3.2 Synthesis of (**Pd14-SBA15**) (**Pd16**).*

Complex **Pd16** was synthesized following the procedure described for complex **Pd15** using **Pd14** (0.1g, 0.16 mmol) and SBA15 (1.0 g). Yellow solid; yield = 0.90 g. IR vmax/ cm^{-1}: ν *(C=N)* = 1657, ν *(Si-O-Si)* = 1059.

*5.2.3.3 Synthesis of (**Pd14-Fe$_3$O$_4$**) (**Pd17**).*

Complex **Pd17** was prepared by following the procedure described for complex **Pd15** using **Pd14** (0.1 g, 0.32 mmol) and Fe$_3$O$_4$ (1.0 g). Brown solid; yield = 0.80 g. IR vmax/ cm^{-1}: ν *(C=N)* = 1597,ν *(Si-O)* = 1053, ν *(Si-OH)=3341,* ν *(Fe-O).= 583*

*5.2.3.4 Synthesis of (Pd14-MCM41@5% wt) (**Pd18**).*

To a solution of **Pd14** (0.05 g, 0.08 mmol) in toluene (15 ml) was added MCM-41 (1.0 g), and the mixture was sonicated for 20 min. The mixture was then refluxed for 24 h, cooled and filtered. The residue was then washed with ethanol (2x3 ml) and dried in the oven for 24 h to give **Pd18** as a yellow powder. Yield, 0.90 g. IR vmax/ cm^{-1}: ν *(C=N)* = 1653,ν *(Si-O-Si)* = 1052

*5.2.3.5 Synthesis of (**Pd14MCM41@15%wt**) (**Pd19**).*

To a solution of **Pd14** (0.15 g, 0.03 mmol) in toluene (15 ml) was added MCM-41 (1.0 g), and the mixture was sonicated for 20 min. The mixture was then refluxed for 24 h, cooled and filtered. The residue was then washed with ethanol (2x3 ml) and dried in the oven for 24 h to give **Pd19** as a yellow powder. Yield, 0.93 g. IR vmax/ cm^{-1}: ν *(C=N)* = 1650 ,ν *(Si-O-Si)* = 1049.

*5.2.3.6 Synthesis of (Pd14-SBA15@150 °C) (**Pd20**).*

Complex **Pd20** was synthesized following the procedure described for complex **Pd15** using **Pd14** (0.1 g, 0.16 mmol) and SBA15 (1.0 g). The resulting yellow solid was then calcined at a temperature of 150 °C for 24 h to afford **Pd20** as bright yellow powder. Yield = 0.91 g. IR νmax/ cm^{-1}: ν *(C=N) = 1652,*ν *(Si-O-Si) = 1053.*

5.2.3.7 Synthesis of (Pd14-SBA15@200 °C) (Pd21).

Complex **Pd20** was synthesized following the procedure described for complex **Pd15** using **Pd14** (0.1g, 0.16 mmol) and SBA15 (1.0 g). The resulting yellow solid was then calcined at a temperature of 200 °C for 24 h to afford **Pd20** as bright yellow powder. Yield = 0.87 g. IR νmax/ cm^{-1}: ν *(C=N) = 1648,*ν *(Si-O-Si) = 1058.*

5.4 Results and discussion

5.5.1 Synthesis and characterization of (amino) phenyl ligands, homogeneous palladium(II) complexes and their respective immobilized complexes.

The diimine ligand (**L12**) was made through a procedure modified from literature (Scheme 5.1), and a below-average yield of 43% was obtained. **L13** was synthesized by functionalization of ligand **L12** using CTPES in good yield (87%). The respective palladium(II) complexes (**Pd13** and **Pd14**) were synthesized at ambient temperature under nitrogen for a duration of 24 h to give the complexes good yields (75 and 80%). ^{1}H NMR, ^{13}C NMR, FTIR spectroscopy, elemental analyses and mass spectrometry were used in characterizing the compounds. On the other hand, - the immobilized complexes (**Pd15-Pd21**) were synthesized through a convergence immobilization route (Scheme 5. 2). The new immobilized compounds were characterized by applying TEM, IR, SEM-EDX, BET analysis, ICP- OES, and power XRD.
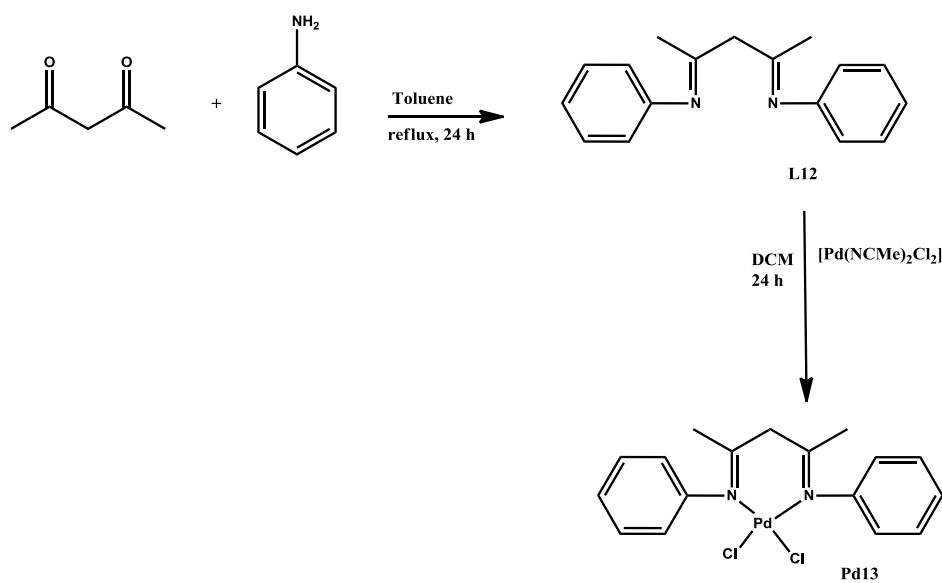
Scheme 5.1: Synthesis of diimine ligand and the homogeneous palladium(II) complex
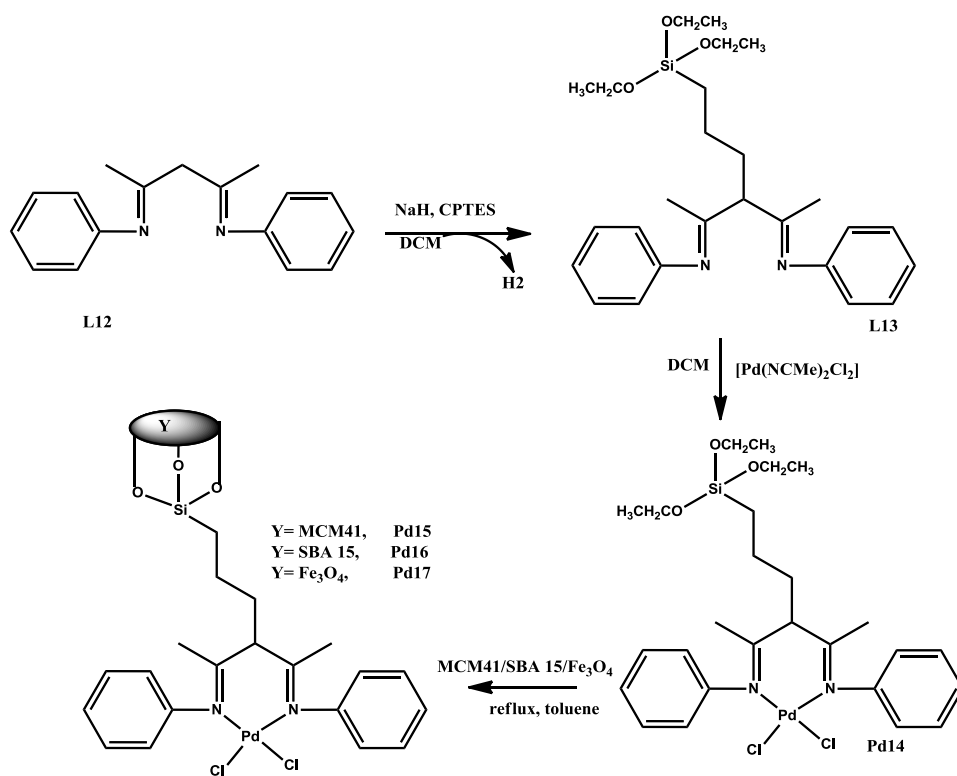
Scheme 5.2: Synthesis of immobilized palladium(II) complexes using a covalent convergence strategy

The ^{1}H NMR helped in determining the identity of the compounds formed. For instance, the formation of ligand **L12** was established by the olefinic proton upward shift from 5.39 ppm in acetylacetone to 4.92 ppm in ligand **L12** (Figure 5.1). A similar shift was observed by Rossetto *et al*., whose peak was reported at 4.89 ppm [18]. In addition, the synthesis of ligand **L13** from **L12** was confirmed by the presence of an additional upfield peak associated with the silane backbone (Figure 5.1). Another observation worth mentioning is the disappearance of β-CH from ligand **L13** relative to ligand **L12,** confirming the successful attachment of 3-chloropropyl triethoxy silane. The resonances displayed by the olefinic proton was further used to assess the formation of the complexes. While the olefinic proton resonated at 4.92 ppm in ligand **L12**, the same proton was observed to undergo an up field shift to 4.83 ppm upon coordination to form complex **Pd13.**
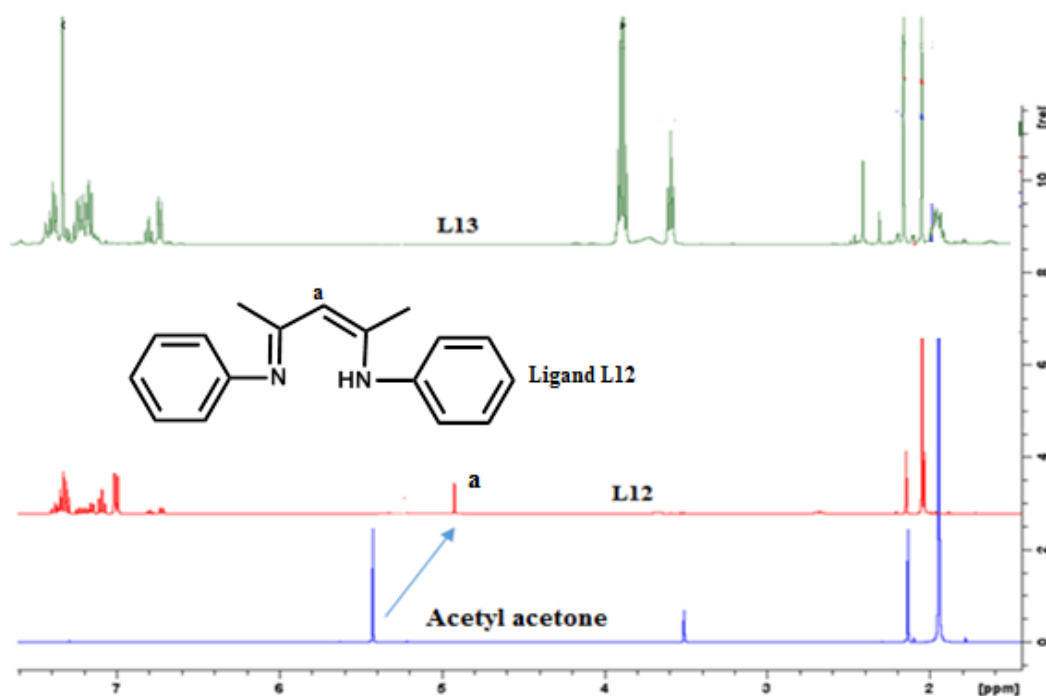
Figure 5.1: Overlaid ^{1}H NMR spectra of acetylacetone and **L12** showing olefinic proton (a) shift from 5.39 ppm to 4.93 ppm and the disappearance of the olefinic proton in **L13**.

Another important characterization tool that was used to deduce the successful formation of the proposed compounds is Fourier-transform infrared spectroscopy. The appearance of the imine bond was also useful in confirming the formation of the diimine ligands. For example, in ligand **L12,** the value at 1635 cm^{-1} is associated with the $\nu(C=N)$ bond, signalling its successful formation. The complexes were also characterized using the same technique, where shifts in the wave numbers of the $\nu(C=N)$ bond signalled a change in the chemical environment hence successful complication (Figure 5. 2). As a demonstration, the $\nu(C=N)$ was observed at 1635 and 1644 cm^{-1} in **L1** and **Pd13,** respectively. Table 5.1 shows a summary of the FT-IR values for the ligands and the respective palladium(II) coordination compounds.
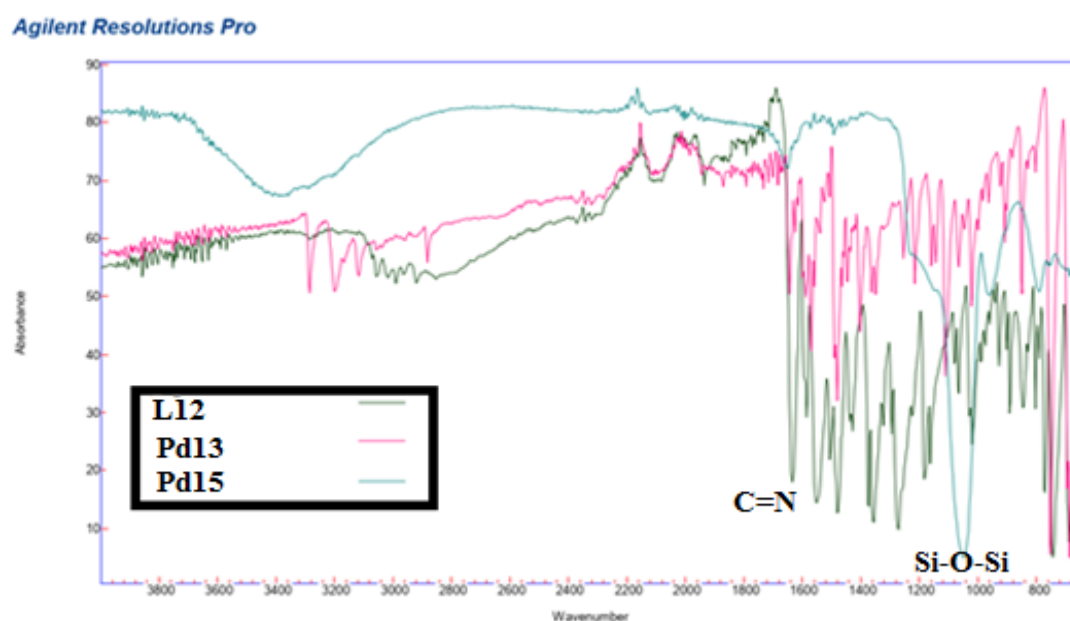
Figure 5.2: An overlaid FT-IR spectra of ligand **L12** and complexes **Pd13** and **Pd15** showing signature peaks.

5.5.2 Characterization of the immobilized compounds

The silica and magnetic nanoparticle supported palladium(II) complexes were also characterized using Fourier-transform infrared spectroscopy. The observed wavenumbers

between 1050-1080 cm^{-1} in the MCM-41 and SBA-15 immobilized complexes were particularly important in inferring the successful immobilization of the silane palladium(II) complexes onto the silica supports, MCM-41 and SBA-15. These wave numbers have been associated with the Si-O-Si vibrations [19, 20]. Besides, all the complexes displayed characteristic $\nu(C=N)$ wavenumbers between 1611-1644 cm^{-1}, indicating the retention of the organic core. The Fe$_3$O$_4$ nanoparticles supported palladium complexes also displayed diagnostic peaks. Apart from the $\nu(C=N)$ wave numbers, there were also lower and higher wave numbers observed (Table 5. 1). For example, complex **Pd17** showed wavenumbers at 3341 and 583 cm^{-1} which can be assigned to $\nu(Si-OH)$ and $\nu(Fe-O)$, respectively. Asadi *et al.* observed similar vibrations at 3457 and 607 cm^{-1}, respectively [21].

Table 5.1: IR and mass spectral values of compounds **L12**, **L13** and **Pd13**-**Pd17**

Ligands and complexes	$\nu(C=N)$ (cm^{-1})	$\nu(Si-O-Si)$ (cm^{-1})	$\nu(Si-OH)$ (cm^{-1})	$\nu(Fe-O)$ (cm^{-1})	Molar mass (gmol^{-1})	m/z (amu)
L12	1635	-	-	-	250.15	251 (M$^+$ + H)
Pd13	1644	-	-	-	426.66	355 (M$^+$ - 2Cl)
L13	1622	1055	-	-	453.30	454 (M$^+$ + H)
Pd14	1641	1060	-	-	482.76	483 (M$^+$ + H)
Pd15	1653	1052	-	-	-	-
Pd16	1652	1053	-	-	-	-
Pd17	1613	-	3341	583	-	-

The surface morphology, qualitative elemental composition and the particle size of the immobilized complexes, the synthesized immobilized materials were characterized using

SEM-EDX and TEM. From the SEM micrographs (Figure 5.3), a morphology surface analysis revealed that predominantly cylindrical particles (Figure 5.3 A). The surface of complex **Pd16** formed by using SBA-15 as a support agent is similar to the support except that additional spherical particles can be observed, indicating a successful immobilization of the complex.
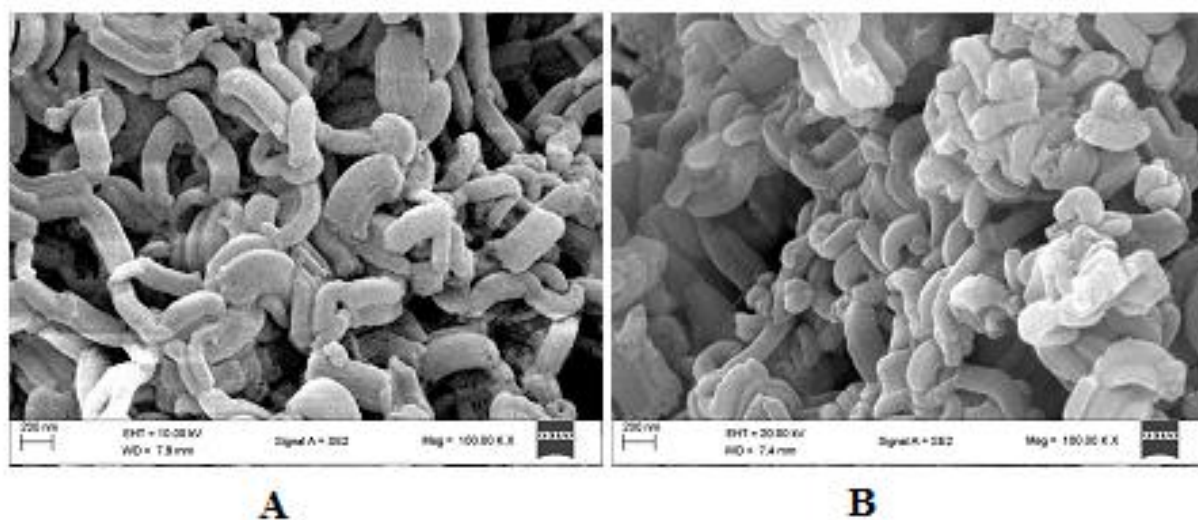
Figure 5.3: SEM images of SBA-15 and complex **Pd16** showing cylindrical particles

SEM-EDX was also used in the investigation of the elemental compositions. As shown in the EDX spectrum for complex **Pd16**, it is evident that the synthesized immobilized complexes had the expected elemental composition, with the complexes having a range of qualitative metallic compositions (Figure 5.4). A summary of the elemental compositions of complexes **Pd15**-**Pd17** has been given in Table 5. 2. Figure 5.4 (inset) shows the dispersion of the elements on the surface of complex **Pd16**. The Figure shows the location of Pd, O, N, Cl, C and Si atoms across the selected region. It is evident that the concentration of Si is appreciable much higher in comparison to the rest of the atoms. This implies that the support material-SBA-15 is the

core material where the metallic and organic functions are all anchored. In addition, the atoms are also homogeneously distributed across the surface, implying the absence of aggregation.
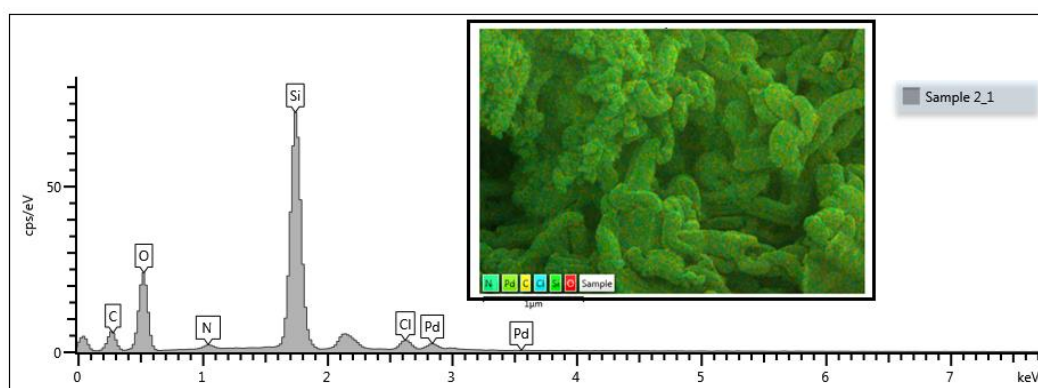
Figure 5.4: An EDX spectrum of complex **Pd16** showing the elemental peaks. Inset (elemental mapping for complex **Pd16**)

Table 5.2: EDX qualitative elemental analysis of the immobilized complexes **Pd15**-**Pd17**.

Element	Pd15		Pd16		Pd17	
	Weight%	Atomic%	Weight%	Atomic%	Weight%	Atomic%
C K	10.94	19.01	12.33	18.33	11.98	17.21
N K	6.87	9.91	6.91	10.03	7.33	10.11
O K	35.43	47.31	32.43	46.77	37.54	43.69
Cl K	12.45	7.56	10.32	8.55	11.35	7.21
Pd L	11.81	3.03	12.21	3.41	9.92	2.95
Si K	22.76	13.18	25.80	12.91	-	-
FeK	-	-	-	-	21.88	18.33
Totals	100.00		100.00		100.00	

In further efforts to understand the morphology and the particle sizes of the synthesized immobilized compounds, TEM analysis was employed. As displayed in Figure 5. 5, there is a variance in surface morphology between the native SBA-15 support and the immobilized complex **Pd16.** The SBA15 shows groups of mesoporous channels. Upon the use of the material to support complex **Pd14,** the mesoporous channels are still visible, and there are additional quasi-spherical particles with diameters ranging from 11.20 nm-12.00 nm. The observations clearly indicate that the immobilization of the complex onto the silica support was successful and that the silica retained its structure. Similar observations were made by Han *et al.* [22] and Veisi et al. [23] in palladium catalysts supported on SBA15 applied in Heck coupling and Suzuki-Miyaura catalytic reactions, respectively.
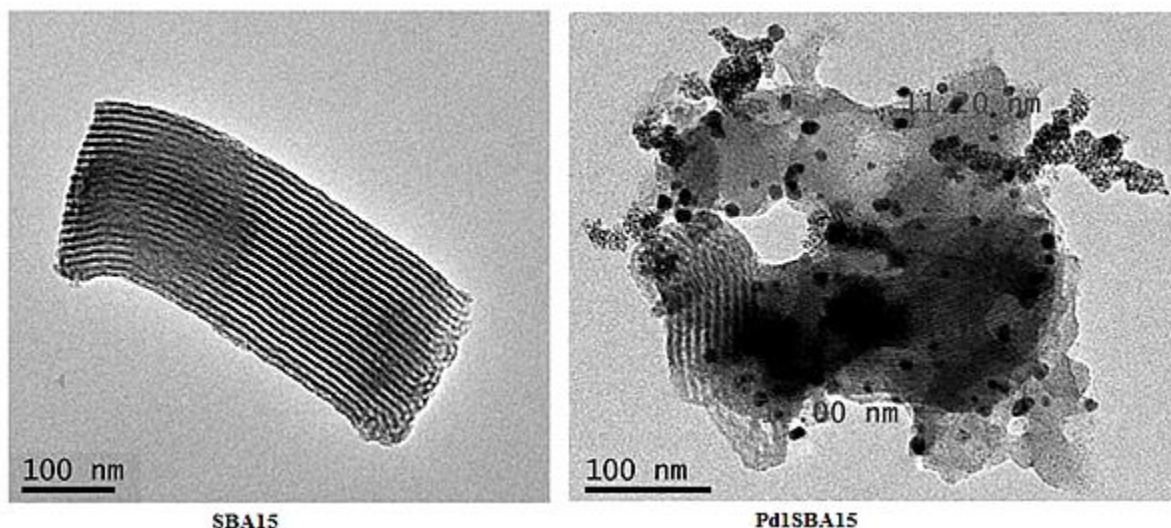
Figure 5.5: TEM images showing additional deposition of quasi-spherical particles on the native SBA15 to give immobilized complex **Pd16**.

ICP-OES was applied in determining the quantitative loading of palladium. A summary of the values is shown in Table 5.3. The synthetic protocol used in making the complexes appeared to have a significant effect on the resultant palladium metal loading. The SBA15 supported complexes were observed to have a higher loading of palladium when compared to MCM-41, and Fe_3O_4 supported complexes. For example, while the palladium loading for **Pd15** and **Pd17** had loadings of 2.65% and 1.91, respectively, the corresponding complex **Pd16** was observed to have a higher metal loading of 2.79%. This observation could be due to the larger pore and pore volume exhibited by the SBA15 support [24].

Table 5.3: Qualitative and quantitative palladium content using EDX and ICP-OES respectively

Entry	Complex	EDX%	ICP-OES (%)
1	**Pd15**	3.03	2.65
2	**Pd16**	3.41	2.79
3	**Pd17**	2.95	1.91
4	**Pd18**	2.59	2.11
5	**Pd19**	3.37	3.03
6	**Pd20**	3.11	2.75
7	**Pd21**	3.03	2.76

In efforts to examine the phase composition and crystallinity of the synthesized immobilized complexes, power XRD was conducted. The wide-angle XRD analysis of the native MCM41 showed sharp diffraction peaks at 100 (5.3º) and 110 (7.1º), typical of the hexagonal nature of MCM-41 [25]. Upon using MCM as a support, the immobilized complex **Pd1-MCM41** showed characteristic peaks at 40.1º, 46.4º and 68.1º (Figure 5.6), which can be assigned h,k, l values of (111), (200) and (220) and is related to palladium nanoparticles [26].
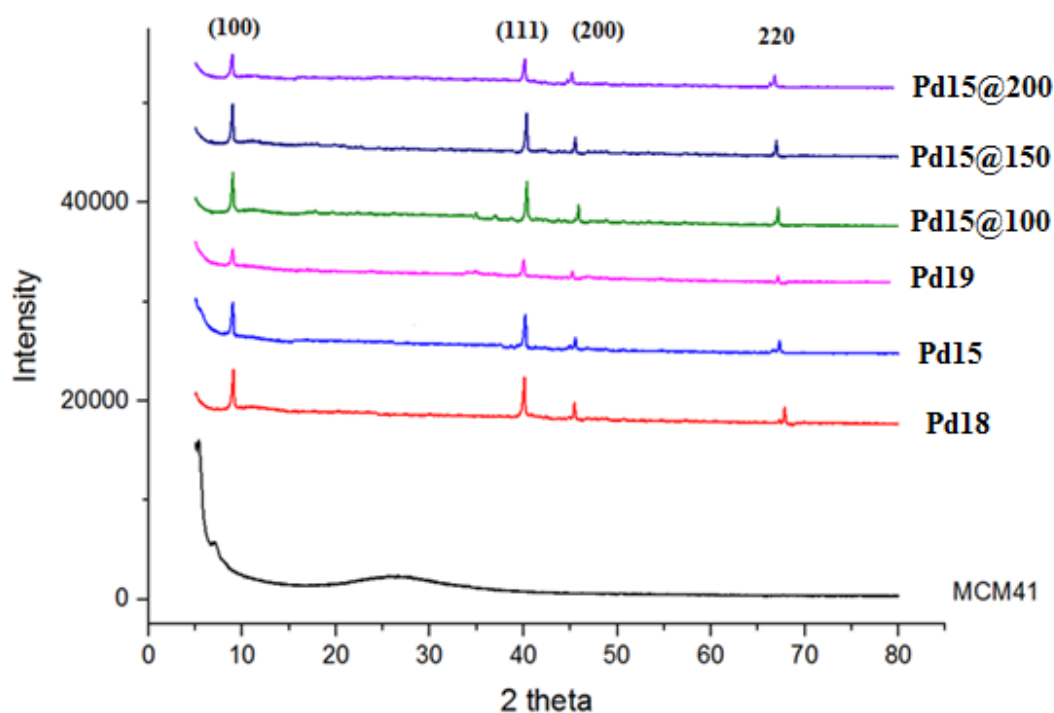
Figure 5.6: XRD pattern and Bragg's reflections observed for the immobilized complexes showing typical Pd silica immobilized complexes.

The magnetic iron particles supported palladium(II) complexes were also characterized using wide-angle XRD. From Figure 5.7, six characteristic peaks of Fe_3O_4 nanomaterial can be observed at 2θ of 35.3^o, 41.7^o, 50.8^o, 63.3^o, 67.7^o and 74.7^o, which respectively be assigned the hkl values of (220), (311), (400), (422), (511) and (440) and has been associated with the cubic spinal structure [27, 28]. Upon using the Fe_3O_4 nanomaterial as a support to the homogenous palladium(II) catalyst, the diffraction patterns were maintained, indicating that the crystalline phase of the Fe_3O_4 nanomaterial remained stable upon immobilization. It is worth noting that extra diffraction peaks at 18.5^o, 22.8^o and 30.2^o observed in the palladium complexes grafted on the Fe_3O_4 nanomaterial confirms the successful formation of the Fe_3O_4 supported palladium(II) complexes [29].
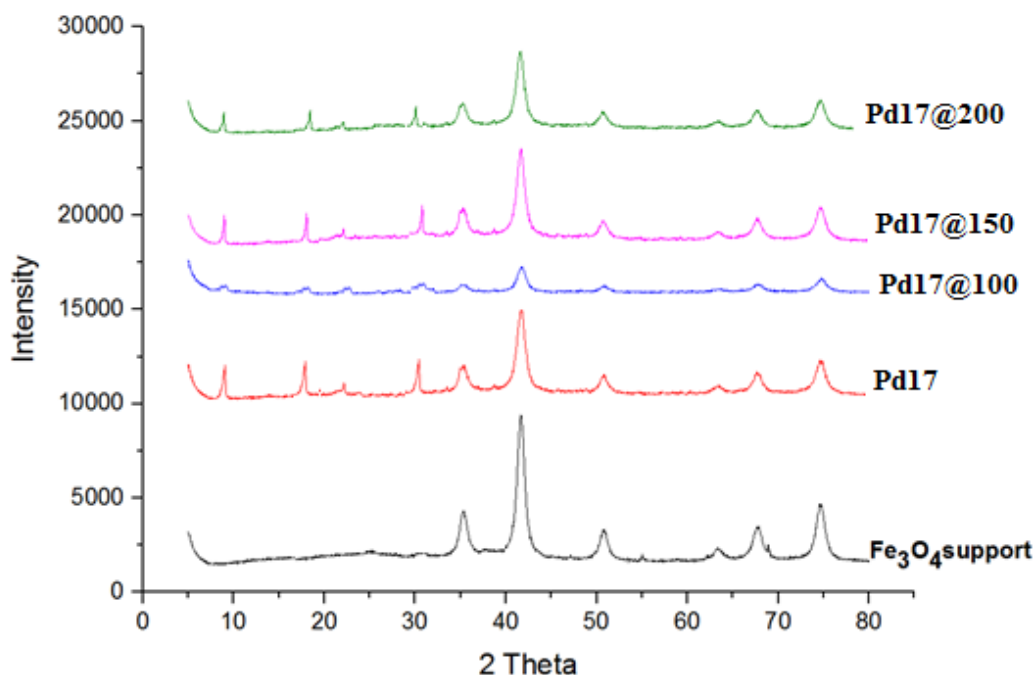
Figure 5.7: XRD pattern and Bragg's reflections observed for the immobilized complexes showing typical Pd iron nanoparticles immobilized complexes.

5.6 Catalytic behaviour of the homogeneous and immobilized complexes in the methoxycarbonylation of olefins

5.6.1. Initial probe of the homogeneous Pd13 in methoxycarbonylation of 1- hexene

The initial probe of the behaviours of the new complexes in the methoxycarbonylation was done with starting reaction conditions of 60 bar and 90 °C as CO gas pressure and the reactor temperature, respectively, using homogeneous complex **Pd13**. Complex **Pd13** was selected for the initial probe as a homogeneous complex to find the optimum conditions to be used for testing the immobilized complexes. The Pd: PPh$_3$: PTSA: 1-hexene ratios were 1:2:10:300, a set-up that gave an equivalence of 0.33 mol% of the palladium metal content with respect to the substrate. In identifying and quantifying the major ester products obtained, GC and GC-

MS were used in addition to ethylbenzene and commercial methyl heptanoate as the internal standard and authentic sample, respectively. Methyl heptanoate and 2-methylhexanoate were revealed as the major compounds formed. The TON values were then calculated from percentage yields obtained. Under the initial reaction conditions, complex **Pd13** gave a yield of 94%, an equivalent of a TON of 282 (Table 5.4, entry 3). In addition, 65% of the linear ester product was observed. An attempt to run a reaction without PPh_3 was met with negligible activity (Table 5.4, entry 14), underpinning the importance of the phosphine additive in the methoxycarbonylation reactions [30].

Table 5.4: Initial screening and optimization using **Pd13** in methoxycarbonylation of 1-hexene[a].

Entry	Pd:1-hexene	Temperature (°C)	Yield (%)[b]	B/L(%)[c]	TON[d]
1	1:100	90	90	33/67	90
2	1:200	90	98	36/64	196
3	1:300	90	94	34/66	282
4	1:400	90	88	35/65	352
5	1:500	90	65	38/62	325
6	1:400	100	93	40/60	372
7	1:400	110	81	44/56	324
8	1:400	100	74	38/62	296
9	1:300	70	68	39/61	204
10[e]	1:300	100	8	43/57	24
11[f]	1:300	100	35	41/59	105
12[g]	1:300	100	59	40/60	186
13[h]	1:300	100	78	40/60	234
14[i]	1:400	100	Trace	-	-

[a]Reaction conditions: Solvent, methanol/toluene (40 mL); Pd:PPh$_3$:PTSA:hexene ratio; 1: 2: 30; time, 24 h. [b]% yields and conversions obtained using an internal standard (ethylbenzene) from GC. [c]Molar ratio between branched and linear esters computed using commercial sample (linear methyl heptanoate). [d]TON = (mol.product/mol. Pd).[efgh] Reactions done for 2, 6, 12 and 18 h respectively.

5.6.2 Optimization of the methoxycarbonylation reaction conditions

Having observed the preliminary catalytic behaviour of complex **Pd13**, various reaction conditions were probed to get the best and relevant reaction conditions. To examine the optimum catalyst loading, the TON values were computed for catalyst loadings of 1:500 (0.2 mol %) to 1: 100 (1 mol %). Increasing the catalysts loading from 1:500 to 1:200 presented

with an increase in percentage yield from 65% to 98%; however, a further increase to 1:100 saw a drop of yield to 90%, an observation that can be attributed to catalyst aggregation at higher loadings [31, 32]. Even though higher yields were observed at higher catalyst loading, there were remarkable reducing TON values. For example, while loading of 1:200 gave an excellent yield of 98% as compared to loading of 1:500 (yield of 65%), it coincided with a lower TON of 196, a value which is comparatively lower than 325 obtained with the 1:500 ratio (Table 5.4 entry 2 vs 5). Catalyst loading of 0.25 mol% (1:400) proved to be the optimum loading and therefore was used in subsequent reactions.

In attempts to determine the best reaction temperature, the reactor's temperature was varied from 90 to 105 $^{\circ}C$. Whereas a temperature of 90 $^{\circ}C$ gave a yield of 88%, an increased value of 100 $^{\circ}C$ saw the activity improve to 93%. Nonetheless, a further enhanced temperature of 110 $^{\circ}C$ was met with a decline of yield to 81% (Table 5, entry 7), an observation that can be associated with partial decomposition of the catalyst, deduced from observed palladium black in the reactor [33]. No notable changes in regioselectivity resulted from the reaction temperatures variations made.

The focus was then turned to varying the amounts of PPh_3 additive. Lowering or increasing the amount of PPh_3 to obtain a Pd: PPh_3 ratio of 1:1 and 1:3, respectively, led to lower catalytic activities (Table 5.5, entries 1 and 3). While the relatively inferior catalytic activities observed at smaller amounts of PPh_3 could be associated with the active species insufficient stabilization, the reduced activities at higher PPh_3 amounts are connected to competition for the coordination centre [34]. It is worth noting that changing the amounts of PPh_3 did not cause a subsequent

change in regioselectivities. Varying the amounts of the acid promoter in the methoxycarbonylation reactions have been shown to impact the activity of catalysts [35].

Table 5.5: Optimization of the Pd:PPh$_3$ and Pd:PTSA ratios using complex **Pd13**[a]

Entry	Pd:PPh$_3$	Pd: PTSA	Yield (%)[b]	B/L(%)[c]	TON[d]
1	1:1	1:10	74	36/64	296
2	1:2	1:10	93	40/60	372
3	1:3	1:10	80	33/67	320
4	1:2	1:20	98	37/63	392
5	1:2	1:30	85	37/63	340

[a]Reaction conditions: Solvent: methanol/toluene (40 mL); Pd: hexene ratio, 1:200; time, 24 h; temp: 90 °C; Pressure: 60 bar**;** [b]% yields and conversions obtained using an internal standard (ethylbenzene) from GC. [c]Molar ratio between branched and linear esters computed using commercial sample (linear methyl heptanoate). [d]TON = (mol. prod/mol. Pd).

The methoxycarbonylation catalytic process largely takes place under reducing conditions; the palladium(II) is usually reduced to palladium(0), which the acid additive is required to reactivate the active palladium(II) species [36]. As such, the amounts of Pd: PTSA acid ratios were varied from 1:10 to 1:30. An increase from the ratio of 1:10 to 1:20 coincided with improved catalytic activity from a yield of 93% to 98% (Table 5.5, entries 2 and 4). However, a further increase to a ratio of 1:30 resulted in a dip in yield to 85%, pointing to possible hydrolysis of the active species. The optimum reaction conditions were therefore concluded to be Pd:PPh$_3$: substrate: PTSA (1:2:400:20), and a temperature of 100 °C. The optimized reaction

conditions for complex **Pd13** were then applied in the further investigation of immobilized silica and iron nanomaterial immobilized complexes.

5.6.3 Investigation of the behaviour of the immobilized complexes in methoxycarbonylation reactions

5.6.3.1 Effect of the nature on the catalytic activities

The supports used in immobilizing homogeneous catalysts to form hybrid catalysts have been shown to have varied effects on the eventual catalysts behaviour due to variance in pore sizes, pore volumes, surface area, particle size, acidity, stability and the number of active sites [37]. It is worth noting that the catalyst support may interact with the active component or may be inert. Such an interaction influences the behaviour of the catalysts [37]. As such, the influence of three different supports, MCM-41, SBA-15 and magnetic iron nanoparticles (Fe_3O_4), were studied. Using the same reaction conditions, an activity trend was observed in the order of **Pd16**> **Pd15**> **Pd17** (SBA-15, MCM-41, and magnetic ion nanoparticles supported, respectively) (Table 5.6, entries 1-3)**.** The trend could be attributed to the larger pore size exhibited by the SBA-15 supported catalysts as compared to the MCM-41 supported catalysts, which are known to have relatively smaller pore sizes [38], pointing to the activities being largely controlled by internal diffusion [39]. The lower activity observed for complex **Pd1Fe$_3$O$_4$ (Pd17)** can be connected to limited porosity.

Table 5.6: Behaviour of immobilized catalyst in the methoxycarbonylation of 1-hexene[a]

Entry	Catalyst	Yield (%)[b]	B/L(%)[c]	TON[d]
1	**Pd15**	85	33/67	340
2	**Pd16**	90	37/63	360
3	**Pd17**	81	33/67	324
4	**Pd20**	93	35/65	372
5	**Pd21**	82	36/64	328
6	**Pd18**	74	38/62	296
7	**Pd19**	80	37/63	320

[a]Reaction conditions: Solvent: methanol/toluene (40 mL); Pd: hexene ratio, 1:400; time, 24 h; temp: 100 °C; Pressure: 60 bar;[b]% yields and conversions obtained using an internal standard (ethylbenzene) from GC. [c]Molar ratio between branched and linear esters computed using commercial sample (linear methyl heptanoate). [d]TON = (mol. prod/mol. Pd).

5.6.3.2 Effect of calcination temperatures

Calcination temperature has been shown to have an influence on the activities of supported catalyst, and depending on a range of surface properties, enhanced or reduced catalytic activities can be observed [40]. Therefore, the other two variants of **Pd16** was made through calcination at temperatures of 150 °C and 200 °C for 24 h. While the **Pd16**, calcined at 100 °C, gave a yield of 90% within 24 h, complex **Pd20** gave an improved catalytic activity of 93% (Table 5.6 entries 2 vs 4), an observation that could be associated with increased pore sizes to enhance diffusion rates [41]. Unexpectedly, complex **Pd21** gave a lower yield of 82% (Table 5.7, entry 5). Even though bigger pore sizes are expected for the complex, the lower activity could be as a result of a partial collapse of the pore and particle sintering [40]. In addition, no substantial change in the regioselectivity of the formed products was observed with the change

in calcination temperature as the complexes still gave predominantly linear ester products (62-67%).

5.6.3.3 Effect of palladium loading

To investigate the effect of palladium loading in catalytic activity, various synthetic protocols were applied to make variants of catalysts **Pd15** having different loadings. As predicted, under the same reaction conditions, the complexes gave varying catalytic activities. While complex **Pd18** gave a yield of 74%, complexes **Pd15** and **Pd19** gave yields of 85% and 80%, respectively. The higher catalytic activity observed for the **Pd15** (10% weight) as compared to **Pd18** (5% weight) can be attributed to an increased number of palladium active sites. On the other hand, a drop in activity at 15% weight implies that the higher loading is not industrially beneficial. This observation has previously been made in the catalytic process of methane combustions using palladium supported catalysts, where higher metal loadings coincided with lower yields of the methane combustion products [42]. In addition, the lower activity at higher loadings has been associated with deformation of the ordered structure of the catalyst support as more of the ordered silica get replaced at higher metal loading [43].

5.6.4 Recyclability studies of the immobilized complexes and leaching studies

The major aim of this chapter was to develop recyclable palladium(II) catalysts for methoxycarbonylation of olefins. Having optimized the reaction conditions and examined the catalytic behaviour of the immobilized complexes, attention was turned towards investigating the recyclability potential of complexes **Pd15**, **Pd16** and **Pd17.** The reactions were done using optimized reaction conditions of a temperature of 100 ºC, CO pressure of 60 bar. The three catalysts were used for five runs (Figure 5.8). While there was minimal loss of catalytic activity

in the first four cycles, the fifth cycle presented with a significant loss of catalytic activities in all three complexes. In efforts to determine if the leaching was responsible for the reduced catalytic activities in the last cycles, the catalysts were filtered off the filtrate analyzed using ICP-OES. From the results obtained, leaching was negligible. Hence the observed reduction in catalytic activities in subsequent runs can be attributed to catalyst abrasion and changes in the physical surface properties of the immobilized catalysts [44].
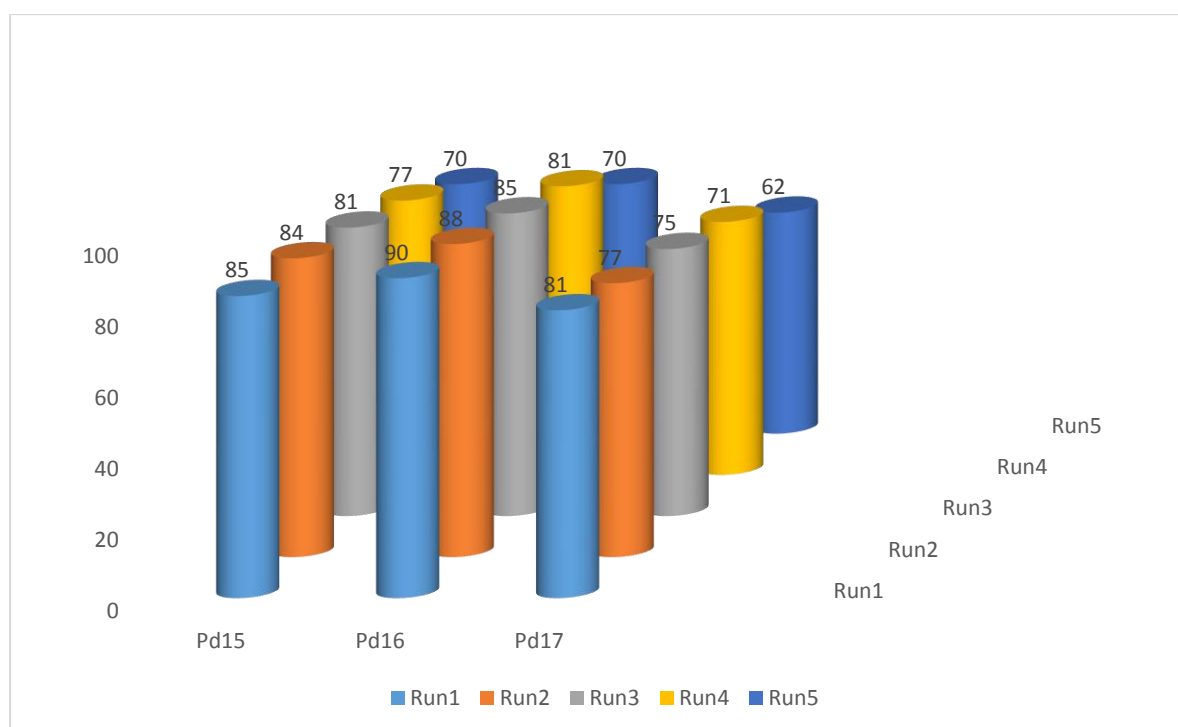
Figure 5.8: A Figure showing the recyclability studies of complexes **Pd15**-**Pd17**

5.6.4.1 Investigation of the nature of the active species

We also investigated the nature of active species in the homogeneous catalyst **Pd13** and its immobilized counterpart **Pd16**; Hg poisoning was employed [45]. When an excess amount of mercury was added to complex **Pd13,** a slight drop in yield to 91% 98% was obtained, indicating that the presence of homogenous active species. On the other hand, the addition of excess mercury to the reaction set-up with immobilized complex **Pd16** coincided with a notable drop of yield from 93% to 61%, indicating that while the homogeneous active species are

present, there was a notable formation of the heterogeneous species too (Figure 5.9). A similar trend was reported for complex **Pd17,** with reduced yields of 56% recorded upon the addition of a few drops of Hg. This observation implies that, while the synthesized compounds were immobilized complexes, they partially formed ligand stabilized palladium nanoparticles during catalysis.
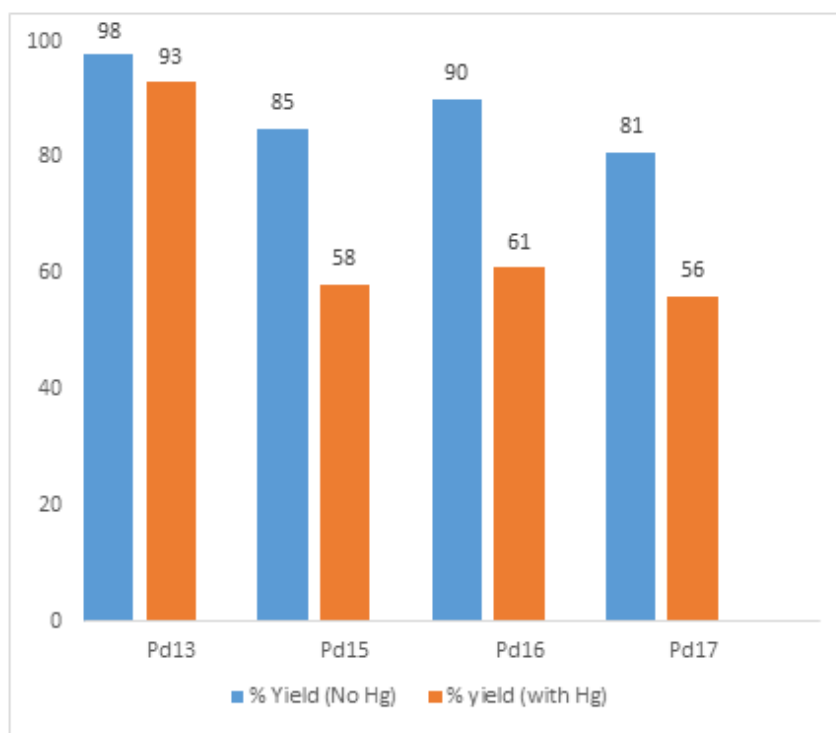
Figure 5.9: A graph showing the poisoning tests for homogeneous (Pd13) and immobilized complexes (Pd15-Pd17)5.6.4.2 Post recycling catalyst characterization

We also sought to determine possible causes of lower catalytic activities after the fifth cycle by studying the nature of the recycled catalyst after the fifth run. Both SEM, TEM and EDX characterization tools were used in this respect. The first step taken was an analysis of the recycled catalysts using ICP-OES and EDX. The palladium content in the recycled complex **Pd16** was revealed to be 1.83% and 2.28% using ICP-OES and EDX, respectively. This show a decline from the original content of 2.79% and 3.41%, respectively. The diminishing quantities of palladium can therefore explain the lower catalytic activity observed in

subsequent cycles. Our next focus turned to TEM to establish if there were any morphological changes. From the images shown in Figure 5.10, it is evident that there was a notable change of morphology after five cycles of catalyst use. As opposed to the fresh catalyst, where there was a homogeneous distribution of particles, a possible agglomeration of particles and partial surface damage was observed, giving a hint of the possible cause of the reduced catalytic activity at the end of the fifth cycle. Therefore, physical damage of the catalytic surface can also be implicated in the diminishing catalytic activities displayed in subsequent cycles [46].
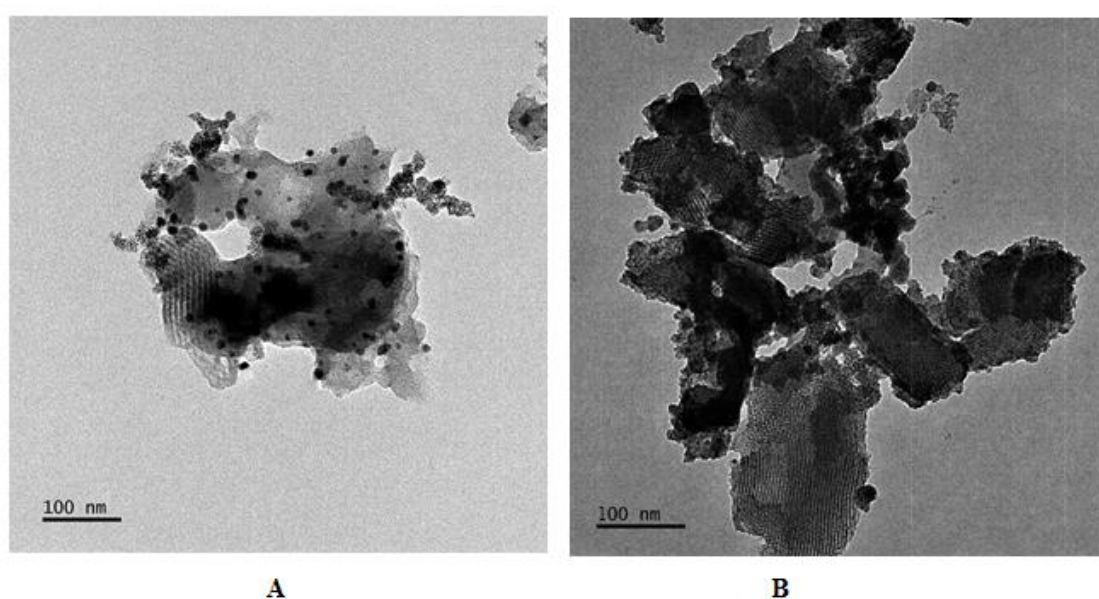
Figure 5.10: A figure showing fresh catalyst **Pd16** (A) and used catalyst (B) indicating a change in morphology

5.7 Conclusions

In conclusion, two ligands, **L12**- **L3** and their respective homogeneous complexes, **Pd13**-**Pd14,** have been synthesized. Respective silica and iron nanoparticle immobilized complexes (**Pd15-Pd21**) were then synthesized following a convergent synthetic route. While the homogeneous complexes were characterized using ^{1}H NMR, ^{13}C NMR, FTIR, Mass

174

spectrometry, the immobilized complexes were characterized using FTIR, SEM-EDX, TEM, XRD, and ICP-OES. The catalytic activities and selectivities of the homogeneous complexes were influenced by the coordination environment around the palladium centre, with the complexes predominantly forming linear esters. On the other hand, the catalytic behaviours of the immobilized catalysts depended on the nature of support and calcination temperatures. In addition, the catalytic activities were observed to depend on the reaction temperature, catalyst loading, amounts of PPh_3 and acid promoters. The immobilized complexes **Pd15**, **Pd16** and **Pd17,** were recycled up to five times. While Hg poisoning was used in determining the true nature of the active species, ICP-OES was useful in leaching evaluation.

The next chapter presents a comparative evaluation of the homogeneous and silica immobilized complexes in the hydrogenation of alkenes, alkynes and functionalized benzenes. This set of complexes were used during the masters of science as catalysts in methoxycarbonylation of olefins; impressed with their behaviours in terms of activity and recyclability, the work was extended to hydrogenation catalytic reactions.

5.8 References

[1] J. Hagen, Industrial catalysis: a practical approach, John Wiley & Sons2015.

[2] W. Abdussalam-Mohammed, A. Qasem Ali, A. O Errayes, Green chemistry: principles, applications, and disadvantages, Chem. Methodol., 4 (2020) 408-423.

[3] R.A. Sheldon, Engineering a more sustainable world through catalysis and green chemistry, J. R. Soc. Interface, 13 (2016) 20160087.

[4] O. Piermatti, R. Abu-Reziq, L. Vaccaro, Strategies to Immobilized Catalysts: A Key Tool for Modern Chemistry, Catalyst Immobilization: Methods and Applications, (2020) 1-22.

[5] I.V. Gürsel, T. Noël, Q. Wang, V. Hessel, Separation/recycling methods for homogeneous transition metal catalysts in continuous flow, Green Chem., 17 (2015) 2012-2026.

[6] B. Dutta, S. Omar, S. Natour, R. Abu-Reziq, Palladium nanoparticles immobilized on magnetic nanoparticles: an efficient semi-heterogeneous catalyst for carbonylation of aryl bromides, Catal. Commun., 61 (2015) 31-36.

[7] I. Beletskaya, O. Ganina, Hydroxy-and alkoxycarbonylation of aryl iodides catalyzed by polymer-supported palladium, Reaction Kinetics, Mechanisms and Catalysis, 99 (2010) 1-4.

[8] X. Chen, H. Zhu, T. Wang, C. Li, L. Yan, M. Jiang, J. Liu, X. Sun, Z. Jiang, Y. Ding, The 2V-P, N polymer supported palladium catalyst for methoxycarbonylation of acetylene, J. Mol. Catal. A: Chem., 414 (2016) 37-46.

[9] S. Doherty, J.G. Knight, M. Betham, The first insoluble polymer-bound palladium complexes of 2-pyridyldiphenylphosphine: highly efficient catalysts for the alkoxycarbonylation of terminal alkynes, Chem. Commun., (2006) 88-90.

[10] S.O. Akiri, S.O. Ojwach, Synthesis of MCM-41 Immobilized (Phenoxy) Imine Palladium (II) Complexes as Recyclable Catalysts in the Methoxycarbonylation of 1-Hexene, Catalysts, 9 (2019) 143.

[11] K. Mukhopadhyay, B.R. Sarkar, R.V. Chaudhari, Anchored Pd complex in MCM-41 and MCM-48: novel heterogeneous catalysts for hydrocarboxylation of aryl olefins and alcohols, J. Am. Chem. Soc., 124 (2002) 9692-9693.

[12] V.I. Isaeva, O.L. Eliseev, V.V. Chernyshev, T.N. Bondarenko, V.V. Vergun, G.I. Kapustin, A.L. Lapidus, L.M. Kustov, Palladium nanoparticles embedded in MOF matrices: Catalytic activity and structural stability in iodobenzene methoxycarbonylation, Polyhedron, 158 (2019) 55-64.

[13] A.E. Collis, I.T. Horvath, Heterogenization of homogeneous catalytic systems, Catal. Sci. Technol., 1 (2011) 912-919.

[14] C.M. Standfest-Hauser, T. Lummerstorfer, R. Schmid, H. Hoffmann, K. Kirchner, M. Puchberger, A.M. Trzeciak, E. Mieczyńska, W. Tylus, J.J. Ziółkowski, Rhodium phosphine complexes immobilized on silica as active catalysts for 1-hexene hydroformylation and arene hydrogenation, J. Mol. Catal. A: Chem., 210 (2004) 179-187.

[15] J.M. Thomas, R. Raja, Catalytic significance of organometallic compounds immobilized on mesoporous silica: economically and environmentally important examples, J. Organomet. Chem., 689 (2004) 4110-4124.

[16] R. Sang, C. Schneider, R. Razzaq, H. Neumann, R. Jackstell, M. Beller, Palladium-catalyzed carbonylations of highly substituted olefins using CO-surrogates, Org. Chem. Front., 7 (2020) 3681-3685.

[17] H. Veisi, J. Gholami, H. Ueda, P. Mohammadi, M. Noroozi, Magnetically palladium catalyst stabilized by diaminoglyoxime-functionalized magnetic Fe3O4 nanoparticles as active and reusable catalyst for Suzuki coupling reactions, J. Mol. Catal. A: Chem., 396 (2015) 216-223.

[18] E. Rossetto, M. Caovilla, D. Thiele, R.F. de Souza, K. Bernardo-Gusmão, Ethylene oligomerization using nickel-β-diimine hybrid xerogels produced by the sol–gel process, Appl Catal A-Gen, 454 (2013) 152-159.

[19] M. Nikoorazm, A. Ghorbani-Choghamaranai, M. Khanmoradi, P. Moradi, Synthesis and characterization of Cu (II)-Adenine-MCM-41 as stable and efficient mesoporous catalyst for the synthesis of 5-substituted 1 H-tetrazoles and 1 H-indazolo [1, 2-b] phthalazine-triones, J. Porous Mater., 25 (2018) 1831-1842.

[20] A. Ghorbani-Choghamarani, B. Tahmasbi, R.H. Hudson, A. Heidari, Supported organometallic palladium catalyst into mesoporous channels of magnetic MCM-41 nanoparticles for phosphine-free CC coupling reactions, Microporous Mesoporous Mater., 284 (2019) 366-377.

[21] F.D. Firuzabadi, Z. Asadi, F. Panahi, Immobilized NNN Pd-complex on magnetic nanoparticles: efficient and reusable catalyst for Heck and Sonogashira coupling reactions, RSC adv., 6 (2016) 101061-101070.

[22] P. Han, X. Wang, X. Qiu, X. Ji, L. Gao, One-step synthesis of palladium/SBA-15 nanocomposites and its catalytic application, J. Mol. Catal. A: Chem., 272 (2007) 136-141.

[23] H. Veisi, M. Hamelian, S. Hemmati, Palladium anchored to SBA-15 functionalized with melamine-pyridine groups as a novel and efficient heterogeneous nanocatalyst for Suzuki–Miyaura coupling reactions, J. Mol. Catal. A: Chem., 395 (2014) 25-33.

[24] C. He, J. Li, J. Cheng, L. Li, P. Li, Z. Hao, Z.P. Xu, Comparative studies on porous material-supported Pd catalysts for catalytic oxidation of benzene, toluene, and ethyl acetate, Ind. Eng. Chem. Res., 48 (2009) 6930-6936.

[25] N.A. Ivashchenko, W. Gac, V.A. Tertykh, V.V. Yanishpolskii, S.A. Khainakov, A.V. Dikhtiarenko, S. Pasieczna-Patkowska, W. Zawadzki, Preparation, characterization and catalytic activity of palladium nanoparticles embedded in the mesoporous silica matrices, World j. nano sci. eng., 2 (2012) 117.

[26] M. Nikoorazm, A. Ghorbani-Choghamarani, M. Khanmoradi, Application of Pd-2A3HP-MCM-41 to the Suzuki, Heck and Stille coupling reactions and synthesis of 5-substituted 1H-tetrazoles, Appl. Organomet. Chem., 30 (2016) 705-712.

[27] L.Q. Yu, L.J. Zheng, J.X. Yang, Study of preparation and properties on magnetization and stability for ferromagnetic fluids, Mater. Chem. Phys., 66 (2000) 6-9.

[28] R.K. Sharma, M. Yadav, R. Gaur, R. Gupta, A. Adholeya, M.B. Gawande, Synthesis of iron oxide palladium nanoparticles and their catalytic applications for direct coupling of acyl chlorides with alkynes, ChemPlusChem, 81 (2016) 1312.

[29] S. Verma, D. Verma, A.K. Sinha, S.L. Jain, Palladium complex immobilized on graphene oxide–magnetic nanoparticle composites for ester synthesis by aerobic oxidative esterification of alcohols, Appl Catal A-Gen, 489 (2015) 17-23.

[30] I. del Río, C. Claver, P.W. van Leeuwen, On the mechanism of the hydroxycarbonylation of styrene with palladium systems, Eur. J. Inorg. Chem., 2001 (2001) 2719-2738.

[31] A.F. Schmidt, A. Al-Halaiqa, V.V. Smirnov, Effect of macrokinetic factors on the ligand-free Heck reaction with non-activated bromoarenes, J. Mol. Catal. A: Chem., 250 (2006) 131-137.

[32] H.A. Ghaly, A.S. El-Kalliny, T.A. Gad-Allah, N.E.A. El-Sattar, E.R. Souaya, Stable plasmonic Ag/AgCl–polyaniline photoactive composite for degradation of organic contaminants under solar light, RSC adv., 7 (2017) 12726-12736.

[33] J.J. de Pater, B.J. Deelman, C.J. Elsevier, G. van Koten, Multiphase systems for the recycling of alkoxycarbonylation catalysts, Adv. Synth. Catal., 348 (2006) 1447-1458.

[34] G. Kiss, Palladium-catalyzed Reppe carbonylation, Chem. Rev., 101 (2001) 3435-3456.

[35] D.B.G. Williams, M.L. Shaw, M.J. Green, C.W. Holzapfel, Aluminum Triflate as a Highly Active and Efficient Nonprotic Cocatalyst in the Palladium-Catalyzed Methoxycarbonylation Reaction, Angew. Chem. Int. Ed., 47 (2008) 560-563.

[36] A. Behr, L. Johnen, A. Wintzer, A. Willstumpf, M. Dinges, First methoxycarbonylation of the renewable β-myrcene: high selectivity through reduced isomerisation, Catal. Sci. Technol., 3 (2013) 1573-1578.

[37] P.S. Shinde, P.S. Suryawanshi, K.K. Patil, V.M. Belekar, S.A. Sankpal, S.D. Delekar, S.A. Jadhav, A Brief Overview of Recent Progress in Porous Silica as Catalyst Supports, J. Compos. Sci., 5 (2021) 75.

[38] N.T. Phan, C.W. Jones, Highly accessible catalytic sites on recyclable organosilane-functionalized magnetic nanoparticles: An alternative to functionalized porous silica catalysts, J. Mol. Catal. A: Chem., 253 (2006) 123-131.

[39] U. Wilkenhöner, G. Langhendries, F. van Laar, G.V. Baron, D.W. Gammon, P.A. Jacobs, E. van Steen, Influence of pore and crystal size of crystalline titanosilicates on phenol hydroxylation in different solvents, J. Catal., 203 (2001) 201-212.

[40] C.A. Akinnawo, N. Bingwa, R. Meijboom, Surface properties vs activity of meso-ZrO2 catalyst in chemoselective Meerwein-Ponndorf-Verley reduction of citral: Effect of calcination temperature, Microporous Mesoporous Mater., 311 (2021) 110693.

[41] H. Wang, J. Lu, A review on particle size effect in metal-catalyzed heterogeneous reactions, Chin. J. Chem . 38 (2020) 1422-1444.

[42] Z.-j. Wang, Y. Liu, P. Shi, C.-j. Liu, Y. Liu, Al-MCM-41 supported palladium catalyst for methane combustion: Effect of the preparation methodologies, Appl Catal B- Environ., 90 (2009) 570-577.

[43] G.z. Fan, S.q. Cheng, M.f. Zhu, X.l. Gao, Palladium chloride anchored on organic functionalized MCM-41 as a catalyst for the Heck reaction, Appl. Organomet. Chem., 21 (2007) 670-675.

[44] I. Ziccarelli, H. Neumann, C. Kreyenschulte, B. Gabriele, M. Beller, Pd-Supported on N-doped carbon: improved heterogeneous catalyst for base-free alkoxycarbonylation of aryl iodides, Chem. Commun., 52 (2016) 12729-12732.

[45] R.H. Crabtree, Resolving heterogeneity problems and impurity artifacts in operationally homogeneous transition metal catalysts, Chem. Rev., 112 (2011) 1536-1554.

[46] K. Yu, W. Sommer, M. Weck, C.W. Jones, Silica and polymer-tethered Pd–SCS-pincer complexes: evidence for precatalyst decomposition to form soluble catalytic species in Mizoroki–Heck chemistry, J. Catal., 226 (2004) 101-110.

Chapter 6

Comparative study of homogeneous and silica immobilized N^N and N^O palladium (II) complexes as catalysts for hydrogenation of alkenes, alkynes and functionalized benzenes

This chapter is adapted from the paper published in Catalysis Letters (2020): 2850 – 2862 and is wholly based on the work of the first author, Saphan Akiri. The contribution of the first author, Saphan Akiri, include ligand and complex synthesis and characterization, hydrogenation catalysis as well as drafting the manuscript.

6.1 Introduction

The molecular hydrogenation reaction of saturated substrates is among the vital catalytic processes in synthetic organic chemistry, both in industrial and academic laboratories, largely due to its cleaner process [1]. The industrial applications of hydrogenation reactions range from pharmaceuticals, petrochemical and fine chemicals syntheses. Traditionally, catalysts obtained from platinum have been used in catalysing the hydrogenation of alkenes, alkynes, and other unsaturated hydrocarbons [2-4]. Besides, the catalysts have been in the past and at present derived from a pool of metals such as palladium [5], iron [6], rhodium [7], chromium [8], ruthenium [9], and platinum[10]. However, palladium catalysts have gained prominence since they possess a better surface to volume ratio as compared to platinum. A classic example is Lindlar's catalyst, which has been widely applied in food industries in the hydrogenation of alkynes [11].

The substrates' functionalisation through hydrogenation transformation can either be done using molecular hydrogen or achieved *via* hydrogen surrogates in what has been widely known as transfer hydrogenation in the presence of a transition metal catalyst. First incorporated into

science by Paul Sabatier, culminating in winning a Nobel Prize award in 1912 [12], several improvements have since been made in the process to open avenues for functionalisation of a wide range of industrial feedstocks for value addition. It is worth noting that hydrogen is largely unreactive towards the substrates in the absence of a transition metal catalyst. However, in the presence of catalysts, hydrogen's versatility in organic reactions is reflected in the conversion of unsaturated substrates to numerous industrial feedstocks and useful domestic consumables [2, 4]

Phosphine-donor palladium catalysts are the most studied systems, even though they suffer from air and moisture sensitivity and poor stability. Therefore, nitrogen-donor catalysts have seen increased interest due to their improved stability and ease of synthesis [13, 14]. In one of the reports, phosphine donor palladium (II) complexes bearing (2,5-dimethylphospholano)benzene applied by Drago and Pregosin afforded a conversion of 40% in the hydrogenation of 3-methyl-2-cyclohexene within 24 h [15]. Mixed P and N donor catalysts have also been utilized in hydrogenation reactions. Chelating P^N donor palladium (II) systems bearing phosphino hydrazonic ligands displayed conversion of 77% to 100% of styrene to ethyl benzene within 48 h [16].

Hydrogenation of benzene and its derivatives is another area that continues to attract interest both in industry and academia [17]. For example, selective hydrogenation of nitrobenzene is vital in the production of anilines, an important intermediate in the pharmaceutical industry [18]. The major challenge in this process is the low reactivity of the benzene molecule and achieving good selectivity in multiple-functionalized benzene substrates [19-21]. For example, the hydrogenation of 4-nitro acetophenone and 4-nitro benzaldehyde occur in complex

multistep pathways due to the competitive hydrogenation reactions between the nitro and carbonyl groups [22]. In one such example in the hydrogenation of 4-nitroacetophenone, using palladium catalyst supported on a melamino-formaldehyde polymer, Cao *et al.* reported selective hydrogenation of the nitro group to give 4-aminoacetophenone [20]. Using the same substrate, Hawkins and Makowski observed a mixture of 4-aminoacetophenone (59%) and 1-(4-aminophenyl) ethanol (34%) using Rh/Al$_2$O$_3$ catalysts [23]. Currall and Jackson, on the other hand, reported a mixture of 1-(4-aminophenyl) ethanol, 4-aminoacetophenone and 1-(4-aminocyclohexyl) ethanol using Rh/silica catalyst [24], an indication that the hydrogenation of benzenes containing more than two sites for the electrophilic attack is not a straightforward and obvious reaction. From these accounts, it is clear that this is an area that requires intense research to formulate more active and selective catalysts.

These hydrogenation reactions are carried out under both homogeneous and heterogeneous conditions, with varied outcomes. While homogeneous catalysts display superior selectivity [25-28], they suffer from a lack of separation and recycling of the active species [29-31]. On the other hand, heterogeneous catalysts are separable and recyclable [32] but display poor selectivity [33]. Therefore, efforts geared towards exploiting the advantages of both catalyst systems with the aim of achieving selective and recyclable systems have been on the rise [34]. Various methods have since been developed, such as using polymer supports [35-38], silica [39-41], magnetic nanoparticles [42-44], and biphasic systems [45-47]. We recently applied homogeneous and immobilized palladium(II) compounds in the methoxycarbonylation of olefins during masters work and published the findings [48]. Both catalyst systems display comparable catalytic activities, and regio-selectivity and the immobilized systems can be recycled [49]. Encouraged by these results in the methoxycarbonylation of olefins, we choose to extend the use of these systems in molecular hydrogenation reactions of alkenes, alkynes,

and functionalized benzenes. This chapter, therefore, reports the comparative catalytic behaviour, reaction kinetics and catalyst poisoning studies of these homogeneous and immobilized palladium(II) complexes in these reactions.

6.2 Experimental

6.2.1 Materials and methods.

All air sensitive reactions were manipulated using standard Schlenk techniques. (2-phenyl-2-((3(triethoxysilyl)propyl)imino)ethanol) (**L14**) and (4-methyl-2-((3(triethoxysilyl)propyl)imino)methyl)phenol) (**L15**), and their supported ligands, **L114**-MCM-41 (**L16**), and **L15**-MCM-41 (**L17**) were synthesized following previously reported procedures [48, 49]. The respective homogeneous and immobilized palladium complexes [Pd (**L14**)$_2$ (**Pd22**), [Pd (**L15**)$_2$] (**Pd23**), [Pd (**L14**)(Cl$_2$)] (**Pd24**), [Pd (**L5**)(Cl$_2$)] (**Pd25**) and [Pd(**L14**)$_2$]-MCM 41] (**Pd26**); [Pd(**L15**)$_2$]-MCM 41(**Pd27**); [Pd(**L14**)(Cl$_2$)]-MCM 41] (**Pd28**) and [Pd (**L15**)(Cl$_2$)]-MCM 41] (**Pd29**) were synthesized following our recently described procedures [49].

6.2.2 Standard procedure for the hydrogenation of substrates

Hydrogenation catalysis was accomplished using a stainless steel autoclave Parr reactor with an inbuilt cooling system, sampling valve and a temperature regulation unit. In a typical experiment, the reactor was pre-heated, evacuated and flushed with nitrogen and cooled to room temperature. A solution of styrene (0.25 ml, 2.10 mmol) and complex **Pd24** (0.0014 g, 0.0027 mmol) in toluene (20 ml) was then introduced using a cannula. The reactor was then purged with hydrogen gas several times, and then the desired pressure and reaction temperature were set and stirred for the specified time. At the end of the reaction period, the reactor was

then cooled, the gas supply closed, and excess hydrogen gas vented off. The samples were then collected for GC analyses using a syringe equipped with 0.45 µm micro filters and analysed by a Varian CP-3800 GC (ZB-5HT Column 30 m x 0.25 mm x 0.1 µm) to establish percentage conversions. The percentage conversions were calculated by comparison of the substrate peak areas to those of the products, assuming a 100% mass balance. The kinetic reactions were done by monitoring the change in substrate consumption over time at regular intervals. The rate constants were then derived from graphical plots of $\ln[\text{substrate}]_0/[\text{substrate}]_t$ versus time. The catalysis products were identified using the standard authentic samples as well as GC-MS.

6.2.3 Recycling of the immobilized catalysts procedure

The recycling experiments were carried out using the immobilized complexes (**Pd26** – **Pd29**) through the use of a centrifuge where the reaction mixture was centrifuged at 8000 rotations per minute for 10 min after the preceding reaction. The solid catalyst was recovered following a decantation process of the supernatant liquid and reintroduced into the reactor together with a fresh substrate. The fresh reaction was run under the pre-set reaction conditions, and analyses were done with GC as outlined in section 6.2.2.

6.3 Results and discussion

6.3.1 Preliminary evaluation of the homogeneous and immobilized palladium complexes as catalysts in hydrogenation reactions of styrene.

Preliminary catalytic hydrogenation of styrene reactions using homogeneous and immobilized complexes **Pd22**-**Pd25** and **Pd26** – **Pd29** respectively, (Figure 6.1), were carried out at 30 ºC,

5 bar and at Pd: styrene ratio of 1:800 (Table 6.1). All the complexes afforded conversions of between 72% and 88% within 1 h under these reaction conditions. To determine if indeed the catalytic activities displayed were due to the palladium complexes, we set up a typical hydrogenation reaction without any palladium complex and obtained negligible conversions of 2% (Table 6.1, entry 9), confirming that the higher conversions obtained were due to the palladium complexes.
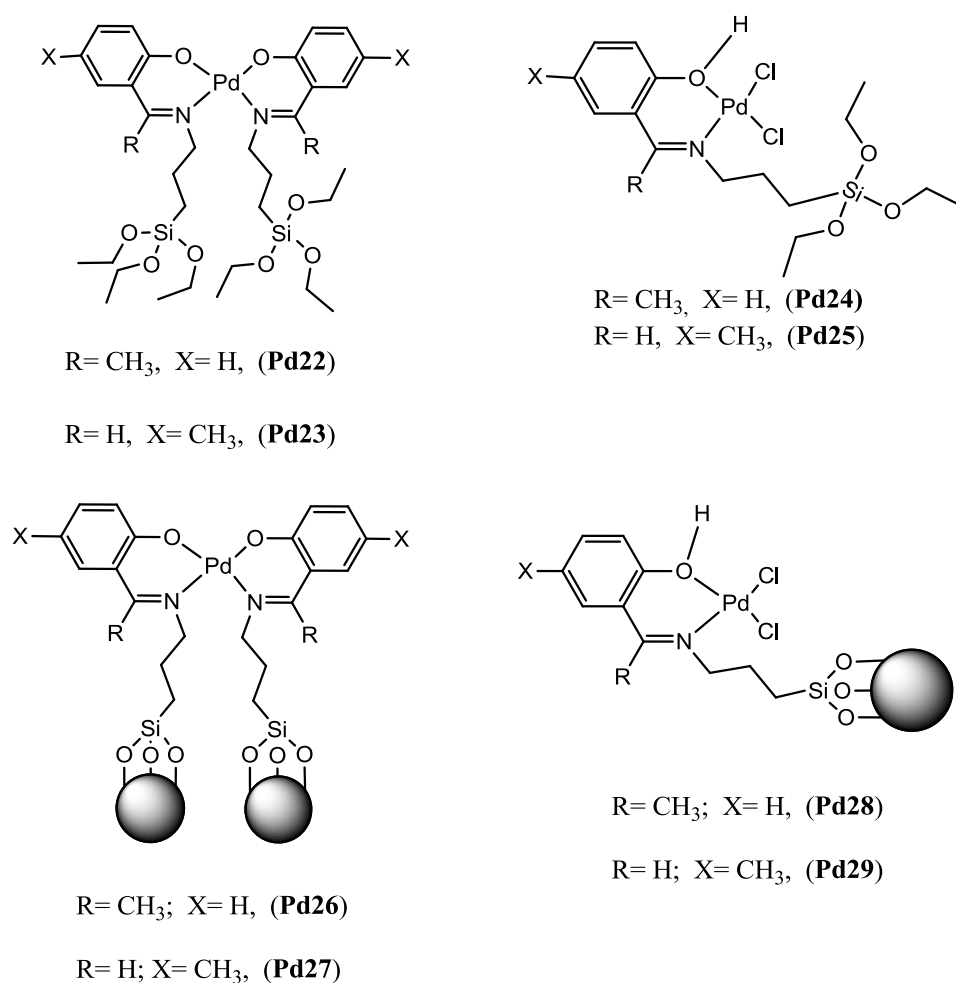

R= CH₃, X= H, (**Pd22**)

R= H, X= CH₃, (**Pd23**)

R= CH₃, X= H, (**Pd24**)
R= H, X= CH₃, (**Pd25**)

R= CH₃; X= H, (**Pd26**)

R= H; X= CH₃, (**Pd27**)

R= CH₃; X= H, (**Pd28**)

R= H; X= CH₃, (**Pd29**)

Figure 6.1: Structures of homogeneous (**Pd22**-**Pd25**) and immobilized (**Pd26** – **Pd29**) palladium complexes used as catalysts in hydrogenation reactions in this study.

Table 6.1: Hydrogenation of styrene using homogeneous and immobilized complexes[a]

Entry	catalyst	Conv(%)[b]	k_{obs} (h^{-1})	[c]TOF (h^{-1})
1	**Pd22**	86	1.86 (± 0.12)	688
2	**Pd23**	81	1.62(± 0.09)	640
3	**Pd24**	88	2.02 (± 0.05)	704
4	**Pd25**	84	1.75 (± 0.09)	672
5	**Pd26**	78	1.41(± 0.12)	624
6	**Pd27**	72	1.17(± 0.10)	576
7	**Pd28**	83	1.59(± 0.14)	664
8	**Pd29**	76	1.37 (± 0.12)	608
9	**-**	2	-	16
10[d]	**Pd24**	85	-	

[a]Reaction conditions: Pressure, 5 bar; time: 1 h; temp 30 ^{o}C; Solvent, toluene (20 ml); catalyst concentration, 0.125 mol % (Pd/substrate:1:800); styrene (0.5 ml, 4.4 mmol) [b]% of styrene converted to ethyl benzene; [c]TOF (mol. sub/mol. Pd h^{-1}). [d] Reaction centrifuged midway.

6. 3.2 Kinetic studies of the catalytic hydrogenation reactions

6.3.2.1 Effects of complex structure on the kinetics of hydrogenation of styrene

The influence of the structure of the complex on the kinetics of hydrogenation reactions of styrene was carried out for both the homogeneous (**Pd22-Pd245**) and immobilized complexes (**Pd26 – Pd29**) at 5 bar and temperature of 30 ^{o}C. The kinetic plots of time *vs* percentage conversion showed different profiles for the homogeneous and immobilized palladium catalysts (Figure 6. 2). The sigmoid curves obtained for the immobilized complexes **Pd26**-

Pd29 depicted their heterogeneous behaviour and possible formation of active Pd(0) nanoparticles (discussed later), while the smooth curves obtained for complexes **Pd22**-**Pd25** are typical of homogeneous active species [50, 51]. A similar trend was observed by Gross *et al.*, where the SBA-15 supported palladium catalyst gave sigmoid-shaped plots [52]. Nonetheless, the plots of $\ln[\text{Styrene}]_o/[\text{Styrene}]_t$ *vs* time for homogeneous catalysts displayed linear relationships corresponding to *pseudo*-first-order kinetics. From the linearity of the plot, the reaction rate with respect to the substrate is shown 6.1 in Eq. 1.

$$\text{Rate} \quad = \quad k[\text{Styrene}]^1 \quad \dots\dots\dots\dots\dots\dots\dots\dots\dots\dots\dots\dots\dots\dots\text{Eq.} \quad 6.1$$
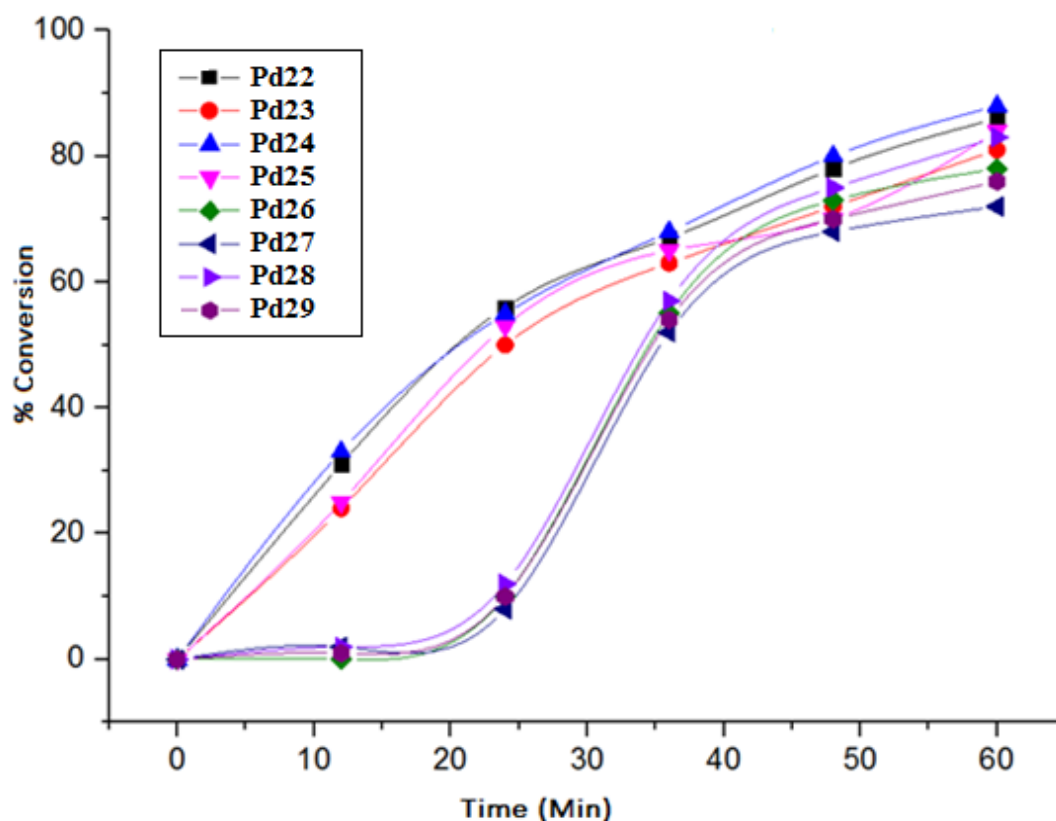

Figure 6.2: Plots of time vs percentage conversion of styrene to ethylbenzene showing smooth and sigmoid curves for the homogeneous (**Pd22**-**Pd25**) and immobilized palladium catalysts (**Pd26** – **Pd29**), respectively.

The observed rate constants (k_{obs}) exhibited by the catalysts were calculated from the linear plots in (Figure 6.3) and applied in evaluating the influence of complex structures on catalytic activities (Table 6.1). The catalytic activities of the homogenous catalysts demonstrated dependence on the coordination sphere of the metal centre. For instance, the mono(chelated) complex **Pd24** gave a higher rate constant of 2.02 ± 0.05 h^{-1} as compared to a value of 1.86 ± 0.12 h^{-1} obtained for the corresponding bis(chelated) **Pd22** complex (Table 6.1, entries 1 and 3). Two reasons can be fronted for this observation. First, the easier generation of the palladium-hydride species from the Pd-Cl bond (**Pd24**), which is believed to be the active species [53]. Secondly, we hypothesize that the bis(chelated) complexes **Pd22** and **Pd23** may require the dissociation of one ligand unit to allow for styrene substrate coordination. Similar trends were observed for the immobilized catalysts **Pd26** – **Pd29**. However, this current observation contradicts our recent reports using the same complexes in the methoxycarbonylation of olefins [48]. A plausible reason is that the bis(chelated) complexes exhibit higher thermal stability required for the methoxycarbonylation reactions (90 ^{o}C), as opposed to room temperature conditions employed in the current hydrogenation reactions. A comparison of the catalytic behaviours of the two systems revealed diminished catalytic activities of the immobilized systems. For instance, rate constants of 1.86 ± 0.12 h^{-1} and 1.41 ± 0.12 h^{-1} for **Pd22** and **Pd26,** respectively, were observed (Table 6.1 entries 1 and 5). This is consistent with the expected behaviour [54] and agrees well with the results observed in the methoxycarbonylation reactions using the same catalysts [48, 49].
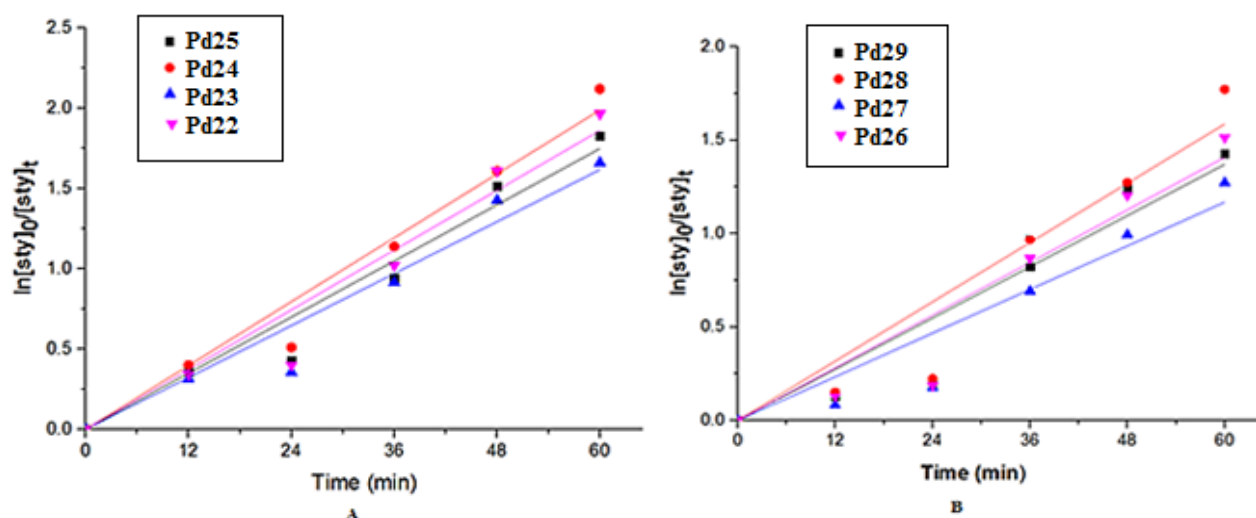
Figure 6.3: Kinetics plots for homogeneous complexes (**Pd22**-**Pd25**) and immobilized complexes (**Pd26**-**Pd29**).

In comparison to the widely reported catalysts in hydrogenation reactions of various substrates [55-58], the present catalysts displayed moderate catalytic activities. For example, the palladium (II) catalysts bearing perfluoroalkylated S^O- ligand reported by Kani and co-workers [59] display TOFs of 372 h^{-1} in the hydrogenation of styrene, which is lower than the TOF of 704 h^{-1} we observed using the homogeneous catalyst **Pd24.** In the same vein, Altinel *et al.* [60] perfluorinated Rh–BINAP catalysts exhibit much lower TOF of 71.5 h^{-1} in the hydrogenation of styrene when compared to our catalysts. The TOFs of 624 h^{-1} observed for the immobilized complex **Pd28** is much higher when compared to the values of 1.33 h^{-1} recorded for the soluble iron nanoparticles stabilized by $MgCl_2$ reported by Phua *et al.* in the hydrogenation of 1- hexene [61]. In some recent literature, palladium catalysts display comparable or higher catalytic activities relative to the immobilized catalysts **Pd26**– **Pd29** in this study. For example, the palladium nanoparticles stabilized by polyethylene glycol reported by Harazz *et al.* [62] and Pan *et al.* palladium nanoparticles anchored on uncoordinated carbonyl groups MOFs [63] exhibit TOFs of 660 h^{-1} and 703 $h^{-1,}$ respectively, which are close

to TOFs of 576 h^{-1} to 624 h^{-1} for complexes **Pd26** – **Pd29**. On the other hand, the Pd catalysts immobilized on polymerized 2-(acetoacetoxy)ethyl methacrylate reported by Lan *et al* [64] and Gao *et al.'s* Pd–pyridyl catalytic films [65] display much higher catalytic activities of 1449 h^{-1} and 6944 h^{-1} respectively in the styrene hydrogenation.
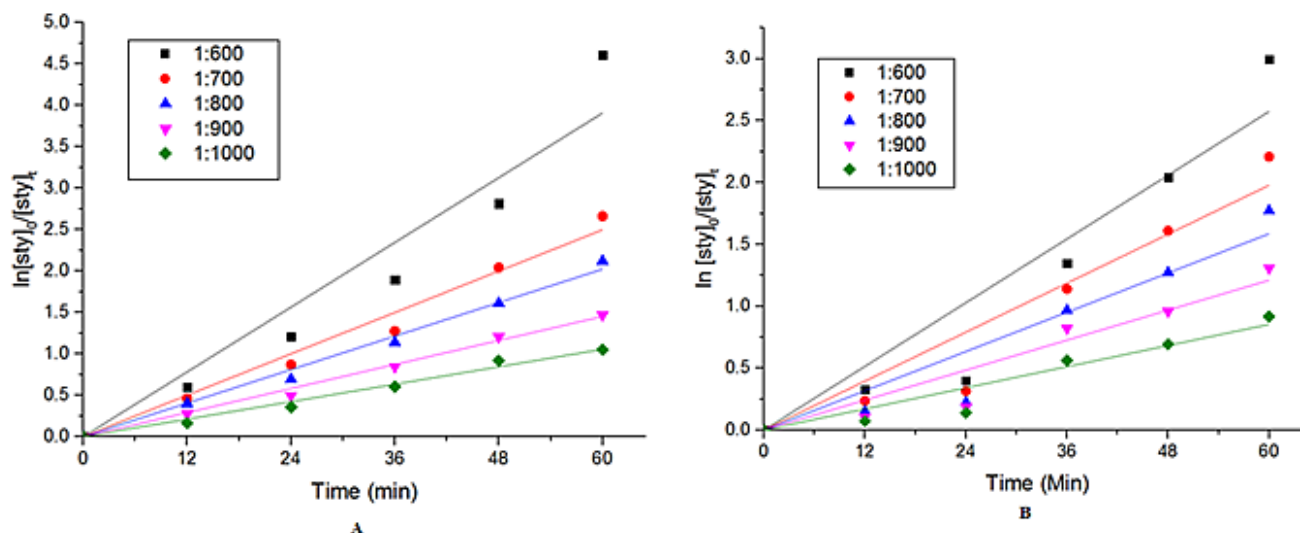

Figure 6.4: Graphical Plot of In[styrene]$_0$/[styrene]$_t$ vs time for effect of catalyst concentration using complex **Pd24** (A) and **Pd28** (B). The [styrene]/[**Pd24/Pd28**] was varied from 600 to 1000 at fixed concentration of styrene.

6. 3.2.2 Dependence of kinetics on hydrogen pressure and catalyst loading

Having established that both the homogeneous and immobilized complexes afford active catalysts in the hydrogenation of styrene, the most active homogeneous and immobilized complexes, **Pd24** and **Pd28,** respectively, were employed in further investigations. The impact of catalyst concentration was examined by varying the styrene/Pd ratios from 600 to 1000 at a constant styrene concentration. Plots of In[styrene]$_0$/[styrene]$_t$ *vs* time for complexes **Pd24** and **Pd28** at different catalyst concentrations (Figure 6.4) allowed us to determine the rate constant at each catalyst concentration. While the rates of the reactions appear to increase with an

191

increase in catalyst concentration, a different trend was observed in the examination of the TOF values (Figure 6.5). For instance, increasing the catalyst concentration of **Pd28** from 0.10 mol % to 0.125 mol % led to higher k_{obs} (from 0.85 h^{-1} to 1.59 h^{-1}) and TOFs (from 580 h^{-1} to 664 h^{-1}), respectively. However, beyond catalyst loading of 0.125%, the TOF dropped significantly (Figure 6.5). This clearly shows that the apparent increase in the rate is of lower magnitude in comparison to the amount of catalyst added. Hence, a lower catalyst loading of 0.125% would be qualitatively preferred from an industrial perspective.
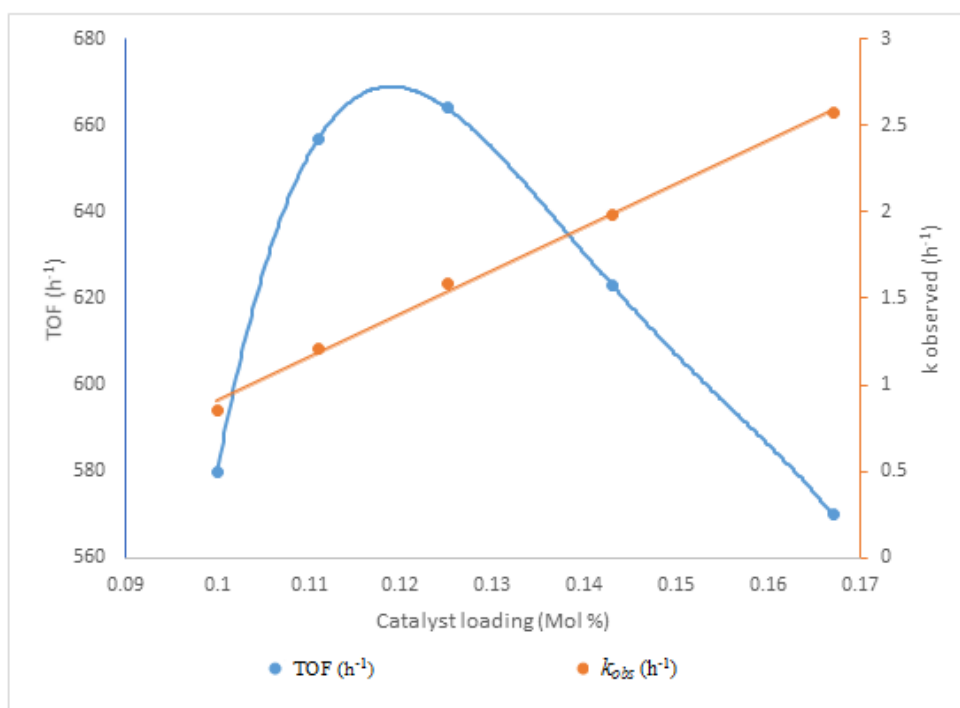
Figure 6.5:   A double plot of TOF and k_{obs} observed against catalyst loading for complex **Pd28** indicating optimum catalyst loading at about 0.14 mol%

The plots of $-\ln(k_{obs})$ vs $-\ln[$**Pd24**$]$ and $-\ln[$**Pd28**$]$ were used to obtain the reaction order related to **Pd24** and **Pd28** as 2.34 ± 0.18 h^{-1} and 2.07 ± 0.15 h^{-1} respectively (Figure 6.6). The reaction orders with reference to catalysts **Pd24** and **Pd28** is an indication that the rates of the hydrogenations reactions are sensitive to the changes in catalyst concentration. A more

interesting observation can be derived from the non-integer values of 2.34 and 2.07 for the homogeneous and immobilized **Pd24** and **Pd28** catalysts, respectively. Since fractional orders are associated with catalyst aggregation [66, 67], one would expect a higher fraction in the order with respect to the immobilized catalyst **Pd28**, as the active species is likely to be heterogeneous in nature. While the integer order of 2.07 can be attributed to a possible uniformly dispersed palladium catalyst, it is not sufficient to account for this discrepancy. The fractional-order with respect to **Pd24** may be assigned to aggregation and or resultant Pd(0) as part of the active species [66, 67]. The rate laws of the hydrogenation reactions of styrene with respect to catalyst concentrations are shown in Eq. 6.2.

$$\text{Rate} = k[\text{Styrene}]^1 \, [\textbf{Pd24}]^{2.34}$$

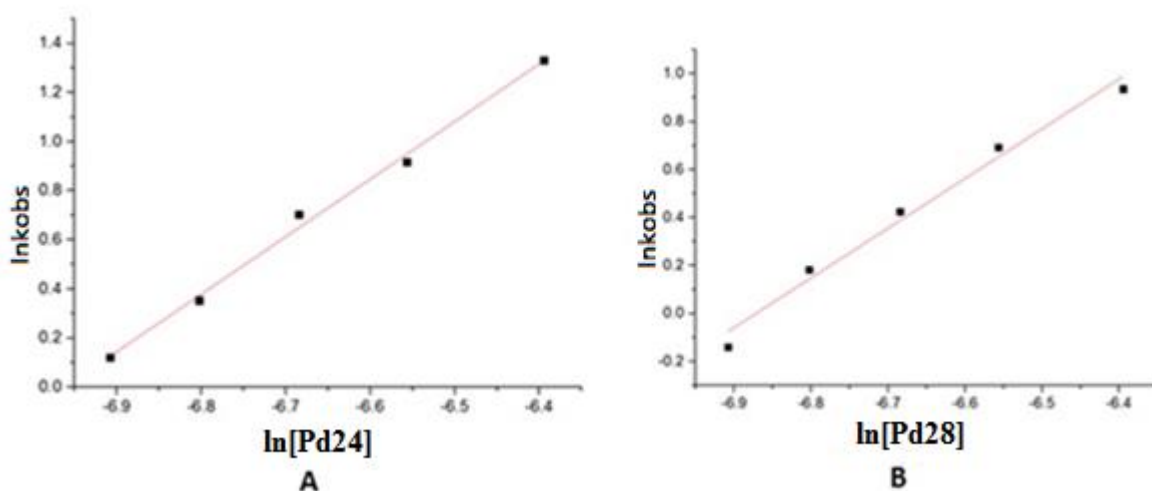$$\text{Rate} = k[\text{Styrene}]^1 \, [\textbf{Pd28}]^{2.07} \quad \dots\dots\dots\dots\dots\dots\dots\dots\text{Eq. 6.2}$$

Figure 6.6: Graphs of $\text{In}(k_{obs})$ vs $\text{In}[\textbf{Pd24}]$ (A) and $\text{In}[\textbf{Pd28}]$ (B) used in determining the reaction order with respect to complexes **Pd24** and **Pd28,** respectively.

We also investigated the effects of varying the hydrogenation pressure using complexes **Pd24** and **Pd28** by varying the hydrogen pressure from 2.5 to 10 bar. Plots of $In[styrene]_0/[styrene]_t$ *vs* time for complexes **Pd24** and **Pd28** at different hydrogen pressures (Figure 6.7) afforded linear relationships, from which the rate constant at each pressure was determined. For example, using complex **Pd24** at 2.5 bar, the observed rate constant was 1.62 ($\pm$ 0.10) h^{-1}, a value which expectedly increased dramatically to 3.74 ($\pm$ 0.37) h^{-1} at a pressure of 10 bar. Similar increase trends were observed for complex **Pd28**. Kinetic plots of the observed rate constants against pressure gave reaction orders with respect to pressure of 0.28 $\pm$ 0.05 and 0.27 $\pm$ 0.04 for **Pd24** and **Pd28,** respectively, an indication of similar response to changes in hydrogen pressure for both systems. The lower reaction orders are indicative of the formation of the monohydride compound as the active intermediate [68, 69]. The overall rate law combining the substrate, catalyst concentration, and hydrogen pressure for complexes **Pd24** and **Pd28** can be represented as in Eq. 3.
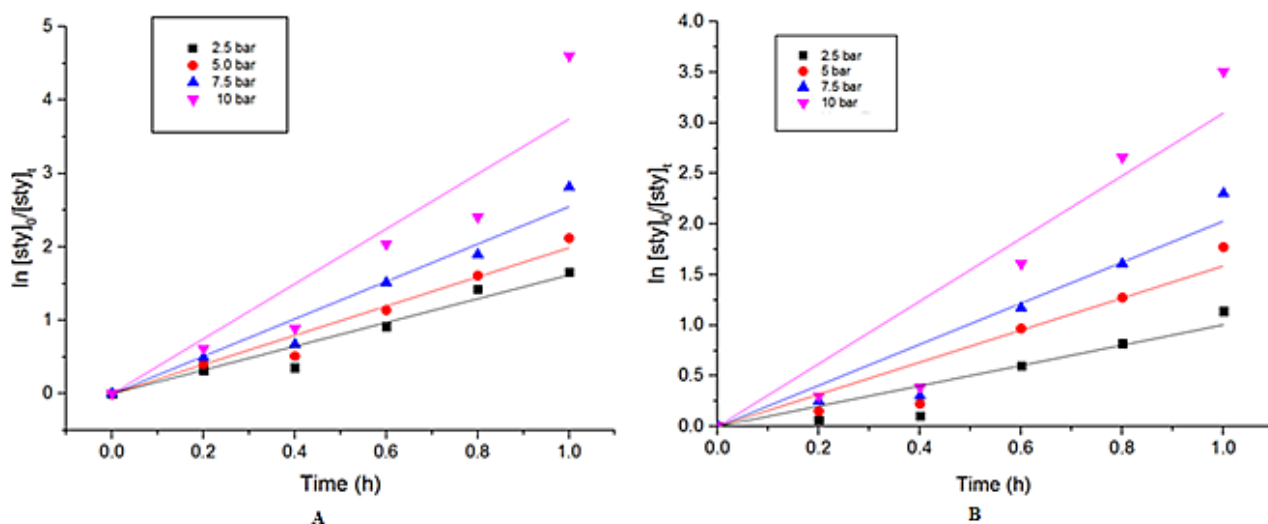
Figure 6.7: Plot of In[styrene]0/[styrene]t vs time for hydrogenation pressures for complex **Pd24** (A) and **Pd28** (B). Reaction conditions: styrene of 0.45 g (4.36 mmol); solvent, toluene (20 mL); time, 1 h; pressure, 5 bar; temperature, 30 °C.

Rate = k[styrene]^1 [**Pd24**]$^{2.36}$ [P$_{H2}$]$^{0.28}$

Rate = k[styrene]^1 [**Pd28**]$^{2.07}$ [P$_{H2}$]$^{0.27}$ …………Eq. 3.

6.3.2.3 Dependence of kinetics of hydrogenation of styrene on the reaction temperature

To determine the influence of reaction temperature using catalysts **Pd24** and **Pd28,** the reaction temperatures were varied from 30 °C to 60 °C. By plotting a graph of In[styrene]$_0$/[styrene]$_t$ vs time at different temperatures, the observed rate constants were extracted. In general and expectedly, raised temperature was followed by concomitant enhanced rate constants [70, 71]. For instance, using catalyst **Pd24**, at 30 °C and 60 °C, the observed rate constants of 2.02 h^{-1} and 5.95 h$^{-1,}$ respectively, were realized (Table 6.2). The activation parameters of complexes **Pd24** and **Pd28** were calculated from the Arrhenius plots as 31.22 ± 0.3 kJ/mol and 39.85± 0.8 kJ/mol, respectively (Figure 6.8). These values are significant in that they show that complex **Pd28** indeed behaved largely as a heterogeneous catalyst since typical heterogeneous catalysts

are known to exhibit higher activation energies than homogeneous systems [72-74]. The observations are in harmony with those reported by Semagina *et al.,* where they obtained activation energies of 30 kJ/mol and 36 kJ/mol for the homogeneous and supported palladium catalysts, respectively [72].

Table 6.2: Effect of temperature variation on k_{obs} values using complexes **Pd23** and **Pd27**[a]

Temperature (°C)	k_{obs}	
	Pd24	**Pd28**
30	2.02 ± 0.10	1.59 ± 0.14
40	2.55 ± 0.10	1.81 ± 0.15
50	4.00 ± 0.12	2.21 ± 0.15
60	5.95± 0.22	5.83 ± 0.20

[a]Reaction conditions: Time: 1 h, pressure: 5 bar, Solvent: toluene 20 ml; where styrene was 0.5 ml, 4.4 mmol. Catalyst loading, 0.125 mol%.

Pd24   **Pd28**
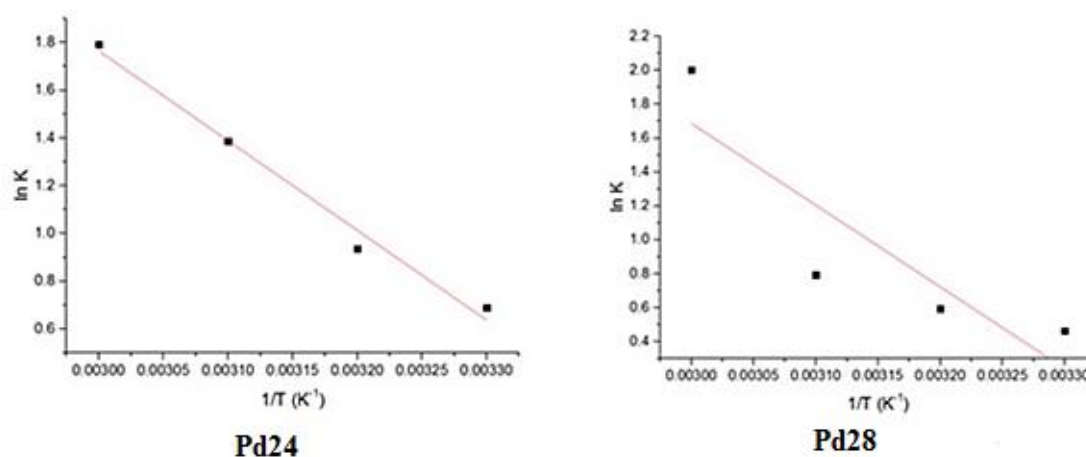
Figure 6.8: Arrhenius plot for the determination of activation parameters. Values of $E_a = 31.22 \pm 0.3$ kJ mol^{-1} (**Pd24**) and 39.95± 0.8 kJ/mol (**Pd28**); $R^2 = 0.9806$; slope $= -3762$;

Intercept $= 13$ (**Pd24**), $R^2 = 0.864$; slope $= -4817$; Intercept $= 16$ (**Pd28**) for the hydrogenation of styrene were obtained.

6.3.3 Investigations of the scope of the substrate in the hydrogenation reactions

6.3.3.1 Hydrogenation of alkenes and alkynes

Complexes **Pd24** and **Pd28** were used in the hydrogenation of 1-octyne, 1-hexyne, 1-hexene, phenyl-acetylene, 1-decene, 1-nonene and 1-octene to evaluate their viability in a wide range of olefins and alkynes (Table 6.3). The study revealed that the nature of the substrate had a notable impact on catalytic behaviour. For instance, using complex **Pd28**, we observed that varying chain lengths from 1-hexene to 1-octene resulted in a decreased rate of reaction from 1.39 ± 0.12 h^{-1} and 1.22 ± 0.11 $h^{-1,}$ respectively (Table 6.3, entries 1 and 2). This is expected as increased chain length results in higher steric hindrance and/or enhanced electron density and have the overall influence of hindering the coordination of the substrate [75, 76]. The higher rate constants observed for the more electron-deficient alkyne substrates support the hypothesis (Table 6.3, entries 4 and 5).
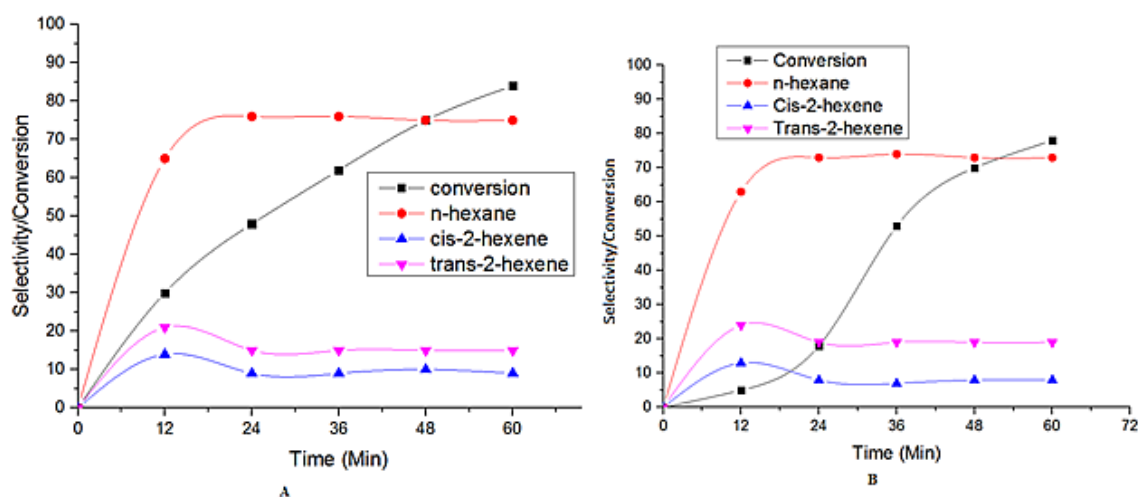
Figure 6.9: Selectivity /Conversion vs. time profile for hydrogenation of 1-hexene using **Pd24** (A) and **Pd28** (B) H$_2$ pressure, 5 bar, temperature, 30 °C; solvent, toluene (50 mL) time, 1 h.

We also studied the selectivity of the hydrogenation reactions for the various substrates using complexes **Pd24** and **Pd28** (Figure 6.10). The compositions of the hydrogenation products were found to be dependent on the substrate identity. We observed that terminal alkenes displayed considerable isomerization products in addition to the hydrogenation products (Table 6.3, entries 1, 2 and 5). For instance, **Pd24** afforded chemoselectivity of 76% for n-hexane, and isomerization products, *cis*-2-hexene (9%) and *trans*-2-hexene (15%) in the hydrogenation of 1-hexene (Fig. S13). More significantly, the immobilized complex **Pd28** gave a similar chemo-selectivity of 73% for n-hexane, indicating that the immobilization did not change the selectivity of the resultant catalyst. The hydrogenation of phenyl acetylene was found to occur in two steps; *via* the formation of styrene (Figure 6.11). The final product composition comprised of 91% ethylbenzene and 9% styrene (Figure 6.11), consistent with previous results
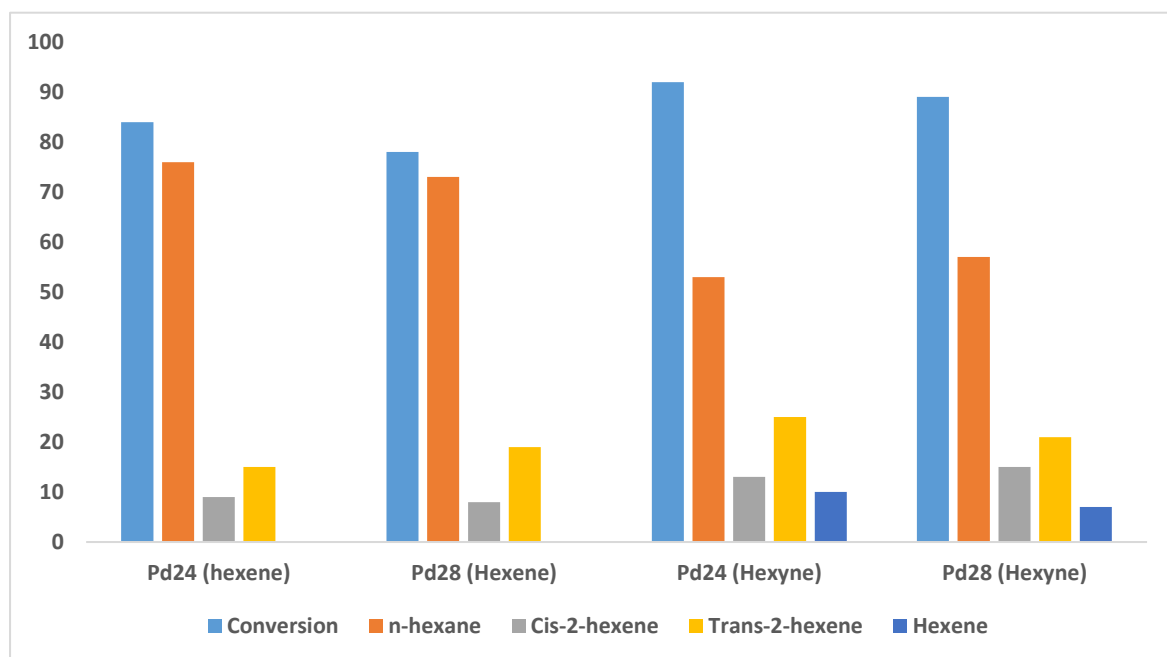
[77].

Figure 6.10: Hydrogenation and isomerization of 1-hexene and hexyne using **Pd24** and **Pd28**.

H_2 pressure; 5 bar; temperature; 30 °C; Solvent; toluene (50 mL).

Table 6.3: Effect of alkene and alkyne substrate on the hydrogenation reactions

Entry	Substrate	k_{obs} (h^{-1})		% Alkane		% Isomers	
		Pd24	**Pd28**	**Pd24**	**Pd28**	**Pd24**	**Pd28**
1	1-Hexene	1.75 (± 0.03)	1.39 (± 0.12)	76	73	24	27
2	1-Octene	1.57(± 0.03)	1.22(± 0.11)	65	63	35	37
3	Styrene	2.02(± 0.05)	1.59(± 0.14)	>99	98	-	-
4	Phenyl acetylene	2.82 (± 0.10)	2.06(± 0.17)	91	86	-	-
5	1-Hexyne	3.85 (± 0.13)	2.70 (± 0.22)	67	67	33	33

[a]Reaction conditions: Pressure, 5 bar; time: 1 h; temp 30 °C; Solvent, toluene (20 ml); catalyst concentration, 0.125 mol % (Pd: substrate = 1:800).
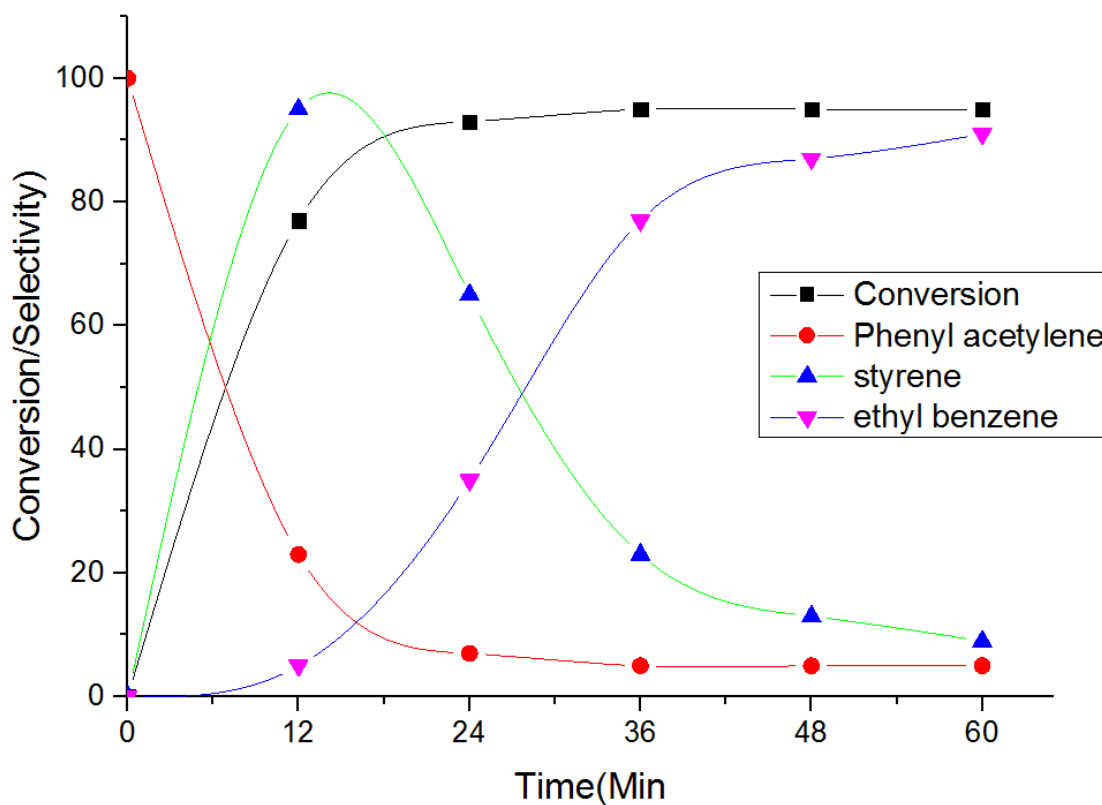
Figure 6.11: Selectivity /Conversion vs. time profile for hydrogenation of phenyl acetylene using **Pd3**, H_2 pressure: 5 bar; temperature, 30 °C; solvent, toluene (50 mL; time, 1 h.

6.4 Hydrogenation of substituted benzenes using complexes Pd24 and Pd28

As highlighted in the introduction, the development of active and selective catalysts for the hydrogenation of benzene and its derivatives to more useful intermediates is currently attracting significant attention [18, 78-80]. We thus used compounds **Pd24** and **Pd28** in the hydrogenation of various substituted benzenes (Table 6.4 and Figure 6.12).
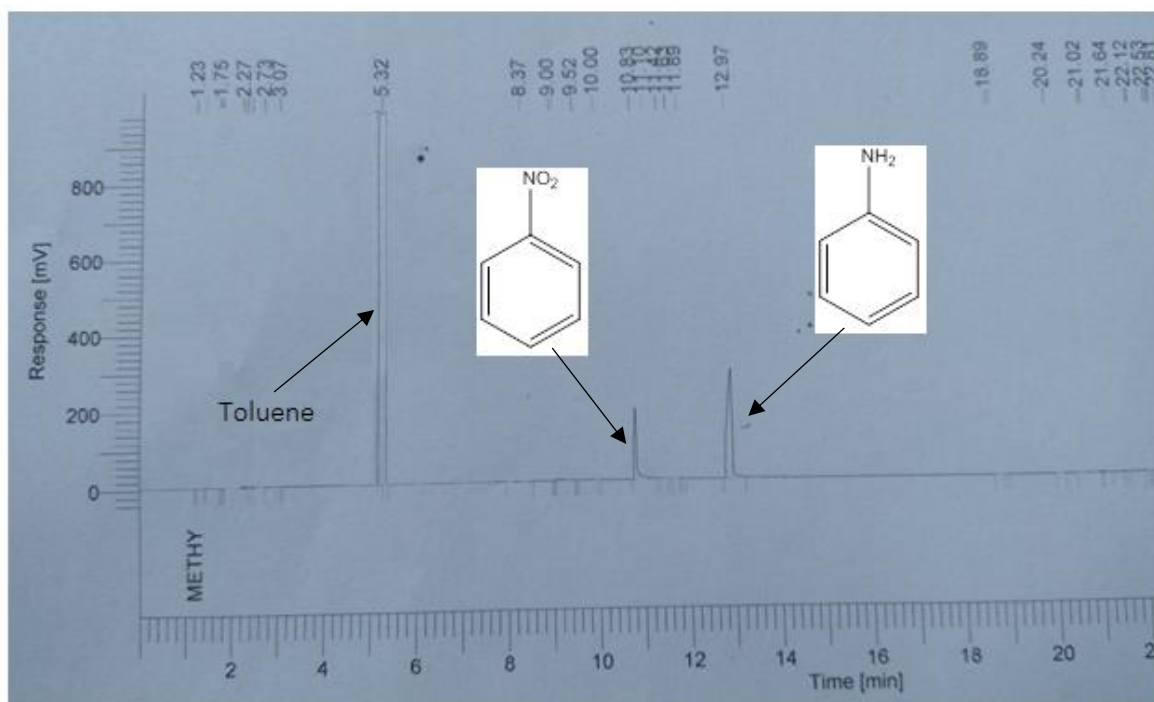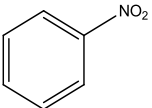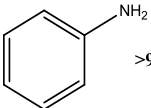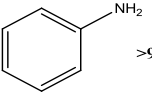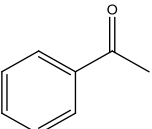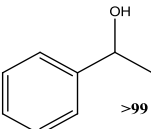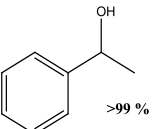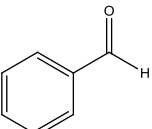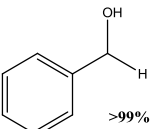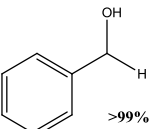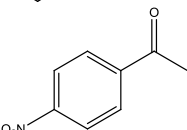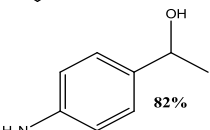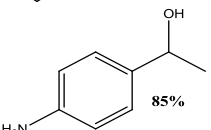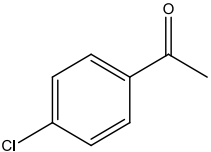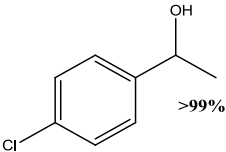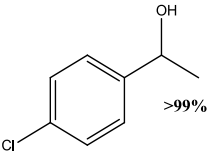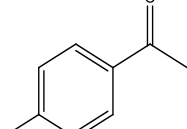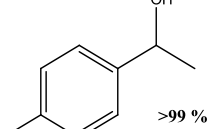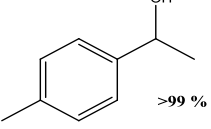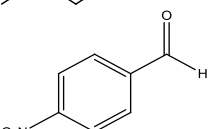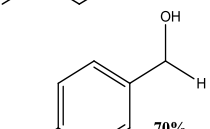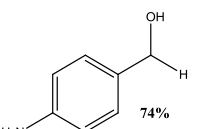
Figure 6.12: A GC trace showing the selective hydrogenation of nitrobenzene to aniline using **Pd24**

From Table 6.4, the complexes were active, with the catalytic activity being largely depending on substrate identity. As a demonstration, while the hydrogenation of nitrobenzene displayed conversions of 98% (TOF of 490 h^{-1}), acetophenone substrate afforded only 10% conversion (TOF of 50 h^{-1}) within 1 h using complex **Pd24** (Table 6.4, entries 1 and 2). A similar trend was noted for the immobilized compound **Pd28,** though with relatively lower conversions in comparison to the homogeneous complex **Pd24**. The higher reactivity of nitrobenzene is expected behaviour since the nitro- group is more reactive and is in line with previous results [24]. In addition, hydrogenation of the benzaldehyde gave comparable conversions of 93% (TOF of 465 h^{-1}) to those observed for nitrobenzene. Interestingly, using acetophenone substrate derivatives with electron-withdrawing or electron-donating groups at the *para-* position resulted in enhanced catalytic activities (Table 6.4, entries 2, 4-6). For example, 4-

201

nitro-acetophenone and 4-methyl-acetophenone substrates recorded conversions of 95% and 90%, respectively, compared to 10% posted by acetophenone. These reactivity trends could be attributed to resonance and inductive effects and are in good agreement with previous reports [81-83].

Table 6.4: Hydrogenation of various substituted benzenes using complexes **Pd24** and **Pd28**

Entry	Substrate	%Conv[b]		TOF[c]		Major products	
		Pd24	Pd28	Pd24	Pd28	Pd24	Pd28
1		98	87	490	435	>99 %	>99 %
2		10	7	50	35	>99 %	>99 %
3		93	86	465	430	>99%	>99%
4[d]		95	85	475	425	82%	85%
5		93	83	465	415	>99%	>99%
6		90	80	450	400	>99 %	>99 %
7[e]		88	77	440	385	70%	74%

[a]Reaction conditions: Pressure, 5 bar; time: 1 h; temp 30 °C; Solvent, toluene (20 ml); catalyst concentration, 0.2 mol % (Pd/substrate:1:500); [b]% of substrate converted to total products; [c]TOF (mol. sub/mol. Pd h^{-1}). [d]minor products include 4 amino acetophenone (15% and 13%) and 4-nitrobenzylethanol (3% and 2%,) for **Pd24** and **Pd28** respectively. [e]Minor product is 4 amino benzaldehyde 30% and 26 % for **Pd24** and **Pd28** respectively.

With respect to chemo-selectivity, hydrogenation reactions of nitrobenzene, acetophenone and benzaldehyde using **Pd24** and **Pd28** gave selectivity of >99% towards aniline, phenylethanol and phenylmethanol, respectively. However, the double-functionalized benzenes gave a mixture of products (Table 6.4 and Figure 6.13). For instance, from the kinetics profiles (Figure 6.13), hydrogenation of 4-nitroacetophenone initially formed 4-amino-acetophenone to give a final composition of 82% 4-aminophenylethanol and 15% 4-amino-acetophenone. Similar compositions of 85% and 13% for 4-aminophenylethanol and 4-amino-acetophenone were reported for the immobilized complex **Pd28** (Table 6.4, entry 4). The observed chemo-selectivities are both comparable and different to the literature reports in the hydrogenation reactions of bifunctional benzenes. For example, Cao *et al.* observed selective hydrogenation of 4-nitroacetophenone substrate to give only 4-amino-acetophenone using a Pd-MgO complex supported on melamino-formaldehyde polymer [20]. On the other hand, Hawkins and Makowski reported similar results to ours, where a mixture of 4-amino-acetophenone (59%) and 1-(4-aminophenyl) ethanol (34%) using Rh/Al_2O_3 catalyst were observed [23]. Interestingly, for 4-nitrobenzaldehyde, relatively lower selectivity towards 4-(aminophenyl)methanol of 70% and 74% was observed for complexes **Pd24** and **Pd28,** respectively (Table 6.4, entry 7). The minor product is 4-amino-benzaldehyde. In both cases, the results support the higher reactivity observed for nitrobenzene. The homogeneous and heterogeneous nature of complexes **Pd24** and **Pd28** was evident from the smooth and sigmoid curves of their kinetics profiles [50, 51] given in Figure 6.13.
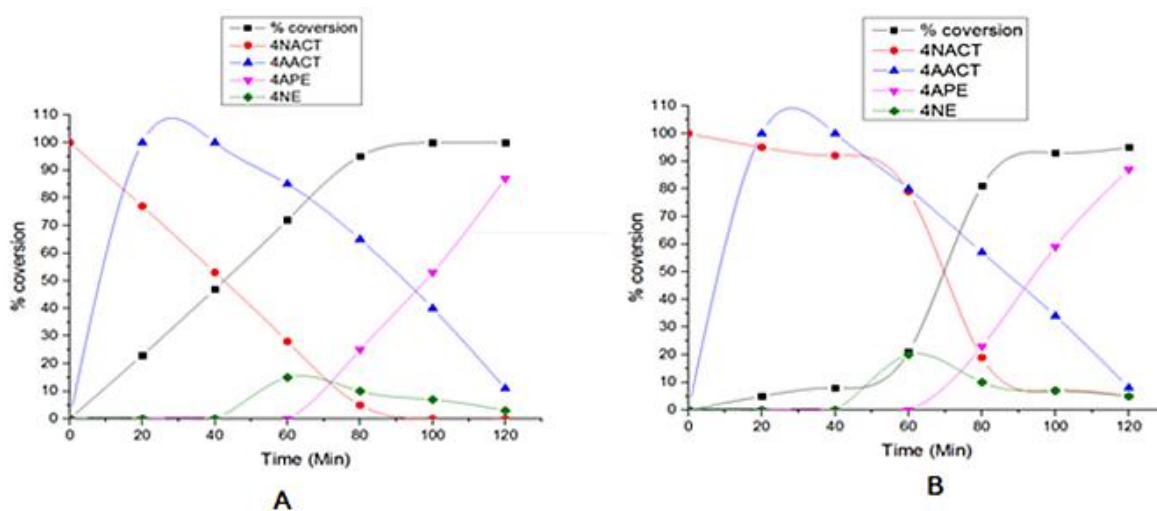
Figure 6.13: Selectivity /conversion vs. time profile for hydrogenation of 4-nitroacetophenone using **Pd24** (A) and **Pd28** (B), H_2 pressure, 5 bar, temperature, 30 °C; solvent, toluene (20 mL) time, 2 h. 4NACT (4-nitroacetophenone); 4AACT (4-amino-acetophenone); 4APE (4-aminophenylethanol); 4NE (4- nitroethanol).

6.5 Investigation of recovery and re-use of the immobilized catalysts

Another important aspect of this work was to formulate easily recoverable and recyclable catalysts in the hydrogenation reactions. Thus, we investigated the propensity of the immobilized complexes **Pd26**- **Pd29** to be recycled under optimized conditions (Figure 6.14). Significantly, all the immobilized complexes showed appreciable catalytic activities for five consecutive cycles (Figure 6.14) in the hydrogenation of styrene and nitrobenzene. For example, complex **Pd26** showed conversions of 98%, 84% and 70% in the first, fourth and fifth cycles, respectively, in the hydrogenation of styrene. The significant drop witnessed between the fourth and fifth cycle showed that the catalyst remains stable within the fourth run but undergo significant deactivation thereafter. Similar trends were observed for the other complexes, **Pd27 – Pd29** (Figure 6.14).
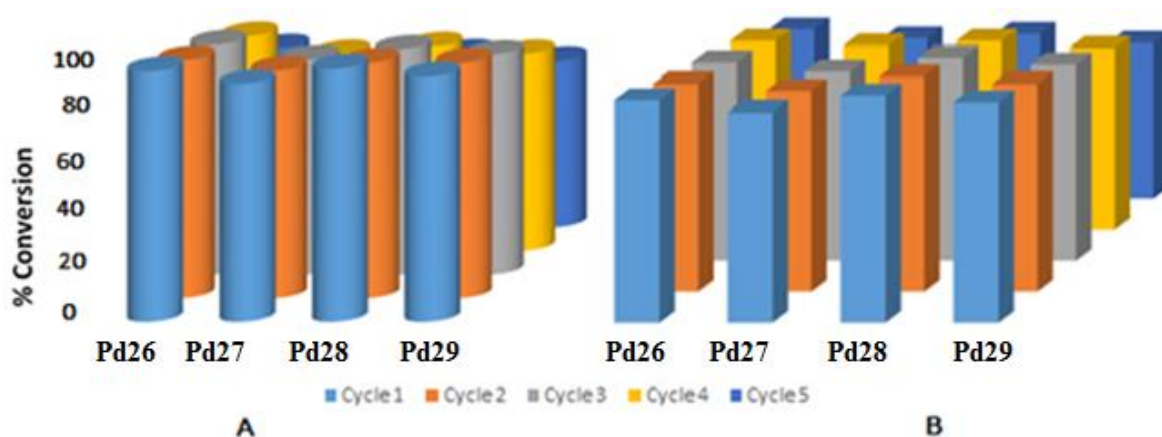
Figure 6.14: A graph showing catalytic activities of complexes **Pd25**- **Pd28** with % conversions of subsequent cycles in the hydrogenation of styrene (A) and nitrobenzene (B). Reaction conditions: time, 1.5 h; P$_{H2}$: 5 bar; temp, 30 ^{o}C; solvent, toluene (20 mL).

In order to understand the factors behind this loss of catalytic activities in the fifth cycle, we performed hot filtration experiments using complex **Pd28** to establish if leaching might account for the observed loss of catalytic activities in subsequent cycles. In a typical experiment, the reaction was run for 30 min to achieve about 40% percentage conversion, then the reaction mixture was cooled, filtered, and the supernatant liquid introduced into the reactor and run for a further 1 h. We observed that there was no increase in percentage conversion (42%, representing only 2% increase), indicating the absence of leaching. This result is a further indication that the immobilized complexes were insoluble in the reaction mixture, thus depicting a largely non-homogeneous reaction pathway. Thus the reductions in catalytic activities in subsequent runs may be assigned to physical damage to the catalyst system, consistent with the results we reported in the methoxycarbonylation reactions [49]. The EDX data (Table 6.5) showed the existence of Pd in catalysts (1.18 to 14.15%) and was indicative that the Pd metal remained immobilized even after the catalysis experiments. These results also

reflect those obtained by Ziccarelli *et al*., where losses in catalytic activities drop in the subsequent cycles in the alkoxycarbonylation of aryl halides were associated with catalyst abrasion [84].

Table 6.5: EDX data for the recycled immobilized complexes showing elemental compositions

Element	Pd26		Pd27		Pd28		Pd29	
	Weight (%)	Atomic (%)	Weight (%)	Atomic (%)	Weight (%)	Atomic (%)	Weight (%)	Atomic (%)
C	7.16	9.88	10.33	12.78	14.87	25.52	12.73	17.63
N	11.48	17.51	12.02	16.05	8.44	8.85	8.08	11.64
O	48.59	49.65	46.42	49.87	31.94	41.97	34.27	45.11
Si	31.44	21.78	29.71	20.04	18.47	12.67	19.13	15.56
Cl	-	-	-	-	12.13	8.32	13.21	8.05
Pd	1.33	1.18	1.52	1.26	14.15	2.67	12.58	2.01
Totals	100.00		100.00		100.00		100.00	

6.6 Investigation of the nature of the active species in the hydrogenation reactions.

Among the major goals of this chapter was to establish the real active species of the homogeneous and immobilized **Pd24** and **Pd28** complexes by employing mercury poisoning

[85] and sub-stoichiometric poisoning agents [50, 86], as depicted in Figures 6.15 and 6.16. This was to determine the possible formation of nanoparticles in both systems during the reducing conditions. First, we employed mercury-poisoning experiments by adding excess mercury using catalysts **Pd24** and **Pd28**. It is a common feature to use the term "excess mercury" in the catalysis community; however, to date, what is meant by excess mercury is not clear [50]. Thus at the start of the reaction, we first used three drops of mercury and complex **Pd28** and styrene and recorded a drop in conversion from 83% (1.59 ± 0.14) to 54% (0.77 ± 0.04). On the other hand, the use of seven drops saw the percentage conversion drop to 31%, while ten drops led to near-complete poisoning of the catalyst, achieving trace conversions of 4% (Figure 6.16). Thus in this work, ten drops of mercury could be regarded as excess.
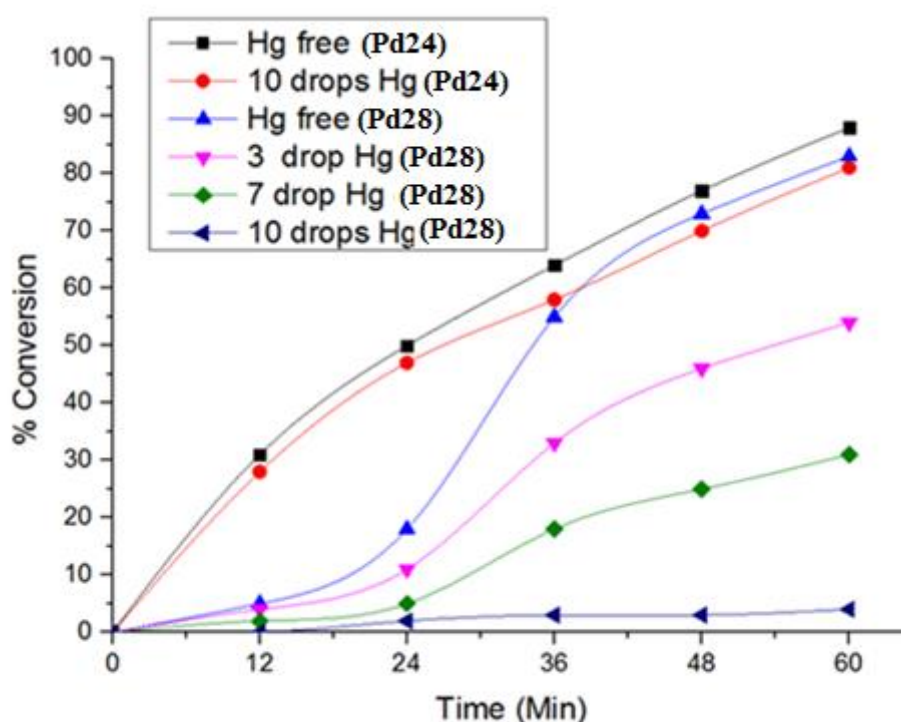

Figure 6.15: A Plot showing the effect of a varying number of drops of mercury in the hydrogenation of styrene using **Pd24** and **Pd28**

We further studied the impact of adding mercury at 50% conversion (once the active catalyst species is generated). Similarly, we recorded complete poisoning of the pre-formed catalyst (Figure 6.15). This showed that the addition of mercury has the effect of stopping the formation of the active species as well as deactivating the pre-formed active catalysts. The reduction in catalytic activities of complex **Pd28** upon addition of excess mercury thus implicates the formation of Pd(0) nanoparticles as the active species [50]. Comparatively, the addition of ten drops of mercury to the complex **Pd24** resulted in a slight drop in percentage conversion from 88% ($k_{obs} = 2.02 \pm 0.09$) to 81 % ($k_{obs} = 1.78 \pm 0.09$), indicating that complex **Pd24** forms mainly homogeneous active species [52] and possible little amounts of nanoparticles. To further understand the active species type generated from complexes **Pd24** and **Pd28**, we also used sub-stoichiometric poisoning agents PPh_3 and PCy_3 (Figure 6.16). We observed that the addition of 20 and 100% of PPh_3 to the **Pd28** complex system led to near-complete poisoning of the active catalyst, recording only 6% and 2% percentage conversions, respectively. On the other hand, the addition of 20 and 100% of the PPh_3 to the **Pd24** catalyst system resulted in very slight reductions in percentage conversion from 88% to 83% and 79%, respectively (Figure 6.16). Thus, mercury and sub-stoichiometric poisoning data point to the presence of a combination of catalytically active homogeneous and Pd(0) nanoparticle species for complex **Pd24**. On the other hand, Pd(0) nanoparticle species was responsible for the catalytic activity displayed by **Pd28**, consistent with the kinetics profiles reported earlier.
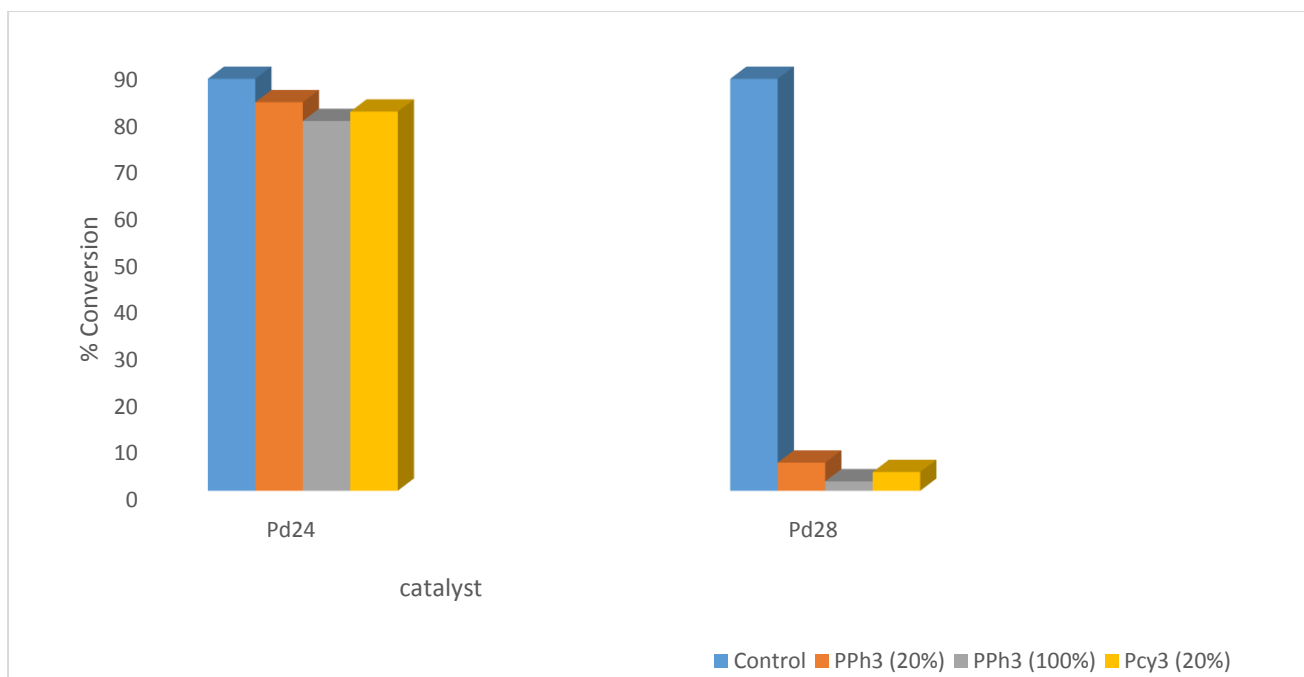
Figure 6.16: Graphical plot showing stoichiometric poisoning using 20% and 100% PPh3 and PCy₃ in the hydrogenation of styrene using **Pd24** and **Pd28**.

6.7 Conclusions

In summary, we have shown that homogeneous palladium complexes (**Pd22**-**Pd25**) and their immobilized counterparts (**Pd26**- **Pd29**) form active catalysts in the hydrogenation of alkenes alkynes and functionalized benzenes. In general, the homogeneous complexes exhibited higher catalytic activities than their corresponding immobilized complexes. More importantly, the immobilized complexes displayed comparative selectivities to the homogeneous systems across the substrates tested. The use of double-functionalized benzenes resulted in both partial and complete hydrogenation products. Changes in reaction parameters affected the kinetics of the hydrogenation reactions. Kinetics experiments, mercury and sub-stoichiometric poisoning data supported the homogeneous nature of complexes **Pd22-Pd25**, while **Pd26-Pd29** formed nanoparticles. The immobilized catalysts displayed significant catalytic behaviour for five cycles in the hydrogenation reactions of styrene and nitrobenzene.

210

The next and final chapter, chapter 7, entails general conclusion remarks and future recommendations. A possible prediction of the future outlook of methoxycarbonylation as olefin value addition reaction will be discussed.

6.8 References

[1] H.U. Blaser, C. Malan, B. Pugin, F. Spindler, H. Steiner, M. Studer, Selective hydrogenation for fine chemicals: Recent trends and new developments, Adv. Synth. Catal., 345 (2003) 103-151.

[2] Z. Dobrovolná, P. Kačer, L. Červený, Competitive hydrogenation in alkene–alkyne–diene systems with palladium and platinum catalysts1, J. Mol. Catal. A: Chem., 130 (1998) 279-284.

[3] S.M.A. Sohel, R.-S. Liu, Carbocyclisation of alkynes with external nucleophiles catalysed by gold, platinum and other electrophilic metals, Chem. Soc. Rev., 38 (2009) 2269-2281.

[4] R. Abu-Reziq, D. Wang, M. Post, H. Alper, Platinum nanoparticles supported on ionic liquid-modified magnetic nanoparticles: Selective hydrogenation catalysts, Adv. Synth. Catal., 349 (2007) 2145-2150.

[5] K. Sonogashira, E. Negishi, A. de Meijere, Handbook of Organopalladium Chemistry for Organic Synthesis Wiley, Interscience, NewYork, 2002.

[6] C. Bianchini, A. Meli, M. Peruzzini, P. Frediani, C. Bohanna, M.A. Esteruelas, L.A. Oro, Selective hydrogenation of 1-alkynes to alkenes catalyzed by an iron (II) cis-hydride. eta. 2-dihydrogen complex. A case of intramolecular reaction between. eta. 2-H2 and. sigma.-vinyl ligands, Organometallics, 11 (1992) 138-145.

[7] E. Drinkel, A. Briceno, R. Dorta, R. Dorta, Hemilabile P-Alkene Ligands in Chiral Rhodium and Copper Complexes: Catalytic Asymmetric 1, 4 Additions to Enones. 2, Organometallics, 29 (2010) 2503-2514.

[8] B. Han, P. Ma, X. Cong, H. Chen, X. Zeng, Chromium-and Cobalt-Catalyzed, Regiocontrolled Hydrogenation of Polycyclic Aromatic Hydrocarbons: A Combined Experimental and Theoretical Study, J. Am. Chem. Soc., 141 (2019) 9018-9026.

[9] B.G. Schieweck, P. Jürling-Will, J.r. Klankermayer, Structurally versatile ligand system for the ruthenium catalyzed one-pot hydrogenation of CO2 to methanol, ACS Catal., 10 (2020) 3890-3894.

[10] N. Singh, U. Sanyal, G. Ruehl, K.A. Stoerzinger, O.Y. Gutiérrez, D.M. Camaioni, J.L. Fulton, J.A. Lercher, C.T. Campbell, Aqueous phase catalytic and electrocatalytic hydrogenation of phenol and benzaldehyde over platinum group metals, J. Catal., 382 (2020) 372-384.

[11] Y. Zhang, S. Liao, Y. Xu, D. Yu, Catalytic selective hydrogenation of cinnamaldehyde to hydrocinnamaldehyde, Appl Catal A-Gen., 192 (2000) 247-251.

[12] P. Sabatier, How I Have Been Led to the Direct Hydrogenation Method by Metallic Catalysts1, Ind. Eng. Chem. Res., 18 (1926) 1005-1008.

[13] M.W. van Laren, M.A. Duin, C. Klerk, M. Naglia, D. Rogolino, P. Pelagatti, A. Bacchi, C. Pelizzi, C.J. Elsevier, Palladium (0) complexes with unsymmetric bidentate nitrogen ligands for the stereoselective hydrogenation of 1-phenyl-1-propyne to (Z)-1-phenyl-1-propene, Organometallics, 21 (2002) 1546-1553.

[14] K.-T. Chan, Y.-H. Tsai, W.-S. Lin, J.-R. Wu, S.-J. Chen, F.-X. Liao, C.-H. Hu, H.M. Lee, Palladium complexes with carbene and phosphine ligands: synthesis, structural characterization, and direct arylation reactions between aryl halides and alkynes, Organometallics, 29 (2009) 463-472.

[15] D. Drago, P.S. Pregosin, Palladium− Duphos Structural and Enantioselective Hydroarylation Chemistry, Organometallics, 21 (2002) 1208-1215.

[16] A. Bacchi, M. Carcelli, M. Costa, A. Leporati, E. Leporati, P. Pelagatti, C. Pelizzi, G. Pelizzi, Palladium (II) complexes containing a P, N chelating ligand Part II. Synthesis and characterisation of complexes with different hydrazinic ligands. Catalytic activity in the hydrogenation of double and triple CC bonds, J. Organomet. Chem., 535 (1997) 107-120.

[17] G.C. Bond, Metal-catalysed reactions of hydrocarbons, Springer2005.

[18] H. Blaser, U. Siegrist, H. Steiner, M. Studer, Aromatic nitro compounds, Fine Chemicals Through Heterogeneous Catalysis, (2001) 389-406.

[19] M.J. Sharif, S. Yamazoe, T. Tsukuda, Selective hydrogenation of 4-nitrobenzaldehyde to 4-aminobenzaldehyde by colloidal RhCu bimetallic nanoparticles, Top. Catal., 57 (2014) 1049-1053.

[20] S. Cao, S. Xu, S. Xu, Hydrogenation of nitroaromatics containing a carbonyl group catalyzed by the palladium complex of MgO-supported melamino–formaldehyde polymer, Polym. Adv. Technol., 10 (1999) 43-47.

[21] G. Li, C. Zeng, R. Jin, Chemoselective hydrogenation of nitrobenzaldehyde to nitrobenzyl alcohol with unsupported au nanorod catalysts in water, J. Phys. Chem. C ., 119 (2015) 11143-11147.

[22] K. Currall, S.D. Jackson, Hydrogenation of 4-nitroacetophenone over Rh/silica, Appl Catal A-Gen., 484 (2014) 59-63.

[23] J.M. Hawkins, T.W. Makowski, Optimizing selective partial hydrogenations of 4-nitroacetophenone via parallel reaction screening, Org Process Res Dev, 5 (2001) 328-330.

[24] K. Currall, S.D. Jackson, Hydrogenation of 4-Nitroacetophenone Over Rh/Silica: Understanding Selective Hydrogenation of Multifunctional Molecules, Top. Catal., 57 (2014) 1519-1525.

[25] D.J. Cole-Hamilton, Homogeneous catalysis--new approaches to catalyst separation, recovery, and recycling, Science, 299 (2003) 1702-1706.

[26] E.L. Goetheer, A.W. Verkerk, L.J. van den Broeke, E. de Wolf, B.-J. Deelman, G. van Koten, J.T. Keurentjes, Membrane reactor for homogeneous catalysis in supercritical carbon dioxide, J. Catal., 219 (2003) 126-133.

[27] P.G. Jessop, T. Ikariya, R. Noyori, Homogeneous catalysis in supercritical fluids, Chem. Rev., 99 (1999) 475-494.

[28] K. De Smet, S. Aerts, E. Ceulemans, I.F. Vankelecom, P.A. Jacobs, Nanofiltration-coupled catalysis to combine the advantages of homogeneous and heterogeneous catalysis, Chem. Commun., (2001) 597-598.

[29] P.T. Anastas, M.M. Kirchhoff, Origins, current status, and future challenges of green chemistry, Acc. Chem. Res., 35 (2002) 686-694.

[30] I.W. Davies, L. Matty, D.L. Hughes, P.J. Reider, Are heterogeneous catalysts precursors to homogeneous catalysts?, J. Am. Chem. Soc., 123 (2001) 10139-10140.

[31] C. de Bellefon, N. Tanchoux, S. Caravieilhes, New reactors and methods for the investigation of homogeneous catalysis, J. Organomet. Chem., 567 (1998) 143-150.

[32] S. Alexander, V. Udayakumar, V. Gayathri, Hydrogenation of olefins by polymer-bound palladium (II) Schiff base catalyst, J. Mol. Catal. A: Chem., 314 (2009) 21-27.

[33] H.H. Brintzinger, D. Fischer, R. Mülhaupt, B. Rieger, R.M. Waymouth, Stereospecific olefin polymerization with chiral metallocene catalysts, Angew. Chem. Int. Ed., 34 (1995) 1143-1170.

[34] J.J. de Pater, B.J. Deelman, C.J. Elsevier, G. van Koten, Multiphase systems for the recycling of alkoxycarbonylation catalysts, Adv. Synth. Catal., 348 (2006) 1447-1458.

[35] B. Wan, S. Liao, D. Yu, Polymer-supported palladium–manganese bimetallic catalyst for the oxidative carbonylation of amines to carbamate esters, Appl Catal A- Gen, 183 (1999) 81-84.

[36] H. Ishii, K. Takeuchi, M. Asai, M. Ueda, Oxidative carbonylation of phenol to diphenyl carbonate catalyzed by Pd–pyridyl complexes tethered on polymer support, Catal. Commun., 2 (2001) 145-150.

[37] X. Chen, H. Zhu, T. Wang, C. Li, L. Yan, M. Jiang, J. Liu, X. Sun, Z. Jiang, Y. Ding, The 2V-P, N polymer supported palladium catalyst for methoxycarbonylation of acetylene, J. Mol. Catal. A: Chem., 414 (2016) 37-46.

[38] M. Hronec, Z. Cvengrošová, M. Kralik, G. Palma, B. Corain, Hydrogenation of benzene to cyclohexene over polymer-supported ruthenium catalysts, J. Mol. Catal. A: Chem., 105 (1996) 25-30.

[39] Y. Chen, J. Qiu, X. Wang, J. Xiu, Preparation and application of highly dispersed gold nanoparticles supported on silica for catalytic hydrogenation of aromatic nitro compounds, J. Catal., 242 (2006) 227-230.

[40] W. Huang, J.N. Kuhn, C.-K. Tsung, Y. Zhang, S.E. Habas, P. Yang, G.A. Somorjai, Dendrimer templated synthesis of one nanometer Rh and Pt particles supported on mesoporous silica: catalytic activity for ethylene and pyrrole hydrogenation, Nano Lett., 8 (2008) 2027-2034.

[41] S.G. Shore, E. Ding, C. Park, M.A. Keane, Vapor phase hydrogenation of phenol over silica supported Pd and Pd · Yb catalysts, Catal. Commun., 3 (2002) 77-84.

[42] V. Polshettiwar, B. Baruwati, R.S. Varma, Nanoparticle-supported and magnetically recoverable nickel catalyst: a robust and economic hydrogenation and transfer hydrogenation protocol, Green Chem., 11 (2009) 127-131.

[43] M.J. Jacinto, P.K. Kiyohara, S.H. Masunaga, R.F. Jardim, L.M. Rossi, Recoverable rhodium nanoparticles: synthesis, characterization and catalytic performance in hydrogenation reactions, Appl Catal A- Gen, 338 (2008) 52-57.

[44] Q.M. Kainz, R. Linhardt, R.N. Grass, G. Vilé, J. Pérez-Ramírez, W.J. Stark, O. Reiser, Palladium Nanoparticles Supported on Magnetic Carbon-Coated Cobalt Nanobeads: Highly Active and Recyclable Catalysts for Alkene Hydrogenation, Adv. Funct. Mater., 24 (2014) 2020-2027.

[45] J. Schulz, A. Roucoux, H. Patin, Stabilized rhodium (0) nanoparticles: a reusable hydrogenation catalyst for arene derivatives in a biphasic water-liquid system, Chem. Eur. J., 6 (2000) 618-624.

[46] L. Plasseraud, G. Süss-Fink, Catalytic hydrogenation of benzene derivatives under biphasic conditions, J. Organomet. Chem., 539 (1997) 163-170.

[47] K. Demmans, O. Ko, R. Morris, Aqueous biphasic iron-catalyzed asymmetric transfer hydrogenation of aromatic ketones, RSC Adv., 6 (2016) 88580-88587.

[48] S.O. Akiri, S.O. Ojwach, Methoxycarbonylation of olefins catalysed by homogeneous palladium (II) complexes of (phenoxy) imine ligands bearing alkoxy silane groups, Inorg. Chim. Acta, 489 (2019) 236-243.

[49] S.O. Akiri, S.O. Ojwach, Synthesis of MCM-41 Immobilized (Phenoxy) Imine Palladium (II) Complexes as Recyclable Catalysts in the Methoxycarbonylation of 1-Hexene, Catalysts, 9 (2019) 143.

[50] J.A. Widegren, R.G. Finke, A review of the problem of distinguishing true homogeneous catalysis from soluble or other metal-particle heterogeneous catalysis under reducing conditions, J. Mol. Catal. A: Chem., 198 (2003) 317-341.

[51] J.F. Sonnenberg, R.H. Morris, Distinguishing homogeneous from nanoparticle asymmetric iron catalysis, Catal. Sci. Technol., 4 (2014) 3426-3438.

[52] E. Gross, J.H.-C. Liu, F.D. Toste, G.A. Somorjai, Control of selectivity in heterogeneous catalysis by tuning nanoparticle properties and reactor residence time, Nature chemistry, 4 (2012) 947.

[53] L.S. Hegedus, Transition metals in the synthesis of complex organic molecules, University Science Books1999.

[54] B.G. van Ravensteijn, D.J. Schild, W.K. Kegel, R.J. Klein Gebbink, The Immobilization of a Transfer Hydrogenation Catalyst on Colloidal Particles, ChemCatChem, 9 (2017) 440-450.

[55] Y. Niu, L.K. Yeung, R.M. Crooks, Size-selective hydrogenation of olefins by dendrimer-encapsulated palladium nanoparticles, J. Am. Chem. Soc., 123 (2001) 6840-6846.

[56] H. Abe, H. Amii, K. Uneyama, Pd-catalyzed asymmetric hydrogenation of α-fluorinated iminoesters in fluorinated alcohol: A new and catalytic enantioselective synthesis of fluoro α-amino acid derivatives, Org. Lett., 3 (2001) 313-315.

[57] M.-W. Chen, Y. Duan, Q.-A. Chen, D.-S. Wang, C.-B. Yu, Y.-G. Zhou, Enantioselective Pd-catalyzed hydrogenation of fluorinated imines: facile access to chiral fluorinated amines, Org. Lett., 12 (2010) 5075-5077.

[58] Y.-Q. Wang, S.-M. Lu, Y.-G. Zhou, Palladium-catalyzed asymmetric hydrogenation of functionalized ketones, Org. Lett., 7 (2005) 3235-3238.

[59] F. Yılmaz, A. Mutlu, H. Ünver, M. Kurtça, İ. Kani, Hydrogenation of olefins catalyzed by Pd (II) complexes containing a perfluoroalkylated S, O-chelating ligand in supercritical CO_2 and organic solvents, J Supercrit Fluids, 54 (2010) 202-209.

[60] H. Altinel, G. Avsar, M. Yilmaz, B. Guzel, New perfluorinated rhodium–BINAP catalysts and hydrogenation of styrene in supercritical CO_2, J Supercrit Fluids, 51 (2009) 202-208.

[61] P.-H. Phua, L. Lefort, J.A. Boogers, M. Tristany, J.G. de Vries, Soluble iron nanoparticles as cheap and environmentally benign alkene and alkyne hydrogenation catalysts, Chem. Commun., (2009) 3747-3749.

[62] F. Harraz, S. El-Hout, H. Killa, I. Ibrahim, Palladium nanoparticles stabilized by polyethylene glycol: Efficient, recyclable catalyst for hydrogenation of styrene and nitrobenzene, J. Catal., 286 (2012) 184-192.

[63] Y. Pan, D. Ma, H. Liu, H. Wu, D. He, Y. Li, Uncoordinated carbonyl groups of MOFs as anchoring sites for the preparation of highly active Pd nano-catalysts, J. Mater. Chem., 22 (2012) 10834-10839.

[64] Y. Lan, M. Zhang, W. Zhang, L. Yang, Enhanced Pd-Catalyzed Hydrogenation of Olefins within Polymeric Microreactors under Organic/Aqueous Biphasic Conditions, Chem. Eur. J., 15 (2009) 3670-3673.

[65] S. Gao, W. Li, R. Cao, Palladium–pyridyl catalytic films: A highly active and recyclable catalyst for hydrogenation of styrene under mild conditions, J. Colloid Interface Sci., 441 (2015) 85-89.

[66] C.M. Starks, M. Halper, Phase-transfer catalysis: fundamentals, applications, and industrial perspectives, Springer Science & Business Media2012.

[67] Q. Ashton Acton, Carboxylic Acids—Advances in Research and Application, Atlanta, GA: Scholarly Editions, (2013).

[68] P.J. Rheinländer, J. Herranz, J. Durst, H.A. Gasteiger, Kinetics of the hydrogen oxidation/evolution reaction on polycrystalline platinum in alkaline electrolyte reaction order with respect to hydrogen pressure, J. Electrochem. Soc., 161 (2014) F1448-F1457.

[69] M.H. Kim, E.K. Lee, J.H. Jun, S.J. Kong, G.Y. Han, B.K. Lee, T.-J. Lee, K.J. Yoon, Hydrogen production by catalytic decomposition of methane over activated carbons: kinetic study, Int. J. Hydrogen Energy, 29 (2004) 187-193.

[70] E. Díaz, A. Mohedano, L. Calvo, M. Gilarranz, J. Casas, J. Rodríguez, Hydrogenation of phenol in aqueous phase with palladium on activated carbon catalysts, Chem. Eng. J., 131 (2007) 65-71.

[71] A. Borodziński, G.C. Bond, Selective hydrogenation of ethyne in ethene-rich streams on palladium catalysts. Part 1. Effect of changes to the catalyst during reaction, Catal. Rev., 48 (2006) 91-144.

[72] N. Semagina, E. Joannet, S. Parra, E. Sulman, A. Renken, L. Kiwi-Minsker, Palladium nanoparticles stabilized in block-copolymer micelles for highly selective 2-butyne-1, 4-diol partial hydrogenation, Appl Catal A-Gen, 280 (2005) 141-147.

[73] Y. Mei, G. Sharma, Y. Lu, M. Ballauff, M. Drechsler, T. Irrgang, R. Kempe, High catalytic activity of platinum nanoparticles immobilized on spherical polyelectrolyte brushes, Langmuir, 21 (2005) 12229-12234.

[74] Y. Mei, Y. Lu, F. Polzer, M. Ballauff, M. Drechsler, Catalytic activity of palladium nanoparticles encapsulated in spherical polyelectrolyte brushes and core− shell microgels, Chem. Mater., 19 (2007) 1062-1069.

[75] R. Pruvost, J. Boulanger, B. Léger, A. Ponchel, E. Monflier, M. Ibert, A. Mortreux, T. Chenal, M. Sauthier, Synthesis of 1, 4: 3, 6-Dianhydrohexitols Diesters from the Palladium-Catalyzed Hydroesterification Reaction, ChemSusChem, 7 (2014) 3157-3163.

[76] J.C. Chadwick, R. Duchateau, Z. Freixa, P.W. Van Leeuwen, Homogeneous catalysts: activity-stability-deactivation, John Wiley & Sons2011.

[77] S.D. Jackson, L.A. Shaw, The liquid-phase hydrogenation of phenyl acetylene and styrene on a palladium/carbon catalyst, Applied Catalysis A: General, 134 (1996) 91-99.

[78] C.M. Peres, S.N. Agathos, Biodegradation of nitroaromatic pollutants: from pathways to remediation, (2000).

[79] J.C. Spain, J.B. Hughes, H.-J. Knackmuss, Biodegradation of nitroaromatic compounds and explosives, CRC Press2000.

[80] S. Ram, R.E. Ehrenkaufer, A general procedure for mild and rapid reduction of aliphatic and aromatic nitro compounds using ammonium formate as a catalytic hydrogen transfer agent, Tetrahedron Lett., 25 (1984) 3415-3418.

[81] K. Ganguli, S. Shee, D. Panja, S. Kundu, Cooperative Mn (I)-complex catalyzed transfer hydrogenation of ketones and imines, Dalton Trans. (2019).

[82] A.J. Watson, A.J. Fairbanks, Ruthenium-Catalyzed Transfer Hydrogenation of Amino- and Amido-Substituted Acetophenones, Eur. J. Org. Chem., 2013 (2013) 6784-6788.

[83] K. Li, X. Zhu, S. Lu, X.-Y. Zhou, Y. Xu, X.-Q. Hao, M.-P. Song, Catalyst-Free Friedel–Crafts Alkylation of Imidazo [1, 2-α] pyridines, Synlett, 27 (2016) 387-390.

[84] I. Ziccarelli, H. Neumann, C. Kreyenschulte, B. Gabriele, M. Beller, Pd-Supported on N-doped carbon: improved heterogeneous catalyst for base-free alkoxycarbonylation of aryl iodides, Chem. Commun., 52 (2016) 12729-12732.

[85] R.H. Crabtree, Resolving heterogeneity problems and impurity artifacts in operationally homogeneous transition metal catalysts, Chem. Rev., 112 (2011) 1536-1554.

[86] Y. Lin, R.G. Finke, A More General Approach to Distinguishing" Homogeneous" from" Heterogeneous" Catalysis: Discovery of Polyoxoanion-and Bu4N$^+$-Stabilized, Isolable and Redissolvable, High-Reactivity Ir. apprx. 190-450 Nanocluster Catalysts, Inorg. Chem., 33 (1994) 4891-4910.

Chapter 7

7.1 Overall Conclusion

This last Chapter presents general conclusions and possible future prospects based on the findings of the investigations of various catalytic systems in the methoxycarbonylation and hydrogenation reactions, as discussed in Chapters 3 to 6. In Chapter 3, (pyridyl)benzamidine ligands **L1**-**L5** coordinate to the palladium centre in bidentate mode to form typical square planar N^N (pyridyl) benzamidine palladium complexes **Pd1**-**Pd5.** The water-soluble (phenoxyimine) anionic ligands **L6-L8** and their non-water-soluble counterparts ligands **L9-L11,** reported in Chapter 4, contribute two ligand units each to form bischelated square planar (phenoxyimine) palladium(II) complexes, **Pd6-Pd11** respectively. On the other hand, the use of ligand (**L9**) gave a cationic complex **Pd12.**
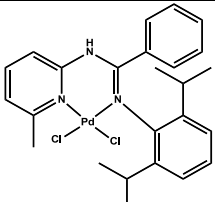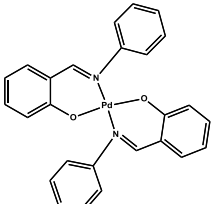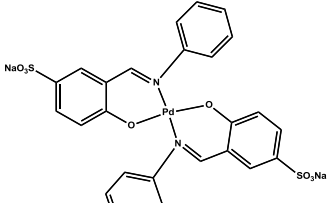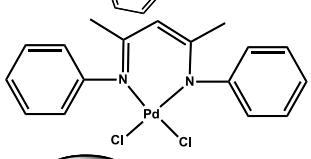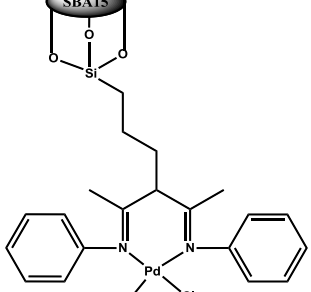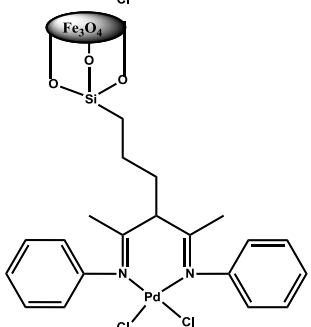
Reactions of (amino)phenyl ligand **L12** with 3-chloropropyl triethoxy silane led to the formation of (triethoxysilyl)propyl (amino)phenyl ligand **L13**. Ligands **L12** and **L13** both coordinate to palladium centre to form homogeneous complexes **Pd13** and **Pd14,** respectively, with complex **Pd14** used in making immobilized complexes reported in Chapter 5. Three different types of solid supports, MCM-41, SBA-15 and Fe_3O_4 nanoparticles, were used as immobilization agents for complex **Pd14** to form immobilized complexes **Pd15**-**Pd17**, respectively. Derivatives of complex **Pd15** were obtained by varying the palladium loading to form complexes **Pd18** and **Pd19**. Calcinations of complex **Pd16** at various temperatures lead to the formation of complexes **Pd20** and **Pd21. In Chapter 6,** the (phenoxy)imine homogeneous and silica-supported palladium(II) complexes were also obtained from the reactions of (phenoxy)imine ligands **L14** and **L15**. Immobilization of ligands **L14** and **L15** results in the formation of immobilized ligands **L16** and **L17**. The ligands **L14** and **L15** give

homogeneous palladium(II) complexes **Pd22**-**Pd25** upon coordination to the palladium. Besides, immobilized complexes **Pd26** and **Pd27** are obtained from immobilization of complexes **Pd22** and **Pd23** through a convergence approach, while complexes **Pd28** and **Pd29** are achieved upon the complexation of immobilized ligands **L16** and **L17** via sequential strategy.

The (pyridyl) benzamidine palladium complexes **Pd1-Pd5** formed active catalysts in the methoxycarbonylation of a range of higher olefins, both internal and terminal, with the catalytic activities and selectivities mainly controlled by steric factors. While the highest TON observed was 282, the lowest value observed in this set of complexes is 222. Besides, the best regioselectivity in the methoxycarbonylation of 1-hexene was 75% in favour of the linear ester product. The product distribution also depends on the identity of the substrate used, with other substrates such as trans-2-hexene, styrene, 1-heptene, 1-octene, 1-decene, trans-4-octene, 1-dodecene and tetradecene giving varying amounts of branched and linear ester products. Apart from the water-soluble (phenoxyimine) palladium(II) complexes **Pd6**-**Pd8** affording active catalysts, the complexes could be recycled up to five times. The activities of the water-soluble complexes **Pd6**-**Pd8** are comparable to their respective non-water-soluble complexes **Pd9**-**Pd11** with a TON of up to 372 observed. In addition, the regioselectivity of up to 77% of linear ester product was observed. Immobilized complexes **Pd15**-**Pd21** also formed active catalysts in the methoxycarbonylation of olefins, with the catalytic activities largely depending on the nature of the support. While SBA-15 supported catalysts gave the best activities (a TON of 360), the Fe_3O_4 magnetic nanoparticles supported catalysts were the least active (TON of 324) in this series. However, the nature of support did not notably impact the regioselectivity of the resultant catalysts, as 62%-67% of linear ester products were observed. Complexes **Pd15**-**Pd17** are also recyclable up to five times.

Homogeneous complexes **Pd22**-**Pd25** and their silica immobilized counterparts, complexes **Pd26**-**Pd29** were also active in catalytic hydrogenation of styrene, alkenes, alkynes and functionalized benzenes. While styrene selectively formed ethylbenzene as the sole product, product distribution in functionalized benzenes vary from one substrate to another. The highest and lowest TOF values observed in the hydrogenation of styrene was 704 and 576 mol. sub/mol. Pd h^{-1} respectively. The catalytic activities of the two sets of complexes were comparable; again, the supported compounds were reused five times in the hydrogenation of styrene and nitrobenzene.

Table 7.1: Comparative catalytic activities and selectivities observed for complexes

Entry	Catalyst	Type	Activity (TON)	Selectivity (Linear product %)
1		Homogeneous	222	75
2		Homogeneous	288	70
3		Water soluble	276	69
4		Homogeneous	372	60
5		SBA-15 immobilized	360	63
6		Fe_3O_4 immobilized	324	67

In general, the catalytic activities of the homogenous compounds, water-soluble complexes and immobilized complexes in methoxycarbonylation reactions were comparable, with the homogeneous systems showing slightly higher catalytic activities as compared to the water-soluble complexes and immobilized complexes (Table 7.1). On the other hand, the observed selectivities are influenced by the ligand design forming part of the complex network, with the more bulky systems yielding higher quantities of linear ester products. From this work, it is evident that the regioselectivity of the products formed in the methoxycarbonylation catalytic process can effectively be controlled by modifying the steric encumbrance around the metal centre.

## 7.2 Suggestions for Further Analysis

This thesis has explored comprehensive synthesis, characterization and catalytic applications of various classes of palladium(II) complexes. However, some extra work can improve the quality of the research achieved thus far. For instance, some characterization techniques can be instrumental in revealing the nature of the immobilized complexes better. BET analysis is recommended as part of extra work to help in determining the real particle sizes and compare with what is already in the literature. Other characterization techniques that can be appropriate for the immobilized complexes include:

-TPD to quantify the acid and basic sites on the catalyst surface

-XPS to determine the catalyst surface chemical composition, such as the oxidation states of the active sites.

7.3 Future recommendations

Chapters 3-6 of this thesis have presented a systematic catalyst design that supports green chemistry, starting with pure homogeneous systems and transitioning to recyclable water-soluble systems and immobilized systems that can be recycled. However, one aspect of methoxycarbonylation, which is still a dark spot, is the application of toxic and relatively more expensive CO gas as the carbonyl source. Guided by the principles of green chemistry, there is a need to design systems that can be used in the methoxycarbonylation that can use other sources of carbonyl such as carbon dioxide and formates, among other sources, while at the same time recyclable. Future methoxycarbonylation reactions should not only focus on recyclable catalysts but also the elimination of the use of toxic and expensive CO gas. The implication is those catalyst systems that can generate CO *in-situ* from other sources should be given priority to help drive the industry forward. For instance, CO2 can be used as a CO surrogate during a methoxycarbonylation reaction (Scheme 7.1).
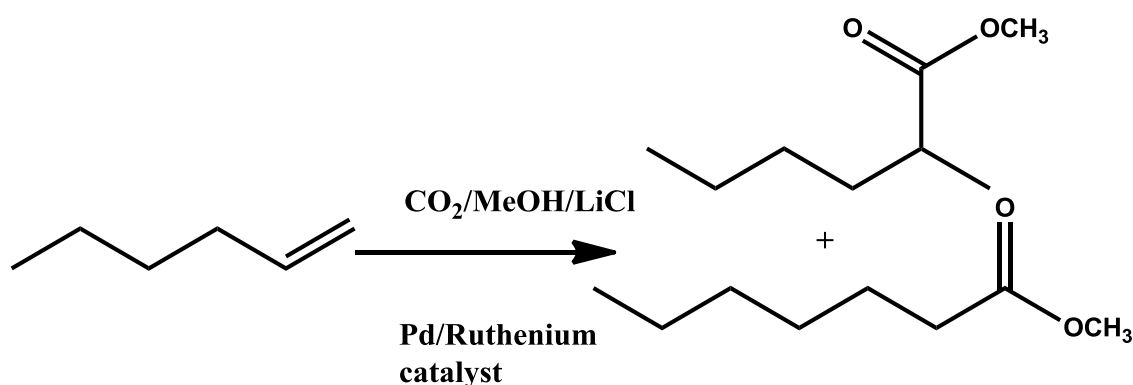
Scheme 7.1: The use of CO_2 as a CO surrogate in methoxycarbonylation of olefin.

As a future prospect, a homogenous and supported catalyst that can be used in methoxycarbonylation reaction as a recyclable catalyst while avoiding the use of toxic carbon

dioxide is presented in Figure 7.1. The catalyst system can generate CO *in-situ* from carbon

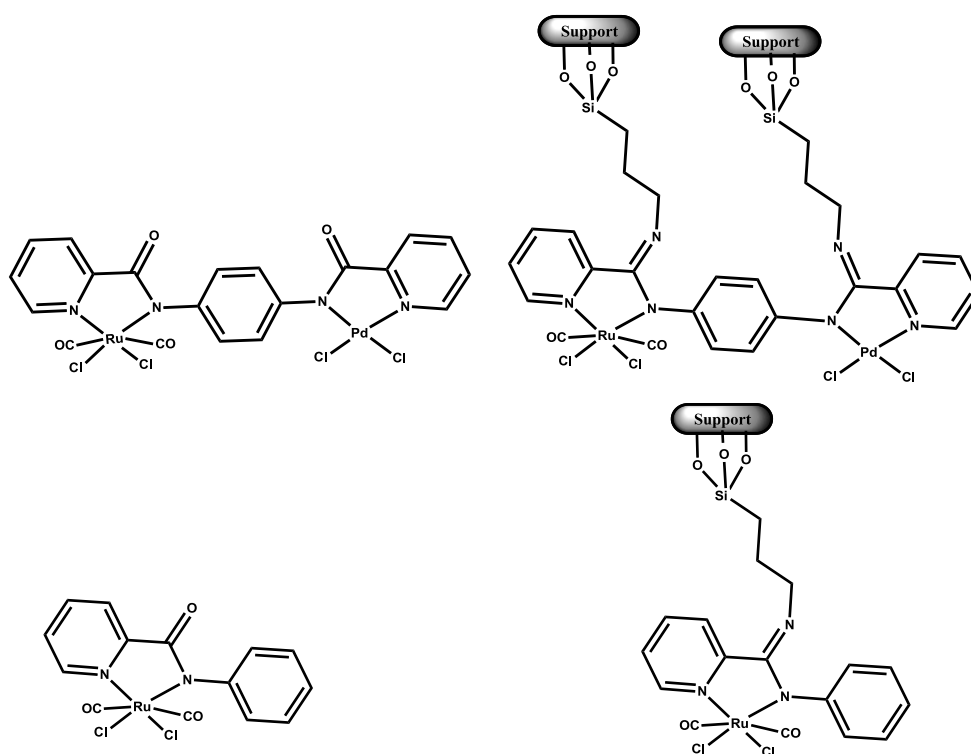dioxide, which is far much cheaper and less toxic than carbon monoxide gas.

Figure 7.1: Potential homogenous and supported ruthenium catalysts for possible methoxycarbonylation of olefins using CO_2

From the literature review, it has been shown that catalysts majorly employed in the methoxycarbonylation catalysis are *in situ* generated, with some of the best systems currently commercialized. As deduced from the previous chapters, the regioselectivity of products formed in a methoxycarbonylation reaction can be controlled by controlling steric hindrance around the metal coordination sphere. In addition, this present study has provided a unique insight where preformed/discrete catalysts performed better than their *in situ* generated

counterparts in methoxycarbonylation reactions. The implication of these insights is that part of the future recommendation should be pre- syntheses and isolation and of some of the best *in situ* generated catalysts and investigate them in the methoxycarbonylation reactions.